

2022

## Utilizing the K18-hACE2 mouse model to develop protective COVID-19 vaccines

Ting Y. Wong

*West Virginia University School of Medicine, Vaccine Development Center at West Virginia University Health Sciences Center, twong4@mix.wvu.edu*

Follow this and additional works at: <https://researchrepository.wvu.edu/etd>



Part of the [Diseases Commons](#), [Immunology and Infectious Disease Commons](#), and the [Microbiology Commons](#)

---

### Recommended Citation

Wong, Ting Y., "Utilizing the K18-hACE2 mouse model to develop protective COVID-19 vaccines" (2022). *Graduate Theses, Dissertations, and Problem Reports*. 11414.  
<https://researchrepository.wvu.edu/etd/11414>

This Dissertation is protected by copyright and/or related rights. It has been brought to you by the The Research Repository @ WVU with permission from the rights-holder(s). You are free to use this Dissertation in any way that is permitted by the copyright and related rights legislation that applies to your use. For other uses you must obtain permission from the rights-holder(s) directly, unless additional rights are indicated by a Creative Commons license in the record and/ or on the work itself. This Dissertation has been accepted for inclusion in WVU Graduate Theses, Dissertations, and Problem Reports collection by an authorized administrator of The Research Repository @ WVU. For more information, please contact [researchrepository@mail.wvu.edu](mailto:researchrepository@mail.wvu.edu).

**Utilizing the K18-hACE2 mouse model to develop protective COVID-19 vaccines**

**Ting Y. Wong**

**Dissertation submitted to the School of Medicine at West Virginia University in partial fulfillment of the requirements for the degree of**

**Doctor of Philosophy in Immunology and Microbial Pathogenesis**

**F. Heath Damron, PhD, Committee Chair**

**Gordon Meares, PhD**

**Cory Robinson, PhD**

**Paul Lockman, PhD**

**Robert Shanks, PhD**

**C. Garret Cooper, MD, PhD**

**Department of Microbiology, Immunology, and Cell Biology**

**Morgantown, West Virginia**

**2022**

**Keywords: SARS-CoV-2, COVID-19, VOC, RBD, K18-hACE2 mouse, human convalescent plasma, BReC-CoV-2, BECC470, RBD-EcoCRM, HBsAg, SWE, intranasal vaccination, mucosal immunity, hybrid immunity, vaccine break through immunity**

**Copyright 2022 Ting Y. Wong**

# Abstract

## Utilizing the K18-hACE2 mice model to develop protective COVID-19 vaccines

Ting Y. Wong

The ongoing Coronavirus Disease 2019 (COVID-19) pandemic is caused by the respiratory virus Severe Acute Respiratory Syndrome Coronavirus 2 (SARS-CoV-2). Similar to other respiratory viruses, SARS-CoV-2 is transmitted through inhalation of respiratory droplets and aerosols from infected individuals. Once inhaled, SARS-CoV-2 utilizes the receptor binding domain (RBD) on the spike protein to bind to human Angiotensin Converting Enzyme 2 (hACE2) receptor to gain entrance into host cells to begin viral replication. SARS-CoV-2 infection can result in mild to severe cases of COVID-19 ranging from asymptomatic infections, cold or flu like symptoms to respiratory failure. The onset of the pandemic in 2019 triggered a push to develop vaccines and therapeutics to prevent and treat SARS-CoV-2 infections. At the end of 2020, companies such as Moderna and Pfizer began to administer the first COVID-19 mRNA vaccines, and now in 2022, there are ten World Health Organization (WHO) approved vaccines with many more vaccines in clinical trials and pre-clinical development. At this time, approximately 12 billion doses have been administered worldwide accounting for 61% of the global population being fully vaccinated. However, with the continual emergence of SARS-CoV-2 variants of concern (VOC), each harboring new mutations that can negatively impact vaccine efficacy, there is a need to study and develop new vaccine approaches to improve immunity against VOC. Here, we devised three approaches to help improve vaccine efficacy against SARS-CoV-2 using the pre-clinical Keratin promoter 18-human Angiotensin Converting Enzyme 2 (K18-hACE2) mouse model. First, we evaluated the pathogenesis and response of VOC against human convalescent plasma (HCP) obtained from patients infected with the ancestral strain of SARS-CoV-2. Second, we assessed the vaccine efficacy of four adjuvanted Beta VOC or ancestral strain derived RBD Virus-like

particle (VLP) vaccines against Alpha and Beta VOC challenge. Third, we evaluated intranasal administration of a RBD carrier protein-based vaccine adjuvanted with a lipid A mimetic. K18-hACE2 challenge models were used to establish SARS-CoV-2 VOC lethal challenge doses for Alpha, Beta, and Delta. Once a lethal viral dose was determined for each VOC, we evaluated the VOC response against polyclonal antibodies obtained from high titer HCP in a passive immunization study. The objective of the study was to assess the efficacy of antibodies derived from the ancestral strain on emerging VOC since binding and neutralizing antibodies against SARS-CoV-2 are the main correlates of protection for measuring immunity against SARS-CoV-2. Passive immunization of HCP and challenge using ancestral strain, Alpha, Beta or Delta resulted in protection against ancestral strain (100% survival), partial protection against Alpha (60%), and no protection against Beta or Delta challenge (0% survival). Survival outcomes of passive immunization and VOC challenge were also reflected on disease outcomes, viral RNA levels in the lung, brain, and nasal wash (Delta challenge only), and lung pathology. Despite poor outcomes, human RBD and nucleocapsid IgG levels remained stable in the serum and lung in the HCP treated and VOC challenged animals. Therefore, the VOC challenge mouse model established in this study was further used to study vaccine efficacy. Additionally, the HCP passive immunization study demonstrated to us that antibodies generated against the ancestral strain may not protect against VOC. Therefore, to better improve vaccine efficacy against VOC, Beta specific RBD antigens were utilized to study the efficacy of a VLP delivery approach in a murine challenge model. In this study, vaccines were formulated with RBD from either the ancestral strain (Wu) or Beta VOC conjugated to Hepatitis B surface antigen (HBsAg) VLP and adjuvanted with Aluminum hydroxide (Alum) or Squalene-in-water emulsion (SWE) and compared against Pfizer mRNA vaccine. Overall, all RBD-VLP vaccines generated RBD binding antibodies against multiple VOC RBD, broadly neutralizing antibodies against VOC RBD, decreased viral burden in the lung and brain, and lowered inflammation in the lung similar to Pfizer mRNA. However, only Beta and Wu RBD VLP adjuvanted with Alum, and Beta RBD VLP adjuvanted with SWE were



able to protect mice (100% survival) against both Alpha and Beta challenge. Next, we evaluated intranasal (IN) vaccination as an approach to improve vaccine efficacy against SARS-CoV-2. We developed a prototype RBD vaccine conjugated to a diphtheria toxoid carrier protein Economical CRM<sub>197</sub> (EcoCRM) and adjuvanted with a toll-like receptor agonist 4 (TRL4), Bacterial Enzymatic Combinatorial Chemistry (BECC) called BReC-CoV-2 (BECC+ RBD-EcoCRM COVID-19 vaccine). Overall, IN immunization with BReC-CoV-2 resulted in protection against SARS-CoV-2, decreased viral burden in the lung, brain and nasal wash, generated high levels of RBD IgG in the serum and lung that were capable of neutralizing VOC RBD, as well as induced mucosal IgA in the lung and nasal wash compared to intramuscular (IM) vaccination of BReC-CoV-2. Furthermore, heterologous IN prime and IM boost strategy with BReC-CoV-2 resulted in protection (100% survival) against a lethal Delta challenge. Altogether, the three approaches to improve vaccine efficacy demonstrated that the addition of VOC vaccine antigens accompanied with immunostimulatory adjuvants can improve vaccine responses to VOC and intranasal immunization can enhance vaccine protection by inducing mucosal antibody responses at the site of infection. Together, these vaccine approaches can help improve vaccine efficacy against emerging VOC in future COVID-19 vaccines.

# Dedication

This work presented here is dedicated to my parents, and my 爷爷 and 奶奶. Thank you for all the sacrifices you have made to provide the opportunities I have today. You all are a true testament to hard work, perseverance, and strength, the real MVPs.

# Acknowledgements

It truly takes a village to raise a PhD student...

First, I would like to give the biggest thank you to my mentor Dr. Heath Damron. Thank you for giving me a second chance at science: for hiring me as a research technician whenever I had no idea what I was doing, for encouraging me to pursue a PhD, for supporting me all the way through my PhD journey, and for shaping me into scientist. I would also like to thank Dr. Mariette Barbier: for your kindness, support, and encouragement throughout the years, and for the many hours in your office troubleshooting experiments, designing, and fixing manuscripts and presentations and so much more. Thank you both for all the countless hours you invest into the labs and the members of the lab. The foundation that you have established within the DB lab is an environment unlike any other, and one that I will never forget.

To the DB lab fam: you all are my second family and I have no idea how I would have gotten through my PhD without you all. To Jesse Hall, Dylan Boehm, Emel Sen-Kilic, Catherine Blackwood, Allison Wolf, Paz Gutierrez, Justin Bevere, Jason Kang, Megan DeJong, Graham "JEFFF" Bitzer, Gage Pyles, Kelly Weaver, Willy Witt, Katie Lee, Nate "Radadaa" Rader, Olivia Miller, Sebastian Dziadowicz, Melissa Cooper, Annalisa Huckaby, Jo Miller, Matt Warden, Casey Cunningham, Brynna Russ, Alex Horspool, Josh Chapman, Eddie the Box, Barb, Bridgette, and Edgardo thank you all for always being there, for helping in any situation, and for making the DB lab so much fun. You guys are the best. I look forward to celebrating what awesome adventures the future holds for you all.

I would also like to thank my dissertation committee. Thank you all for your support, advice, and constructive input on my projects throughout the years. Your guidance and insight have been truly helpful and fully appreciated throughout all the projects and ideas I have shared with you all. Overall, thank you for making me critically think, and for always challenging me to think outside the box.

Thank you to everyone in the Microbiology, Immunology, and Cell Biology Department. Thank you all for being so collaborative and willing to share ideas, research, and reagents. I would like to also thank Dr. Kathleen Brundage for teaching us how to operate the Fortessa and MSD plate reader and for helping us troubleshoot experiments. I would also like to thank Dr. Ivan Martinez and Michael Winters for helping us culture SARS-CoV-2 and prepare the virus for our challenge studies. Thank you to Dr. Ali Elliott and Matt Stinoski for teaching us how to do experiments in the BLS3 safely, and for keeping the facility running smoothly.

Lastly, I would like to thank my family and friends. To my family, thank you for everything. Thank you for your support even when I make dumb mistakes, for all the encouraging talks and advice, for the tough love, and for being my unbreaking foundation. Thank you for pushing me to never give up. To my friends, thank you all for your constant support, encouragement, taking time out your busy lives to listen to me rant, and offering a shoulder to cry on every once in a while. Without you all, I would be lost.

# Table of Contents

<b>Abstract</b> .....	<b>ii</b>
<b>Dedication</b> .....	<b>iv</b>
<b>Acknowledgements</b> .....	<b>v</b>
<b>Table of Contents</b> .....	<b>vi</b>
<b>Chapter 1: Introduction</b> .....	<b>1</b>
1.1 COVID-19 pandemic .....	1
1.2 SARS-CoV-2 Pathogenesis and disease.....	1
1.3 Immune responses against SARS-CoV-2 infection.....	2
1.4 SARS-CoV-2 Variants of Concern .....	4
1.5.1 Non-replicating adenovirus COVID-19 vaccines.....	7
1.5.2 mRNA COVID-19 vaccines. ....	8
1.5.3 Protein subunit vaccines .....	9
1.5.4 Inactivated SARS-CoV-2 vaccines .....	10
1.6 Adjuvants for COVID-19 vaccines .....	13
1.6.1 Alum.....	13
1.6.2 Toll like receptor agonist .....	14
1.6.3 Oil in water adjuvants.....	15
1.7 Vaccine nanoparticles and carrier proteins .....	17

1.8 COVID-19 vaccine immunological correlates of protection .....	18
1.9.1 Mice .....	22
1.9.2 Syrian Hamsters.....	23
1.9.3 Ferrets .....	24
1.9.4 Non-human primates.....	24
1.10 SARS-CoV-2 mucosal immune response .....	25
1.11 Nasal vaccination .....	29
1.12 COVID-19 vaccine overview .....	30
1.13 Premise .....	31
1.14 References .....	33
<b>Chapter 2: Evaluating antibody mediated protection against Alpha, Beta, and Delta SARS-CoV-2 variants of concern in K18-hACE2 transgenic mice.....</b>	<b>46</b>
2.1 ABSTRACT .....	48
2.3. INTRODUCTION .....	49
2.4 METHODS: .....	51
2.5 RESULTS.....	57
2.6 DISCUSSION .....	62
2.7 ACKNOWLEDGEMENTS.....	64
2.8 FIGURES .....	66
2.9 REFERENCES:.....	73
<b>Chapter 3: RBD-VLP vaccines adjuvanted with Alum or SWE protect K18-hACE2 mice against SARS-CoV-2 VOC challenge .....</b>	<b>85</b>

3.2 Importance .....	89
3.3 Introduction.....	90
3.4 Methods .....	93
3.5 Results .....	97
3.6 Discussion.....	104
3.7 Acknowledgements .....	109
3.8 Figures. ....	111
3.9 Supplemental Figures.....	119
3.9 References .....	127
<b>Chapter 4: Intranasal administration of BReC-CoV-2 COVID-19 vaccine protects K18-hACE2 mice against lethal SARS-CoV-2 challenge .....</b>	<b>138</b>
4.1 Abstract .....	140
4.2 Introduction.....	141
4.3 Results .....	143
4.4 Discussion.....	153
4.5 Methods .....	159
4.6 Acknowledgements .....	167
4.7 Figures .....	169
4.7 Supplementary Figures.....	183
4.8 References .....	188
<b>Chapter 5: Discussion .....</b>	<b>196</b>
5.1 Overview .....	196

5.2 Pandemic response .....	199
5.2.1 Repurposing of animal models .....	200
5.2.2 Implementation of antibody-based therapeutics and antivirals to treat COVID-19 ...	201
5.2.3 Local community response to COVID-19 .....	202
5.2.4 Global response to vaccine inequity .....	203
5.3 Manufacturability of COVID-19 vaccines for developing countries .....	204
5.4 The impact of SARS-CoV-2 zoonosis and recombination events.....	204
5.4.2 SARS-CoV-2 spillover and spillback events .....	205
5.4.3 Prediction on future emerging SARS-CoV-2 variants .....	206
5.5 Improving COVID-19 vaccines.....	208
5.5.1 Improving longevity .....	210
5.5.2 Improving vaccine responses against VOC .....	212
5.6 Developing protective nasal COVID-19 vaccines.....	213
5.5.1 Potential nasal adjuvants .....	217
5.5.2 Other uses for nasal vaccination .....	218
5.6 Concluding remarks.....	218
5.7 References .....	220

## **Table of Figures and Supplemental material**

<b>Chapter 1: Introduction.....</b>	<b>1</b>
Figure 1. Timeline of the emergence of SAR-CoV-2 variants of concern.....	6
Figure 2. Types of SARS-CoV-2 immunity.....	21
Figure 3. Summary of animal models used to study SARS-CoV-2.....	27
<b>Chapter 2: Evaluating antibody mediated protection against Alpha, Beta, and Delta SARS-CoV-2 variants of concern in K18-hACE2 transgenic mice.....</b>	<b>46</b>
Figure 1. Characterization of early pandemic human convalescent plasma and in vitro characterization of SARS-CoV-2 variants.....	66
Figure 2 Effect of convalescent plasma treatment on SARS-CoV-2 VoC infection in K18-hACE2 transgenic mice.....	68
Figure 3 Survival and viral infection of serum-treated K18-hACE2 transgenic mice infected with SARS-CoV-2 VoC.....	69
Figure 4 Human anti-SARS-CoV-2 IgGs in serum-treated K18-hACE2 transgenic mice challenged with SARS-CoV-2 VoC.....	70
Figure 5 Histopathological analysis of VoC challenged lungs.....	71
Figure 6 HCP passive immunization was insufficient to protect against Delta variant challenge.....	72
<b>Chapter 3: RBD-VLP vaccines adjuvanted with Alum or SWE protect K18-hACE2 mice against SARS-CoV-2 VOC challenge.....</b>	<b>85</b>
Figure 1. Characterization of RBD IgG antibody responses against 10 SARS-CoV-2 VOC RBDs.....	112
Figure 2. Evaluation of RBD-VLP and mRNA vaccine protection against VOC challenge.....	113
Figure 3. Determination of viral RNA burden in VOC challenged mice.....	115
Figure 4. RBD HBsAg+SWE induced broadly neutralizing antibodies against VOC RBD.....	116
Figure 5. Histopathological analysis of the lung in vaccinated mice challenged with VOC.....	118



Supplemental Figure 1 RBD IgG titers from 2 weeks post prime (prime) and 4 weeks post 2 <sup>nd</sup> dose (boost 2) against Wuhan, Alpha, Beta, and Delta RBD VOC. ....	122
Supplemental Figure 2 Evaluation of weight and temperature change from K18-hACE2 vaccinated mice against Alpha or Beta challenge .....	123
Supplemental Figure 3 Analysis of vaccine induced neutralizing antibodies against 5 major VOC during Alpha challenge.....	124
Supplemental Figure 5 Chronic and acute inflammation in non-vaccinated and vaccinated lungs. ....	126
<b>Chapter 4: Intranasal administration of BReC-CoV-2 COVID-19 vaccine protects K18-hACE2 mice against lethal SARS-CoV-2 challenge.....</b>	<b>138</b>
Figure 1. Mouse immunogenicity studies to identify vaccine candidates. ....	169
Figure 2. Analysis of antibody responses and neutralization capacity of IN and IM BreC-CoV-2 vaccines.....	170
Figure 3. Intranasal administration of BReC-CoV-2 protected mice from SARS-CoV2 challenge. ....	171
Figure 4. Determination of viral RNA levels in challenged mice.....	173
Figure 5. Serological analysis of serum, lung, and nasal antibodies.....	174
Figure 6. Analysis of RBD-ACE2 neutralization capacity of serum. ....	175
Figure 7. Analysis of CXCL13 in serum or lungs in relation to immunization. ....	176
Figure 8. Histopathological analysis of naïve or vaccinated mice challenged with SARS-CoV-2. ....	177
Figure 9. RNAseq analysis reveals IN BReC-CoV-2 vaccination results in unique gene expression signatures enriched for T cell responses.....	180
Figure 10. IM BReC-CoV-2 prime followed by IN boost afforded protection against SARS-CoV-2 Delta variant challenge.....	181
Supplementary Figure 1 Disease scoring schematic.....	185

Supplementary Figure 2 BReC-CoV-2 vaccination demonstrated a balanced Th1/Th2 response..  
.....186

Supplementary Figure 3 IN BreC-CoV-2 decreased IFN $\gamma$  in the lung .....187

**Chapter 5: Discussion.....196**

Figure 1. SARS-CoV-2 zoonosis and VOC evolution .....207

Figure 2. Mucosal and systemic immunity against SARS-CoV-2.....209

Figure 3. Experimental vaccine approaches to improve COVID-19 vaccine efficacy. ....216

## List of Tables

<b>Chapter 1: Introduction.....</b>	<b>1</b>
Table 1: Eleven WHO approved COVID-19 vaccines.....	12
<b>Chapter 3: RBD-VLP vaccines adjuvanted with Alum or SWE protect K18-hACE2 mice against SARS-CoV-2 VOC challenge.....</b>	<b>85</b>
Supplemental Table 1. COVID-19 vaccine formulations.....	119
Supplemental Table 2 Statistical analysis of VOC RBD IgG levels at 2 weeks post prime and 4 weeks post second boost. ....	120
<b>Chapter 4: Intranasal administration of BReC-CoV-2 COVID-19 vaccine protects K18-hACE2 mice against lethal SARS-CoV-2 challenge.....</b>	<b>138</b>
Supplementary Table 1. COVID-19 vaccine formulations and routes for CD1 immunogenicity studies. ....	183
Supplementary Table 2. Statistical analysis of RBD IgG titers in CD1 mice vaccinated with BREC-CoV-2 or RBD + BECC470 (figure 2). ....	184

# Chapter 1: Introduction

## 1.1 COVID-19 pandemic

In late December 2019, multiple pneumonia cases caused by an unidentified respiratory pathogen was detected in Wuhan, Hubei Province, China, and linked to the Huanan Seafood Wholesale Market (1,2). As the year 2019 ended and 2020 began, the unidentified respiratory pathogen was unveiled through genetic sequencing as a novel coronavirus named Severe Acute Respiratory Syndrome Coronavirus 2 (SARS-CoV-2) (1,2). The newly identified coronavirus was closely monitored by the World Health Organization (WHO) and declared a public health emergency of international concern at the end of January (1,2). In February 2020, the disease caused by SARS-CoV-2 was coined Coronavirus Disease 2019 (COVID-19), with cases increasing to over 160,000 cases world-wide (1,2). On March 11, 2020, the WHO declared COVID-19 a pandemic, initiating shut down and stay-at-home orders world-wide. As soon as the genetic sequence for SARS-CoV-2 was known, vaccine development began (1,2). Due to an abundance of previous research on similar coronaviruses, as well as more than 30 years of research on development of mRNA technology, Pfizer-BioNTech and Moderna administered the first mRNA COVID-19 vaccines under emergency use authorization in December 2020.

## 1.2 SARS-CoV-2 Pathogenesis and disease

Transmission of SARS-CoV-2 can occur through inhalation of aerosols or respiratory droplets of infected individuals. SARS-CoV-2 establishes infection in the host, utilizing structural proteins as well as other non-structural and accessory proteins. The RNA virus is composed of four main structural proteins including spike, membrane, envelope, and nucleocapsid that play crucial roles in pathogenesis. Unlike the other structural proteins, the spike protein of SARS-CoV-2 remains an important target for vaccine and therapeutic development. The spike protein is composed of

two subunits, S1 and S2, and is responsible for viral entry into host cells. The S1 and S2 are divided by S1 and S2 cleavage sites (3). Therefore, the S1 subunit of the spike protein contains the receptor binding domain (RBD), which allows for the binding of the spike protein to the host human angiotensin converting enzyme 2 (ACE2). In turn this enables the protease cleavage at the S2 site, triggering S2 subunit fusion of the host and virion membranes (3–6). The membrane protein of SARS-CoV-2 is the most abundant structural protein with the main role of viral particle assembly (5). Envelope protein of SARS-CoV-2 engages in viral assembly as well as plays a role in viral lysis, release of virions once inside of the host cell, and activates the inflammasome (5–7). Nucleocapsid is the only structural protein on the inside of the virion and is responsible for protecting the viral RNA by forming ribonucleoprotein complexes. Nucleocapsid could also play a role with interfering with host immune responses (5,6,8).

Once SARS-CoV-2 begins replication in the upper respiratory tract, different symptoms of COVID-19 can occur ranging from asymptomatic to mild to severe. Dissemination of SARS-CoV-2 and rapid replication of SARS-CoV-2 in the lungs can result in severe cases of COVID-19, which can cause hyperactivation of the immune system causing increased inflammation, lung damage, and respiratory failure. However, SARS-CoV-2 does not have a single organotropism for pulmonary tissue, but can cause disease in other organ systems expressing ACE2 such as the cardiovascular, vascular, gastrointestinal, renal, as well as the central nervous system (4,9–14).

### **1.3 Immune responses against SARS-CoV-2 infection**

The body defends against foreign invaders using the innate and adaptive immune system. Typically, during viral infection, the first responder to the infection is the innate immune system. The innate immune system provides rapid, non-specific response to the pathogen by inhibiting entry of virus into the cell, destroying infected cells, triggering inflammation, and thereby slowing the establishment of infection and signaling for help of the adaptive immune system (15). Key innate immune features involved with SARS-CoV-2 infection include the induction of type I and type III interferon responses. Induction of interferons during the beginning of infection are

important to the severity of COVID-19. Limited or delayed interferon responses can result in severe, life-threatening COVID-19 disease (16). Therefore, due to the intrinsic ability of SARS-CoV-2 to avoid triggering anti-viral interferon responses, establishment of infection can manifest in severe COVID-19 symptoms in naïve individuals (16).

The adaptive immune system, on average, needs approximately 6-10 days after initial infection to generate antigen specific B and T cells to control and eliminate infection (17). Three main adaptive immune system components play a large role in eliminating SARS-CoV-2 infection: 1) CD4<sup>+</sup> T-cells 2) CD8<sup>+</sup> cytotoxic T-cells and 3) B-cells and antibodies. During viral infection, CD4<sup>+</sup> T-cells can function by activating cytotoxic T-cells, maturing B-cells, and triggering the release of anti-viral cytokines. CD8<sup>+</sup> T-cells, with the help of CD4<sup>+</sup> T-cells, can kill infected cells with the release of cytotoxic granules. CD4<sup>+</sup> T-cells can also differentiate into T follicular helper cells, which can promote the affinity maturation of B-cells and result in the production of SARS-CoV-2 specific antibodies that can help neutralize SARS-CoV-2. B-cells can also generate SARS-CoV-2 specific antibodies including IgM, IgG and IgA contributing to systemic and mucosal protection. Even though a majority of patients who are infected with SARS-CoV-2 generate antibodies against SARS-CoV-2, studies have shown that neutralizing antibodies during a primary infection does not likely contribute to reducing viral load and disease burden in infected patients (17–19).

Convalescent individuals that have recovered from COVID-19 develop memory against SARS-CoV-2. Immune memory cells acquired during infection such as memory CD4<sup>+</sup> T-cells, CD8<sup>+</sup>T cells and B-cells can be triggered during re-infection with SARS-CoV-2 and can persist at least up to 8 months post infection (20). T-cells play an important role in controlling and decreasing disease severity in acute SARS-CoV-2 infection; however, SARS-CoV-2 specific antibodies, particularly spike neutralizing antibodies, are necessary for protection against secondary infection (21).

#### **1.4 SARS-CoV-2 Variants of Concern**

One year after SARS-CoV-2 was discovered in Wuhan, China, strains of SARS-CoV-2 containing mutations on the spike protein were detected and began negatively impacting vaccine and therapeutic development for COVID-19. Reports of increased transmission, infectivity, and immune evasion arose due to the newly emerging strains. Thus, the World Health Organization (WHO) developed a system to classify and monitor variants of concern (VOC) of SARS-CoV-2. VOC are characterized as variants of SARS-CoV-2 harboring mutations that can cause increased transmissibility, probability of severe disease including hospitalization or death, evasion of neutralizing SARS-CoV-2 antibodies due to vaccination or infection, and lastly, decreased effectiveness of therapeutics, vaccines, treatments, and detection assays (WHO and CDC).

Throughout the two years of the pandemic, there has been 5 alarming SARS-CoV-2 VOC (Fig. 1). On December 2020, the WHO declared both Alpha (B.1.1.7) and Beta (B.1.351) as VOC (Fig.1). Alpha was first detected in the United Kingdom and contained two major concerning mutations on the spike protein, D614G and N501Y (RBD) (22). D614G mutation on the spike protein is known to increase viral replication, whereas the N501Y mutation on the RBD of spike protein allows the spike protein to bind with higher affinity to host receptors, promoting increased transmissibility (GAVI). Beta VOC was first discovered in South Africa, and harbors two additional mutations on the RBD compared to Alpha VOC, E484K and K417N (22). E484K and K417N mutations on the RBD increase the virus evasiveness from neutralizing antibodies generated against infection with the original strain or vaccination. Overall, Beta VOC did not have as high of frequency in the population as the Alpha variant, and eventually slowly disappeared from circulation (23). Approximately one year following the designations of Alpha and Beta VOC, the Gamma VOC was detected in Brazil in January 2021 (Fig.1). Similar to the Beta variant, the Gamma variant contained N501Y and E484K mutations on the RBD, but accumulated a key new mutation on the RBD, K417T, which promoted enhanced binding to host cells increasing transmissibility of the variant (22). As Alpha and Gamma were still in circulation in the population,

Delta was declared a VOC in May 2021 (Fig.1). Delta VOC was first detected in India and contained the same D614G mutation as the previous variants of concern; however, unlike the previous variants, Delta obtained three to four new mutations on the spike, and RBD protein such as P681R, L452R and T478K (22). P681R mutation on the spike protein can cause increased probability of severe disease, L452R mutation on the RBD was found to promote infectivity of the Delta variant, and mutation T478K on the RBD was responsible for enhanced immune evasion (22). As the world was recovering from the damage brought on by the Delta variant, Omicron emerged as the most current and dominant circulating variant of concern in November 2021 (Fig.1). Omicron was first detected in South Africa, and unlike the predecessor SARS-CoV-2 VOC, Omicron harbored more than 50 viral mutations, 30-40 mutations on the spike protein, and approximately 15 mutations on the RBD alone. These newly acquired mutations on the spike protein have made Omicron highly transmissible by increasing the ability of the variant to evade immune responses such as neutralizing antibodies generated from vaccination and previous infection with other strains of SARS-CoV-2 as well as approved monoclonal antibody therapeutics (24–29). Currently, Omicron has 5 lineages: BA.1, BA.2, BA.3, BA.4, and BA.5. Although BA.1 and BA.2 were the predominant circulating strains of Omicron in late 2021 into early 2022, currently BA.4 and BA.5 are the dominant global subvariants (30–33).



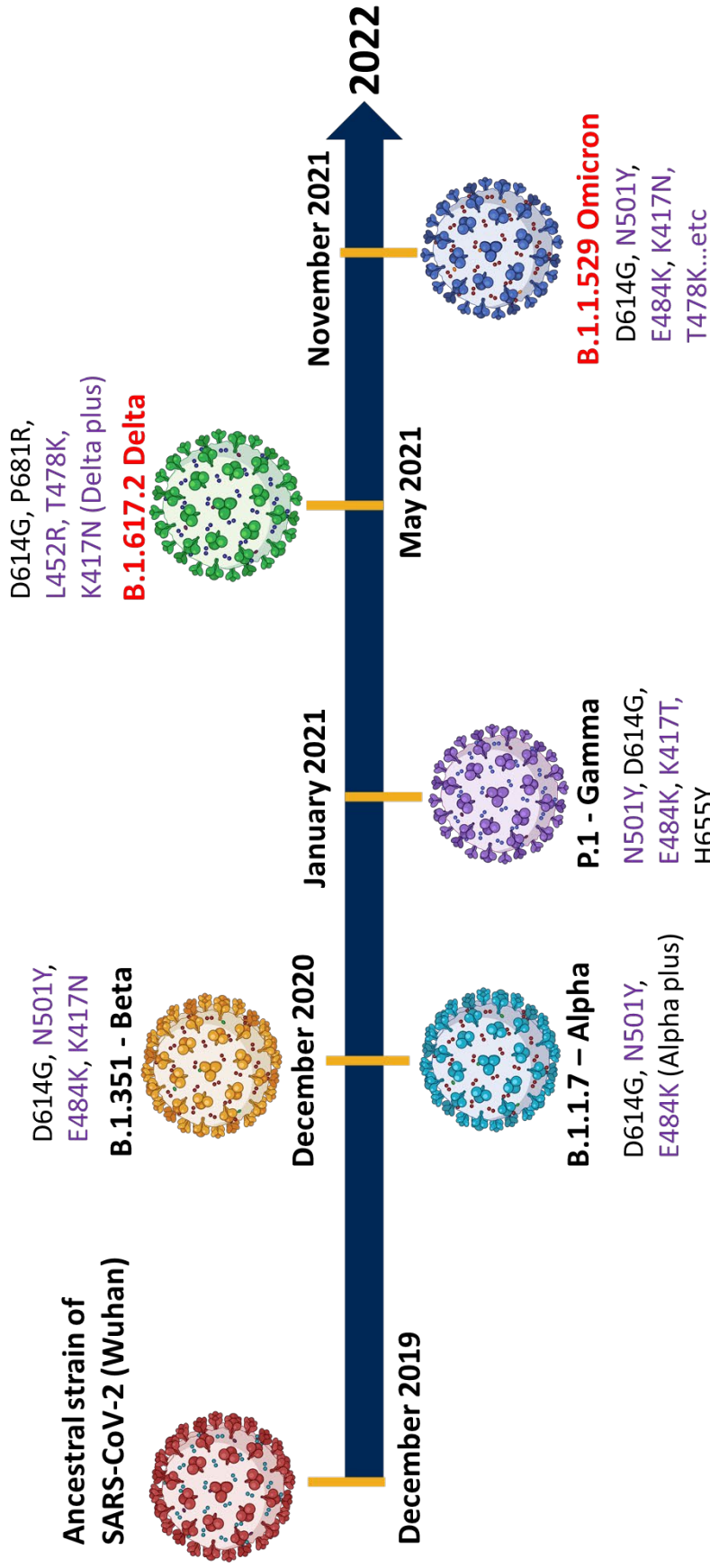


**Figure 1. Timeline of the emergence of SARS-CoV-2 variants of concern.** Amino acid changes in purple represents mutations on the RBD, black represents mutations on the spike protein. Red represents current predominant VOC.

## **1.5 COVID-19 Vaccines**

The WHO has approved eleven vaccines for Emergency Use Listing worldwide (Table 1). Vaccine platforms utilized include protein subunit, mRNA, non-replicating adenovirus, and inactivated virus all formulated with either the spike protein or inactivated virus from the ancestral strain of SARS-CoV-2. Thus far, non-replicating adenovirus vaccines such as Ad26.COV.S (Jansen), Vaxzevria (Oxford/AstraZeneca), Covishield (Serum Institute of India), and Convidecia/Ad5-nCoV (CanSino) have been approved in 310 countries, making the adenovirus COVID-19 vaccines the most widely approved COVID-19 vaccine platform in the world. Closely following adenovirus-based vaccines, mRNA vaccines including Comirnaty (Pfizer/BioNTech) and Spikevax (Moderna) have approval in 232 countries and are FDA approved in the United States. After mRNA vaccines, inactivated viral vaccines such as Bharat Biotech Covaxin, Sinopharm Covilo, and Sinovac CoronaVac are approved for use in 161 countries. Lastly, protein subunit vaccines developed by Novavax (Nuvaxovid) or manufactured by the Serum Institute of India (COVOVAX) have been granted approval in 43 countries.

### **1.5.1 Non-replicating adenovirus COVID-19 vaccines.**

Adenovirus vectors have been historically used for gene therapy; however, advancement of adenovirus vector technology has allowed for the application of adenoviruses in vaccines and cancer immunotherapies (34). Adenovirus vectors used for COVID-19 vaccines are attenuated DNA viruses most commonly originating from humans or chimpanzees with the genes responsible for replication removed and substituted with target genes of interest such as the spike protein. Vaccine adenovirus vectors function by infecting host cells and incorporating the gene encoding spike protein into the nucleus of the cell which is transcribed into mRNA to eventually produce the spike protein. Ad.26.COV2-S utilizes a non-replicating human adenovirus serotype 26 as the vector to express the pre-fusion stabilized spike protein of ancestral SARS-CoV-2 (35). Phase 3 clinical trials showed that a single dose of Ad.26.COV2-S exhibited 66.9% vaccine efficacy against moderate to severe COVID-19 14 days post vaccination and 66.1% vaccine efficacy 28

days post vaccination (36). At the time of the phase 3 clinical trial, Beta was the predominant variant amongst clinical trial participants (86 out of 91 cases) in South Africa (36). Additionally, ChAdOX1-nCoV (Vaxzevria), unlike Jansen's vaccine utilizes a chimpanzee adenoviral vector. Similar to Ad.26.COV2-S, ChAdOX1-nCoV also expresses the ancestral spike protein; however, without S2 stabilizing mutations (37). In phase 3 clinical trials, two doses of ChAdOX1-nCoV resulted in 74% vaccine efficacy against mild COVID-19 (38). However, genomic sequencing of SARS-CoV-2 samples in the participant pool revealed a low frequency of variants of concern (38). Nevertheless, recent studies assessing ChAdOX1-nCoV protection against severe COVID-19 caused by the Delta variant showed a 90% vaccine efficacy after two doses of ChAdOX1-nCoV (39). The most recent WHO approved vaccine, Convidecia/Ad5-nCoV (CanSino) utilizes a non-replicating human adenovirus 5 to express the full-length spike protein (35). Phase 3 clinical trials demonstrated that one dose of Convidecia/Ad5-nCoV resulted in 57.5% efficacy against mild COVID-19 and 90% effectiveness against severe COVID-19 (40). Omicron, Alpha and the ancestral strain were detected in the Convidecia/Ad5-nCoV phase 3 clinical trial (40). The advantages provided by adenoviral vaccines include thermostability, ease of scalability, and the ability for the vector to induce a robust immune response (35). However, disadvantages to adenoviral vector vaccines include previous immunity generated from human adenoviruses limiting immunogenicity of the vaccine, as well as thrombocytopenia, a rare but serious side effect induced by vaccination (35,41).

### **1.5.2 mRNA COVID-19 vaccines.**

The COVID-19 pandemic provided the first opportunity for mRNA vaccines to be used in humans. The contribution of multiple scientists and over 30 years of research has culminated in the rapid development and rollout of COVID-19 mRNA vaccines (42). Development of mRNA vaccines began in the 1980s with the synthesis of mRNA in the laboratory along with the utilization of lipids to deliver mRNA (43). Advancements in the stabilization of mRNA progressed into the first pre-clinical studies in mice with cancer mRNA therapy, and mRNA vaccines for influenza in the 1990s

(44). In the early 2000s, methods were developed to manufacture lipid nanoparticles which eventually lead to the first lipid nanoparticle mRNA vaccines for influenza in clinical trials in 2015 (43). Other mRNA based vaccines that were also developed and evaluated in clinical trials include vaccines against HIV, rabies, and Zika (45).

Current approved COVID-19 mRNA vaccines developed by Pfizer/BioNTech (46) and Moderna (47) are formulated with mRNA encoding pre-fusion spike protein from the ancestral strain of SARS-CoV-2 encapsulated within lipid nanoparticles (LNPs). COVID-19 mRNA vaccines utilize LNP delivery systems to protect mRNA from degradation and to promote entry into the host cell. Once inside the host cell, mRNA is transcribed into the spike protein and is expressed on the surface of the cell where they are displayed to antigen presenting cells to initiate immune responses. In clinical trials, two doses of either Pfizer/BioNTech or Moderna mRNA vaccines provided high vaccine efficacy (over 95%) against the Delta variant; however, vaccine efficacy sharply dropped against the Omicron variant to 65.5% and 75.1% respectively, decreasing rapidly in efficacy over time after the second dose. The third dose of either Pfizer/BioNTech or Moderna mRNA vaccines provided an increase in vaccine efficacy to 67.7% and 73.9% respectively (48). Ten weeks after the third dose, Pfizer/BioNTech mRNA vaccine efficacy waned from 67.7% to 45.7%, whereas Moderna mRNA vaccine efficacy dropped from 73.9% to 64.4% after five to nine weeks following the third dose against Omicron infection (48). Advantages of mRNA vaccine technology include safety of the vaccine, speed of producibility and scalability in cell free bioreactors as well as the ability to express multiple antigens at once within one vaccine. However, despite many doses of mRNA vaccines distributed world-wide, cold-chain requirements for mRNA vaccines deter distribution to low-income countries.

### **1.5.3 Protein subunit vaccines**

In general, protein subunit vaccines are considered to be the conventional method of immunization. Protein-based vaccines can include full or subunits of proteins that can be assembled on nanoparticles, virus-like particles (VLPs), or carrier proteins. Typically, most

protein-based vaccines are adjuvanted to enhance antigen specific immune responses. Despite the common use of protein vaccines, there is only one COVID-19 protein subunit vaccine, Nuvaxovid/COVOVAX, that has been currently approved by the WHO. Nevertheless, there are over 46 protein-based vaccines in clinical development (49). Unlike mRNA or adenovirus vaccines, Nuvaxovid/ COVOVAX is composed of ancestral strain full-length spike protein produced in insect cells. The spike protein is displayed on nanoparticles, and adjuvanted with Matrix-M, a saponin extracted from soap bark trees (50–52). In phase 3 clinical trials, two doses of Nuvaxovid resulted in 100% protection against COVID-19 caused by non-variants of concern of SARS-CoV-2 and demonstrated 92.6% vaccine efficacy against primarily the Alpha variant which was the predominant variant at the time of the study (51). Regardless of the slower development period of protein-based vaccines for COVID-19, this platform offers advantages such as: familiarity with the platform, safety amongst immunocompromised individuals, and thermostability (53). However, there are disadvantages including longer development to implementation periods of the vaccine into the population compared to adenovirus and mRNA platforms.

#### **1.5.4 Inactivated SARS-CoV-2 vaccines**

Over 11 billion COVID-19 vaccines have been distributed worldwide (54). Despite only approved for use in 160 countries, approximately 5 billion of inactivated SARS-CoV-2 vaccines have been administered globally. (54). Currently, CoronaVac developed by Sinovac, leads in the most vaccines distributed and used world-wide with almost 2.5 million doses allocated (54). Approved inactivated SARS-CoV-2 vaccines are developed by chemically inactivating live ancestral SARS-CoV-2 with beta-propiolactone, and adjuvanting the dead virus with aluminum hydroxide (55,56). Vaccine efficacy of CoronaVac, Covaxin, and Covilo showed 81.3%, 93.4%, and 79% respectively against severe COVID-19 after two doses (57–59). Advantages of using inactivated virus vaccines include speed of development and ease of manufacturing, thermostability which allows vaccines to be distributed to low-income countries, and capability of administration to

immunocompromised individuals (60). Similar to mRNA, adenovirus and protein based COVID-19 vaccines, inactivated SARS-CoV-2 have demonstrated waning vaccine efficacy against the Omicron variant of SARS-CoV-2. However, due to increased immune evasion of Omicron towards inactivated vaccines, different boosting strategies with other vaccine platforms such as mRNA, are recommended for protection against VOC (25,61).

## WHO approved COVID-19 vaccines

Company	Type	Countries approved
Moderna (mRNA-1273)	mRNA-spike	86
Pfizer-BioNTech (BNT162b2)	mRNA-spike	146
Oxford/Astrazeneca/ SII Covishield	Adenovirus - spike	140/49
Janssen (Ad26.COV2.S)	Adenovirus - spike	111
CanSino (Convidecia/Ad5-nCoV)	Adenovirus - spike	10
Novavax/ SII COVOVAX	Recombinant protein - spike adjuvanted with Matrix M	38/5
Bharat Biotech (Covaxin)	Inactivated SARS-CoV-2 with Alum adjuvant	14
Sinopharm (Covilo)	Inactivated SARS-CoV-2 with Alum adjuvant	91
Sinovac (CoronaVac)	Inactivated SARS-CoV-2 with Alum adjuvant	56

**Table 1: Eleven WHO approved COVID-19 vaccines.**

## 1.6 Adjuvants for COVID-19 vaccines

Currently, there are a variety of adjuvants used for approved intramuscular vaccines as well as new adjuvants that are being developed to help stimulate a safe and robust immune response. Conventionally, adjuvants are utilized in vaccine formulations to enhance the immunogenicity of the candidate vaccine antigen, promote longevity of the vaccine response, and provide dose sparing for vaccine antigens. Current approved adjuvant platforms traditionally used in intramuscular protein subunit vaccines or inactivated vaccines include Alum, oil in water emulsions, lipid A, Cytosine phosphoguanosine (CpG), and the AS0 adjuvant systems (AS01, AS03, and AS04). Thus far, approved COVID-19 vaccines have utilized adjuvants such as LNPs for mRNA vaccines as well as saponin or Matrix M used by Novavax. However, COVID-19 vaccines under pre-clinical as well as clinical development have utilized other adjuvants to enhance vaccine responses. Here, common adjuvants used for vaccine development and novel vaccine adjuvant platforms are discussed.

### 1.6.1 Alum

Aluminum hydroxide or Alum is the most frequently used adjuvant in vaccines. Alum has been used in vaccine formulations to prevent bacterial, viral, or parasitic diseases such as Diphtheria, Tetanus, Pertussis, *Haemophilus influenzae*, human papillomaviruses (HPV), Japanese encephalitis, bacterial meningitis, *pneumococcus*, shingles, SARS-Cov-2, and malaria. In general, Alum stimulates a strong antibody mediated response through mechanisms such as triggering tissue damage through the induction of uric acid activation of dendritic cells to promote a Th2 facilitated response (62,63). Alum also can cause the release of neutrophil extracellular traps. The DNA released from neutrophils can also help mediate a Th2 induced humoral response (64,65). Currently, alum adjuvants are used in WHO approved inactivated viral vaccines, as well as protein subunit and virus like particle vaccines adjuvanted with alum are being evaluated in pre-clinical studies. Studies performed in mice demonstrated that alum adjuvanted COVID-19 vaccines generated increased neutralizing antibody titers (66).



### 1.6.2 Toll like receptor agonist

Toll-like receptors (TRLs) are pattern recognition receptors located either on the cell surface (TLR1, TLR2, TR4, TLR5, TLR6) or in endosomes (TLR3, TLR7, TLR8, and TLR9) (15). TLRs are most commonly found on innate immune cells such as dendritic cells, monocytes, macrophages and neutrophils, and play an important role in recognizing pathogen-associated molecular patterns (PAMPs), such as lipid polysaccharides (LPS) for Gram-negative bacteria or nucleic acid (15). Overall, activation of TLRs with appropriate PAMPs can trigger the release of pro-inflammatory cytokines that can stimulate the immune response to the pathogen. Therefore, adjuvant platforms that utilize the activation of TLRs can help stimulate the appropriate cellular and humoral immune responses to vaccine antigens. Adjuvants such as Monophosphoyl lipid (MPL) and CpG are agonist for TLR4 and TLR9 respectively.

MPL is a low toxicity lipid A derived from the LPS of *Salmonella*. Since MPL is a TLR4 agonist, it can activate antigen presenting cells such as dendritic cells to elicit a pro-inflammatory Th1 driven immune response (67). In licensed vaccines, MPL is formulated with the AS0 adjuvant systems developed by GlaxoSmithKline (68). In the adjuvant system AS04, MPL is adsorbed to alum. AS04 is used in licensed vaccines for hepatitis B (HBV) and HPV and studies have demonstrated that the addition of MPL to alum generated improved vaccine efficacy in the HPV and HBV vaccines, increased antibody response to pathogen, and increased longevity of the vaccine immune response compared to alum alone (62,68). MPL is also combined in the adjuvant system AS01 with saponin (QS-21) and delivered in liposomes (69). AS01 is currently used in vaccine formulations for shingles in older adults (70). Together, MPL and QS-21 provide synergistic affects when administered together and can promote both a strong cellular and functional antibody response (70). TLR4 agonist adjuvants can enhance the immune response of a vaccine by generating robust cellular and antibody responses. However, few methods exist for developing novel TLR4 agonists that can be used as safe and efficacious adjuvants in vaccines. Bacterial Enzymatic Combinatorial Chemistry (BECC) is a novel method developed to generate lipid A

mimetics that are TLR4 agonist by harnessing LPS on Gram-negative bacteria. In general, BECC generates TLR4 agonists by reprogramming the lipid A biosynthesis pathway in Gram-negative bacteria by the addition of exogenous or removal of endogenous lipid A modifying enzymes under different temperature conditions (71). The BECC method provided two candidate lipid A mimetics, BECC438 and BECC470, that could be used as vaccine adjuvants. Pre-clinical studies in murine models have demonstrated that BECC adjuvants improved the vaccine efficacy in protein subunit vaccines for both bacterial and viral pathogens such as *Yersinia pestis*, *Bordetella pertussis*, *Staphylococcus aureus*, HPV, influenza A, and SARS-CoV-2 (72–75). Both BECC438 and BECC470 elicited a balanced cellular and functional antibody driven response to the vaccine antigen overall improving vaccine efficacy.

Lastly, CpG is a TLR9 agonist adjuvant that has been used in licensed vaccines such as Heplisav, to prevent HBV infections. When formulated in vaccines, CpG induced a Th1 skewed response that can stimulate the activation of B and NK cells (62). CpG, similar to MPL, can be used in combination with other adjuvants such as alum to increase immunogenicity of the vaccine response. SARS-CoV and MERS-CoV vaccine studies with CpG and alum showed increased production of neutralizing antibodies and stimulated robust cellular response (76,77). Additionally, CpG has been used in a two-dose virus like particle SARS-CoV-2 vaccines that are currently in phase 1 clinical trials (78).

### **1.6.3 Oil in water adjuvants**

Oil in water adjuvants have been commonly used in vaccines to increase immunogenicity. MF59, Montanide ISA 51, ISA 720 and AS03 are all oil in water adjuvants that have been used in human vaccine clinical trials. Particularly, MF59 is utilized in licensed influenza vaccines for the elderly (Fluad) as well as for the pandemic influenza vaccines (79). The composition of MF59 includes squalene obtained from shark liver, and the surfactants Tween 80 and Span 85 combined into oil droplets. MF59 functions to stimulate the recruitment of antigen presenting cells to the injection site leading to enhanced antigen uptake and trafficking into the draining lymph nodes, resulting

in the activation of B and T-cells. Vaccines formulated with MF59 stimulate a strong CD4+ T-cell response that can overall promote the production of affinity matured functional antibodies as well as enhance the durability of the antibody responses compared to alum. Additionally, studies have demonstrated that MF59 can limit the amount of antigen needed to mount an immunogenic response. MF59 has been used in vaccine formulations for SARS-CoV and MERS in pre-clinical studies which demonstrated that the addition of MF59 to spike protein induced elevated levels of neutralizing antibodies as well as stimulated both CD4 and CD8 T-cell responses (66). Currently, pre-clinical studies are underway evaluating SARS-CoV-2 inactivated and protein subunit vaccines adjuvanted with MF59 (66).

The COVID-19 pandemic has emphasized the on-going global vaccine disparity. As a result of the vaccine disparity, developing countries have less access to vaccines to prevent infectious diseases. The establishment of non-profit companies such as the Vaccine Formulation Institute (VFI) in Switzerland allowed for the focus on providing adjuvants, vaccine adjuvant research, and pre-clinical vaccine development to aid developing countries, as well as to offer open access to available adjuvants to the vaccine community (80). VFI developed a squalene in water emulsion (SWE) adjuvant similar to MF59 to aid in the global distribution and development of vaccines. Together with Seppic, they have generated and manufactured Good Manufacturing Practice (GMP) grade SWE that is open access to the vaccine community. SWE similar to MF59 is composed of squalene, and surfactants sorbitan trioleate similar to Span 85, and polyoxyethylene sorbitan monooleate. SWE has been utilized in pre-clinical studies evaluating vaccine candidates for both bacterial and viral pathogens such as Polio, Influenza, RSV, Rabies, SARS-CoV-2 and group A *Streptococcus* (81–85). COVAC-2, a SARS-CoV-2 protein subunit vaccine formulated with S1 protein and SWE, is of the first COVID-19 vaccine adjuvanted with SWE to enter phase 1/2 clinical trials (86,87).

## 1.7 Vaccine nanoparticles and carrier proteins

Nanoparticles are utilized in vaccine formulations as antigen delivery systems that can enhance the immunogenicity of candidate vaccine antigens. In general, antigens can be delivered on the surface of the nanoparticle or encapsulated within the nanoparticle. Nanoparticle material can include lipid nanoparticle (LNP), virus-like particle (VLP), protein, polymer, micelle, and liposomes with each nanoparticle possessing a unique method of displaying and delivering vaccine antigen (88). WHO approved COVID-19 vaccines that utilize the nanoparticle delivery system include Moderna and Pfizer-BioNTech mRNA vaccines (LNPs) and Novavax protein subunit vaccine (Micelle). LNPs are commonly used to deliver nucleic acid encoding vaccine antigen such as the mRNA COVID-19 vaccines in order to help prevent the degradation of the nucleic acid. The LNP also holds immunostimulatory properties and can act as an adjuvant to increase immunogenicity of nucleic acid vaccines. Other than Moderna and Pfizer-BioNTech mRNA COVID-19 vaccines which are WHO approved, there are approximately 14 additional nucleic acid derived COVID-19 vaccines in clinical trials (88). The Micelle delivery system is currently used by the Novavax protein subunit vaccine, Nuvaxovid to display the full-length spike protein. Micelles are normally derived from amphiphilic compounds, such as Tween 80 used by the novavax vaccine, and allows for the presentation of antigens in their native conformations (88).

VLPs are another vaccine antigen delivery platform that have been used in COVID-19 vaccine development. VLPs are viral structural proteins utilized to display vaccine antigen. Homologous antigen display (same antigen) on the VLP can elicit highly specific neutralizing antibodies against the displayed antigen whereas heterologous display on the VLP (multiple antigens) can allow for the induction of more cross-reactive B-cells which can lead to increased breadth of neutralizing antibodies against multiple variant types (88). Furthermore, there are over five COVID-19 VLP vaccines in clinical trials and numerous VLP vaccine being evaluated in pre-clinical studies. The company Medicago has developed a Coronavirus-like particle vaccine (CoVLP) produced in plants that displays the pre-fusion spike protein adjuvanted with AS03 which has completed phase

3 clinical trials (89). Additional VLP vaccines in clinical trials include RBD antigen displayed on Hepatitis B surface antigen (HBsAg) using SpyBiotech SpyTag/SpyCatcher technology. SpyTag and SpyCatcher is a protein conjugation system derived from *Streptococcus pyogenes* and allows for the spontaneous conjugation of the vaccine antigen to the surface of the VLP (90). SpyTag is located on the vaccine antigen and the SpyCatcher is on the surface of the VLP, together this conjugation system can display antigen in high density on the VLP increasing the immunogenicity of the vaccine antigen (84). The RBD HBsAg VLP vaccine was developed by the Serum Institute of India and is in Phase 1/2 clinical trials in Australia (91).

Similar to VLPs, vaccine antigens can also be displayed on bacterial carrier proteins. Carrier proteins are commonly used for polysaccharide vaccines against encapsulated bacteria to induce a T-cell dependent response. Licensed carrier proteins include, diphtheria toxoid, tetanus toxoid, CRM<sub>197</sub>, and Haemophilis protein D (92). Particularly, CRM<sub>197</sub>, is a detoxified diphtheria toxin and has been used in licensed vaccines for *Haemophilis influenzae*, *Streptococcus pneumoniae*, and *Neisseria meningitidis*. Additionally, FinaBio has developed an *E. coli* expression system to increase manufacturability of CRM<sub>197</sub> and has been used to as a carrier protein for not only encapsulated bacteria but also for viral proteins and bacterial peptides (93,94). Therefore, similar to VLPs, protein-based vaccine antigens conjugated to bacterial carrier proteins can increase immunogenicity to the vaccine antigen by increasing the number of antigens displayed on the carrier protein compared to the soluble form of the protein.

### **1.8 COVID-19 vaccine immunological correlates of protection**

Generally, there are three types of immunity against COVID-19: 1) convalescence after SARS-CoV-2 infection, 2) vaccine mediated immunity, and 3) hybrid immunity, a combination of both immunity from infection and vaccination. Generation of immunity to COVID-19 could result in protection from SARS-CoV-2 infection, severe disease, hospitalization, and death. In order to evaluate immunological protection, types of immune responses are measured to assess the contribution of the response to protection, defined as an immunological correlate of protection.

Generation of neutralizing antibodies and binding antibodies against SARS-CoV-2 are key components of protection of the three types of immunity. Convalescence after SARS-CoV-2 infection can elicit SARS-CoV-2 specific antibody responses dominated by mucosal IgA at the site of infection such as in the upper respiratory tract which includes the nasal cavity, pharynx, and trachea, as well as induce a systemic antibody response dominated by serum IgG transported to the lower respiratory tract such as the lung (Fig. 2A)(41). Intramuscular vaccine mediated responses are driven by robust systemic IgG production; however, lack induction of mucosal IgA in the upper respiratory tract (Fig. 2B)(41). Lastly, hybrid immunity or vaccine break through immunity caused by infection and vaccination, or vaccination and infection lead to the generation of both mucosal IgA due to infection and systemic IgG responses caused by both vaccination and infection (Fig. 2C)(95). Additionally, cellular responses such as CD4<sup>+</sup> and CD8<sup>+</sup> T cell responses also contribute to limiting the severity of disease(17). Studies performed in non-human primates demonstrated that polyclonal antibodies from convalescent rhesus macaques were able to protect against SARS-CoV-2 challenge in a dose dependent manner without the assistance of cellular immune responses (96). Also in the same study, depletion of CD8<sup>+</sup> T-cells in convalescent rhesus macaques with waning SARS-CoV-2 antibody titers decreased protection against SARS-CoV-2 challenge in the upper respiratory tract (96). For vaccine mediated immunity, neutralizing antibodies also play a large role in protection. Passive immunization studies conducted in non-human primates showed that polyclonal antibodies obtained from rhesus macaques immunized with Moderna mRNA-1273 COVID-19 vaccine protected hamsters from SARS-CoV-2 challenge (97). Human vaccine studies demonstrated the importance of neutralizing and binding IgG antibodies against spike and RBD to protection with the ChAdOx1 nCoV-19, Moderna mRNA-1273, and Pfizer Bio-N-Tech BNT162b2 COVID-19 vaccines (98,99). Furthermore, hybrid immunity, denoted by SARS-CoV-2 infection before COVID-19 vaccination, or vaccine break through immunity described as SARS-CoV-2 infection after COVID-19 vaccination offered the highest levels of neutralizing antibody titers against SARS-CoV-2 when compared to vaccine

mediated only and convalescent responses. Studies concluded that hybrid and vaccine break through immunity provided increased breadth, potency, and longevity of neutralizing antibody responses against SARS-CoV-2 (100,101). Overall, neutralizing antibodies generated against SARS-CoV-2 are the main correlate of protection for immunity against SARS-CoV-2 infection (102). More immune correlates of protection to SARS-CoV-2 are currently being investigated, such as T-cell responses and other functional antibody roles including antibody mediated complement activation and other Fc mediated effector functions (103,104).

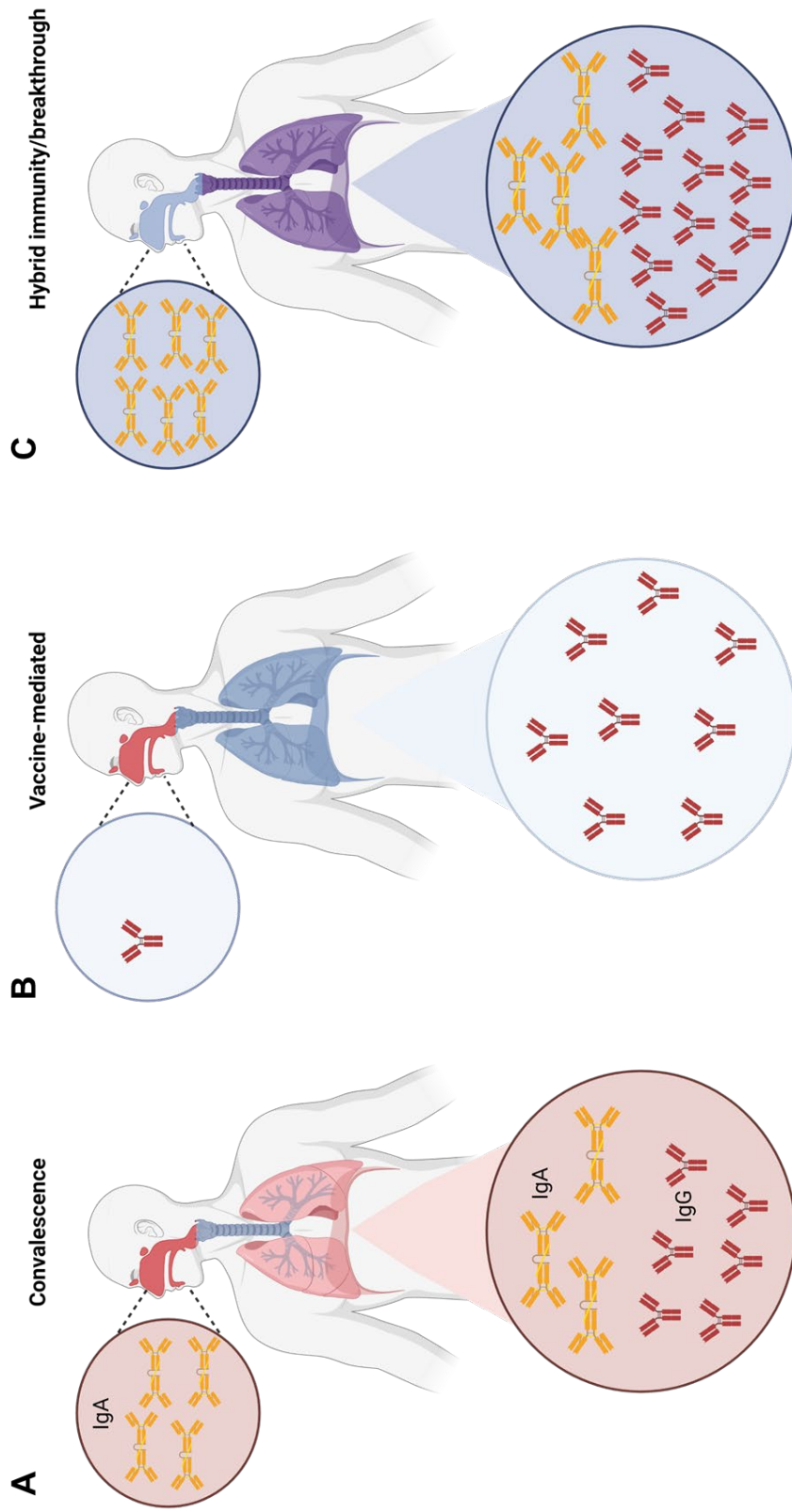


**Figure 2. Types of SARS-CoV-2 immunity.** A) SARS-CoV-2 convalescent immunity B) Intramuscular vaccine mediated immunity C) Immunity acquired through infection and vaccination (hybrid) or vaccination and infection (vaccine breakthrough).



## **1.9 Animal models to study COVID-19**

Animal models provide a pre-clinical avenue to study SARS-CoV-2 pathogenesis, transmission as well as vaccine and therapeutic efficacy. Animal models offer advantages such as control over variables in the study; for example, time frame of study, virus dose used in animals, and ability to assess and necropsy all tissue samples. However, there are also disadvantages in using animal models, including animals used not reciprocating similar disease or immune phenotypes observed in humans. Mice, hamsters, ferrets, and non-human primates (NHPs) currently represent the models that have been most frequently utilized to study SARS-CoV-2 (Fig. 3) (105).

### **1.9.1 Mice**

Utilizing mouse models to study SARS-CoV-2 have been useful to evaluate pathogenesis of SARS-CoV-2 as well as to examine vaccine and therapeutic efficacy. However, conventional wild-type inbred, and outbred mice strains cannot be used as a lethal SARS-CoV-2 challenge model because these mice lack the human ACE2 receptor needed for SARS-CoV-2 infection. Previous studies have shown that the ancestral strain of SARS-CoV-2 could not bind to the mouse ACE2 receptor and that wild-type mice were not susceptible to ancestral SARS-CoV-2 challenge (106–108). However, with the emergence of SARS-CoV-2 variants of concern, studies have shown that the Alpha and Beta variants of concern could bind to mouse hACE2, replicate in the in the lung and trachea to high viral RNA burden, and cause pathological damage to the upper and lower respiratory tract (109,110). Despite the ability of the SARS-CoV-2 variants of concern to bind to mouse ACE2 receptor, wild-type mice do not become morbid, show drastic weight or temperature loss, or demonstrate outward disease manifestations (111). Nevertheless, a lethal challenge model would be ideal to evaluate protection against SARS-CoV-2 challenge.

Therefore, transgenic mice that expressed human ACE2 were used to establish a lethal challenge mouse model of SARS-CoV-2 to evaluate vaccine and therapeutic efficacy. The most widely used lethal transgenic mouse model is the K18-hACE2 (B6. Cg-Tg (K18-ACE2)2PrImn/J) mice developed by McCray and Perlman to originally study SARS-CoV challenge since both viruses

utilized the same human ACE2 receptor for infection. The K18-hACE2 mice utilize the human keratin 18 promoter to express human ACE2 in epithelial cells including in the lung, liver, kidney, brain, heart, and the gastrointestinal tract (112–114). K18-hACE2 mice intranasally challenged with SARS-CoV-2 resulted in morbidity, demonstrating severe weight and temperature loss, lack of grooming and hunched appearance, lethargic activity, eye closure, and rapid or slowed respiration (75,115,116). Lethality in the K18-hACE2 model could be contributed to the viral dissemination into the brain. Overall, the K18-hACE2 mouse model provides a lethal SARS-CoV-2 challenge model that can be used to measure overall vaccine protection and therapeutic efficacy. However, due to the high expression of human ACE2 in the K18-hACE2 mouse, this model does not recapitulate the disease observed in humans, in particular, the lethal brain infection. Other human ACE2 transgenic mouse models to study SARS-CoV-2 infection include the lethal AC70 transgenic mouse lineage utilizing a cytomegalovirus immediate early enhancer and chicken  $\beta$ -actin promoter to express human ACE2 (117), and the non-lethal mouse ACE2 promoter human ACE2 transgenic mouse model (118).

### **1.9.2 Syrian Hamsters**

In contrast to the human ACE2 transgenic mouse model, the Syrian hamster model is not a lethal model of SARS-CoV-2 infection and portrays a similar respiratory disease phenotype as humans. Studies have demonstrated that SARS-CoV-2 spike protein can bind to Syrian hamster ACE2 to initiate infection, thus not needing further genetic altering to express human ACE2 (119). Intranasal challenge with SARS-CoV-2 in Syrian hamsters resulted in initial weight loss of the hamsters, elevated viral replication in the respiratory tract, and histopathology in the lungs; however, due to the mild to moderate disease outcomes, hamsters usually recover from infection after 2 weeks post challenge. Furthermore, unlike the mouse challenge models, Syrian hamsters can be used to evaluate transmission of SARS-CoV-2 which can be beneficial for vaccine and therapeutic studies (120–122). Conversely, even though Syrian hamsters are a useful tool to

study SARS-CoV-2 transmission and evaluate vaccine and therapeutic efficacy, research using the hamster model is restricted due to the lack of reagents for immunological analysis (105).

### **1.9.3 Ferrets**

Ferrets share similar disease outcomes during SARS-CoV-2 infection compared to humans. Similar to hamsters, SARS-CoV-2 can bind to ferret ACE2 receptor and infect cells. Intranasal SARS-CoV-2 challenge in ferrets result in similar clinical symptoms as in humans such upper respiratory symptoms including runny nose, wheezing, and sneezing. Other symptoms similar to human COVID-19 shown in ferrets also include lethargy and diarrhea. Viral replication in ferrets is maintained in the upper respiratory tract particularly in the nose and oropharynx, with limited lung pathology (105). Interestingly, ferrets have been historically used to study transmission in respiratory viruses such as influenza; therefore, this model of transmission has also been applied to study SARS-CoV-2 transmission (123). Studies have demonstrated that ferrets can transmit SARS-CoV-2 to non-challenged ferrets through direct contact as well as their aerosolized particles (124,125). Overall, ferrets are a robust model to study SARS-CoV-2 in the context of vaccine break through cases, and transmission.

### **1.9.4 Non-human primates**

Non-human primates have been an important model used to evaluate vaccine and therapeutic efficacy before entering human clinical trials. Rhesus macaques, cynomolgus macaques, and African green monkeys are the most frequently used non-human primates to study COVID-19. SARS-CoV-2 challenge studies performed in rhesus macaques demonstrated that disease outcomes were similar to mild to moderate COVID-19 observed in humans (126,127). Rhesus macaques challenged with SARS-CoV-2 showed viral shedding in the nose, viral replication in both the upper and lower respiratory tract, as well as mild lung histopathology (126,128). Cynomolgus macaques provided a asymptomatic model for SARS-CoV-2 infection, showing limited clinical symptoms, viral shedding from the nasal and oral pharynx, and replication in both

the upper and lower respiratory tract (129). Lastly, the African green monkey model established a severe COVID-19 phenotype, supported by higher viral replication in the respiratory tract compared to rhesus macaques and cynomolgus macaques, as well as developed substantial viral pneumonia (130). Furthermore, COVID-19 vaccine efficacy studies have utilized the rhesus macaque as the primary non-human primate model. Pfizer-BioNTech (131), Moderna (132), and Oxford/AstraZeneca (133) as well as other vaccine platforms have evaluated their vaccine candidates in rhesus macaques before entering clinical trials or simultaneously during clinical trials (134–136).

### **1.10 SARS-CoV-2 mucosal immune response**

The mucosal immune system is derived from mucosa-associated lymphoid tissue (MALT) which is composed of three main compartments in humans: 1) gut associated lymphoid tissue (GALT), 2) nasopharynx lymphoid tissue and tonsils (NALT) and 3) bronchus associated lymphoid tissue (BALT) (137). In general, these mucosal lymphoid tissues are comprised of induction sites where antigens from a pathogen or vaccine are sampled by microfold cells, processed by antigen presenting cells such as dendritic cells in order to stimulate T-cells which can help promote the activation of IgA secreting B-cells. The mucosal induction sites such as the NALT are composed of two major zones: 1) follicle and 2) parafollicular zone (137). The follicle zone largely contains germinal center B cells whereas the parafollicular zone is comprised of T cells and dendritic cells. In the follicle zone, mucosal B-cells in the germinal centers undergo T-cell dependent B-cell somatic hypermutation and class switch recombination favoring IgA (137). After activation in the induction sites, B and T-cells then travel to effector mucosal tissue sites, for example the nasal cavity in the upper respiratory tract, where antigen specific T-cells can help B-cells further differentiate into IgA secreting plasma cells to help alleviate infection (138). Since SARS-CoV-2 is a respiratory pathogen, induction of the mucosal immune response mostly relies on the NALT and tonsils in humans, and NALT in rodents. The BALT contributes little to mucosal immunity in

humans, since BALT is rarely present adults and only present during childhood and/or adolescence.

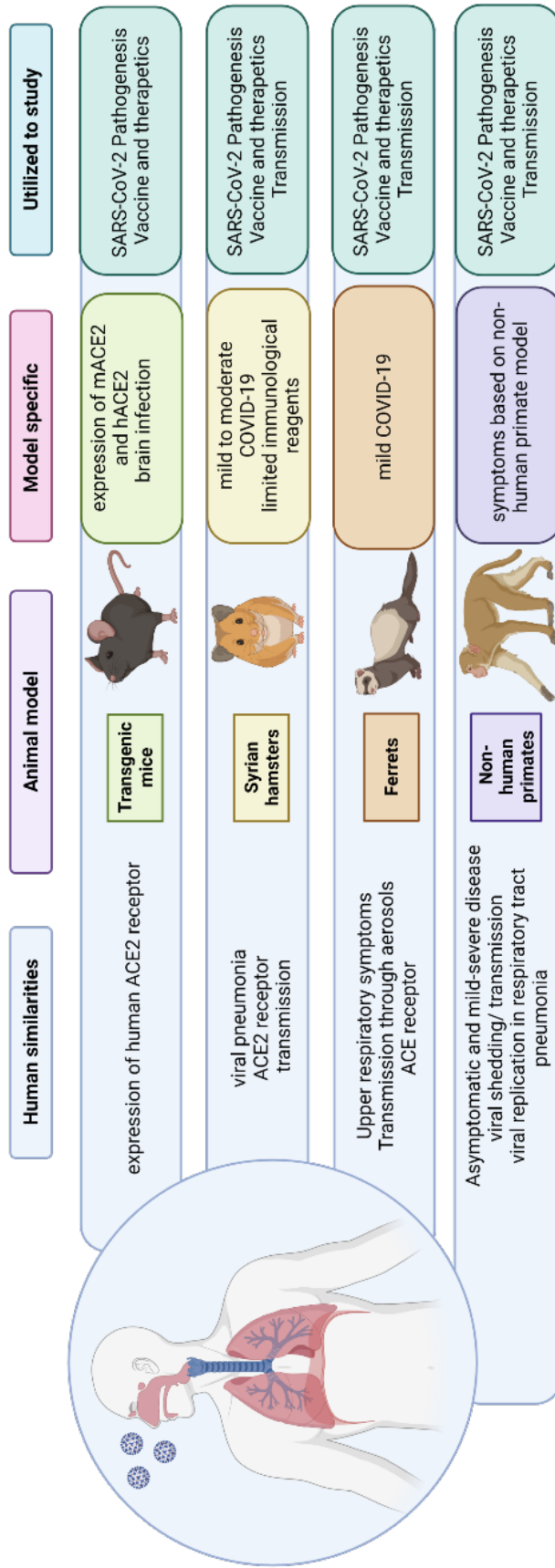


**Figure 3. Summary of animal models used to study SARS-CoV-2.**

The antibody response in the respiratory tract is composed heavily of secretory IgA in the upper respiratory tract and IgG in the lower respiratory tract. Secretory IgA plays an important role in the mucosal immune response towards respiratory pathogen infection or vaccination. Functions of secretory IgA in the mucosae include removal of foreign antigen, neutralization, and agglutination. In the upper respiratory tract, secretory IgA is the predominant immunoglobulin accounting for approximately 70% of the immunoglobulin pool whereas IgG accounts for approximately 80% in the lung (137). Furthermore, mucosal lymphoid tissue is responsible for eliciting the majority of secretory IgA in the upper respiratory tract while IgG found in the lower respiratory tract comes from systemic circulation (137). Overall, SARS-CoV-2 infection generates the production of both secretory IgA and IgG in the respiratory tract; however, during intramuscular COVID-19 vaccination only, there is a robust production of systemic IgG but limited induction of secretory IgA in the upper respiratory tract (41)(Fig. 2).

Cellular responses can also contribute to the mucosal immune response against respiratory pathogens. Generally, antibodies are responsible for protection against secondary infection whereas cellular responses can provide the ability to prevent severe disease by eliminating infected cells as well protect against future infection by assisting B-cells to produce high affinity antibodies (17). CD4<sup>+</sup> T-cells help activate and help drive B-cell maturation and differentiation into plasma cells in the mucosal induction and effector sites, as well as can also promote activation of cytotoxic CD8<sup>+</sup> T-cells that can eliminate infected cells. Memory T-cells including T effector memory cells and T resident memory cells also contribute largely to the durability of the immune response to a respiratory pathogen, in particular T resident memory (T<sub>RM</sub>) cells (139). T<sub>RM</sub> cells that reside in the respiratory tract are generated after infection or nasal vaccination. Overall, the function of T<sub>RM</sub> cells in the respiratory tract is to respond quickly to local infection by coordinating local immune responses to clear the active infection (137,140). Moreover, studies have shown that CD4<sup>+</sup> and CD8<sup>+</sup> T<sub>RM</sub> cells can provide protection against influenza and respiratory syncytial viral infection in the respiratory tract (141).

### **1.11 Nasal vaccination**

SARS-CoV-2 infection is acquired through inhalation of respiratory droplets and/or aerosols. The mucosal immune response plays a large role at initially controlling respiratory infection through humoral and cellular mediated responses. Therefore, immunization at the site of infection could provide optimal protection against SARS-CoV-2. Nasal vaccination similar to SARS-CoV-2 infection can provide the necessary protection in the mucosal tissue in regard to generation of antigen specific IgA in the upper respiratory tract as well as stimulate a systemic IgG response in the lung (41). Currently, the only approved intranasal vaccine for human use is Flumist, a vaccine for influenza. Flumist is a live attenuated vaccine containing cold adapted attenuated influenza A and B viruses that can only replicate within lower temperatures found in the nose (142–144). Intranasal administration with Flumist provides protection by generating both a mucosal IgA and systemic IgG response, with an overall efficacy of approximately 60-70%, comparable to the intramuscular influenza vaccine (145). Interestingly, there are no approved intranasal COVID-19 vaccines for human use; although, many intranasal vaccines are in pre-clinical and clinical trials. Intranasal vaccine platforms utilized include vectored based vaccines such as adenovirus, Newcastle disease virus, live attenuated influenza virus, parainfluenza virus, and respiratory syncytial virus as well as SARS-CoV-2 live attenuated virus and recombinant protein vaccines are currently in phase I, II, and III clinical trials globally (143,146,147). Most of the vectored intranasal vaccines in clinical trials utilize the full-length spike protein, for example, adenovirus vectored ChAdOx1 nCoV-19 (AstraZeneca/University of Oxford) and ChAd-SARS-CoV-2-S (Bharat Biotech International Limited/University of Washington St. Louis) (148–151). Though, Ad5-nCoV nasal vaccine developed by CanSino Biologics with the Beijing Institute of Biotechnology use the RBD as the candidate vaccine antigen (147). At this time, CoviLiv is the only nasal SARS-CoV-2 live attenuated vaccine in clinical trials. CoviLiv, developed by the company Codagenix, is formulated with attenuated ancestral strain of SARS-CoV-2 (147,152). Lastly, there are two nasal protein subunit vaccines in clinical trials, CIGB-669 developed by



Center of Genetic Engineering and Biotechnology in Cuba, and Razi Cov Pars, developed by the Razi Vaccine and Serum Research Institute in Iran (147). CIGB-669 utilizes the RBD as the vaccine antigen with Hepatitis B core antigen whereas Razi Cov Pars uses the spike trimer adjuvanted with oil in water adjuvant system RAS-01 (Razi Adjuvant system-1) (153).

### **1.12 COVID-19 vaccine overview**

All current WHO approved vaccines are administered through the intramuscular route. Despite these intramuscular COVID-19 vaccines preventing severe disease, hospitalization, and death, we are still facing transmission of SARS-CoV-2 and vaccine break through cases. We hypothesize, intranasal vaccination can help mitigate vaccine break through cases and viral transmission because nasal vaccination can induce mucosal immunity at the site of infection. Intramuscular vaccination with the current approved COVID-19 vaccines offers robust systemic immune responses such as the presence of neutralizing antibodies in the lower respiratory tract and strong CD4<sup>+</sup> and CD8<sup>+</sup> T-cell responses (17). COVID-19 mRNA vaccine studies demonstrated that secretory IgA was detected in the saliva in patients vaccinated with mRNA vaccines; however, higher SARS-CoV-2 IgA titers were observed at convalescence, or with hybrid immunity (154). In contrast to intramuscular immunization, nasal immunization similar to respiratory infection can elicit both localized protection in the mucosal tissue as well as systemic induction of neutralizing antibodies. Studies have shown that nasal vaccination can induce high levels of secretory IgA in the upper and lower respiratory tract as well as stimulate systemic IgG in the lower respiratory tract (41). Furthermore, the optimal level of protection from SARS-CoV-2 infection originates from both infection and vaccination (100,101). Infection and vaccination or vice versa generates magnitude, breadth and durability of antibody and cellular responses against SARS-CoV-2 (100). Therefore, to harness the level of protection acquired from infection and vaccination into a vaccine strategy, a heterologous prime and boost strategy can be utilized. Studies have demonstrated that an intramuscular prime and intranasal boost can promote both robust systemic and mucosal immunity as well as induce T and B cell memory responses (155).

### **1.13 Premise**

The COVID-19 pandemic allowed for a surge of global scientific research and collaborations in order to reach a common goal of preventing the spread of COVID-19. The overall premise of this body of work is to contribute to the world-wide effort of defeating SARS-CoV-2 through the utilization of pre-clinical models to study the mechanisms of immunity against SARS-CoV-2 via passive and active immunization. The lethal K18-hACE2 mouse model played an instrumental role in the study of SARS-CoV-2 pathogenesis as well as evaluation of the correlates of protection in prototype vaccine formulations. The work performed in chapter 2 established the passive immunization and challenge model in K18-hACE2 transgenic mice to study antibody mediated protection against SARS-CoV-2 VOC. Chapter 2 emphasized the importance of functional antibodies against SARS-CoV-2 and the significance of broadly neutralizing antibodies against SARS-CoV-2 VOC through passive immunization with convalescent plasma (HCP) obtained from a patient infected with the ancestral strain of SARS-CoV-2. Passive immunization with HCP resulted in total protection from the ancestral strain of SARS-CoV-2 and Alpha, partial protection against Beta, and no protection against Delta. Overall, this study demonstrated that the passive immunization model can be utilized to evaluate SARS-CoV-2 antibody efficacy against emerging VOC which can provide vital information for developing future therapeutics and vaccines.

In chapter 3, the K18-hACE2 mouse challenge model was utilized to evaluate the vaccine efficacy of RBD-VLP vaccines against Alpha or Beta challenge. RBD-VLP vaccines were developed by the Serum Institute of India and Spy Biotech utilizing the Hepatitis B surface antigen decorated with the homologous display of RBD from the ancestral strain of SARS-CoV-2 and/or Beta adjuvanted with either Alum or SWE. Four RBD-VLP formulations administered intramuscularly in three doses were compared to the standard 2 dose Pfizer-BioNTech mRNA vaccine series. Overall, the combination of ancestral strain RBD-VLP with Beta RBD-VLP adjuvanted with Alum and the ancestral strain RBD-VLP adjuvanted with SWE provided protection against both Alpha and Beta challenge similar to the Pfizer-BioNTech mRNA vaccine.

Lastly, in chapter 4, we developed a prototype vaccine formulated with RBD conjugated to the bacterial carrier protein EcoCRM adjuvanted with a TLR4-agonist BECC470 (BReC-CoV-2). Intranasal administration of BreC-CoV-2 resulted in the induction of both systemic IgG and localized IgA response which led to the overall protection against the ancestral strain of SARS-CoV-2. A heterologous prime and boost strategy was also implemented with BReC-CoV-2 where BreC-CoV-2 was administered intramuscularly first then given intranasally as a boost. The heterologous vaccine strategy resulted in 100% protection against a lethal Delta variant challenge in the K18-hACE2 mouse model.

Overall, the following chapters utilize the K18-hACE2 mouse model to establish a platform to study vaccine efficacy against SARS-CoV-2 challenge. The results demonstrated the importance of the antibody mediated responses against SARS-CoV-2 as well as the significance of the contribution of mucosal immunity to protection against SARS-CoV-2. Furthermore, the story represented here establishes the pipeline that can be used to improve on vaccine efficacy for future COVID-19 vaccines.

## 1.14 References

1. Timeline of WHO's response to COVID-19 [Internet]. [cited 2022 Jul 13]. Available from: <https://www.who.int/emergencies/diseases/novel-coronavirus-2019/interactive-timeline#!>
2. CDC Museum COVID-19 Timeline | David J. Sencer CDC Museum | CDC [Internet]. [cited 2022 Jul 13]. Available from: <https://www.cdc.gov/museum/timeline/covid19.html>
3. Walls AC, Park YJ, Tortorici MA, Wall A, McGuire AT, Velesler D. Structure, Function, and Antigenicity of the SARS-CoV-2 Spike Glycoprotein. *Cell* [Internet]. 2020 Apr 16 [cited 2022 May 3];181(2):281-292.e6. Available from: <https://pubmed.ncbi.nlm.nih.gov/32155444/>
4. Lamers MM, Haagmans BL. SARS-CoV-2 pathogenesis. *Nat Rev Microbiol* 2022 205 [Internet]. 2022 Mar 30 [cited 2022 Apr 27];20(5):270–84. Available from: <https://www.nature.com/articles/s41579-022-00713-0>
5. Yang H, Rao Z. Structural biology of SARS-CoV-2 and implications for therapeutic development. *Nat Rev Microbiol* 2021 1911 [Internet]. 2021 Sep 17 [cited 2022 Apr 27];19(11):685–700. Available from: <https://www.nature.com/articles/s41579-021-00630-8>
6. Yadav R, Chaudhary JK, Jain N, Chaudhary PK, Khanra S, Dhamija P, et al. Role of Structural and Non-Structural Proteins and Therapeutic Targets of SARS-CoV-2 for COVID-19. *Cells* [Internet]. 2021 Apr 1 [cited 2022 Apr 27];10(4):821. Available from: </pmc/articles/PMC8067447/>
7. Nieto-Torres JL, Verdiá-Báguena C, Jimenez-Guardeño JM, Regla-Nava JA, Castaño-Rodríguez C, Fernandez-Delgado R, et al. Severe acute respiratory syndrome coronavirus E protein transports calcium ions and activates the NLRP3 inflammasome. *Virology* [Internet]. 2015 Nov 1 [cited 2022 Apr 27];485:330–9. Available from: <https://pubmed.ncbi.nlm.nih.gov/26331680/>
8. Lu X, Pan J, Tao J, Guo D. SARS-CoV nucleocapsid protein antagonizes IFN- $\beta$  response by targeting initial step of IFN- $\beta$  induction pathway, and its C-terminal region is critical for the antagonism. *Virus Genes* [Internet]. 2011 Feb 1 [cited 2022 Apr 27];42(1):37. Available from: </pmc/articles/PMC7088804/>
9. Puelles VG, Lütgehetmann M, Lindenmeyer MT, Sperhake JP, Wong MN, Allweiss L, et al. Multiorgan and Renal Tropism of SARS-CoV-2. *N Engl J Med* [Internet]. 2020 Aug 6 [cited 2022 Apr 27];383(6):590–2. Available from: <https://www.nejm.org/doi/10.1056/NEJMc2011400>
10. Bhatnagar J, Gary J, Reagan-Steiner S, Estetter LB, Tong S, Tao Y, et al. Evidence of Severe Acute Respiratory Syndrome Coronavirus 2 Replication and Tropism in the Lungs, Airways, and Vascular Endothelium of Patients With Fatal Coronavirus Disease 2019: An Autopsy Case Series. *J Infect Dis* [Internet]. 2021 Mar 3 [cited 2022 Apr 27];223(5):752–64. Available from: <https://academic.oup.com/jid/article/223/5/752/6121320>
11. Lindner D, Fitzek A, Bräuninger H, Aleshcheva G, Edler C, Meissner K, et al. Association of Cardiac Infection With SARS-CoV-2 in Confirmed COVID-19 Autopsy Cases. *JAMA Cardiol* [Internet]. 2020 Nov 1 [cited 2022 Apr 27];5(11):1281–5. Available from: <https://jamanetwork.com/journals/jamacardiology/fullarticle/2768914>
12. Lamers MM, Beumer J, Vaart J Van Der, Knoops K, Puschhof J, Breugem TI, et al. SARS-CoV-2 productively infects human gut enterocytes. *Science* (80- ) [Internet]. 2020 Jul 3 [cited 2022 Apr 27];369(6499):50–4. Available from:

<https://www.science.org/doi/full/10.1126/science.abc1669>

13. Mao L, Jin H, Wang M, Hu Y, Chen S, He Q, et al. Neurologic Manifestations of Hospitalized Patients With Coronavirus Disease 2019 in Wuhan, China. *JAMA Neurol* [Internet]. 2020 Jun 1 [cited 2022 Apr 27];77(6):683–90. Available from: <https://pubmed.ncbi.nlm.nih.gov/32275288/>
14. Liu J, Li Y, Liu Q, Yao Q, Wang X, Zhang H, et al. SARS-CoV-2 cell tropism and multiorgan infection. *Cell Discov* 2021 71 [Internet]. 2021 Mar 23 [cited 2022 Apr 27];7(1):1–4. Available from: <https://www.nature.com/articles/s41421-021-00249-2>
15. Tak MW, Mary SE, Bradley JD, editors. *Primer to The Immune Response*. Elsevier; 2014.
16. Galani IE, Rovina N, Lampropoulou V, Triantafyllia V, Manioudaki M, Pavlos E, et al. Untuned antiviral immunity in COVID-19 revealed by temporal type I/III interferon patterns and flu comparison. *Nat Immunol* 2020 221 [Internet]. 2020 Dec 4 [cited 2022 May 3];22(1):32–40. Available from: <https://www.nature.com/articles/s41590-020-00840-x>
17. Sette A, Crotty S. Adaptive immunity to SARS-CoV-2 and COVID-19. *Cell* [Internet]. 2021 Feb 18 [cited 2022 Feb 28];184(4):861–80. Available from: <https://pubmed.ncbi.nlm.nih.gov/33497610/>
18. Rydzynski C, Moderbacher C, Ramirez SI, Dan JM, Grifoni A, Hastie KM, Weiskopf D, et al. Antigen-Specific Adaptive Immunity to SARS-CoV-2 in Acute COVID-19 and Associations with Age and Disease Severity. *Cell* [Internet]. 2020 Nov 12 [cited 2022 May 3];183(4):996–1012.e19. Available from: <https://pubmed.ncbi.nlm.nih.gov/33010815/>
19. Soresina A, Moratto D, Chiarini M, Paolillo C, Baresi G, Focà E, et al. Two X-linked agammaglobulinemia patients develop pneumonia as COVID-19 manifestation but recover. *Pediatr Allergy Immunol* [Internet]. 2020 Jul 1 [cited 2022 May 3];31(5):565–9. Available from: <https://pubmed.ncbi.nlm.nih.gov/32319118/>
20. Dan JM, Mateus J, Kato Y, Hastie KM, Yu ED, Faliti CE, et al. Immunological memory to SARS-CoV-2 assessed for up to 8 months after infection. *Science* (80- ) [Internet]. 2021 Feb 5 [cited 2022 Feb 28];371(6529). Available from: <https://www.science.org/doi/abs/10.1126/science.abf4063>
21. Deng W, Bao L, Liu J, Xiao C, Liu J, Xue J, et al. Primary exposure to SARS-CoV-2 protects against reinfection in rhesus macaques. *Science* [Internet]. 2020 Aug 14 [cited 2022 May 3];369(6505):818–23. Available from: <https://pubmed.ncbi.nlm.nih.gov/32616673/>
22. From Alpha to Omicron: Everything you need to know about SARS-CoV-2 variants of concern | Gavi, the Vaccine Alliance [Internet]. [cited 2022 Jul 13]. Available from: <https://www.gavi.org/vaccineswork/alpha-omicron-everything-you-need-know-about-coronavirus-variants-concern>
23. Nextstrain / ncov / gisaid / global [Internet]. [cited 2022 Mar 28]. Available from: <https://nextstrain.org/ncov/gisaid/global>
24. Jung C, Kmiec D, Koepke L, Zech F, Jacob T, Sparrer KMJ, et al. Omicron: What Makes the Latest SARS-CoV-2 Variant of Concern So Concerning? *J Virol* [Internet]. 2022 Mar 23 [cited 2022 Apr 27];96(6). Available from: <https://journals.asm.org/doi/full/10.1128/jvi.02077-21>
25. Cheng SMS, Mok CKP, Leung YWY, Ng SS, Chan KCK, Ko FW, et al. Neutralizing antibodies against the SARS-CoV-2 Omicron variant BA.1 following homologous and

- heterologous CoronaVac or BNT162b2 vaccination. *Nat Med* 2022 283 [Internet]. 2022 Jan 20 [cited 2022 Apr 27];28(3):486–9. Available from: <https://www.nature.com/articles/s41591-022-01704-7>
26. Yu J, Collier AY, Rowe M, Mardas F, Ventura JD, Wan H, et al. Neutralization of the SARS-CoV-2 Omicron BA.1 and BA.2 Variants. *N Engl J Med* [Internet]. 2022 Apr 21 [cited 2022 Apr 27];386(16):1579–80. Available from: <https://www.nejm.org/doi/full/10.1056/NEJMc2201849>
  27. GeurtsvanKessel CH, Geers D, Schmitz KS, Mykytyn AZ, Lamers MM, Bogers S, et al. Divergent SARS CoV-2 Omicron-reactive T- and B cell responses in COVID-19 vaccine recipients. *Sci Immunol* [Internet]. 2022 Feb 3 [cited 2022 Feb 28]; Available from: <https://www.science.org/doi/abs/10.1126/sciimmunol.abo2202>
  28. Liu L, Iketani S, Guo Y, Chan JFW, Wang M, Liu L, et al. Striking antibody evasion manifested by the Omicron variant of SARS-CoV-2. *Nat* 2021 6027898 [Internet]. 2021 Dec 23 [cited 2022 Mar 7];602(7898):676–81. Available from: <https://www.nature.com/articles/s41586-021-04388-0>
  29. VanBlargan LA, Errico JM, Halfmann PJ, Zost SJ, Crowe JE, Purcell LA, et al. An infectious SARS-CoV-2 B.1.1.529 Omicron virus escapes neutralization by therapeutic monoclonal antibodies. *Nat Med* 2022 283 [Internet]. 2022 Jan 19 [cited 2022 Apr 27];28(3):490–5. Available from: <https://www.nature.com/articles/s41591-021-01678-y>
  30. Statement on Omicron sublineage BA.2 [Internet]. [cited 2022 Apr 27]. Available from: <https://www.who.int/news/item/22-02-2022-statement-on-omicron-sublineage-ba.2>
  31. Viana R, Moyo S, Amoako DG, Tegally H, Scheepers C, Althaus CL, et al. Rapid epidemic expansion of the SARS-CoV-2 Omicron variant in southern Africa. *Nat* 2022 6037902 [Internet]. 2022 Jan 7 [cited 2022 Apr 27];603(7902):679–86. Available from: <https://www.nature.com/articles/s41586-022-04411-y>
  32. Hadfield J, Megill C, Bell SM, Huddleston J, Potter B, Callender C, et al. NextStrain: Real-time tracking of pathogen evolution. *Bioinformatics*. 2018 Dec 1;34(23):4121–3.
  33. Callaway E. What Omicron's BA.4 and BA.5 variants mean for the pandemic. *Nature*. 2022 Jun 30;
  34. Singh S, Kumar R, Agrawal B. Adenoviral Vector-Based Vaccines and Gene Therapies: Current Status and Future Prospects. 2016 [cited 2022 Jul 13]; Available from: <http://dx.doi.org/10.5772/intechopen.79697>
  35. Mendonça SA, Lorincz R, Boucher P, Curiel DT. Adenoviral vector vaccine platforms in the SARS-CoV-2 pandemic. *npj Vaccines* 2021 61 [Internet]. 2021 Aug 5 [cited 2022 Apr 29];6(1):1–14. Available from: <https://www.nature.com/articles/s41541-021-00356-x>
  36. Sadoff J, Gray G, Vandebosch A, Cárdenas V, Shukarev G, Grinsztejn B, et al. Safety and Efficacy of Single-Dose Ad26.COV2.S Vaccine against Covid-19. *N Engl J Med* [Internet]. 2021 Jun 10 [cited 2022 Jul 14];384(23):2187–201. Available from: <https://www.nejm.org/doi/full/10.1056/NEJMoa2101544>
  37. Heinz FX, Stiasny K. Distinguishing features of current COVID-19 vaccines: knowns and unknowns of antigen presentation and modes of action. *npj Vaccines* 2021 61 [Internet]. 2021 Aug 16 [cited 2022 Apr 29];6(1):1–13. Available from: <https://www.nature.com/articles/s41541-021-00369-6>

38. Falsey AR, Sobieszczyk ME, Hirsch I, Sproule S, Robb ML, Corey L, et al. Phase 3 Safety and Efficacy of AZD1222 (ChAdOx1 nCoV-19) Covid-19 Vaccine. *N Engl J Med* [Internet]. 2021 Dec 16 [cited 2022 Jul 14];385(25):2348–60. Available from: <https://www.nejm.org/doi/full/10.1056/NEJMoa2105290>
39. Sheikh A, Robertson C, Taylor B. BNT162b2 and ChAdOx1 nCoV-19 Vaccine Effectiveness against Death from the Delta Variant. *N Engl J Med* [Internet]. 2021 Dec 2 [cited 2022 Jul 14];385(23):2195–7. Available from: <https://www.nejm.org/doi/full/10.1056/NEJMc2113864>
40. Halperin SA, Ye L, MacKinnon-Cameron D, Smith B, Cahn PE, Ruiz-Palacios GM, et al. Final efficacy analysis, interim safety analysis, and immunogenicity of a single dose of recombinant novel coronavirus vaccine (adenovirus type 5 vector) in adults 18 years and older: an international, multicentre, randomised, double-blinded, placebo-controlled phase 3 trial. *Lancet* [Internet]. 2022 Jan 15 [cited 2022 Jul 14];399(10321):237–48. Available from: <http://www.thelancet.com/article/S0140673621027537/fulltext>
41. Krammer F. SARS-CoV-2 vaccines in development. *Nat* 2020 5867830 [Internet]. 2020 Sep 23 [cited 2022 Mar 1];586(7830):516–27. Available from: <https://www.nature.com/articles/s41586-020-2798-3>
42. Fang E, Liu X, Li M, Zhang Z, Song L, Zhu B, et al. Advances in COVID-19 mRNA vaccine development. *Signal Transduct Target Ther* 2022 71 [Internet]. 2022 Mar 23 [cited 2022 Jul 14];7(1):1–31. Available from: <https://www.nature.com/articles/s41392-022-00950-y>
43. Dolgin E. The tangled history of mRNA vaccines. *Nature*. 2021 Sep 1;597(7876):318–24.
44. Sahin U, Karikó K, Türeci Ö. mRNA-based therapeutics — developing a new class of drugs. *Nat Rev Drug Discov* 2014 1310 [Internet]. 2014 Sep 19 [cited 2022 Jul 13];13(10):759–80. Available from: <https://www.nature.com/articles/nrd4278>
45. Pardi N, Hogan MJ, Porter FW, Weissman D. mRNA vaccines—a new era in vaccinology. *Nat Rev Drug Discov*. 2018 Mar 28;17(4):261–79.
46. Polack FP, Thomas SJ, Kitchin N, Absalon J, Gurtman A, Lockhart S, et al. Safety and Efficacy of the BNT162b2 mRNA Covid-19 Vaccine. *N Engl J Med* [Internet]. 2020 Dec 31 [cited 2022 Jun 7];383(27):2603–15. Available from: <https://www.nejm.org/doi/full/10.1056/nejmoa2034577>
47. Baden LR, El Sahly HM, Essink B, Kotloff K, Frey S, Novak R, et al. Efficacy and Safety of the mRNA-1273 SARS-CoV-2 Vaccine. *N Engl J Med* [Internet]. 2021 Feb 4 [cited 2022 Jun 7];384(5):403–16. Available from: <https://www.nejm.org/doi/full/10.1056/nejmoa2035389>
48. Andrews N, Stowe J, Kirsebom F, Toffa S, Rickeard T, Gallagher E, et al. Covid-19 Vaccine Effectiveness against the Omicron (B.1.1.529) Variant. *N Engl J Med* [Internet]. 2022 Apr 21 [cited 2022 Jun 22];386(16):1532–46. Available from: <https://www.nejm.org/doi/full/10.1056/NEJMoa2119451>
49. The COVID-19 vaccine race | Gavi, the Vaccine Alliance [Internet]. [cited 2022 Feb 22]. Available from: <https://www.gavi.org/vaccineswork/covid-19-vaccine-race>
50. Heath PT, Galiza EP, Baxter DN, Boffito M, Browne D, Burns F, et al. Safety and Efficacy of NVX-CoV2373 Covid-19 Vaccine. <https://doi.org/101056/NEJMoa2107659> [Internet]. 2021 Jun 30 [cited 2021 Oct 29];385(13):1172–83. Available from:

<https://www.nejm.org/doi/full/10.1056/NEJMoa2107659>

51. Dunkle LM, Kotloff KL, Gay CL, Áñez G, Adelglass JM, Barrat Hernández AQ, et al. Efficacy and Safety of NVX-CoV2373 in Adults in the United States and Mexico. *N Engl J Med* [Internet]. 2022 Feb 10 [cited 2022 Feb 18];386(6):531–43. Available from: <https://www.nejm.org/doi/full/10.1056/NEJMoa2116185>
52. Tian JH, Patel N, Haupt R, Zhou H, Weston S, Hammond H, et al. SARS-CoV-2 spike glycoprotein vaccine candidate NVX-CoV2373 immunogenicity in baboons and protection in mice. *Nat Commun* 2021 121 [Internet]. 2021 Jan 14 [cited 2022 Feb 18];12(1):1–14. Available from: <https://www.nature.com/articles/s41467-020-20653-8>
53. What is the Novavax vaccine, and why does the world need another type of COVID-19 vaccine? | Gavi, the Vaccine Alliance [Internet]. [cited 2022 May 3]. Available from: <https://www.gavi.org/vaccineswork/what-novavax-vaccine-and-why-does-world-need-another-type-covid-19-vaccine>
54. Dolgin E. Omicron thwarts some of the world's most-used COVID vaccines. *Nature*. 2022 Jan 1;601(7893):311.
55. How Bharat Biotech's Covaxin Vaccine Works - The New York Times [Internet]. [cited 2022 May 3]. Available from: <https://www.nytimes.com/interactive/2021/health/bharat-biotech-covid-19-vaccine.html>
56. How the Sinovac Covid-19 Vaccine Works - The New York Times [Internet]. [cited 2022 May 3]. Available from: <https://www.nytimes.com/interactive/2020/health/sinovac-covid-19-vaccine.html>
57. Cerqueira-Silva T, Andrews JR, Boaventura VS, Ranzani OT, de Araújo Oliveira V, Paixão ES, et al. Effectiveness of CoronaVac, ChAdOx1 nCoV-19, BNT162b2, and Ad26.COV2.S among individuals with previous SARS-CoV-2 infection in Brazil: a test-negative, case-control study. *Lancet Infect Dis* [Internet]. 2022 Jun 1 [cited 2022 Jul 14];22(6):791–801. Available from: <http://www.thelancet.com/article/S1473309922001402/fulltext>
58. Ella R, Reddy S, Blackwelder W, Potdar V, Yadav P, Sarangi V, et al. Efficacy, safety, and lot-to-lot immunogenicity of an inactivated SARS-CoV-2 vaccine (BBV152): interim results of a randomised, double-blind, controlled, phase 3 trial. *Lancet* [Internet]. 2021 Dec 11 [cited 2022 Jul 14];398(10317):2173–84. Available from: <http://www.thelancet.com/article/S0140673621020006/fulltext>
59. The Sinopharm COVID-19 vaccine: What you need to know [Internet]. [cited 2022 Jul 14]. Available from: <https://www.who.int/news-room/feature-stories/detail/the-sinopharm-covid-19-vaccine-what-you-need-to-know>
60. What are whole virus vaccines and how could they be used against COVID-19? | Gavi, the Vaccine Alliance [Internet]. [cited 2022 May 3]. Available from: <https://www.gavi.org/vaccineswork/what-are-whole-virus-vaccines-and-how-could-they-be-used-against-covid-19>
61. Pérez-Then E, Lucas C, Monteiro VS, Miric M, Brache V, Cochon L, et al. Immunogenicity of heterologous BNT162b2 booster in fully vaccinated individuals with CoronaVac against SARS-CoV-2 variants Delta and Omicron: the Dominican Republic Experience. *medRxiv* [Internet]. 2021 Dec 29 [cited 2022 May 3];2021.12.27.21268459. Available from: <https://www.medrxiv.org/content/10.1101/2021.12.27.21268459v1>



62. Pulendran B, S. Arunachalam P, O'Hagan DT. Emerging concepts in the science of vaccine adjuvants. *Nat Rev Drug Discov* 2021 206 [Internet]. 2021 Apr 6 [cited 2021 Sep 16];20(6):454–75. Available from: <https://www.nature.com/articles/s41573-021-00163-y>
63. Kool M, Soullié T, Van Nimwegen M, Willart MAM, Muskens F, Jung S, et al. Alum adjuvant boosts adaptive immunity by inducing uric acid and activating inflammatory dendritic cells. *J Exp Med* [Internet]. 2008 Apr 14 [cited 2022 Jun 14];205(4):869–82. Available from: <https://pubmed.ncbi.nlm.nih.gov/18362170/>
64. Wu Z, Liu K. Overview of vaccine adjuvants. *Med Drug Discov*. 2021 Sep 1;11.
65. Pulendran B, S. Arunachalam P, O'Hagan DT. Emerging concepts in the science of vaccine adjuvants. *Nat Rev Drug Discov* 2021 206 [Internet]. 2021 Apr 6 [cited 2022 Jun 13];20(6):454–75. Available from: <https://www.nature.com/articles/s41573-021-00163-y>
66. Liang Z, Zhu H, Wang X, Jing B, Li Z, Xia X, et al. Adjuvants for Coronavirus Vaccines. *Front Immunol*. 2020 Nov 6;11:2896.
67. Wang YQ, Bazin-Lee H, Evans JT, Casella CR, Mitchell TC. MPL Adjuvant Contains Competitive Antagonists of Human TLR4. *Front Immunol*. 2020 Oct 16;11:2716.
68. Garçon N, Chomez P, Van Mechelen M. GlaxoSmithKline Adjuvant Systems in vaccines: Concepts, achievements and perspectives. *Expert Rev Vaccines*. 2007 Oct;6(5):723–39.
69. AM D, B L, A DP, N H, C C, N G. Adjuvant system AS01: helping to overcome the challenges of modern vaccines. *Expert Rev Vaccines* [Internet]. 2017 Jan 2 [cited 2021 Aug 10];16(1):55–63. Available from: <https://pubmed.ncbi.nlm.nih.gov/27448771/>
70. Pulendran B, S. Arunachalam P, O'Hagan DT. Emerging concepts in the science of vaccine adjuvants. *Nat Rev Drug Discov* 2021 206 [Internet]. 2021 Apr 6 [cited 2022 Jun 14];20(6):454–75. Available from: <https://www.nature.com/articles/s41573-021-00163-y>
71. Gregg KA, Harberts E, Gardner FM, Pelletier MR, Cayatte C, Yu L, et al. Rationally Designed TLR4 Ligands for Vaccine Adjuvant Discovery. *MBio* [Internet]. 2017 May 1 [cited 2021 Jul 20];8(3). Available from: [/pmc/articles/PMC5424205/](https://pubmed.ncbi.nlm.nih.gov/27448771/)
72. Zacharia A, Harberts E, Valencia SM, Myers B, Sanders C, Jain A, et al. Optimization of RG1-VLP vaccine performance in mice with novel TLR4 agonists. *Vaccine*. 2021 Jan 8;39(2):292–302.
73. Gregg KA, Harberts E, Gardner FM, Pelletier MR, Cayatte C, Yu L, et al. A lipid A-based TLR4 mimetic effectively adjuvants a *Yersinia pestis* rF-V1 subunit vaccine in a murine challenge model. *Vaccine* [Internet]. 2018 Jun 27 [cited 2021 Sep 14];36(28):4023. Available from: [/pmc/articles/PMC6057149/](https://pubmed.ncbi.nlm.nih.gov/27448771/)
74. Harberts E, Varisco D, Haupt R, Jain A, Middaugh CR, Ernst RK. Novel lipid A mimetics, BECC438 and BECC470, act as potent adjuvants in bacterial and viral subunit vaccines. *J Immunol*. 2020;204(1 Supplement).
75. Wong TY, Lee KS, Russ BP, Horspool AM, Kang J, Winters MT, et al. Intranasal administration of BReC-CoV-2 COVID-19 vaccine protects K18-hACE2 mice against lethal SARS-CoV-2 challenge. *npj Vaccines* 2022 71 [Internet]. 2022 Mar 14 [cited 2022 Mar 21];7(1):1–15. Available from: <https://www.nature.com/articles/s41541-022-00451-7>
76. Lan J, Deng Y, Chen H, Lu G, Wang W, Guo X, et al. Tailoring subunit vaccine immunity with adjuvant combinations and delivery routes using the Middle East respiratory

- coronavirus (MERS-CoV) receptor-binding domain as an antigen. *PLoS One* [Internet]. 2014 Nov 18 [cited 2022 Jun 15];9(11). Available from: <https://pubmed.ncbi.nlm.nih.gov/25405618/>
77. Zakhartchouk AN, Sharon C, Satkunarajah M, Auperin T, Viswanathan S, Mutwiri G, et al. Immunogenicity of a receptor-binding domain of SARS coronavirus spike protein in mice: implications for a subunit vaccine. *Vaccine* [Internet]. 2007 Jan 2 [cited 2022 Jun 15];25(1):136–43. Available from: <https://pubmed.ncbi.nlm.nih.gov/16919855/>
  78. Ward BJ, Gobeil P, Séguin A, Atkins J, Boulay I, Charbonneau PY, et al. Phase 1 randomized trial of a plant-derived virus-like particle vaccine for COVID-19. *Nat Med* 2021 276 [Internet]. 2021 May 18 [cited 2022 May 10];27(6):1071–8. Available from: <https://www.nature.com/articles/s41591-021-01370-1>
  79. O'Hagan DT, Ott GS, De Gregorio E, Seubert A. The mechanism of action of MF59 – An innately attractive adjuvant formulation. *Vaccine*. 2012 Jun 19;30(29):4341–8.
  80. About us < Vaccine Formulation Institute [Internet]. [cited 2022 Jul 15]. Available from: <https://www.vaccineformulationinstitute.org/about-vaccine-formulation-institute/>
  81. de Jonge J, van Dijken H, de Heij F, Spijkers S, Mouthaan J, de Jong R, et al. H7N9 influenza split vaccine with SWE oil-in-water adjuvant greatly enhances cross-reactive humoral immunity and protection against severe pneumonia in ferrets. *NPJ Vaccines* [Internet]. 2020 Dec 1 [cited 2022 Feb 25];5(1). Available from: </pmc/articles/PMC7214439/>
  82. Marcandalli J, Fiala B, Ols S, Perotti M, de van der Schueren W, Snijder J, et al. Induction of Potent Neutralizing Antibody Responses by a Designed Protein Nanoparticle Vaccine for Respiratory Syncytial Virus. *Cell* [Internet]. 2019 Mar 7 [cited 2022 Feb 25];176(6):1420. Available from: </pmc/articles/PMC6424820/>
  83. Westdijk J, Koedam P, Barro M, Steil BP, Collin N, Vedvick TS, et al. Antigen sparing with adjuvanted inactivated polio vaccine based on Sabin strains. *Vaccine* [Internet]. 2013 Feb 18 [cited 2022 Feb 25];31(9):1298. Available from: </pmc/articles/PMC3570672/>
  84. Dalvie NC, Rodriguez-Aponte SA, Hartwell BL, Tostanoski LH, Biedermann AM, Crowell LE, et al. Engineered SARS-CoV-2 receptor binding domain improves manufacturability in yeast and immunogenicity in mice. *Proc Natl Acad Sci U S A* [Internet]. 2021 Sep 21 [cited 2022 Feb 25];118(38). Available from: <https://www.pnas.org/content/118/38/e2106845118>
  85. Rivera-Hernandez T, Rhyme MS, Cork AJ, Jones S, Segui-Perez C, Brunner L, et al. Vaccine-Induced Th1-Type Response Protects against Invasive Group A Streptococcus Infection in the Absence of Opsonizing Antibodies. *MBio* [Internet]. 2020 Mar 1 [cited 2022 Feb 25];11(2). Available from: </pmc/articles/PMC7064752/>
  86. A Clinical Trial of COVAC-2 in Adults - Full Text View - ClinicalTrials.gov [Internet]. [cited 2022 Jun 15]. Available from: <https://clinicaltrials.gov/ct2/show/NCT05209009>
  87. A Clinical Trial of COVAC-2 in Healthy Adults - Full Text View - ClinicalTrials.gov [Internet]. [cited 2022 Jun 15]. Available from: <https://clinicaltrials.gov/ct2/show/NCT04702178>
  88. Vu MN, Kelly HG, Kent SJ, Wheatley AK. Current and future nanoparticle vaccines for COVID-19. *eBioMedicine* [Internet]. 2021 Dec 1 [cited 2022 Jun 16];74:103699. Available from: <http://www.thelancet.com/article/S235239642100493X/fulltext>
  89. Hager KJ, Marc GP, Gobeil P, Diaz RS, Heizer G, Llapur C, et al. Efficacy and Safety of a Recombinant Plant-Based Adjuvanted Covid-19 Vaccine.

- <https://doi.org/10.1056/NEJMoa2201300> [Internet]. 2022 May 4 [cited 2022 May 10]; Available from: <https://www.nejm.org/doi/full/10.1056/NEJMoa2201300>
90. Reddington SC, Howarth M. Secrets of a covalent interaction for biomaterials and biotechnology: SpyTag and SpyCatcher. *Curr Opin Chem Biol*. 2015 Dec 1;29:94–9.
  91. | Australian Clinical Trials [Internet]. [cited 2021 Sep 14]. Available from: <https://www.australianclinicaltrials.gov.au/anzctr/trial/ACTRN12620000817943>
  92. Micoli F, Adamo R, Costantino P. molecules Protein Carriers for Glycoconjugate Vaccines: History, Selection Criteria, Characterization and New Trends. [cited 2022 Jun 16]; Available from: [www.mdpi.com/journal/molecules](http://www.mdpi.com/journal/molecules)
  93. Hickey JM, Toprani VM, Kaur K, Mishra RPN, Goel A, Oganessian N, et al. Analytical Comparability Assessments of 5 Recombinant CRM197 Proteins From Different Manufacturers and Expression Systems. *J Pharm Sci*. 2018 Jul 1;107(7):1806–19.
  94. Oganessian N, Lees A. Expression and Purification of CRM197 and Related Proteins. US; 10093704, 2018.
  95. Crotty S. Hybrid immunity. *Science* (80- ) [Internet]. 2021 Jun 25 [cited 2022 Jun 22];372(6549):1392–3. Available from: <https://www.science.org/doi/10.1126/science.abj2258>
  96. McMahan K, Yu J, Mercado NB, Loos C, Tostanoski LH, Chandrashekar A, et al. Correlates of protection against SARS-CoV-2 in rhesus macaques. *Nat* 2020 5907847 [Internet]. 2020 Dec 4 [cited 2022 Jun 2];590(7847):630–4. Available from: <https://www.nature.com/articles/s41586-020-03041-6>
  97. Corbett KS, Nason MC, Flach B, Gagne M, O’Connell S, Johnston TS, et al. Immune correlates of protection by mRNA-1273 vaccine against SARS-CoV-2 in nonhuman primates. *Science* (80- ) [Internet]. 2021 Sep 17 [cited 2022 Jun 2];373(6561). Available from: <https://www.science.org/doi/full/10.1126/science.abj0299>
  98. Gilbert PB, Montefiori DC, McDermott AB, Fong Y, Benkeser D, Deng W, et al. Immune correlates analysis of the mRNA-1273 COVID-19 vaccine efficacy clinical trial. *Science* (80- ) [Internet]. 2022 Jan 7 [cited 2022 Jun 2];375(6576):43–50. Available from: <https://www.science.org/doi/full/10.1126/science.abm3425>
  99. Wei J, Pouwels KB, Stoesser N, Matthews PC, Diamond I, Studley R, et al. Antibody responses and correlates of protection in the general population after two doses of the ChAdOx1 or BNT162b2 vaccines. *Nat Med* 2022 285 [Internet]. 2022 Feb 14 [cited 2022 Jun 2];28(5):1072–82. Available from: <https://www.nature.com/articles/s41591-022-01721-6>
  100. Bates TA, McBride SK, Leier HC, Guzman G, Lyski ZL, Schoen D, et al. Vaccination before or after SARS-CoV-2 infection leads to robust humoral response and antibodies that effectively neutralize variants. *Sci Immunol* [Internet]. 2022 Feb 18 [cited 2022 Jun 3];7(68):8014. Available from: <https://www.science.org/doi/full/10.1126/sciimmunol.abn8014>
  101. Walls AC, Sprouse KR, Bowen JE, Joshi A, Franko N, Navarro MJ, et al. SARS-CoV-2 breakthrough infections elicit potent, broad, and durable neutralizing antibody responses. *Cell* [Internet]. 2022 Mar 3 [cited 2022 Jun 3];185(5):872-880.e3. Available from: <http://www.cell.com/article/S0092867422000691/fulltext>

102. Krammer F. A correlate of protection for SARS-CoV-2 vaccines is urgently needed. *Nat Med* 2021 277 [Internet]. 2021 Jul 8 [cited 2022 Jun 3];27(7):1147–8. Available from: <https://www.nature.com/articles/s41591-021-01432-4>
103. Richardson SI, Manamela NP, Motsoeneng BM, Kaldine H, Ayres F, Makhado Z, et al. SARS-CoV-2 Beta and Delta variants trigger Fc effector function with increased cross-reactivity. *Cell Reports Med*. 2022 Feb 15;3(2):100510.
104. Lim WW, Cowling BJ. Mechanistic correlates of protection for SARS-CoV-2 Vaccines. *Epidemiology* [Internet]. 2022 Jan 1 [cited 2022 Jun 6];33(1):E1. Available from: [https://journals.lww.com/epidem/Fulltext/2022/01000/Mechanistic\\_Correlates\\_of\\_Protection\\_for.18.aspx](https://journals.lww.com/epidem/Fulltext/2022/01000/Mechanistic_Correlates_of_Protection_for.18.aspx)
105. Muñoz-Fontela C, Dowling WE, Funnell SGP, Gsell P-S, Riveros-Balta AX, Albrecht RA, et al. Animal models for COVID-19. *Nat* 2020 5867830 [Internet]. 2020 Sep 23 [cited 2021 Jul 31];586(7830):509–15. Available from: <https://www.nature.com/articles/s41586-020-2787-6>
106. Zhou P, Yang X Lou, Wang XG, Hu B, Zhang L, Zhang W, et al. A pneumonia outbreak associated with a new coronavirus of probable bat origin. *Nat* 2020 5797798 [Internet]. 2020 Feb 3 [cited 2022 Jul 15];579(7798):270–3. Available from: <https://www.nature.com/articles/s41586-020-2012-7>
107. Jackson CB, Farzan M, Chen B, Choe H. Mechanisms of SARS-CoV-2 entry into cells. *Nat Rev Mol Cell Biol* 2021 231 [Internet]. 2021 Oct 5 [cited 2022 Jul 15];23(1):3–20. Available from: <https://www.nature.com/articles/s41580-021-00418-x>
108. Xavier Montagutelli A, Prot M, Levillayer L, Baquero Salazar E, Jouvion G, Conquet L, et al. Variants with the N501Y mutation extend SARS-CoV-2 host range to mice, with contact transmission. *bioRxiv* [Internet]. 2021 Dec 7 [cited 2022 Jul 15];2021.03.18.436013. Available from: <https://www.biorxiv.org/content/10.1101/2021.03.18.436013v2>
109. Shuai H, Fuk-Woo Chan J, Tsz-Tai Yuen T, Yoon C, Hu J-C, Wen L, et al. Emerging SARS-CoV-2 variants expand species tropism to murines. 2021 [cited 2022 Jun 7]; Available from: <https://doi.org/10.1016/j.ebiom.2021.103643>
110. Pan T, Chen R, He X, Yuan Y, Deng X, Li R, et al. Infection of wild-type mice by SARS-CoV-2 B.1.351 variant indicates a possible novel cross-species transmission route. *Signal Transduct Target Ther* 2021 61 [Internet]. 2021 Dec 14 [cited 2022 Jun 7];6(1):1–12. Available from: <https://www.nature.com/articles/s41392-021-00848-1>
111. Wong TY, Horspool AM, Russ BP, Ye C, Lee KS, Winters MT, et al. Evaluating antibody mediated protection against Alpha, Beta, and Delta SARS-CoV-2 variants of concern in K18-hACE2 transgenic mice. *J Virol* [Internet]. 2022 Jan 26 [cited 2022 Feb 25]; Available from: <https://pubmed.ncbi.nlm.nih.gov/35080423/>
112. PB M, L P, C W-L, M H, L M, L S, et al. Lethal infection of K18-hACE2 mice infected with severe acute respiratory syndrome coronavirus. *J Virol* [Internet]. 2007 Jan 15 [cited 2021 Aug 8];81(2):813–21. Available from: <https://pubmed.ncbi.nlm.nih.gov/17079315/>
113. Winkler ES, Bailey AL, Kafai NM, Nair S, McCune BT, Yu J, et al. SARS-CoV-2 infection of human ACE2-transgenic mice causes severe lung inflammation and impaired function. *Nat Immunol* 2020 2111 [Internet]. 2020 Aug 24 [cited 2021 Aug 8];21(11):1327–35. Available from: <https://www.nature.com/articles/s41590-020-0778-2>

114. Yinda CK, Port JR, Bushmaker T, Owusu IO, Purushotham JN, Avanzato VA, et al. K18-hACE2 mice develop respiratory disease resembling severe COVID-19. *PLOS Pathog* [Internet]. 2021 Jan 19 [cited 2021 Aug 11];17(1):e1009195. Available from: <https://journals.plos.org/plospathogens/article?id=10.1371/journal.ppat.1009195>
115. Zheng J, Wong LYR, Li K, Verma AK, Ortiz ME, Wohlford-Lenane C, et al. COVID-19 treatments and pathogenesis including anosmia in K18-hACE2 mice. *Nature* [Internet]. 2021 Jan 28 [cited 2022 Jun 7];589(7843):603–7. Available from: <https://pubmed.ncbi.nlm.nih.gov/33166988/>
116. Golden JW, Cline CR, Zeng X, Garrison AR, Carey BD, Mucker EM, et al. Human angiotensin-converting enzyme 2 transgenic mice infected with SARS-CoV-2 develop severe and fatal respiratory disease. *JCI insight* [Internet]. 2020 Oct 2 [cited 2022 Jun 7];5(19). Available from: <https://pubmed.ncbi.nlm.nih.gov/32841215/>
117. Tseng C-TK, Huang C, Newman P, Wang N, Narayanan K, Watts DM, et al. Severe Acute Respiratory Syndrome Coronavirus Infection of Mice Transgenic for the Human Angiotensin-Converting Enzyme 2 Virus Receptor. *J Virol* [Internet]. 2007 Feb [cited 2022 Jun 7];81(3):1162–73. Available from: <https://journals.asm.org/doi/full/10.1128/JVI.01702-06>
118. Bao L, Deng W, Huang B, Gao H, Liu J, Ren L, et al. The pathogenicity of SARS-CoV-2 in hACE2 transgenic mice. *Nat* 2020 5837818 [Internet]. 2020 May 7 [cited 2022 Jun 7];583(7818):830–3. Available from: <https://www.nature.com/articles/s41586-020-2312-y>
119. Chan JFW, Zhang AJ, Yuan S, Poon VKM, Chan CCS, Lee ACY, et al. Simulation of the clinical and pathological manifestations of Coronavirus Disease 2019 (COVID-19) in golden Syrian hamster model: implications for disease pathogenesis and transmissibility. *Clin Infect Dis An Off Publ Infect Dis Soc Am* [Internet]. 2020 Nov 1 [cited 2022 Jun 7];71(9):2428–46. Available from: <https://pubmed.ncbi.nlm.nih.gov/34220377/>
120. Sia SF, Yan LM, Chin AWH, Fung K, Choy KT, Wong AYL, et al. Pathogenesis and transmission of SARS-CoV-2 in golden hamsters. *Nat* 2020 5837818 [Internet]. 2020 May 14 [cited 2022 Jun 7];583(7818):834–8. Available from: <https://www.nature.com/articles/s41586-020-2342-5>
121. Imai M, Iwatsuki-Horimoto K, Hatta M, Loeber S, Halfmann PJ, Nakajima N, et al. Syrian hamsters as a small animal model for SARS-CoV-2 infection and countermeasure development. *Proc Natl Acad Sci* [Internet]. 2020 Jul 14 [cited 2021 Aug 12];117(28):16587–95. Available from: <https://www.pnas.org/content/117/28/16587>
122. Langel SN, Johnson S, Martinez CI, Tedjakusuma SN, Peinovich N, Dora EG, et al. Adenovirus type 5 SARS-CoV-2 vaccines delivered orally or intranasally reduced disease severity and transmission in a hamster model. *Sci Transl Med* [Internet]. 2022 May 5 [cited 2022 Jun 7]; Available from: <https://www.science.org/doi/full/10.1126/scitranslmed.abn6868>
123. Kim Y-I, Kim S-G, Kim S-M, Webby RJ, Jung JU, Choi Correspondence YK. Infection and Rapid Transmission of SARS-CoV-2 in Ferrets. [cited 2022 Jun 7]; Available from: <https://doi.org/10.1016/j.chom.2020.03.023>
124. Richard M, Kok A, de Meulder D, Bestebroer TM, Lamers MM, Okba NMA, et al. SARS-CoV-2 is transmitted via contact and via the air between ferrets. *Nat Commun* 2020 111 [Internet]. 2020 Jul 8 [cited 2022 Jun 7];11(1):1–6. Available from: <https://pubmed.ncbi.nlm.nih.gov/33166988/>


<https://www.nature.com/articles/s41467-020-17367-2>

125. Kutter JS, de Meulder D, Bestebroer TM, Lexmond P, Mulders A, Richard M, et al. SARS-CoV and SARS-CoV-2 are transmitted through the air between ferrets over more than one meter distance. *Nat Commun* 2021 121 [Internet]. 2021 Mar 12 [cited 2022 Jun 7];12(1):1–8. Available from: <https://www.nature.com/articles/s41467-021-21918-6>
126. Munster VJ, Feldmann F, Williamson BN, van Doremalen N, Pérez-Pérez L, Schulz J, et al. Respiratory disease in rhesus macaques inoculated with SARS-CoV-2. *Nat* 2020 5857824 [Internet]. 2020 May 12 [cited 2022 Jun 7];585(7824):268–72. Available from: <https://www.nature.com/articles/s41586-020-2324-7>
127. Shan C, Yao Y-F, Yang X-L, Zhou Y-W, Gao G, Peng Y, et al. Infection with novel coronavirus (SARS-CoV-2) causes pneumonia in Rhesus macaques. [cited 2022 Jun 7]; Available from: <https://doi.org/10.1038/s41422-020-0364-z>
128. Chandrashekar A, Liu J, Martino AJ, McMahan K, Mercad NB, Peter L, et al. SARS-CoV-2 infection protects against rechallenge in rhesus macaques. *Science* (80- ) [Internet]. 2020 Aug 14 [cited 2022 Jun 7];369(6505):812–7. Available from: <https://www.science.org>
129. Rockx B, Kuiken T, Herfst S, Bestebroer T, Lamers MM, Munnink BBO, et al. Comparative pathogenesis of COVID-19, MERS, and SARS in a nonhuman primate model. *Science* (80- ) [Internet]. 2020 May 29 [cited 2022 Jun 7];368(6494):1012–5. Available from: <https://www.science.org/doi/full/10.1126/science.abb7314>
130. Woolsey C, Borisevich V, Prasad AN, Agans KN, Deer DJ, Dobias NS, et al. Establishment of an African green monkey model for COVID-19 and protection against re-infection. *Nat Immunol* 2020 221 [Internet]. 2020 Nov 24 [cited 2022 Jun 7];22(1):86–98. Available from: <https://www.nature.com/articles/s41590-020-00835-8>
131. Vogel AB, Kanevsky I, Che Y, Swanson KA, Muik A, Vormehr M, et al. BNT162b vaccines protect rhesus macaques from SARS-CoV-2. *Nat* 2021 5927853 [Internet]. 2021 Feb 1 [cited 2022 Jun 7];592(7853):283–9. Available from: <https://www.nature.com/articles/s41586-021-03275-y>
132. Corbett KS, Flynn B, Foulds KE, Francica JR, Boyoglu-Barnum S, Werner AP, et al. Evaluation of the mRNA-1273 Vaccine against SARS-CoV-2 in Nonhuman Primates. *N Engl J Med* [Internet]. 2020 Oct 15 [cited 2022 Jun 7];383(16):1544–55. Available from: <https://www.nejm.org/doi/full/10.1056/nejmoa2024671>
133. Lambe T, Spencer AJ, Thomas KM, Gooch KE, Thomas S, White AD, et al. ChAdOx1 nCoV-19 protection against SARS-CoV-2 in rhesus macaque and ferret challenge models. *Commun Biol* 2021 41 [Internet]. 2021 Jul 26 [cited 2022 Jun 7];4(1):1–12. Available from: <https://www.nature.com/articles/s42003-021-02443-0>
134. Yu J, Tostanosk LH, Peter L, Mercad NB, McMahan K, Mahrokhia SH, et al. DNA vaccine protection against SARS-CoV-2 in rhesus macaques. *Science* (80- ) [Internet]. 2020 Aug 14 [cited 2022 Jun 7];369(6505):806–11. Available from: <https://www.science.org>
135. Gao Q, Bao L, Mao H, Wang L, Xu K, Yang M, et al. Development of an inactivated vaccine candidate for SARS-CoV-2. *Science* (80- ) [Internet]. 2020 Jul 3 [cited 2022 Jun 7];369(6499):77–81. Available from: <https://www.science.org/doi/full/10.1126/science.abc1932>
136. Mercado NB, Zahn R, Wegmann F, Loos C, Chandrashekar A, Yu J, et al. Single-shot

- Ad26 vaccine protects against SARS-CoV-2 in rhesus macaques. *Nat* 2020 5867830 [Internet]. 2020 Jul 30 [cited 2022 Jun 7];586(7830):583–8. Available from: <https://www.nature.com/articles/s41586-020-2607-z>
137. Phillip SD, Blumberg SR, Macdonald TT, editors. *Principles of Mucosal Immunology*. 2nd ed. CRC Press Taylor & Francis Group; 2020.
  138. Brandtzaeg P, Kiyono H, Pabst R, Russell MW. Terminology: nomenclature of mucosa-associated lymphoid tissue. *Mucosal Immunol* 2008 11 [Internet]. 2007 Dec 11 [cited 2022 Jun 8];1(1):31–7. Available from: <https://www.nature.com/articles/mi20079>
  139. Wilk MM, Mills KHG. CD4 TRM cells following infection and immunization: Implications for more effective vaccine design. *Front Immunol*. 2018 Aug 10;9(AUG):1860.
  140. Zheng MZM, Wakim LM. Tissue resident memory T cells in the respiratory tract. *Mucosal Immunol* 2021 153 [Internet]. 2021 Oct 20 [cited 2022 Jul 15];15(3):379–88. Available from: <https://www.nature.com/articles/s41385-021-00461-z>
  141. Szabo PA, Miron M, Farber DL. Location, location, location: Tissue resident memory T cells in mice and humans.
  142. Krammer F. The human antibody response to influenza A virus infection and vaccination. *Nat Rev Immunol* [Internet]. [cited 2022 Jul 14]; Available from: <https://doi.org/10.1038/>
  143. Tiboni M, Casettari L, Illum L. Nasal vaccination against SARS-CoV-2: Synergistic or alternative to intramuscular vaccines? *Int J Pharm* [Internet]. 2021 Jun 15 [cited 2021 Aug 10];603:120686. Available from: </pmc/articles/PMC8099545/>
  144. Demystifying FluMist, a new intranasal, live influenza vaccine. [cited 2022 Jul 14]; Available from: [www.ccm.org](http://www.ccm.org)
  145. Vaccine Effectiveness & Efficacy | FluMist® Quadrivalent (Influenza Vaccine Live, Intranasal) [Internet]. [cited 2022 Jul 14]. Available from: <https://www.flumistquadrivalenthcp.com/vaccine-effectiveness-and-efficacy.html>
  146. Chavda VP, Vora LK, Pandya AK, Patravale VB. Intranasal vaccines for SARS-CoV-2: From challenges to potential in COVID-19 management. *Drug Discov Today*. 2021 Nov 1;26(11):2619–36.
  147. Alu A, Chen L, Lei H, Wei Y, Tian X, Wei X. Intranasal COVID-19 vaccines: From bench to bed. *eBioMedicine* [Internet]. 2022 Feb 1 [cited 2022 Jun 22];76:103841. Available from: <http://www.thelancet.com/article/S2352396422000251/fulltext>
  148. Van Doremalen N, Purushotham JN, Schulz JE, Holbrook MG, Bushmaker T, Carmody A, et al. Intranasal ChAdOx1 nCoV-19/AZD1222 vaccination reduces viral shedding after SARS-CoV-2 D614G challenge in preclinical models. *Sci Transl Med* [Internet]. 2021 Aug 18 [cited 2022 Jul 14];13(607):755. Available from: <https://www.science.org/doi/10.1126/scitranslmed.abh0755>
  149. Marsh GA, McAuley AJ, Au GG, Riddell S, Layton D, Singanallur NB, et al. ChAdOx1 nCoV-19 (AZD1222) vaccine candidate significantly reduces SARS-CoV-2 shedding in ferrets. *npj Vaccines* 2021 61 [Internet]. 2021 May 10 [cited 2022 Jul 14];6(1):1–8. Available from: <https://www.nature.com/articles/s41541-021-00315-6>
  150. Hassan AO, Kafai NM, Dmitriev IP, Fremont DH, Curiel DT, Diamond MS. A Single-Dose Intranasal ChAd Vaccine Protects Upper and Lower Respiratory Tracts against SARS-

- CoV-2. 2020 [cited 2021 Jul 31]; Available from: <https://doi.org/10.1016/j.cell.2020.08.026>
151. Hassan AO, Shrihari S, Gorman MJ, Ying B, Yaun D, Raju S, et al. An intranasal vaccine durably protects against SARS-CoV-2 variants in mice. *Cell Rep* [Internet]. 2021 Jul 27 [cited 2021 Jul 31];36(4):109452. Available from: <https://linkinghub.elsevier.com/retrieve/pii/S221112472100869X>
  152. Nose Spray Vaccines Could Quash COVID Virus Variants - Scientific American [Internet]. [cited 2022 Jul 14]. Available from: <https://www.scientificamerican.com/article/nose-spray-vaccines-could-quash-covid-virus-variants/>
  153. Banihashemi SR, Es-haghi A, Fallah Mehrabadi MH, Nofeli M, Mokarram AR, Ranjbar A, et al. Safety and Efficacy of Combined Intramuscular/Intranasal RAZI-COV PARS Vaccine Candidate Against SARS-CoV-2: A Preclinical Study in Several Animal Models. *Front Immunol* [Internet]. 2022 May 26 [cited 2022 Jun 13];0:2390. Available from: <https://www.frontiersin.org/articles/10.3389/fimmu.2022.836745/full>
  154. Sheikh-Mohamed S, Isho B, Chao GYC, Zuo M, Cohen C, Lustig Y, et al. Systemic and mucosal IgA responses are variably induced in response to SARS-CoV-2 mRNA vaccination and are associated with protection against subsequent infection. *Mucosal Immunol* 2022 [Internet]. 2022 Apr 25 [cited 2022 Jun 16];1–10. Available from: <https://www.nature.com/articles/s41385-022-00511-0>
  155. Mao T, Israelow B, Suberi A, Zhou L, Reschke M, Peña-Hernández MA, et al. Unadjuvanted intranasal spike vaccine booster elicits robust protective mucosal immunity against sarbecoviruses. [cited 2022 Jun 16]; Available from: <https://doi.org/10.1101/2022.01.24.477597>





**Chapter 2: Evaluating antibody  
mediated protection against Alpha, Beta,  
and Delta SARS-CoV-2 variants of  
concern in K18-hACE2 transgenic mice**

## **Evaluating antibody mediated protection against Alpha, Beta, and Delta SARS-CoV-2 variants of concern in K18-hACE2 transgenic mice**

Ting Y. Wong<sup>1,2\*</sup>, Alexander M. Horspool<sup>1,2\*</sup>, Brynna P. Russ<sup>1,2</sup>, Chengjin Ye<sup>9</sup>, Katherine S. Lee<sup>1,2</sup>, Michael T. Winters<sup>1</sup>, Justin R. Bever<sup>1,2</sup>, Olivia A. Miller<sup>1,2</sup>, Nathaniel A. Rader<sup>1,2</sup>, Melissa Cooper<sup>1,2</sup>, Theodore Kieffer<sup>4</sup>, Julien Sourimant<sup>5</sup>, Alexander Greninger<sup>6</sup>, Richard K. Plemper<sup>5</sup>, James Denvir<sup>7</sup>, Holly A. Cyphert<sup>8</sup>, Mariette Barbier<sup>1,2</sup>, Jordi B. Torrelles<sup>9</sup>, Ivan Martinez<sup>1,3</sup>, Luis Martinez-Sobrido<sup>9</sup>, F. Heath Damron<sup>1,2\*</sup>.

<sup>1</sup> Department of Microbiology, Immunology, and Cell Biology, West Virginia University, Morgantown, WV, USA

<sup>2</sup> Vaccine Development Center at West Virginia University Health Sciences Center, Morgantown, WV, USA

<sup>3</sup> West Virginia University Cancer Institute, Morgantown, WV, USA

<sup>4</sup> Department of Pathology, Anatomy and Laboratory Medicine, West Virginia University School of Medicine, Morgantown, WV, USA

<sup>5</sup> Institute for Biomedical Sciences, Georgia State University, Atlanta, GA, USA

<sup>6</sup> University of Washington, Department of Laboratory Medicine and Pathology, Seattle, WA, USA

<sup>7</sup> Department of Biomedical Sciences, Marshall University, Huntington, WV, USA

<sup>8</sup> Department of Biological Sciences, Marshall University, Huntington, WV, USA

<sup>9</sup> Host-Pathogen Interactions and Population Health Programs, Texas Biomedical Research Institute, San Antonio, TX, USA.

\* Authors contributed equally to this publication \*\* Corresponding author

Corresponding author email address: [fdamron@hsc.wvu.edu](mailto:fdamron@hsc.wvu.edu)

Keywords: SARS-CoV-2, COVID-19, variants of concern, Alpha, Beta, Delta, K18-hACE2 transgenic mice, convalescent plasma, modeling COVID-19, passive immunity

DOI: <https://doi.org/10.1128/jvi.02184-21>

## **2.1 ABSTRACT**

SARS-CoV-2 variants of concern (VoC) are impacting responses to the COVID-19 pandemic. Here, we utilized passive immunization using human convalescent plasma (HCP) obtained from a critically ill COVID-19 patient in the early pandemic to study the efficacy of polyclonal antibodies generated to ancestral SARS-CoV-2 against the Alpha, Beta, and Delta VoC in the K18 human angiotensin converting enzyme 2 (hACE2) transgenic mouse model. HCP protected mice from challenge with the original WA-1 SARS-CoV-2 strain; however, only partially protected mice challenged with the Alpha VoC (60% survival) and failed to save Beta challenged mice from succumbing to disease. HCP treatment groups had elevated receptor binding domain (RBD) and nucleocapsid IgG titers in the serum; however, Beta VoC viral burden in the lung and brain was not decreased due to HCP treatment. While mice could be protected from WA-1 or Alpha challenge with a single dose of HCP, six doses of HCP could not decrease mortality of Delta challenged mice. Overall, these data demonstrate that VoC have enhanced immune evasion and this work underscores the need for *in vivo* models to evaluate future emerging strains.

## **2.2 IMPORTANCE**

Emerging SARS-CoV-2 VoC are posing new problems regarding vaccine and monoclonal antibody efficacy. To better understand immune evasion tactics of the VoC, we utilized passive immunization to study the effect of early-pandemic SARS-CoV-2 HCP against, Alpha, Beta, and Delta VoC. We observed that HCP from a human infected with the original SARS-CoV-2 was unable to control lethality of Alpha, Beta, or Delta VoC in the K18-hACE2 transgenic mouse model of SARS-CoV-2 infection. Our findings demonstrate that passive immunization can be used as a model to evaluate immune evasion of emerging VoC strains.

### 2.3. INTRODUCTION

The evolution of Severe Acute Respiratory Syndrome CoV-2 (SARS-CoV-2) variants of concern (VoC) has been a source of escalating epidemiological alarm in the currently ongoing coronavirus disease 2019 (COVID-19) pandemic. SARS-CoV-2 VoC have emerged and are thought to be more infectious and more lethal than the early 2020 original Wuhan-Hu-1 or USA-WA1/2020 (WA-1) strains (115–117). The VoC B.1.1.7, also known as Alpha variant (first identified in the United Kingdom (118)), and B.1.351 also known as Beta variant (first identified in South Africa (119)), were two SARS-CoV-2 VoC that rapidly spread around the world and exhibited high levels of infectivity and therapeutic resistance (117,120–125). Both VoC contain important mutations in the receptor binding domain (RBD) of the spike (S) viral glycoprotein (118,119) that are predicted to impact binding to the human angiotensin converting enzyme 2 (hACE2) viral receptor and enhance viral entry to host cells (126–130). In particular, Alpha contains the D614G and N501Y mutations in the SARS-CoV-2 S RBD which are theorized to increase the ability of the virus to bind to hACE2 (126,128). Beta possesses these key mutations in the S RBD, in addition to the K417N and E484K mutations which are not directly implicated in altered viral transmission and hACE2 binding (130,131). In December 2020, the VoC, B.1.617.2 (Delta) of SARS-CoV-2 first appeared in India, becoming quickly the global predominant circulating variant; however, this distinction could be soon displaced by the novel Omicron variant (132–134). The most common Delta variant has two important mutations on the viral S RBD, L452R and T478K, allowing for increased infectivity, transmissibility, as well as its ability of escaping neutralizing antibodies (135–137). The culmination of high infectivity, therapeutic resistance, and key changes in their viral genome suggests that VoC may have an impact on pathogenicity in animal models of SARS-CoV-2, with a subsequent impact on evaluating vaccines and therapeutics.

The K18-hACE2 transgenic mouse model (138) of SARS-CoV-2 infection was established by several groups in 2020 (139–141). K18-hACE2 transgenic mice infected with SARS-CoV-2 exhibit

significant morbidity and mortality, viral tropism of the respiratory and central nervous systems, elevated systemic chemokine and cytokine levels, significant tissue pathologies, and altered gross clinical measures (140–143). The generation of this mouse model has led to numerous studies of SARS-CoV-2 infection for a variety of purposes including understanding SARS-CoV-2 related immunity, and therapeutic/vaccine testing (139,144–149). As the world experiences an increase in the number of SARS-CoV-2 VoC, it is imperative to adapt existing preclinical animal infection models to these newly emerging VoC. Specifically, it is critical to understand if the K18-hACE2 transgenic mouse model first, is useful for studying SARS-CoV-2 VoC infection dynamics and second, if it exhibits any differences after challenge with newly emerged SARS-CoV-2 VoC. An investigation of these key points will provide context for studies important for developing new therapeutics and prophylactics as the COVID-19 pandemic continues and as new VoC emerge. Neutralizing antibodies against SARS-CoV-2 induce by either natural infection or vaccination serve as an important component of protection against secondary SARS-CoV-2 infection (150); however, according to the WHO and recent data, Omicron variant appears to be able to easily infect fully vaccinated. The S protein is a major target of neutralizing antibodies, with RBD encompassing 90% of the neutralizing antibodies within convalescent sera (151,152). Emergence of new VoC with mutations in the S protein and in the RBD could decrease the efficacy of neutralizing antibodies not originally generated against the VoC. Studies have shown that N-terminal domain S and RBD monoclonal antibodies generated against the original SARS-CoV-2 strain lose neutralization activity against VoC especially when administered as a monotherapy (121,153,154). Human convalescent plasma (HCP) also has demonstrated a decrease in neutralizing antibody efficacy against the VoC that specifically harbor the E484K mutation in the S RBD (121,123). Here, we evaluated the polyclonal antibodies of HCP obtained from a patient infected with the original strain of SARS-CoV-2 against the Alpha, Beta, and Delta VoC in the K18-hACE2 transgenic mouse model. Our findings indicate that when compared to the original WA-1 strain, Alpha, Beta and Delta VoC are more resistant to HCP polyclonal antibodies in the

K18-hACE2 transgenic mouse model. This passive immunity model allows for comparison of *in vivo* activity of human antibodies and extends upon *in vitro* studies and will likely assist us understanding immunity among VoC.

## **2.4 METHODS:**

### **Ethics and biosafety**

The HCP used in this study was obtained under West Virginia University (WVU) IRB no. 2004976401 (155). HCP was obtained from a single individual with PCR-confirmed SARS-CoV-2 infection in March 2020. Experiments with live SARS-CoV-2 were conducted in Biosafety Level 3 (BSL-3) at Texas Biomedical Research Institute (TBRI IBC BSC20-004) or at WVU (IBC 20-09-03). All BSL-3 animal experiments were conducted under WVU IACUC protocol no. 2009036460.

### **Assessment of human IgGs against WA-1 SARS-CoV-2 S RBD and N**

Human IgGs against WA-1 SARS-CoV-2 S RBD and N were quantified using ELISA as described (156). WA-1 S RBD (2 µg/mL) or N (1 µg/mL) proteins were coated on plates and blocked with 3% milk in 0.1% Tween 20 +PBS (PBS-T). Plates were washed three times with PBS-T (200 µL) and virus inactivated samples (25 µL) from human plasma or infected mice were added to 100 µL of sample buffer (1% milk + 0.1% Tween 20 diluted in PBS) and serially diluted (5-fold) down the plates. The final row was left with 100 µL of sample buffer as a negative control. Plates were incubated for 10 minutes at room temperature shaking at 60rpm and subsequently washed four times with PBS-T (200 µL). Secondary antibody (100 µL 1:500 anti-human IgG HRP, Invitrogen 31410) was added and plates were incubated for 10 minutes at room temperature shaking at 60 rpm. After incubation, plates were washed five times with PBS-T (200 µL) and SigmaFAST OPD (Sigma-Aldrich P9187, 100 µL) was added to each well of the plate. OPD development was stopped with 25 µL of 3 M hydrochloric acid and plates were read at an absorbance of 492 nm on a Synergy H1 plate-reader. Binding antibody units (BAU) were calculated based on the NIBSC 1<sup>st</sup> WHO International Standard (NIBSC code 20/136).

Area under the curve analysis was completed in GraphPad Prism v.9.

### **Meso Scale Discovery COVID-19 ACE2 Neutralization assay**

SARS-CoV-2 challenged serum was analyzed using the SARS-CoV-2 Plate 11 Multi-Spot 96-well, 10 spot plate following the manufacturer protocol (catalog #: K15458U-2) on the MSD QuickPlex SQ120. The 10 spots contained RBD from different SARS-CoV-2 VoC: 1) B.1427, B.1.429, B.1.526.1 2) B.1.351, B.1.351.1 3) B.1.525, B.1.526, B.1.618, P.2, R.1 4) P.1 5) B.1.526.2 6) B.1.17 7) B.1.17+E484K, P.3 8) B.1.617, B.1.617.1, B.1.617.3 9) AY.3, AY.4, AY.5, AY.6, AY.7, AY.12, AY.14, B.1.617.2, B.1.617.2+Δ144 and 10) A (WT). Three dilutions of serum, 1:10, 1:50 and 1:100 were analyzed for each mouse to perform Area Under the Curve analysis on the electrochemiluminescence using GraphPad Prism v.9.

### **Viral growth and *in vitro* analysis of SARS-CoV-2 replication**

SARS-CoV-2 USA-WA-1/2020 (NR-52281) (WA-1), B.1.1.7/Alpha (NR-54000), and B.1.351/Beta (NR-54008) strains were obtained from BEI Resources, and SARS-CoV-2 Delta variant B.1.617.2 hCoV-19/USA/WV-WVU-WV118685/2021 (GISAID Accession ID: EPI\_ISL\_1742834) was obtained from a patient sample at WVU. These strains were propagated in Vero E6 cells (ATCC-CRL-1586) as described (140,157). Vero E6 cells for viral titrations (6-well plate,  $10^6$  cells/well) were infected with 10-fold serial dilutions of SARS-CoV-2. At 72 hours post-infection, cells were fixed overnight with 10% formalin (Sigma HT501128-4L), permeabilized and immunostained with 1 $\mu$ g/mL of a SARS-CoV cross-reactive N protein antibody 1C7C7, kindly provided by Dr. Thomas Moran at the Icahn School of Medicine at Mount Sinai. For viral growth kinetics, Vero E6 cells (6-well plate,  $10^6$  cells/well, triplicates) were infected (multiplicity of infection, MOI 0.01) with SARS-CoV-2 WA-1, Alpha or beta. At the indicated times after viral infection (12, 24, 48 and 72 hours), tissue culture samples were collected and titrated by plaque assay as described (140).

### **Genome sequencing of SARS-CoV-2 VoC**

SARS-CoV-2 viral RNA from all stocks used for *in vitro* analyses was deep sequenced according to the method described (158). Briefly, we generated libraries using KAPA RNA HyperPrep Kit (Roche KK8541) with a 45 min adapter ligation incubation including 6-cycle of PCR with 100 ng RNA and 7 mM adapter concentration. Samples were sequenced on an Illumina HiSeq X machine. Raw reads were quality filtered using Trimmomatic v0.39 (159) and mapped to a SARS-CoV-2 reference genome (Genbank Accession No. MN985325) with Bowtie2 v2.4.1 (160). Genome coverage was quantified with MosDepth v0.2.6 (161). We genotyped each sample for low frequency VoC with LoFreq\* v2.1.3.1 (162) and filtered sites with allele frequencies less than 20%. SARS-CoV-2 viral RNA from stocks used for K18-hACE2 transgenic mouse infection was deep sequenced and reads were aligned to the MN908947.3 reference genome using BWA v.0.7.17 (163) and trimmed for base-calling quality using iVar v.1.3.1 (164) with default parameters. Consensus sequence and individual mutations relative to the reference genome were determined using iVar, with a minimum allele frequency of 30% used as a threshold for calling a mutation. Coverage was computed using samtools mpileup v.1.11 (165). Lineage was confirmed using pangolin v.2.3.5 and pangoleARN v.2021-03-16 (166). Authentication of the Betastock was performed using metagenomic sequencing as described (167,168). Viral RNA was treated with Turbo DNase I (Thermo Fisher). cDNA was generated from random hexamers using SuperScript III reverse transcriptase, second strand was generated using Sequenase 2.0, and cleaned using 0.8× Ampure XP beads purification on a SciClone IQ (Perkin Elmer). Sequencing libraries were generated using two-fifths volumes of Nextera XT on ds-cDNA with 18 cycles of PCR amplification. Libraries were cleaned using 0.8×Ampure XP beads and pooled equimolarly before sequencing on an Illumina NovaSeq (1×100bp run). Raw fastq reads were trimmed using cutadapt (-q 20) (169). To interrogate potential resistance alleles, reference-based mapping to NC\_045512.2 was carried out using our modified Longitudinal Analysis of Viral Alleles (LAVA - <https://github.com/michellejilin/lava>) (170) pipeline. LAVA constructs a candidate reference



genome from early passage virus using bwa (163), removes PCR duplicates with Picard, calls variants with VarScan (171,172), and converts these changes into amino acid changes with Annovar (173). The genome sequence for strain Betais accession number QWE88973. The genome sequence of the Beta contained the expected mutations spike and has a wild type furin cleavage site. A 52aa deletion was observed in orf7a; however, it is not expected that this deletion has any impact on the *in vivo* infection capacity of this strain as orf7a mutants are observed in surveillance. Beta VoC was able to effectively colonize and cause morbidity in experiments presented in this study.

### **Challenge of K18-hACE2 transgenic mice with SARS-CoV-2 VoC and treatment with HCP**

SARS-CoV-2 WA-1 and Alpha and Beta VoC were thawed from -80°C and diluted in infection medium (Dulbecco's Modified Eagle Medium 4/.5g/L glucose + 2% fetal bovine serum + 1% HEPES + 1% penicillin/streptomycin at 100 units/ $\mu$ g/mL) to a concentration of  $10^6$  plaque forming units (PFU) /mL in the WVU BSL-3 facility. Delta VoC was diluted to a  $10^4$  PFU/dose from a  $2.4 \times 10^5$  PFU/mL stock in 1X Dulbecco's phosphate buffered saline. Male eight to ten weeks old B6.Cg-Tg(K18-hACE2)2PrImn/J mice (Jackson Laboratory 034860) were anesthetized with a single intraperitoneal dose of ketamine (Patterson Veterinary 07-803-6637, 80 mg/kg) + xylazine (Patterson Veterinary 07-808-1947, 8.3 mg/kg) and 50  $\mu$ L infectious dose was administered with a pipette intranasally, 25  $\mu$ L per nare. HCP, 500  $\mu$ L, or healthy human sera (HHS) with known anti-SARS-CoV-2 IgGs and neutralizing Abs (nAbs) were administered intraperitoneally at this time. For the Delta VoC challenge study, 500  $\mu$ L HCP was administered for 6 consecutive days (Figure 6A). Mice were monitored until awake and alert.

### **Cumulative disease scoring of SARS-CoV-2 challenged mice**

Mice were scored daily on a scale encompassing appearance (score of 0-2), eye health (score of 0-2), respiration (score of 0-2), activity (score of 0-3) and weight loss (score of 0-5). Appearance

included visual identification of a combination of mild to severe piloerection (0-2) or lack of grooming (0-2). Eye health scores were defined by observation of squinting (1), prolonged eye closure not related to sleep (2), or eye discharge (0-2) depending on severity. The maximal combined score for eye health was 2. Respiration (assessed visually) outside the range of 80-240 breaths per minute required mandatory euthanasia and scored as 2. Respiration that was abnormal in regularity was scored as 1. Activity was scored as slow (1), immobile (2), or collapsed and immobile (3). Weight loss was scored as 0-5% (0), 5-10% (1), 10-15% (2) 15-20% (3), >20% (4-5). All mice with weight loss greater than 20% were humanely euthanized. Rectal temperature was also monitored daily throughout the experiments.

### **Euthanasia and necropsy of SARS-CoV-2 challenged mice**

Euthanasia was conducted by administering 200  $\mu$ L of pentobarbital (Patterson Veterinary 07-805-9296, 390 mg/kg diluted in 0.9% sterile NaCl) and cardiac puncture. Blood was aliquoted into gold serum separator tubes (BD 365967) and centrifugated at 15,000 x *g* for 5 min. Serum was removed and stored in 1.5 mL tubes at -80°C until needed. Lungs were removed from animals and the right lobes of the lung were homogenized in 1mL of PBS in Miltenyi C tubes (Miltenyi Biotec 130-096-334) using the m\_lung\_02 program on a Miltenyi gentleMACS tissue dissociator. An aliquot of each lung homogenate (300  $\mu$ L) was added to 100  $\mu$ L of TRIReagent (Zymo Research R2050-1-200) and stored at -80°C. Remaining homogenates (300  $\mu$ L) were spun down at 15,000 x *g* and the supernatants collected. Pellets were frozen at -80°C until use. Brain tissue was removed from animals and split down the mid-line. The right brain was added to 1 mL of PBS in Miltenyi C tubes and homogenized using the m\_lung\_02 program. An aliquot of each homogenate (500  $\mu$ L) was added 167  $\mu$ L aliquots of TRIReagent and stored at -80°C until use. Remaining homogenates were frozen at -80°C until use. To inactivate virus from tissue samples, 1% v/v Triton X-100 (Sigma-Aldrich T8787) (141) was added to each sample and incubated for 1

hour at room temperature. Inactivated samples were then removed from the BSL-3 High Containment facility.

### **Evaluating viral copy number in SARS-CoV-2 challenged tissues**

RNA from homogenized virus-inactivated lung and brain tissues of SARS-CoV-2 infected mice was extracted using the Direct-zol RNA MiniPrep Kit (Zymo Research R2051) following the manufacturer's instructions. RT-PCR and qPCR were performed by generating a master mix of: 10  $\mu$ L of TaqMan RT-PCR Mix from the Applied Biosystems TaqMan RNA to CT One Step Kit (Thermo-Fisher Scientific 4392938), 900 nM (1.8  $\mu$ L) of (ATGCTGCAATCGTGCTACAA) forward nucleocapsid primer (141), 900 nM (1.8  $\mu$ L) of (GACTGCCGCCTCTGCTC) reverse nucleocapsid primer (141), 250nM (0.5  $\mu$ L) of TaqMan probe (56-FAM/TCAAGGAAC/ZEN/AACATTGCCAA/3IABkFQ), 0.5  $\mu$ L of TaqMan RT enzyme from the Applied Biosystems TaqMan RNA to CT One Step Kit (Thermo-Fisher Scientific 4392938), 100 ng of RNA, and RNase/DNase free water to make a 20  $\mu$ L total reaction volume. Samples were run in triplicate in Microamp Optical 96-well Fast Reaction Plates (Thermo-Fisher Scientific 4306737) through the following protocol: reverse transcription at 48°C for 15 minutes, activation of AmpliTaq Gold DNA polymerase at 95°C for 10 minutes, and 50 cycles of 95°C denaturing for 10 seconds followed by 60°C annealing for 60 seconds. Samples were run on an Applied Biosystems StepOnePlus Real-Time PCR System. Samples with undetectable virus were assigned a value of 1.  $C_T$  values and copy numbers were calculated and analyzed in Microsoft Excel and GraphPad Prism v.9.0.0.

### **Cytokine analysis of serum-treated SARS-CoV-2 VoC challenged mice**

Virus-inactivated serum samples or lung supernatants from SARS-CoV-2 VoC infected mice were added to a custom 8-plex Mouse Magnetic Luminex Assay (R&D Systems LXSAMSM-08) including IL-6, TNF, IFN- $\gamma$ , IL-10, IL-27, IL-1 $\beta$ , IL-2, IL-13, and IL-17 at the recommended dilution factor (2-fold dilution). Cytokine arrays were read on a Luminex MagPix instrument.

### **Lung Histopathology**

Left lobes of lungs were fixed in 10 mL of 10% neutral buffered formalin. Fixed lungs were paraffin embedded into 5 µm sections. Sections were stained with hematoxylin and eosin (H&E) and sent to iHisto for pathological analysis. Lungs were scored by a pathologist for chronic and acute inflammation in the lung parenchyma, blood vessels, and airways. Pathologist was blinded to the experimental groups but was aware of groups that were challenged with SARS-CoV-2. Each mouse was scored individually using a standard qualitative toxicologic scoring criteria: 0-none; 1-minimal; 2-mild; 3-moderate; 4-marked; 5-severe. Chronic inflammation was marked by lymphocytes, plasma cells, and alveolar macrophages in the parenchyma, blood vessels and airway. Acute inflammation was scored by the presence of neutrophils and edema in the parenchyma, blood vessels and airway.

### **Statistical analyses**

All statistical tests were performed on groups with  $n \geq 5$  in GraphPad Prism v.9.0.0. To compare two-groups, student's *t*-tests were used. To compare three or more groups, one-way ANOVA (parametric data) or Kruskal-Wallis (non-parametric data) were used followed by Tukey's (parametric data) or Dunn's (non-parametric data) multiple comparisons tests. To compare grouped data, two-way ANOVA with no correction was performed followed by Tukey's multiple comparison test. To assess statistical differences between Kaplan-Meier curves, Mantel-Cox log-rank tests were performed.

## **2.5 RESULTS**

**Evaluating human antibodies against original SARS-CoV-2 for their ability to protect VoC challenged mice.** The emergence of SARS-CoV-2 VoC requires re-investigation of their pathogenesis and unique properties. Our goal for this part of the study was to determine if ancestral virus specific antibodies raised in humans would be able to provide protection against Alpha and Beta VoC challenge in K18-hACE2-mouse challenge model. HCP was extensively

used early in the COVID-19 pandemic, but currently it is no longer used as a standard of care. The selected HCP for these studies originated from a patient with severe COVID-19 disease in 2020 and contained 236 antibody binding units (WHO COVID-19 International Standard; BAU). This HCP was compared to other 48 HCP samples from COVID-19 patients taken back in spring of 2020 (Fig. 1A). Next, the selected HCP was compared to serum obtained from pre-vaccine and post Pfizer mRNA vaccinated healthy volunteers. The selected HCP sample was able to neutralize Wuhan, Alpha, Beta, and Delta RBD to ACE2 binding using the MSD hACE2-RBD *in vitro* neutralization assay (Fig. 1B). These data indicate that the selected HCP had high binding and neutralization capacity. *In vitro* cell culture growth experiments were performed to characterize the Alpha and Beta VoC. The Beta variant appeared to have a modest increase in PFU/ml after 24 hours of growth *in vitro* (Fig. 1CD); however, it had a relatively similar growth curve compared to the original WA-1 strain and Alpha VoC. One caveat about using Alpha or Beta challenge strains in mice, is that it is possible the mutations in RBD will allow for binding and engagement of the mouse ACE2 receptor. Mouse adapted SARS-CoV-2 strains are used to challenge wild type, non-transgenic mice (174) and VoC strains are known to replicate in wild type mice (175). We performed a study with Alpha and Beta VoC in wild type C57BL6/J mice; however, morbidity or mortality was not observed (Fig. 1E). We observed low disease scores, and very little detectable viral RNA in the lungs of the wild type challenged mice (Fig. 1FG). Based on these data, we do not believe there is much concern about using Alpha or Beta in mice because it appears their ability to infect through mouse ACE2 is limited.

**Viral challenge and effects of HCP treatment on disease progression in mice challenged with SARS-CoV-2 VoC.** K18-hACE2 transgenic mice were passively immunized with HCP via intraperitoneal administration at day 0 and subsequently challenged with  $10^5$  PFU (lethal dose) of WA-1, Alpha, or Beta VoC (Fig. 2A). WA-1 challenged mice that received human serum from healthy individuals (HHS) exhibited a temperature drop, weight loss, and high cumulative disease

scores (Fig. 2BEH). Mice treated with HCP had normal temperature regulation, maintained weight, and had low disease scores (Fig. 2BEH). Protection from WA-1 lethal challenge in HCP treated mice was expected since convalescent humans have immunity against re-challenge. Challenge with Alpha VoC in HHS treated mice resulted in high temperature loss by day 4 post challenge, up to 20% weight loss, and high cumulative disease scores (Fig. 2 CFH). However, Alpha VoC challenged mice treated with HCP maintained body temperature in two of five animals and similar trends were observed for their body weight loss (Fig. 2CF). These data suggested that HCP was less successful at protecting mice from Alpha VoC challenge compared to WA-1. Disease scores also reflected these observations as HCP treatment was unable to fully suppress disease (Fig. 2H). Unlike WA-1 or Alpha VoC challenged mice, Beta VoC challenged mice treated with HCP compared to HHS had no significant differences by any metric measured (Fig. 2DGH). HCP treatment was unsuccessful in preventing disease and morbidity induced by the Beta VoC. Collectively, these data showed that HCP treatment was able to fully protect against WA-1; partially protect against Alpha VoC; but failed to protect against Beta VoC (Fig. 3AB).

**Effects of HCP treatment on viral RNA burden in lungs and brain of challenged mice.** To determine the viral distribution between the lungs and brain of challenged mice, qRT-PCR was used to quantify nucleocapsid copy number. HCP treatment significantly decreased viral RNA down to the lower limit of detection (LLOD) in the lung of the WA-1 and Alpha challenged mice compared to HHS (Fig. 3C). Similarly, HCP treatment was also able to decrease the Alpha VoC viral burden down to the same low level. Beta variant challenged mice had two logs lower RNA and HCP treatment was able to decrease two of the mice down to the LLOD. A lethal dose of SARS-CoV-2 WA-1 is known to infiltrate the brain of K18-hACE2 transgenic mice (141,176). As expected, brain WA-1 viral copy numbers were decreased due to HCP treatment (Fig. 3D). Similarly, three of five Alpha VoC challenged mice had low viral RNA detected in their brain (Fig. 3D), which correlated with their temperature, weight, and survival data (Fig. 2 and 3). Surprisingly,

HCP treatment did not decrease brain Beta VoC virus RNA copies, further demonstrating the ability of Beta VoC to break through antibody protection that was derived against original Wuhan or WA-1-like viruses (Fig. 3D).

**Human and mouse IgG levels in convalescent plasma treated K18-hACE2 transgenic mice infected with SARS-CoV-2 VoC.** To determine the level of IgGs delivered to HHS and HCP treated mice, we analyzed whether human anti-SARS-CoV-2 IgGs were present within the lung and sera of animals treated with HCP or HHS through the course of infection (Fig. 4AB). Data demonstrate that significant quantities of human anti-SARS-CoV-2 IgGs targeting both the RBD and nucleocapsid proteins were present at two days post-challenge in HCP-treated relative to HHS-treated mice (data not shown). Overall, these data indicate that passive immunization resulted in persistence of human antibodies in mice through the experimental timeframe studied.

**HCP treatment lowered chronic and acute inflammation in the lung caused by SARS-CoV-2 challenge.** Histopathology analysis was performed to characterize disease manifestation in the lung due to inflammation caused by WA-1, Alpha, and Beta challenge during HHS and HCP treatments (Fig. 5). Chronic inflammation was denoted as presence of lymphocytes, plasma cells and alveolar macrophages, whereas acute inflammation was characterized by neutrophils and edema in the lung parenchyma, vasculature, and bronchi. Total inflammation was determined by the addition of chronic and acute inflammation scores. HHS treatment groups challenged with WA-1, and with Alpha and Beta VoC had the highest chronic and acute inflammation scores in the lung parenchyma and surrounding blood vessels compared to the HCP treated mice (Fig. 5ACDE). HHS treated mice challenged with WA-1 and Alpha VoC had the highest average total inflammation scores of 7.4 and 8.8, respectively; whereas Beta VoC challenged mice had an average total inflammation score of 4.0 (Fig. 5CD). HCP treatment groups challenged with WA-1, and Alpha and Beta VoC also had mixed chronic and acute inflammation albeit lower total

inflammation compared to HHS treated mice (Fig. 5BCD). HCP treated mice challenged with WA-1 had the highest average total inflammation score (4.0), characterized by more chronic inflammation than acute (Fig.5CD). Mice treated with HCP and challenged with Alpha VoC had an average inflammation score of 4.4 and decreased acute inflammation compared to HHS treatment (Fig. 5D). Interestingly, HHS and HCP treated mice challenged with Beta VoC had low lung inflammation (Fig. 5CD), which correlated with the low viral RNA burden of Beta VoC (Fig. 3C). Overall, HHS treated, and SARS-CoV-2 challenged mice had elevated levels of both chronic and acute inflammation compared to the HCP treated and challenged mice.

**HCP passive immunization was insufficient to protect against Delta VoC challenge.** Delta VoC contains mutations on the RBD that compromise antibody neutralization (137). We further evaluated whether polyclonal antibodies in the HCP generated from an original virus immune plasma could protect mice from a lethal Delta VoC challenge. Here, we used a challenge dose of  $10^4$  PFU/dose of Delta VoC instead of a  $10^5$  PFU/dose as we previously used for WA-1, Alpha, and Beta VoC. In pilot studies, we demonstrated that  $10^4$  PFU/dose of Delta VoC resulted in 100% morbidity in K18-hACE2 transgenic mice (data not shown). Thus, mice were administered HCP (n=5) or PBS (n=5) intraperitoneally and concurrently intranasally challenged with a lethal Delta VoC dose on day 0 (Fig. 6A). HCP treated mice received treatment for 5 consecutive days after the first dose on day 0. All mice were monitored for disease for 7 days (Fig. 6A). Mice that did not receive HCP treatment succumbed to Delta VoC challenge by day 6 and had elevated cumulative disease scores (Fig 6BC). However, only 20% of mice that received 6 treatments of HCP survived the Delta VoC challenge and had disease scores similar to untreated mice (Fig. 6BC). Viral RNA burden mirrored survival and disease scores for both HCP treated and untreated mice. Lung, brain, and nasal wash (NW) of the HCP treated mice had similar levels of viral RNA compared to untreated mice indicating that HCP treatment did not block viral replication (Fig. 6DEF). Overall, polyclonal antibodies generated against the ancestral SARS-CoV-2 strain did not protect mice



from Delta VoC challenge suggesting that the Delta VoC is resistant to polyclonal antibodies generated against Wuhan-lineage virus strains.

## 2.6 DISCUSSION

SARS-CoV-2 VoC are constantly evolving and dramatically impacting the ongoing COVID-19 pandemic. Since the beginning of the pandemic, three major infection waves have occurred: 1) original virus, 2) Alpha variant, and 3) Delta variant, with a recent wave starting directed by the novel Omicron (B.1.1.529) VoC. Approved vaccines are implemented all around the world with 8 billion total doses administered meaning 1 dose per person in the world. However, there are massive inequities in vaccine coverage with US/Canada, Latin America, Asia-Pacific, and Europe with ~60-70% vaccination with one dose, whereas Africa is only at 10% coverage with one dose. Overall, the world is at 56% vaccine coverage with one dose. All current vaccines are designed against the original virus spike antigen sequence, but two major waves have been fueled by the Alpha and Delta VoC. Vaccine re-development will always be a challenge and new VoC have been constantly arising.

Alpha and Beta VoC spike antigens were extensively studied by binding and neutralization assays that suggested antibodies generated by infection or vaccination would be able to provide protection. Ultimately relatively low numbers of vaccine breakthrough occurred. In order to confirm the *in vitro* predictions regarding Alpha and Beta VoC, we designed this study to use a passive immunization model in K18-hACE2 transgenic mice to compare antibody dependent immunity between original virus vs. VoC. Our observations suggest that Alpha VoC is partially neutralized in K18-hACE2 transgenic mice treated with HCP (Fig. 2 and 3), whether the Beta VoC was not sufficiently neutralized to prevent lethality in this model system (Fig. 2 and 3). HCP treatment dramatically decreased viral RNA burden of the lungs and brain in WA-1 and Alpha VoC challenged mice, but minimal to no decrease was observed in mice challenged by the Beta VoC (Fig. 3CD), which likely contributed to the morbidity and mortality caused by the Beta VoC.

Low viral burden in the lung correlated with low chronic or acute inflammations scores (Fig. 5). Antibody breakthrough and aggressive pathogenesis suggested that the Beta VoC was going to likely be a variant of high concern. When Beta variant appeared, it was able to impact vaccine trial efficacy studies and seemed poised to infect vaccinated people (35,177,178). However, the Beta VoC peaked at a total of 12% genome worldwide frequency by April 2021. Thus, it seems likely that the Beta VoC was not highly transmissible, and our passive immunization model does not take this variable into consideration.

HCP as a treatment was used widely since the onset of the COVID-19 pandemic (179–181), but its efficacy was questionable (182–185) and convalescent plasma therapy for COVID-19 has been replaced as a treatment by monoclonal antibodies. In this study, we used HCP from an early pandemic COVID-19+ severe disease patient to understand how antibodies generated against the original SARS-CoV-2 strain would function against Alpha and Beta VoC. In December 2020, the Delta VoC appeared in India and by mid-2021, this VoC was the dominant variant found in genomic surveillance. To build upon our observations regarding Alpha and Beta VoC in the HCP passive immunity model with K18-hACE2 transgenic mice, we next aimed to evaluate the Delta VoC. Our pilot studies indicated a massive histopathological and inflammatory gene expression in Delta VoC vs. Alpha VoC challenged mice (data not shown). We reasoned that the Delta VoC was more aggressive and would likely need a lower dose to be fully virulent compared to WA-1 strain and would also require more HCP in order to neutralize the virus *in vivo*. Thus, we challenged mice with a lower dose of  $10^4$  PFU and HCP treatment was provided daily out to 6-days post challenge. Unexpectedly, even though we provided 6X more HCP, mice were morbid with high disease scores and high viral burden (Fig. 6). It is now well appreciated that Delta VoC can cause breakthrough cases in previously infected as well as vaccinated humans (186,187). Currently, with the highly mutated Omicron VoC, passive immunity and active immunization studies in pre-clinical models will be important to determine the breakthrough capacity of this new VoC. Furthermore, HCP or mAb passive studies can inform the scientific community about

enhanced virulence or immune subversion of VoC and we anticipate this passive model can be applied going forward for rapid responses to characterize new variants.

In summary, this study provides insights into differences in SARS-CoV-2 VoC pathogenicity in K18-hACE2 transgenic mice in relation to antibody immunity. Passive immunization of mice with human antibodies can allow for robust characterization of breakthrough capacity (134,188). This study demonstrates increased disease pathology for mice challenged with Alpha and Beta VoC, and the lack of protection from HCP in mice challenged with Beta or Delta VoC. These data corroborate observations about Beta and Delta VoC in human populations. The human convalescent plasma passive immunity model presented here can be useful in supporting *in vitro* studies and facilitate decision making and planning of research priorities around the overall immune evasion characteristics of SARS-CoV-2 variants.

## **2.7 ACKNOWLEDGEMENTS**

We would like to express our gratitude to Laura Gibson and Clay Marsh for enabling this research through resources and support. This project was supported by the Vaccine Development Center at the West Virginia University Health Sciences Center. F.H.D. and the VDC are supported by the Research Challenge Grant no. HEPC.dsr.18.6 from the Division of Science and Research, WV Higher Education Policy Commission. Flow cytometry analyses were supported financially by the West Virginia University Flow Cytometry & Single Cell Core Facility, which is supported by the National Institutes of Health equipment grant number S10OD016165 and the Institutional Development Awards (IDeA) from the National Institute of General Medical Sciences of the National Institutes of Health under grant numbers P30GM121322 (TME CoBRE) and P20GM103434 (INBRE).

**AUTHOR CONTRIBUTIONS:** A.M.H, F.H.D, I.M, J.B.T, C.Y and L.M.S designed the experiments. C.Y performed *in vitro* analyses of SARS-CoV-2 VoC, and J.S., A.G, and R.K.P performed sequencing. M.T.W and I.M propagated virus for animal experiments. A.M.H, T.Y.W, B.P.R, K.S.L, O.A.M., M.C., H.A.C. and F.H.D challenged and euthanized animals, dissected organs, and prepared them for analyses. A.M.H, B.P.R, and N.A.R. performed ELISA against SARS-CoV-2 antigens and A.M.H, T.Y.W, H.A.C. and O.A.M. performed qPCR to determine viral load. A.M.H performed cytokine analyses. J.D analyzed sequence data from viral passages used for infection of K18-hACE2 transgenic mice. A.M.H, F.H.D, and T.Y.W. analyzed, formatted, and represented data for publication. All authors contributed to the writing and revision of the manuscript.

**DECLARATION OF INTERESTS:** The authors declare no competing interests.

## 2.8 FIGURES

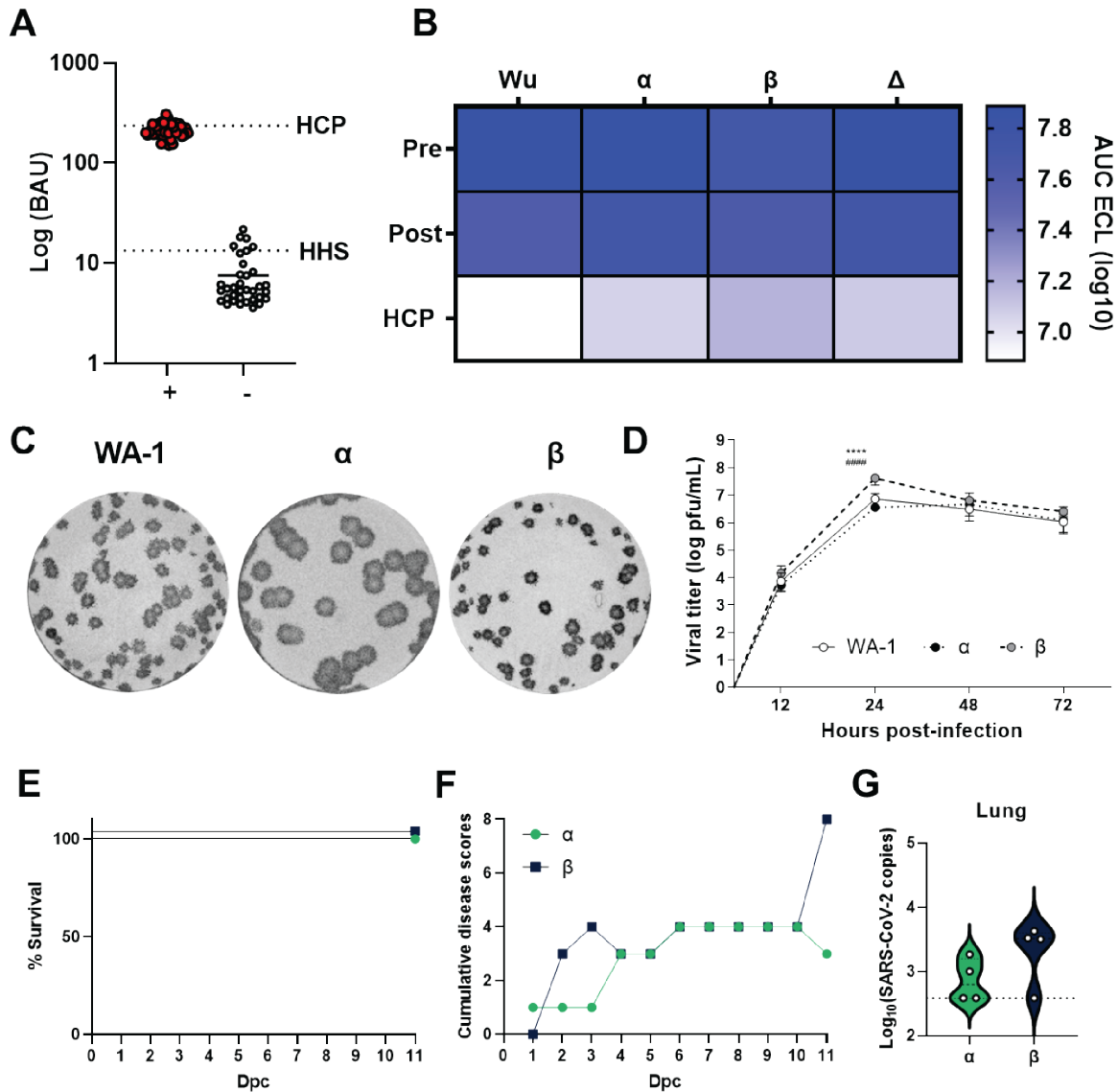


**Figure 1. Characterization of early pandemic human convalescent plasma and in vitro characterization of SARS-CoV-2 variants.**

(A) RBD human IgG Binding antibody units (BAU) of SARS-CoV-2 + (red dots) compared to SARS-CoV-2 – patients (white dots). HCP dotted line indicate the BAU of the human convalescent plasma from a severe COVID-19 patient utilized in passive immunization studies in K18-hACE2 transgenic mice. HHS dotted line indicate the BAU of the healthy human serum used

in passive immunization studies in K18-hACE2 transgenic mice. (B) ACE2-RBD neutralization was assayed, and the human convalescent plasma utilized was more capable of neutralizing receptor binding than mRNA vaccinated human sera. The heat map depicts the log<sub>10</sub> AUC of electro chemiluminescent (ECL) values. (C) Plaque morphology of SARS-CoV-2 WA-1, Alpha or Beta infected VeroE6 cells. (D) Quantification of viral replication of SARS-CoV-2 variants in VeroE6 cells over time was quantified. Statistical analysis of viral replication was completed by two-way ANOVA followed by Tukey's multiple comparison test, or RM ANOVA followed by Tukey's multiple comparison test. \*\*\*\* = P < 0.0001 relative to WA-1, ##### = P < 0.0001 relative to Alpha. C57BL6/J Mice were infected with 105 pfu SARS-CoV-2 VoC monitored for survival (E) and disease score (F). (G) Challenge with Alpha or Beta variants resulted in low detectable virus at day 11 post challenge.

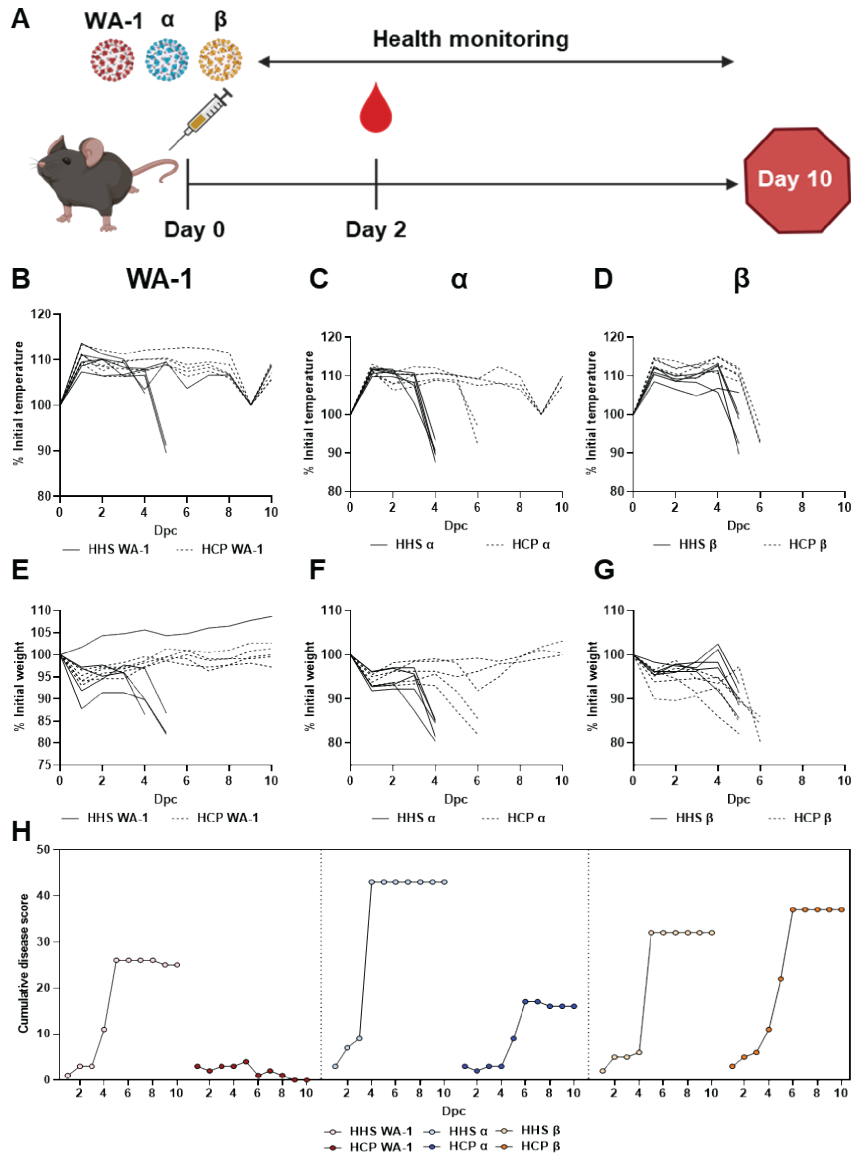


**Figure 2** Effect of convalescent plasma treatment on SARS-CoV-2 VoC infection in K18-hACE2 transgenic mice. (A) Passive immunization and SARS-CoV-2 challenge schematic. Mice were challenged with  $10^5$  PFU of SARS-CoV-2 WA-1 and VoC and simultaneously treated intraperitoneally with 500  $\mu$ L HHS or HCP on day 0. Mice were monitored for temperature (B-D), body weight (E-G) and cumulative clinical score (H) over the 7-day course of infection.

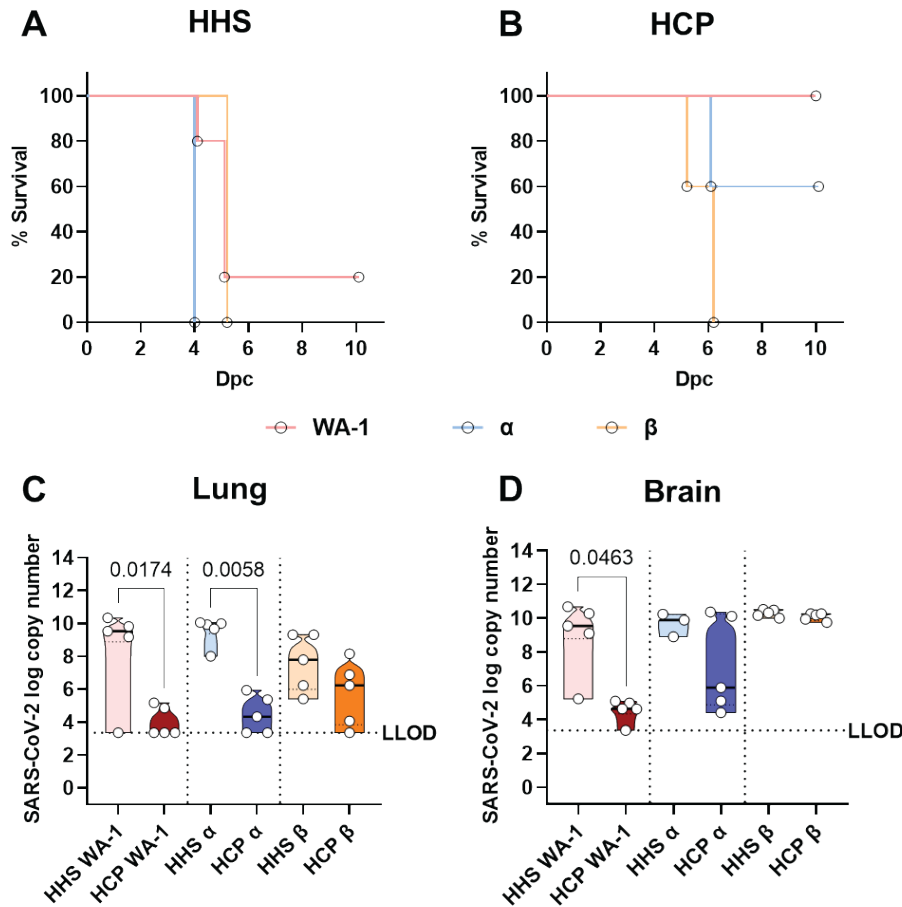


**Figure 3 Survival and viral infection of serum-treated K18-hACE2 transgenic mice infected with SARS-CoV-2 VoC.** Kaplan-Meier survival curves of mice infected with Alpha, beta, or WA-1 treated with HHS (A) or early pandemic SARS-CoV-2 HCP (B). Viral copy numbers in the lung (C) and brain (D) of infected mice. LLOD = lower limit of detection based on a standard curve. Statistical significance of survival curves was assessed with the Mantel-Cox test. For HHS, WA-1 vs Alpha  $P = 0.0143$ ; WA-1 vs Beta  $P = 0.9372$  and Alpha vs Beta  $P = 0.0027$ . For HCP, WA-1 vs Alpha  $P = 0.1336$ ; WA-1 vs Beta  $P = 0.0031$  and Alpha vs Beta  $P = 0.0290$ . Statistical significance between viral copy number was assessed by a Kruskal-Wallis test followed by Dunn's multiple comparisons test.  $n > 3$  subjects per group.  $P$  values for significant differences are reported.



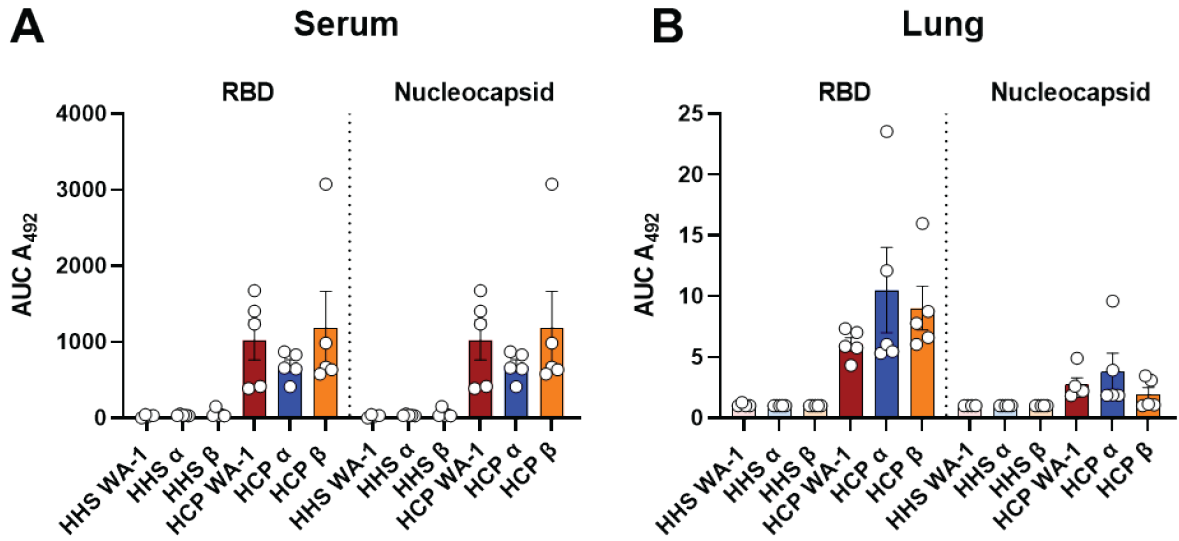


**Figure 4 Human anti-SARS-CoV-2 IgGs in serum-treated K18-hACE2 transgenic mice challenged with SARS-CoV-2 VoC.** Area under the curve (AUC) analyses of anti-RBD IgG levels in the serum (A) or lung (B) of HHS or HCP VoC challenged mice. Statistical significance between AUCs was assessed by a Kruskal-Wallis test followed by Dunn's multiple comparisons test.  $n > 3$  subjects per group.

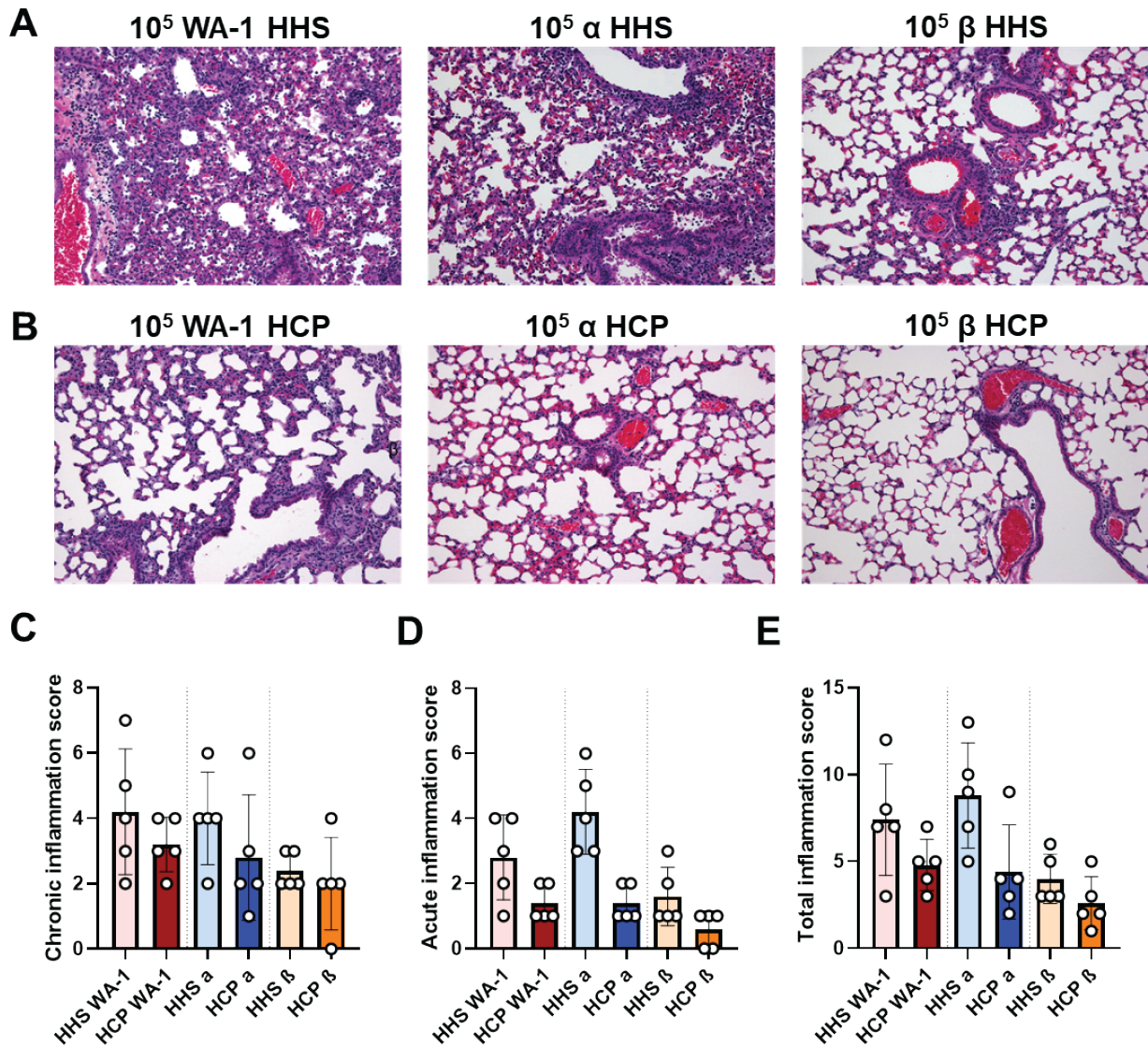


**Figure 5 Histopathological analysis of VoC challenged lungs.** Left lobes of lungs from HHS and HCP treated and SARS-CoV-2 challenge mice were subjected to H&E staining (A) 200X magnification of the lung in HHS treated and SARS-CoV-2 challenged mice (B) 200X magnification of the lung in HCP treated and SARS-CoV-2 challenged mice (C) Total chronic inflammation scores of each mouse. (D) Total acute inflammation score of each mouse. (E) Total inflammation score (chronic + acute) for each mouse. All statistical analysis was performed using Kruskal-Wallis test with Dunn's multiple comparisons test. All results represented as mean  $\pm$ SD.

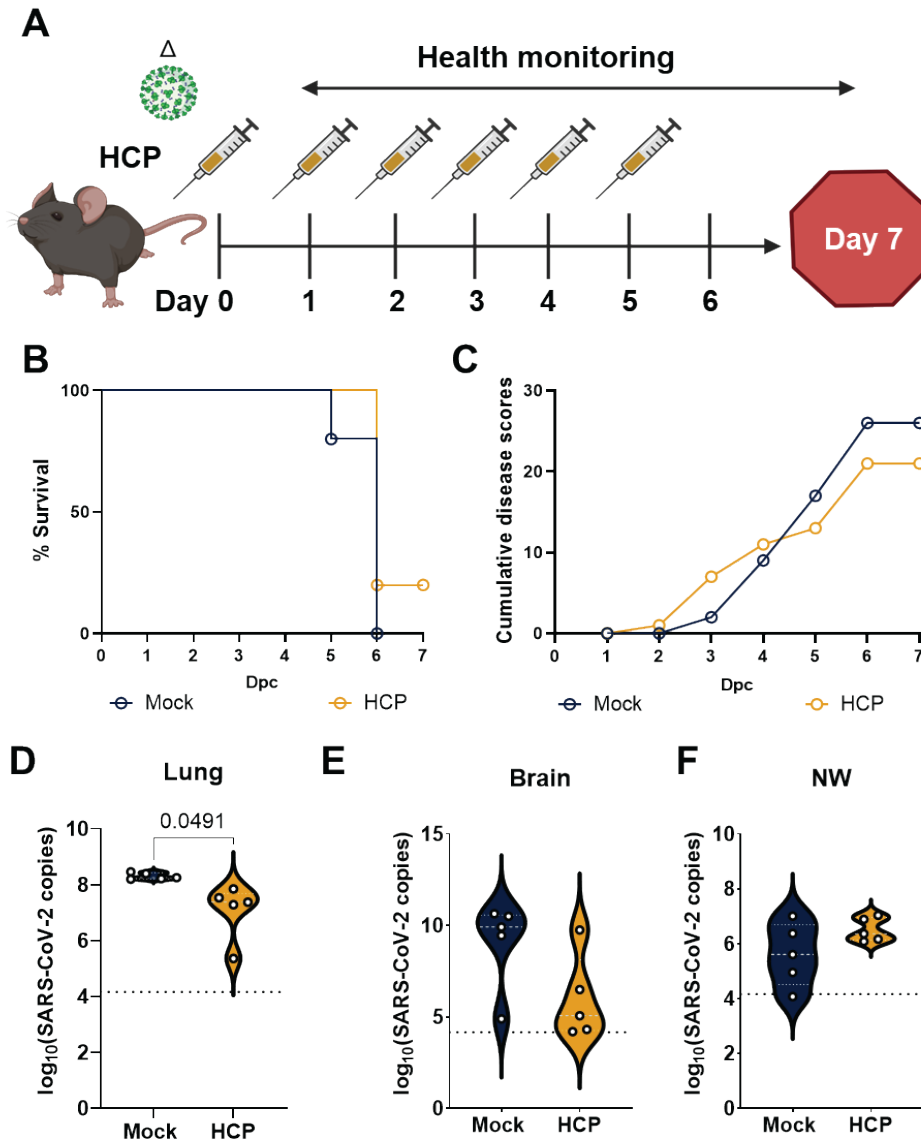


**Figure 6 HCP passive immunization was insufficient to protect against Delta variant challenge.** (A) Experimental workflow of passive immunization study with HCP and challenge with lethal dose of Delta variant ( $10^4$  PFU/dose). (B) Kaplan Meier survival curve comparing Delta challenged mice that received either 1XDPBS vehicle or HCP. (C) Cumulative disease scores comparing Delta challenged mice that received either 1XDPBS vehicle or HCP. SARS-CoV-2 nucleocapsid RNA copies in (A) lung, (B) brain, and (C) nasal wash of untreated and HCP treated and challenged mice. All statistical analysis was performed using Welch's t test.  $P = 0.0491$ .

## 2.9 REFERENCES:

1. Korber B, Fischer WM, Gnanakaran S, Yoon H, Theiler J, Abfalterer W, Hengartner N, Giorgi EE, Bhattacharya T, Foley B, Hastie KM, Parker MD, Partridge DG, Evans CM, Freeman TM, de Silva TI, Angyal A, Brown RL, Carrilero L, Green LR, Groves DC, Johnson KJ, Keeley AJ, Lindsey BB, Parsons PJ, Raza M, Rowland-Jones S, Smith N, Tucker RM, Wang D, Wyles MD, McDanal C, Perez LG, Tang H, Moon-Walker A, Whelan SP, LaBranche CC, Saphire EO, Montefiori DC. 2020. Tracking Changes in SARS-CoV-2 Spike: Evidence that D614G Increases Infectivity of the COVID-19 Virus. *Cell* 182:812-827.e19.
2. Toyoshima Y, Nemoto K, Matsumoto S, Nakamura Y, Kiyotani K. 2020. SARS-CoV-2 genomic variations associated with mortality rate of. *J Hum Genet* 1075–1082.
3. Challen R, Brooks-Pollock E, Read JM, Dyson L, Tsaneva-Atanasova K, Danon L. 2021. Risk of mortality in patients infected with SARS-CoV-2 variant of concern 202012/1: Matched cohort study. *BMJ* 372:1–10.
4. Rambaut A, Loman N, Pybus O, Barclay W, Barrett J, Carabelli A, Connor T, Peacock T, Robertson DL, Volz E. 2020. Preliminary genomic characterisation of an emergent SARS-CoV-2 lineage in the UK defined by a novel set of spike mutations.
5. Tegally H, Wilkinson E, Giovanetti M, Iranzadeh A, Fonseca V, Giandhari J, Doolabh D, Pillay S, San EJ, Msomi N, Mlisana K, von Gottberg A, Walaza S, Allam M, Ismail A, Mohale T, Glass AJ, Engelbrecht S, Van Zyl G, Preiser W, Petruccione F, Sigal A, Hardie D, Marais G, Hsiao M, Korsman S, Davies M-A, Tyers L, Mudau I, York D, Maslo C, Goedhals D, Abrahams S, Laguda-Akingba O, Alisoltani-Dehkordi A, Godzik A, Wibmer CK, Sewell BT, Lourenço J, Alcantara LCJ, Pond SLK, Weaver S, Martin D, Lessells RJ, Bhiman JN, Williamson C, de Oliveira T. 2020. Emergence and rapid spread of a new severe acute respiratory syndrome-related coronavirus 2 (SARS-CoV-2) lineage with multiple spike mutations in South Africa. *medRxiv* 2020.12.21.20248640.

6. Davies NG, Davies NG, Abbott S, Barnard RC, Jarvis CI, Kucharski AJ, Munday JD, Pearson CAB, Russell TW, Tully DC, Washburne AD, Wenseleers T, Gimma A, Waites W, Wong KLM, Zandvoort K Van, Silverman JD, Working CC-, Consortium C-GUKC, Diazordaz K, Keogh R. 2021. Estimated transmissibility and impact of SARS-CoV-2 lineage B.1.1.7 in England 3055:1–16.
7. Wang P, Nair MS, Liu L, Iketani S, Luo Y, Guo Y, Wang M. 2021. Antibody Resistance of SARS-CoV-2 Variants B.1.351 and B.1.1.7. *Nature* <https://doi.org/10.1038/s41586-021-03398-2>.
8. Galloway SE, Prbasaj P, MacCannell DR, Johansson MA, Brooks JT, MacNeil A, Slayton RB, Tong S, Silk BJ, Armstrong GL, Biggerstaff M, Dugan VG. 2021. Emergence of SARS-CoV-2 B.1.1.7 Lineage — United States, December 29, 2020–January 12, 2021 70:95–99.
9. Chen RE, Zhang X, Case JB, Winkler ES, Liu Y, VanBlargan LA, Liu J, Errico JM, Xie X, Suryadevara N, Gilchuk P, Zost SJ, Tahan S, Droit L, Turner JS, Kim W, Schmitz AJ, Thapa M, Wang D, Boon ACM, Presti RM, O'Halloran JA, Kim AHJ, Deepak P, Pinto D, Fremont DH, Crowe JE, Corti D, Virgin HW, Ellebedy AH, Shi P-Y, Diamond MS. 2021. Resistance of SARS-CoV-2 variants to neutralization by monoclonal and serum-derived polyclonal antibodies. *Nat Med* <https://doi.org/10.1038/s41591-021-01294-w>.
10. 2021. FACT SHEET FOR HEALTH CARE PROVIDERS EMERGENCY USE AUTHORIZATION (EUA) OF REGEN-COV™ (casirivimab with imdevimab) 564:1–30.
11. 2021. FACT SHEET FOR HEALTH CARE PROVIDERS EMERGENCY USE AUTHORIZATION (EUA) OF BAMLANIVIMAB AND ETESEVIMAB 1–34.
12. Tian F, Tong B, Sun L, Shi S, Zheng B, Wang Z, Dong X, Zheng P. 2021. Mutation N501Y in RBD of Spike Protein Strengthens the Interaction between COVID-19 and its Receptor ACE2. *bioRxiv* 19:2021.02.14.431117.
13. Shah M, Ahmad B, Choi S, Woo HG. 2020. Mutations in the SARS-CoV-2 spike RBD are responsible for stronger ACE2 binding and poor anti-SARS-CoV mAbs cross-

- neutralization. *Comput Struct Biotechnol J* 18:3402–3414.
14. Ozono S, Zhang Y, Ode H, Sano K, Tan TS, Imai K, Miyoshi K, Kishigami S, Ueno T, Iwatani Y, Suzuki T, Tokunaga K. 2021. SARS-CoV-2 D614G spike mutation increases entry efficiency with enhanced ACE2-binding affinity. *Nat Commun* 12.
  15. Bozdaganyan ME, Sokolova OS, Shaitan K V, Kirpichnikov MP, Orekhov PS. 2021. Effects of Mutations in the Receptor-Binding Domain of SARS-CoV-2 Spike on its Binding Affinity to ACE2 and Neutralizing Antibodies Revealed by Computational Analysis. *bioRxiv* 2021.03.14.435322.
  16. Laffeber C, de Koning K, Kanaar R, Lebbink JH. 2021. Experimental evidence for enhanced receptor binding by rapidly spreading SARS-CoV-2 variants. *bioRxiv*.
  17. Zhou D, Dejnirattisai W, Supasa P, Liu C, Mentzer AJ, Ginn HM, Zhao Y, Duyvesteyn HME, Tuekprakhon A, Nutalai R, Wang B, Paesen GC, Lopez-Camacho C, Slon-Campos J, Hallis B, Coombes N, Bewley K, Charlton S, Walter TS, Skelly D, Lumley SF, Dold C, Levin R, Dong T, Pollard AJ, Knight JC, Crook D, Lambe T, Clutterbuck E, Bibi S, Flaxman A, Bittaye M, Belij-Rammerstorfer S, Gilbert S, James W, Carroll MW, Klenerman P, Barnes E, Dunachie SJ, Fry EE, Mongkolsapaya J, Ren J, Stuart DI, Screaton GR. 2021. Evidence of escape of SARS-CoV-2 variant B.1.351 from natural and vaccine-induced sera. *Cell* <https://doi.org/https://doi.org/10.1016/j.cell.2021.02.037>.
  18. Sarkar R, Lo M, Saha R, Dutta S, Chawla-Sarkar M. S glycoprotein diversity of the Omicron variant <https://doi.org/10.1101/2021.12.04.21267284>.
  19. Cele S, Jackson L, Khan K, Khoury D, Moyo-Gwete T, Tegally H, Scheepers C, Amoako D, Karim F, Bernstein M, Lustig G, Archary D, Smith M, Ganga Y, Jule Z, Reedoy K, San JE, Hwa S-H, Giandhari J, Blackburn JM, Gosnell BI, Karim SA, Hanekom W, NGS-SA, Team C-K, Gottberg A von, Bhiman J, Lessells RJ, Moosa M-YS, Davenport M, Oliveira T de, Moore PL, Sigal A. 2021. SARS-CoV-2 Omicron has extensive but incomplete escape of Pfizer BNT162b2 elicited neutralization and requires ACE2 for infection. *medRxiv*

10:2021.12.08.21267417.

20. Vanblargan LA, Errico JM, Halfmann PJ, Zost SJ, Crowe JE, Purcell LA, Kawaoka Y, Corti D, Fremont DH, Diamond MS, Biotechnology V, Louis S, Mo U. An infectious SARS-CoV-2 B.1.1.529 Omicron virus escapes neutralization by 1 several therapeutic monoclonal antibodies 2 3 <https://doi.org/10.1101/2021.12.15.472828>.
21. Mlcochova P, Kemp SA, Dhar MS, Papa G, Meng B, Ferreira IATM, Datir R, Collier DA, Albecka A, Singh S, Pandey R, Brown J, Zhou J, Goonawardane N, Mishra S, Whittaker C, Mellan T, Marwal R, Datta M, Sengupta S, Ponnusamy K, Srinivasan Radhakrishnan V, Abdullahi A, Charles O, Chattopadhyay P, Devi P, Caputo D, Peacock T, Wattal C, Goel N, Satwik A, Vaishya R, Agarwal M. SARS-CoV-2 B.1.617.2 Delta variant replication and immune evasion. *Chiara Silacci-Fegni* 13:41.
22. Ferreira IATM, Kemp SA, Datir R, Saito A, Meng B, Rakshit P, Takaori-Kondo A, Kosugi Y, Uriu K, Kimura I, Shirakawa K, Abdullahi A, Agarwal A, Ozono S, Tokunaga K, Sato K, Gupta RK. 2021. SARS-CoV-2 B.1.617 Mutations L452R and E484Q Are Not Synergistic for Antibody Evasion. *J Infect Dis* 224:989–994.
23. Planas D, Veyer D, Baidaliuk A, Staropoli I, Guivel-Benhassine F, Rajah MM, Planchais C, Porrot F, Robillard N, Puech J, Prot M, Gallais F, Gantner P, Velay A, Le Guen J, Kassis-Chikhani N, Edriss D, Belec L, Seve A, Courtellemont L, Péré H, Hocqueloux L, Fafi-Kremer S, Prazuck T, Mouquet H, Bruel T, Simon-Lorière E, Rey FA, Schwartz O. 2021. Reduced sensitivity of SARS-CoV-2 variant Delta to antibody neutralization. *Nat* 2021 5967871 596:276–280.
24. McCray PB, Pewe L, Wohlford-Lenane C, Hickey M, Manzel L, Shi L, Netland J, Jia HP, Halabi C, Sigmund CD, Meyerholz DK, Kirby P, Look DC, Perlman S. 2007. Lethal Infection of K18-hACE2 Mice Infected with Severe Acute Respiratory Syndrome Coronavirus. *J Virol* 81:813–821.
25. Moreau GB, Burgess SL, Sturek JM, Donlan AN, Petri WA, Mann BJ. 2020. Evaluation of

- K18-hACE2 Mice as a Model of SARS-CoV-2 Infection. *Am J Trop Med Hyg* 103:1215–1219.
26. Oladunni FS, Park JG, Pino PA, Gonzalez O, Akhter A, Allué-Guardia A, Olmo-Fontáñez A, Gautam S, Garcia-Vilanova A, Ye C, Chiem K, Headley C, Dwivedi V, Parodi LM, Alfson KJ, Staples HM, Schami A, Garcia JI, Whigham A, Platt RN, Gazi M, Martinez J, Chuba C, Earley S, Rodriguez OH, Mdaki SD, Kavelish KN, Escalona R, Hallam CRA, Christie C, Patterson JL, Anderson TJC, Carrion R, Dick EJ, Hall-Ursone S, Schlesinger LS, Alvarez X, Kaushal D, Giavedoni LD, Turner J, Martinez-Sobrido L, Torrelles JB. 2020. Lethality of SARS-CoV-2 infection in K18 human angiotensin-converting enzyme 2 transgenic mice. *Nat Commun* 11.
  27. Winkler ES, Bailey AL, Kafai NM, Nair S, McCune BT, Yu J, Fox JM, Chen RE, Earnest JT, Keeler SP, Ritter JH, Kang LI, Dort S, Robichaud A, Head R, Holtzman MJ, Diamond MS. 2020. SARS-CoV-2 infection of human ACE2-transgenic mice causes severe lung inflammation and impaired function. *Nat Immunol* 21:1327–1335.
  28. Yinda CK, Port JR, Bushmaker T, Owusu IO, Purushotham JN, Avanzato VA, Fischer RJ, Schulz JE, Holbrook MG, Hebner MJ, Rosenke R, Thomas T, Marzi A, Best SM, de Wit E, Shaia C, van Doremalen N, Munster VJ. 2021. K18-hACE2 mice develop respiratory disease resembling severe COVID-19. *PLoS Pathog* 17:1–21.
  29. Zheng J, Wong LYR, Li K, Verma AK, Ortiz ME, Wohlford-Lenane C, Leidinger MR, Knudson CM, Meyerholz DK, McCray PB, Perlman S. 2021. COVID-19 treatments and pathogenesis including anosmia in K18-hACE2 mice. *Nature* 589:603–607.
  30. Hassan AO, Kafai NM, Dmitriev IP, Fox JM, Smith BK, Harvey IB, Chen RE, Winkler ES, Wessel AW, Case JB, Kashentseva E, McCune BT, Bailey AL, Zhao H, VanBlargan LA, Dai YN, Ma M, Adams LJ, Shrihari S, Danis JE, Gralinski LE, Hou YJ, Schäfer A, Kim AS, Keeler SP, Weiskopf D, Baric RS, Holtzman MJ, Fremont DH, Curiel DT, Diamond MS. 2020. A Single-Dose Intranasal ChAd Vaccine Protects Upper and Lower Respiratory



- Tracts against SARS-CoV-2. *Cell* 183:169-184.e13.
31. Pandey K, Acharya A, Mohan M, Ng CL, Reid SP, Byrareddy SN. 2020. Animal models for SARS-CoV-2 research: A comprehensive literature review. *Transbound Emerg Dis* <https://doi.org/10.1111/tbed.13907>.
  32. Liu R, Americo JL, Cotter CA, Earl PL, Erez N, Peng C, Moss B. 2021. One or two injections of MVA-vectored vaccine shields hACE2 transgenic mice from SARS-CoV-2 upper and lower respiratory tract infection. *Proc Natl Acad Sci U S A* 118:1–11.
  33. Silvas J, Morales-Vasquez D, Park J-G, Chiem K, Torrelles JB, Platt RN, Anderson T, Ye C, Martinez-Sobrido L. 2021. Contribution of SARS-CoV-2 accessory proteins to viral pathogenicity in K18 hACE2 transgenic mice. *bioRxiv* 6.
  34. Sarkar J, Guha R. 2020. Infectivity, virulence, pathogenicity, host-pathogen interactions of SARS and SARS-CoV-2 in experimental animals: a systematic review. *Vetinary Res Commun* 44:101–110.
  35. Kumari P, Rothan HA, Natekar JP, Stone S, Pathak H, Strate PG, Arora K, Brinton MA, Kumar M. 2020. Neuroinvasion and encephalitis following intranasal inoculation of SARS-CoV-2 in K18-hACE2 mice. *bioRxiv* <https://doi.org/10.1101/2020.12.14.422714>.
  36. Sette A, Crotty S. 2021. Adaptive immunity to SARS-CoV-2 and COVID-19. *Cell* 184:861–880.
  37. Piccoli L, Park YJ, Tortorici MA, Czudnochowski N, Walls AC, Beltramello M, Silacci-Fregni C, Pinto D, Rosen LE, Bowen JE, Acton OJ, Jaconi S, Guarino B, Minola A, Zatta F, Sprugasci N, Bassi J, Peter A, De Marco A, Nix JC, Mele F, Jovic S, Rodriguez BF, Gupta S V., Jin F, Piumatti G, Lo Presti G, Pellanda AF, Biggiogero M, Tarkowski M, Pizzuto MS, Cameroni E, Havenar-Daughton C, Smithey M, Hong D, Lepori V, Albanese E, Ceschi A, Bernasconi E, Elzi L, Ferrari P, Garzoni C, Riva A, Snell G, Sallusto F, Fink K, Virgin HW, Lanzavecchia A, Corti D, Veessler D. 2020. Mapping Neutralizing and Immunodominant Sites on the SARS-CoV-2 Spike Receptor-Binding Domain by Structure-Guided High-

- Resolution Serology. *Cell* 183:1024.
38. M Brouwer PJ, Caniels TG, van der Straten K, Snitselaar JL, Aldon Y, Bangaru S, Torres JL, A Okba NM, Claireaux M, Kerster G, H Bentlage AE, van Haaren MM, Guerra D, Burger JA, Schermer EE, Verheul KD, van der Velde N, van der Kooi A, van Schooten J, van Breemen MJ, L Bijl TP, Slieden K, Aartse A, Derking R, Bontjer I, Kootstra NA, Joost Wiersinga W, Vidarsson G, Haagmans BL, Ward AB, de Bree GJ, Sanders RW, van Gils MJ. Potent neutralizing antibodies from COVID-19 patients define multiple targets of vulnerability.
  39. Kumar S, Chandele A, Sharma A. 2021. Current status of therapeutic monoclonal antibodies against SARS-CoV-2. *PLOS Pathog* 17:e1009885.
  40. Bursky JM, Chen RE, Zhang X. Resistance of SARS-CoV-2 variants to neutralization by monoclonal and serum-derived polyclonal antibodies. *Nat Med* <https://doi.org/10.1038/s41591-021-01294-w>.
  41. Horspool AM, Kieffer T, Russ BP, DeJong MA, Wolf MA, Karakiozis JM, Hickey BJ, Fagone P, Tacker DH, Bevere JR, Martinez I, Barbier M, Perrotta PL, Damron FH. 2021. Interplay of Antibody and Cytokine Production Reveals CXCL13 as a Potential Novel Biomarker of Lethal SARS-CoV-2 Infection. *mSphere* 6.
  42. Horspool AM, Kieffer T, Russ BP, DeJong MA, Wolf MA, Karakiozis JM, Hickey BJ, Fagone P, Tacker DH, Bevere JR, Martinez I, Barbier M, Perrotta PL, Damron FH. 2021. Interplay of Antibody and Cytokine Production Reveals CXCL13 as a Potential Novel Biomarker of Lethal SARS-CoV-2 Infection. *mSphere* 6.
  43. Case JB, Bailey AL, Kim AS, Chen RE, Diamond MS. 2020. Growth, detection, quantification, and inactivation of SARS-CoV-2. *Virology* 548:39–48.
  44. Ye C, Chiem K, Park J, Oladunni F, Anderson T, Almazan F, Martinez-sobrido L. 2020. Rescue of SARS-CoV-2 from a Single Bacterial Artificial Chromosome 1–10.
  45. Bolger AM, Lohse M, Usadel B. 2014. Genome analysis Trimmomatic : a flexible trimmer

- for Illumina sequence data 30:2114–2120.
46. Langmead B, Salzberg SL. 2012. Fast gapped-read alignment with Bowtie 2 9:357–360.
  47. Pedersen BS, Quinlan AR. 2018. Genome analysis Mosdepth : quick coverage calculation for genomes and exomes 34:867–868.
  48. Wilm A, Poh P, Aw K, Bertrand D, Hui G, Yeo T, Ong SH, Wong CH, Khor CC, Petric R, Hibberd ML, Nagarajan N. 2012. LoFreq : a sequence-quality aware , ultra-sensitive variant caller for uncovering cell-population heterogeneity from high-throughput sequencing datasets 40:11189–11201.
  49. Li H, Durbin R. 2009. Fast and accurate short read alignment with Burrows – Wheeler transform 25:1754–1760.
  50. Grubaugh ND, Gangavarapu K, Quick J, Matteson NL, Jesus JG De, Main BJ, Tan AL, Paul LM, Brackney DE, Grewal S, Gurfield N, Rompay KKA Van, Isern S, Michael SF, Coffey LL, Loman NJ, Andersen KG. 2019. An amplicon-based sequencing framework for accurately measuring intrahost virus diversity using PrimalSeq and iVar 1–19.
  51. Li H, Handsaker B, Wysoker A, Fennell T, Ruan J, Homer N, Marth G, Abecasis G, Durbin R, Data GP, Sam T. 2009. The Sequence Alignment / Map format and SAMtools 25:2078–2079.
  52. O’Toole Á, S. E, Underwood A, Jackson B, Hill V, McCrone J, Ruis C, Abu-Dahab K, Taylor B, Yeats C, du Plessis L, Aanensen D, Holmes E, Pybus O, Rambaut A. Pangolin: lineage assignment in an emerging pandemic as an epidemiological tool.
  53. Addetia A, Crawford KHD, Dingens A, Zhu H, Roychoudhury P, Huang ML, Jerome KR, Bloom JD, Greninger AL. 2020. Neutralizing antibodies correlate with protection from SARS-CoV-2 in humans during a fishery vessel outbreak with high attack rate. medRxiv 58:1–11.
  54. Greninger AL, Waghmare A, Adler A, Qin X, Crowley JL, Englund JA, Kuypers JM, Jerome KR, Zerr DM. 2017. Rule-out outbreak: 24-hour metagenomic next-generation sequencing


- for characterizing respiratory virus source for infection prevention. *J Pediatric Infect Dis Soc* 6:168–172.
55. Martin M. Cutadapt removes adapter sequences from high-throughput sequencing reads. *EMBnet.journal* 17.1:10–12.
  56. Jin M, Shean RC, Makhsous N, Greninger AL. 2019. LAVA: a streamlined visualization tool for longitudinal analysis of viral alleles. *bioRxiv*.
  57. Koboldt DC, Chen K, Wylie T, Larson DE, McLellan MD, Mardis ER, Weinstock GM, Wilson RK, Ding L. 2009. VarScan: Variant detection in massively parallel sequencing of individual and pooled samples. *Bioinformatics* 25:2283–2285.
  58. Koboldt DC, Zhang Q, Larson DE, Shen D, McLellan MD, Lin L, Miller CA, Mardis ER, Ding L, Wilson RK. 2012. VarScan 2: Somatic mutation and copy number alteration discovery in cancer by exome sequencing. *Genome Res* 22:568–576.
  59. Wang K, Li M, Hakonarson H. 2010. ANNOVAR: Functional annotation of genetic variants from high-throughput sequencing data. *Nucleic Acids Res* 38:1–7.
  60. Dinno KH, Leist SR, Schäfer A, Edwards CE, Martinez DR, Montgomery SA, West A, Yount BL, Hou YJ, Adams LE, Gully KL, Brown AJ, Huang E, Bryant MD, Choong IC, Glenn JS, Gralinski LE, Sheahan TP, Baric RS. 2020. A mouse-adapted model of SARS-CoV-2 to test COVID-19 countermeasures. *Nature* 586:560–566.
  61. Montagutelli X, Prot M, Levillayer L, Salazar EB, Jouvion G, Conquet L, Donati F, Albert M, Gambaro F, Behillil S van der, Enouf V, Rousset D, Jaubert J, Rey F, Werf S van der, Simon-Loriere E. 2021. The B.1.351 and P.1 variants extend SARS-CoV-2 host range to mice. *bioRxiv* 1–16.
  62. FS O, JG P, PA P, O G, A A, A A-G, A O-F, S G, A G-V, C Y, K C, C H, V D, LM P, KJ A, HM S, A S, JI G, A W, RN P, M G, J M, C C, S E, OH R, SD M, KN K, R E, CRA H, C C, JL P, TJC A, R C, EJ D, S H-U, LS S, X A, D K, LD G, J T, L M-S, JB T. 2020. Lethality of SARS-CoV-2 infection in K18 human angiotensin-converting enzyme 2 transgenic mice.

Nat Commun 11.

63. Shinde V, Bhikha S, Hoosain Z, Archary M, Borhat Q, Fairlie L, Lalloo U, Masilela MSL, Moodley D, Hanley S, Fouche L, Louw C, Tameris M, Singh N, Goga A, Dheda K, Grobbelaar C, Kruger G, Carrim-Ganey N, Baillie V, de Oliveira T, Lombard Koen A, Lombaard JJ, Mngqibisa R, Borhat AE, Benadé G, Lalloo N, Pitsi A, Vollgraaff P-L, Luabeya A, Esmail A, Petrick FG, Oommen-Jose A, Foulkes S, Ahmed K, Thombrayil A, Fries L, Cloney-Clark S, Zhu M, Bennett C, Albert G, Faust E, Plested JS, Robertson A, Neal S, Cho I, Glenn GM, Dubovsky F, Madhi SA. 2021. Efficacy of NVX-CoV2373 Covid-19 Vaccine against the B.1.351 Variant. *N Engl J Med* 384:1899–1909.
64. Heath PT, Galiza EP, Baxter DN, Boffito M, Browne D, Burns F, Chadwick DR, Clark R, Cosgrove C, Galloway J, Goodman AL, Heer A, Higham A, Iyengar S, Jamal A, Jeanes C, Kalra PA, Kyriakidou C, McAuley DF, Meyrick A, Minassian AM, Minton J, Moore P, Munsoor I, Nicholls H, Osanlou O, Packham J, Pretswell CH, Ramos ASF, Saralaya D, Sheridan RP, Smith R, Soiza RL, Swift PA, Thomson EC, Turner J, Viljoen ME, Albert G, Cho I, Dubovsky F, Glenn G, Rivers J, Robertson A, Smith K, Toback S. 2021. Safety and Efficacy of NVX-CoV2373 Covid-19 Vaccine. <https://doi.org/10.1056/NEJMoa2107659> 385:1172–1183.
65. Falsey AR, Sobieszczyk ME, Hirsch I, Sproule S, Robb ML, Corey L, Neuzil KM, Hahn W, Hunt J, Mulligan MJ, McEvoy C, DeJesus E, Hassman M, Little SJ, Pahud BA, Durbin A, Pickrell P, Daar ES, Bush L, Solis J, Carr QO, Oyedele T, Buchbinder S, Cowden J, Vargas SL, Guerreros Benavides A, Call R, Keefer MC, Kirkpatrick BD, Pullman J, Tong T, Brewinski Isaacs M, Benkeser D, Janes HE, Nason MC, Green JA, Kelly EJ, Maaske J, Mueller N, Shoemaker K, Takas T, Marshall RP, Pangalos MN, Villafana T, Gonzalez-Lopez A. 2021. Phase 3 Safety and Efficacy of AZD1222 (ChAdOx1 nCoV-19) Covid-19 Vaccine. *N Engl J Med* 385:2348–2360.
66. Bloch EM, Shoham S, Casadevall A, Sachais BS, Shaz B, Winters JL, Van Buskirk C,

- Grossman BJ, Joyner M, Henderson JP, Pekosz A, Lau B, Wesolowski A, Katz L, Shan H, Auwaerter PG, Thomas D, Sullivan DJ, Paneth N, Gehrie E, Spitalnik S, Hod EA, Pollack L, Nicholson WT, Pirofski LA, Bailey JA, Tobian AAR. 2020. Deployment of convalescent plasma for the prevention and treatment of COVID-19. *J Clin Invest* 130:2757–2765.
67. Bloch EM. 2020. Convalescent plasma to treat COVID-19. *Blood* 136:654–655.
  68. Chen L, Xiong J, Bao L, Shi Y. 2020. Convalescent plasma as a potential therapy for COVID-19. *Lancet Infect Dis* 20:398–400.
  69. NIH. 2021. NIH halts trial of COVID-19 convalescent plasma in emergency department patients with mild symptoms.
  70. Zhao Q, He Y. 2020. Challenges of Convalescent Plasma Therapy on COVID-19. *J Clin Virol* 127.
  71. Casadevall A, Henderson J, Joyner M, Pirofski L. 2021. SARS-Cov2 variants and convalescent plasma: reality, fallacies, and opportunities. *J Clin Invest* 131.
  72. Cele S, Gazy I, Jackson L, Hwa S-H, Tegally H, Lustig G, Giandhari J, Pillay S, Wilkinson E, Naidoo Y, Karim F, Ganga Y, Khan K, Bernstein M, Balazs AB, Gosnell BI, Hanekom W, Moosa M-YS, Team C, Lessells RJ, de Oliveira T, Sigal A. 2021. Escape of SARS-CoV-2 501Y.V2 from neutralization by convalescent plasma. *medRxiv* 2021.01.26.21250224.
  73. Shastri J, Parikh S, Aggarwal V, Agrawal S, Chatterjee N, Shah R, Devi P, Mehta P, Pandey R. 2021. Severe SARS-CoV-2 Breakthrough Reinfection With Delta Variant After Recovery From Breakthrough Infection by Alpha Variant in a Fully Vaccinated Health Worker. *Front Med* 8:1379.
  74. Lipsitch M, Krammer F, Regev-Yochay G, Lustig Y, Balicer RD. 2021. SARS-CoV-2 breakthrough infections in vaccinated individuals: measurement, causes and impact. *Nat Rev Immunol* 2021 1–9.
  75. Chen RE, Zhang X, Case JB, Winkler ES, Liu Y, VanBlargan LA, Liu J, Errico JM, Xie X,

Suryadevara N, Gilchuk P, Zost SJ, Tahan S, Droit L, Turner JS, Kim W, Schmitz AJ, Thapa M, Wang D, Boon ACM, Presti RM, O'Halloran JA, Kim AHJ, Deepak P, Pinto D, Fremont DH, Crowe JE, Corti D, Virgin HW, Ellebedy AH, Shi PY, Diamond MS. 2021. Resistance of SARS-CoV-2 variants to neutralization by monoclonal and serum-derived polyclonal antibodies. *Nat Med* 2021 27:717–726.



**Chapter 3: RBD-VLP vaccines  
adjuvanted with Alum or SWE protect  
K18-hACE2 mice against SARS-CoV-  
2 VOC challenge**



## **RBD-VLP vaccines adjuvanted with Alum or SWE protect K18-hACE2 mice against SARS-CoV-2 VOC challenge**

Ting Y. Wong<sup>1,2</sup>, Brynna P. Russ<sup>1,2</sup>, Katherine S. Lee<sup>1,2</sup>, Olivia A. Miller<sup>1,2</sup>, Jason Kang<sup>1,2</sup>, Melissa Cooper<sup>1,2</sup>, Michael T. Winters<sup>1</sup>, Sergio A. Rodriguez-Aponte<sup>6,7</sup>, Neil C. Dalvie<sup>7,8</sup>, Ryan S. Johnston<sup>7</sup>, Nathaniel A. Rader<sup>1,2</sup>, Zerial Y. Wong<sup>1,2</sup>, Holly A. Cyphert<sup>5</sup>, Ivan Martinez<sup>1,3</sup>, Umesh Shaligram<sup>9</sup>, Saurabh Batwal<sup>9</sup>, Rakesh Lothe<sup>9</sup>, Rahul Chandrasekaran<sup>9</sup>, Gaurav Nagar<sup>9</sup>, Meghraj Rajurkar<sup>9</sup>, Harish Rao<sup>9</sup>, Justin R. Bevere<sup>1,2</sup>, Mariette Barbier<sup>1,2</sup>, J. Christopher Love<sup>7,8</sup> and F. Heath Damron<sup>1,2\*</sup>.

<sup>1</sup>Department of Microbiology, Immunology, and Cell Biology, West Virginia University, Morgantown, WV, USA

<sup>2</sup> Vaccine Development Center at West Virginia University Health Sciences Center, Morgantown, WV, USA

<sup>3</sup> West Virginia University Cancer Institute, Morgantown, WV, USA School of Medicine, Morgantown, WV, USA

<sup>5</sup> Department of Biological Sciences, Marshall University, Huntington, WV, USA

<sup>6</sup> Department of Biological Engineering, Massachusetts Institute of Technology, Cambridge, Massachusetts 02139, USA

<sup>7</sup> The Koch Institute for Integrative Cancer Research, Massachusetts Institute of Technology, Cambridge, Massachusetts 02139, USA

<sup>8</sup> Department of Chemical Engineering, Massachusetts Institute of Technology, Cambridge, Massachusetts 02139, USA

<sup>9</sup> Serum Institute of India Pvt. Ltd., Pune, India.

\*Corresponding author

Corresponding author email address: [fdamron@hsc.wvu.edu](mailto:fdamron@hsc.wvu.edu)

Keywords: SARS-CoV-2, COVID-19, K18-hACE2 transgenic mouse, vaccines, RBD, HBsAg, VLP, SpyTag, SpyCatcher, SWE

Accepted in mSphere 2022

### 3.1 Abstract

The ongoing COVID-19 pandemic has contributed largely to the global vaccine disparity. Development of protein subunit vaccines can help alleviate shortages of COVID-19 vaccines delivered to low-income countries. Here, we evaluated the efficacy of a three-dose Virus-like particle (VLP) vaccine composed of Hepatitis B surface antigen (HBsAg) decorated with the Receptor Binding Domain (RBD) from Wuhan and/or Beta SARS-CoV-2 strains adjuvanted with either aluminum hydroxide (Alum) or squalene in water emulsion (SWE). RBD HBsAg vaccines were compared to the standard two doses of Pfizer mRNA vaccine. Alum adjuvanted vaccines were composed of either RBD HBsAg conjugated with Beta RBD alone ( $\beta$  RBD HBsAg+Al) or a combination of both Beta RBD HBsAg and Wuhan RBD HBsAg ( $\beta$ /Wu RBD HBsAg+Al). RBD vaccines adjuvanted with SWE were formulated with Beta RBD HBsAg ( $\beta$  RBD HBsAg+SWE) or without HBsAg ( $\beta$  RBD+SWE). Both alum adjuvanted RBD HBsAg vaccines generated functional RBD IgG against multiple SARS-CoV-2 Variants of Concern (VOC), decreased viral RNA burden and lowered inflammation in the lung against Alpha or Beta challenge in K18-hACE2 mice. However, only  $\beta$ /Wu RBD HBsAg+AlOH was able to afford 100% survival to mice challenged with Alpha or Beta VOC. Furthermore, mice immunized with  $\beta$  RBD HBsAg+SWE induced cross reactive neutralizing antibodies against major VOC of SARS-CoV-2, lowered viral RNA burden in the lung and brain, and protected mice from Alpha or Beta challenge similar to mice immunized with Pfizer mRNA. However, RBD+SWE immunization failed to protect mice from VOC challenge. Our findings demonstrate that RBD HBsAg VLP vaccines provided similar protection profiles to the approved Pfizer mRNA vaccines used worldwide and may offer protection against SARS-CoV-2 VOC.

### **3.2 Importance**

Global COVID-19 vaccine distribution to low-income has been a major challenge of the pandemic. To address supply chain issues, RBD Virus-like particle (VLP) vaccines that are cost effective and capable of large-scale production were developed and evaluated for efficacy in pre-clinical mouse studies. We demonstrated that RBD-VLP vaccines protected K18-hACE2 mice against Alpha or Beta challenge similarly to Pfizer mRNA vaccination. Our findings showed that the VLP platform can be utilized to formulate immunogenic and efficacious COVID-19 vaccines.

### 3.3 Introduction

SARS-CoV-2 is the causative agent of the COVID-19 pandemic that has caused more than 446 million cases and over 6 million deaths worldwide. Since January 2020, when the genome of the ancestral strain of SARS-CoV-2 was first released, new variants of concern (VOC) have emerged such as Alpha, Beta, Gamma, Delta, and currently, Omicron. Mutations harbored on the Receptor Binding Domain (RBD) of the spike protein of SARS-CoV-2 such as N501Y and E484K of early VOC (Alpha, Beta, and Gamma) were responsible for increased transmission of SARS-CoV-2 (1,2). Later VOC, such as Delta contained additional mutations on the RBD, L452R and T478K, which were associated with increased infectivity, transmissibility, and evasion of neutralizing antibodies (3,4). Omicron, the current predominant variant of SARS-CoV-2 has 30 mutations on spike protein alone (15 of these are in the RBD) that has led to vaccine breakthrough cases and evasion of monoclonal antibody therapeutics (5). Overall, due to the emergence of VOC, increased vaccine breakthrough cases have been apparent and need to be addressed by the production of vaccines that can broadly neutralize VOC.

Currently, there are 10 WHO-approved COVID-19 vaccines granted for Emergency Use Listing or full approval. These include vaccines formulated with mRNA (Moderna and Pfizer/BioNTech), non-replicating Adenovirus (Jansen, Oxford/AstraZeneca and Serum Institute of India), or protein subunit (Novavax and Serum Institute of India) that utilize the ancestral strain of SARS-CoV-2 spike protein as the vaccine antigen. Bharat Biotech, Sinopharm (Beijing), and Sinovac have also developed approved inactivated SARS-CoV-2 virus vaccines. Overall, Adenovirus non-replicating viral vector COVID-19 vaccines globally lead in approval for use in the most countries (290 countries) followed by the mRNA platform (222 countries), inactivated SARS-CoV-2 (155 countries), and lastly protein subunit (38 countries) (6).

Surprisingly, there is only one approved recombinant protein vaccine formulation, even though historically subunit vaccines have been used for prevention of many infectious diseases. Novavax has developed the first WHO approved recombinant protein COVID-19 vaccine in partnership

with the Coalition for Epidemic Preparedness Innovations (CEPI), and manufacturing collaborations with the Serum Institute of India. The vaccine is formulated with lipid nanoparticle decorated with SARS-CoV-2 spike protein adjuvanted with a Saponin derived Matrix-M adjuvant (7,8). In a phase 3 clinical trial in the United States and Mexico, Novavax vaccine demonstrated 100% vaccine efficacy against moderate to severe COVID-19, and 92.6% efficacy against the variants of concern at that time (not including the Delta variant) (9). Globally, there are also 6 other protein subunit vaccines that are approved for emergency use in Taiwan, China, Russia, Belarus, Turkmenistan, Cuba, Venezuela, and Iran.

With the increase of COVID-19 vaccine development around the world, to date only 56% of the global population is fully vaccinated with 2 doses of a COVID-19 vaccine (10). Global vaccine disparities are evident especially amongst countries in Africa, South America, Eastern Europe, Middle East, and some countries in South Asia. The development of recombinant protein subunit COVID-19 vaccines can help alleviate global vaccine disparities and inequities by increasing the availability of safe and efficacious vaccines to lower-income countries.

To meet the demand of COVID-19 vaccine distribution to lower-income countries, vaccine candidates must have: 1) increased manufacturability and scalability 2) reduced production costs 3) thermostability 4) limited series of doses with long lasting immune responses and 4) generate broadly neutralizing antibodies across VOC. COVID-19 protein subunit vaccines can help address the challenges in developing vaccines for low-income countries. All WHO approved COVID-19 vaccines utilize the full-length spike protein as the vaccine antigen. Although, the spike protein is an immunogenic target, given its size, it is less manufacturable than the RBD. The RBD has become an antigen of interest for protein-based vaccines due to the ability of RBD to be cost efficiently produced in high yields, stability at elevated temperatures, as well as include neutralizing epitopes (11,12). Although, RBD is not sufficiently immunogenic on its own, conjugation to protein nanoparticles, virus-like particles (VLP), or bacterial carrier proteins can elevate immunogenicity by increasing the amount of antigen presented to the immune system

(13–15). Likewise, adjuvants can help boost antigen specific immune responses in vaccines leading to robust cellular and humoral activation. Historically, Aluminum hydroxide (Alum) has been used as an adjuvant for multiple approved protein-based vaccines due to its ability to drive a strong antibody response. Recently, oil-in-water emulsions adjuvants such as MF59 have been utilized to improve the immunogenicity of influenza vaccines to older and immunocompromised populations(16). Alternatively, a Squalene in water emulsion (SWE) adjuvant similar to MF59, has been designed to provide dose-sparing qualities to vaccines by decreasing the amount of antigen necessary for administration. Pre-clinical vaccine studies performed with SWE demonstrated both improved humoral and cellular responses against both viral and bacterial pathogens (17–25). Overall, adjuvants can help limit the vaccine doses needed to be administered as well as increase the duration of the immune response which can benefit low-income countries and alleviate the global vaccine deficit.

In this study, we evaluated a VLP based protein subunit vaccine developed by the Serum Institute of India (SII) and SpyBiotech in comparison to standard Pfizer mRNA vaccine. Experimental vaccines were composed of Hepatitis B surface antigen (HBsAg) VLP decorated with Beta and/or Wuhan RBD and adjuvanted with either Aluminum hydroxide or a squalene in water emulsion (SWE). We hypothesized that 1) combination of both Beta RBD HBsAg and Wuhan RBD HBsAg would provide protection against SARS-CoV-2 VOC compared to Beta RBD HBsAg and 2) conjugation of RBD to HBsAg is necessary to elicit an immunogenic response and protect mice against SARS-CoV-2 VOC. Here, we evaluated 4 experimental RBD HBsAg VLP vaccines compared to Pfizer mRNA against Alpha or Beta challenge in the K18-hACE2 mouse model. Our findings demonstrate that three doses of Beta RBD HBsAg and Wuhan RBD HBsAg adjuvanted with Alum provided better protection against both Alpha and Beta variants similar to Pfizer mRNA vaccination compared to Beta RBD HBsAg adjuvanted with Alum. Additionally, three doses of RBD HBsAg adjuvanted with SWE generated RBD IgG antibody responses against a breadth of VOC comparable to two doses of Pfizer mRNA vaccine and elicited protection against Alpha and

Beta VOC whereas RBD without HBsAg adjuvanted with SWE failed to protect mice against SARS-CoV-2 challenge.

### 3.4 Methods

**Animal welfare and Biosafety.** B6.Cg-Tg(K18-ACE2)2PrImn/J mouse vaccine and SARS-CoV-2 challenge studies were executed under IACUC protocol number 2009036460. All mice were humanely euthanized based on the disease scoring system (26), and no deaths occurred in the cage. All SARS-CoV-2 challenge studies were conducted in the West Virginia University Biosafety Laboratory Level 3 facility under the IBC protocol number 20-04-01. SARS-CoV-2 samples were either inactivated with 1% Triton per volume or Trizol before exiting high containment.

**Production of antigen and vaccine compositions.** RBD protein was cloned, expressed in *Komgataella phaffi* and purified as previously described (27–29). RBD-SpyTag antigens were conjugated overnight onto the HBsAg-SpyCatcher VLP (30,31). Beta RBD used in vaccine formulations was engineered to include mutations L452K and F490W to increase manufacturability and scalability as previously described (13). Vaccine formulations are shown in Supplementary Table 1.

**Mouse immunization.** Female B6.Cg-Tg(K18-ACE2)2PrImn/J mice were purchased from Jackson Laboratory (stock no: 034860) at 4 weeks old. K18-hACE2 mice receiving experimental RBD vaccines were primed at 9 weeks old, boosted 3 weeks later (12 weeks old), and were administered third dose 2 weeks post 2<sup>nd</sup> dose (14 weeks old) with 50µL of vaccine through the intramuscular route in the right leg. Pfizer mRNA immunized K18-hACE2 mice were primed at 9 weeks old with and boosted 3 weeks later (12 weeks old) intramuscularly with 50µL of vaccine in the right leg.



## **Serological analysis**

Pre-challenged serum from vaccinated mice was analyzed for RBD specific IgG using the SARS-CoV-2 Plate 11 Multi-Spot 96-well, 10 spot plate following the manufacturer protocol (catalog #: K15455U) on the MSD QuickPlex SQ120. The 10 spots contained the following RBD antigens, common designations, and lineages: 1) Epsilon - L452R (B.1.427; B.1.429; B.1.526.1) 2) Beta - K417N, E484K, N501Y (B.1.351; B.1.351.1) 3) Eta, Iota, Zeta - E484K (B.1.525; B.1.526; B.1.618; P.2; R.1) 4) Gamma - K417T, E484K, N501Y (P.1) 5) New York - S477N 6) Alpha - N501Y (B.1.1.7) 7) UK, Philippines - E484K, N501Y (B.1.1.7+E484K; P.3) 8) Kappa - L452R, E484Q (B.1.617; B.1.617.1; B.1.617.3) 9) Delta - L452R, T478K (AY.3; AY.4; AY.4.2; AY.5; AY.6; AY.7; AY.12; AY.14; B.1.617.2; B.1.617.2+Δ144) and 10) Wuhan. Serum obtained from non-vaccinated and vaccinated animals at 2 weeks post prime and 4 weeks post 2<sup>nd</sup> dose were evaluated for IgG titers against 10 different VOC RBDs. Non immunized mice sera were diluted at 1:1000, whereas vaccinated mice sera obtained at 2 weeks post prime was diluted at 1:4000-1:512000 and vaccinated sera obtained at 4 weeks post 2<sup>nd</sup> dose was diluted at 1:32000-1:4096000. Titer cut off value was determined by the sum of the average values for non-vaccinated mice added to 2X the standard deviation of non-vaccinated mice electrochemiluminescent (ECL) values. The reciprocal of the dilution showing ECL values above the cutoff were reported as the final titer. Statistical analysis was performed on  $n \geq 8$  mice per group of serum analyzed.

## **SARS-CoV-2 propagation and mouse challenge**

Alpha (NR-54000) and Beta (NR-54008) SARS-CoV-2 variants were obtained from BEI Resources. Alpha and Beta VOC were propagated in Vero E6 cells (ATCC-CRL-1586) and re-sequenced before use in mouse challenge. K18-hACE2 mice were anesthetized using an intraperitoneal injection of ketamine (Patterson Veterinary 07-803-6637, 80 mg/kg) / xylazine (07-808-1947, 8.3 mg/kg) and were intranasally challenged with 50uL of  $10^4$  PFU/dose of Alpha or Beta variant, 25uL per nare. Mice were monitored until fully recovered from the anesthesia.

### **Disease monitoring of SARS-CoV-2 challenged mice**

Challenged K18-hACE2 mice were evaluated daily through both in-person health assessments in the BSL3 and SwifTAG Systems video monitoring for 11 days. Disease assessments of the mice were scored based on five criteria: 1) weight loss (scale 0-5), 2) appearance (scale 0-2), 3) activity (scale 0-3), 4) eye closure (scale 0-2), and 5) respiration (scale 0-2) as previously described (15,26). Briefly, cumulative disease scoring was calculated by adding the disease scores of each mouse from each group. Morbid mice that were euthanized during the study, before day 11, retained their disease score for the remainder of the experiment.

### **Euthanasia and tissue collection**

Challenged mice that were assigned a disease score of 5 or above or reached the end of the experiment were euthanized with an IP injection of Euthasol (390mg/kg) (Pentobarbital) followed by secondary measure of euthanasia with cardiac puncture. Blood from cardiac puncture was collected in BD Microtainer gold serum separator tubes (BD 365967), centrifuged at 15,000 x *g* for 5 minutes and serum was collected for downstream analysis. Lungs were separated into right and left lobes. Right lobe of the lung was homogenized in 1mL of PBS in gentleMACS C tubes (order number: 130-096-334) using the m\_lung\_02 program on the gentleMACS Dissociator. 300µL of lung homogenate was added to 1000µL of TRI Reagent (Zymo research) for downstream RNA purification and 300 µL of lung homogenate was centrifuged at 15,000 x *g* for 5 minutes and the lung supernatant was collected for downstream analyses. Brain was excised from the skull and was homogenized in 1mL PBS in gentleMACS C tubes using the same setting as lung on the gentleMACS Dissociator. 1000µL of TRI Reagent was added to 500µL of brain homogenate for RNA purification.

### **qRT-PCR SARS-CoV-2 viral copy analysis of lung and brain**

As previously described by Wong et. al. (15,26), RNA purification of the lung and brain were performed using the Direct-zol RNA miniprep kit (Zymo Research R2053) following the manufacturer protocol and SARS-CoV-2 copy numbers were assessed through qPCR using the Applied Biosystems TaqMan RNA to CT One Step Kit (Ref: 4392938).

### **Meso Scale Discovery COVID-19 ACE2 neutralization assay**

SARS-CoV-2 challenged serum was analyzed using the SARS-CoV-2 Panel 22 Multi-Spot 96-well, 10 spot plate following the manufacturer protocol (catalog #: K15458U-2 and K15562U-2 respectively) on the MSD QuickPlex SQ120. Panel 22 was utilized for spots containing Beta (B.1.351), Alpha (B.1.1.7), Delta (AY.3; AY.4; AY.4.2; AY.5; AY.6; AY.7; AY.12; AY.14; B.1.617.2; B.1.617.2+Δ144), Gamma (K417T, E484K, N501Y (P.1), Omicron (B1.1.529; BA.1), and Wuhan. Serum dilution of 1:5 was analyzed on the MSD neutralization assay and ECL values of both the blank (calibrator diluent 100) as well as the average biological replicate ECL values were utilized for analysis to calculate percent inhibition for each mouse.

### **Lung Histopathology**

Left lobes of lungs were fixed in 10 mL of 10% neutral buffered formalin and paraffin embedded into 5 μm sections. Sections were stained with hematoxylin and eosin (H&E) and were analyzed by iHisto. Lungs were scored by a pathologist for chronic and acute inflammation in the lung parenchyma, blood vessels, and airways as previously described (15,26).

### **Statistical analyses**

All statistical analyses were performed using GraphPad Prism version 9. Statistical analyses were performed with  $n \geq 4$  for K18-ACE2 mice studies challenged with Alpha or Beta variants. Error bars represent standard deviation. Ordinary one-way ANOVA with Dunnett's multiple comparisons test was used with single pooled variance for data sets following a normal

distribution and Kruskal-Wallis with Dunn's multiple comparisons test for non-parametric distributed datasets. Kaplan-Meier survival curves were utilized, and Log-rank (Mantel-Cox) test were used to test significance of survival between sample groups.

### 3.5 Results

**RBD VLPs adjuvanted with Alum or SWE and Pfizer mRNA immunizations elicited robust immunogenicity in K18-hACE2 mice.** In this study, RBD HBsAg VLP vaccines utilized the SpyCatcher/SpyTag conjugation platform to display the RBD of the spike protein of SAR-CoV-2 on HBsAg (Fig. 1A). The SpyCatcher/SpyTag platform utilizes the SpyCatcher bound to the HBsAg and the SpyTag bound to RBD to form a covalent bond between antigen and VLP to allow for a high quantity of RBD to be displayed on the surface of HBsAg without masking important epitopes (13,32,33) (Fig. 1A). This technology has been used to improve the immunogenicity of viral vaccines against human cytomegalovirus, influenza, and HIV (34–37). Here, our studies were comprised of two main goals. First, since the emergence of VOC has negatively impacted vaccine efficacy, we wanted to assess the immunogenicity and protection profiles of using the VOC Beta variant RBD compared to utilizing both ancestral SARS-CoV-2 RBD and Beta variant RBD as the target vaccine antigens conjugated to HBsAg. Lastly, the second goal was to evaluate the effect of adjuvanting RBD HBsAg or RBD alone with SWE on immunogenicity and protection with the aim of providing a stronger immune response compared to the Alum adjuvant.

In order to evaluate our experimental goals, K18-hACE2 mice were intramuscularly immunized with three doses of either 1) PBS (NVC) (n=10) 2)  $\beta$  RBD HBsAg+Al (n=10) 3)  $\beta$ /Wu RBD HBsAg + Al (n=9) 4)  $\beta$  RBD HBsAg+SWE (n=10) or 5)  $\beta$  RBD+SWE (n=10) (Supp. Table 1, Fig. 1B). After the initial vaccination, mice were administered the second dose 3 weeks after prime and the third dose, 2 weeks after the second dose of vaccine. Pfizer mRNA vaccination was administered at 3 $\mu$ g which is 1/10 the human dose to mice as 2 doses following the same human vaccine schedule with the two doses separated by 3 weeks (Fig. 1 B, Supp. Table 1). To assess the immunogenicity

of RBD HBsAg vaccines adjuvanted with either Alum or SWE compared to the Pfizer mRNA, serological analysis of serum IgG was measured against ten variant RBDs at 2 weeks post prime and 4 weeks post second dose (Fig. 1B).  $\beta$  RBD HBsAg and  $\beta$ /Wu RBD HBsAg adjuvanted with Alum elicited similar RBD IgG levels at 2 weeks post prime and 4 weeks post 2<sup>nd</sup> dose (Fig. 1CD). At two weeks post prime, no significant differences were detected between  $\beta$  RBD HBsAg or  $\beta$ /Wu RBD HBsAg adjuvanted with Alum against Wuhan, Alpha, Beta, or Delta RBD strains (Supp. Table 2). Four weeks after the second dose, mice immunized with  $\beta$ /Wu RBD HBsAg+Al generated higher levels of anti-Wuhan RBD (1336889 AU/mL) (Fig.1E, Supp. Fig.1B) and anti-Delta RBD (1536000 AU/mL) IgG (Fig. 1F, Supp. Fig.1H) compared to Wuhan RBD (1075200 AU/mL) and Delta RBD (1113600 AU/mL) IgG levels in mice vaccinated with  $\beta$  RBD HBsAg+ Al (Fig. 1E-H, Supp. Fig.1B, H). Higher levels of Wuhan and Delta specific RBD IgG suggested that the combination of ancestral and Beta RBD improved the production of cross-reactive antibodies between SARS-CoV-2 strains. Overall, no significant differences between RBD IgG levels were detected between  $\beta$  RBD HBsAg and  $\beta$ /Wu RBD HBsAg adjuvanted with Alum against Wuhan, Alpha, Beta, or Delta RBD strains at 4 weeks post 2<sup>nd</sup> dose (Supp. Table 2).

RBD HBsAg adjuvanted with SWE began to elicit RBD IgG titers post prime, with the highest titers generated against Beta (54400 AU/mL), Delta (54400 AU/mL), Epsilon (60800 AU/mL), Eta, Iota, Zeta (73600 AU/mL), Gamma (80000 AU/mL), and Kappa (108800 AU/mL) RBD variants (Fig.1C). Additionally, at two weeks post prime, RBD HBsAg adjuvanted with SWE immunization generated significantly increased RBD IgG levels compared to Alum adjuvanted RBD HBsAg vaccines, suggesting that SWE improved the initial antibody responses to the RBD variants (Fig 1C, E-H, Supp. Fig.1, Supp. Table 2). Two-weeks after the third vaccine dose, RBD IgG levels in all  $\beta$  RBD HBsAg+SWE vaccinated mice increased significantly amongst Wuhan, Alpha, Beta, and Delta RBD variants compared two weeks post prime (Fig. 1E-H, Supp. Fig.1). RBD HBsAg adjuvanted with SWE generated significant RBD IgG levels compared to  $\beta$  RBD+SWE (Supp. Table 2). Furthermore, mice that received three doses of RBD+SWE generated a lower RBD IgG

response compared to the other vaccine formulations suggesting that the HBsAg VLP was required to develop an immunogenic RBD specific IgG response against SARS-CoV-2 VOC (Fig 1D-H). Interestingly, RBD HBsAg+SWE vaccine generated comparable RBD IgG across all VOC similar to Pfizer mRNA. At 2 weeks post prime, Pfizer mRNA vaccination generated increased RBD IgG levels amongst all RBD variants compared to other RBD HBsAg vaccine formulations (Fig.1C, Supp. Fig. 1, Supp. Table 2). Overall, mice immunized with two doses of Pfizer mRNA or three doses RBD HBsAg+SWE had the highest RBD IgG titers compared to the other vaccine formulations across all RBD variants (Fig. 1CD, Supp. Fig.1) Altogether, RBD HBsAg conjugate vaccines elicited immunogenic RBD IgG responses against SARS-CoV-2 VOC. Therefore, we hypothesized that RBD-VLP immunization would protect mice against Alpha or Beta SARS-CoV-2 challenge.

**$\beta$ /Wu RBD HBsAg+Al,  $\beta$  RBD HBsAg+SWE, and Pfizer mRNA vaccines provided protection against lethal challenge with Alpha or Beta SARS-CoV-2 in K18-hACE2 mice.** Next, to evaluate the protection profile of RBD HBsAg vaccines adjuvanted with either Alum or SWE compared to Pfizer mRNA, vaccinated and non-vaccinated K18-hACE2 mice were challenged with a lethal  $10^4$  PFU/dose of Alpha or Beta SARS-CoV-2 (Fig. 2A). Four to five mice from each vaccine group were challenged with either Alpha or Beta SARS-CoV-2, and five mice that were not challenged with SARS-CoV-2 was used as a control. During the 11-day challenge period, mice were monitored and scored based on the severity of disease symptoms including temperature and weight loss, activity, appearance, respiration, and eye health (Fig. 2A) (15,26). The disease scoring method was also used to determine humane euthanasia points throughout the course of challenge (26). In this study, we utilized survival instead of plaque forming assays as a strong indicator of protection. All PBS vaccinated mice (No Vaccine Challenged (NVC)) challenged with Alpha became morbid by day 6 post challenge and were humanely euthanized (Fig.2B), whereas PBS vaccinated mice (NVC) challenged with Beta also had a low survival rate (20% survival). Mice immunized with  $\beta$  RBD HBsAg+Al had partial survival (60% survival) against

Alpha challenge (Fig.2B) and performed better against Beta challenge with 80% survival (Fig. 2C). Whereas mice immunized with both Beta and Wuhan RBDs HBsAg adjuvanted with Alum afforded mice 100% survival against Alpha or Beta challenge (Fig.2BC). Mice immunized with  $\beta$  RBD HBsAg adjuvanted with SWE were 100% protected against Alpha or Beta challenge (Fig. 2BC). However, without the HBsAg, survival decreased in mice immunized with RBD+SWE against Alpha (60% survival) or Beta (40% survival) challenge (Fig.2BC). Similar to the  $\beta$ /Wu RBD HBsAg+Al and  $\beta$  RBD HBsAg+SWE, Pfizer mRNA also provided 100% protection against Alpha or Beta challenge (Fig.2BC). Overall, immunization with both Beta and Wuhan RBD antigens conjugated onto HBsAg VLP increased protection against Alpha or Beta challenge compared to immunization with Beta RBD HBsAg. Additionally, SWE adjuvanted RBD HBsAg vaccines were also able to protect mice from lethal challenge doses of Alpha or Beta VOC.

Poor survival was correlated in the daily increasing disease scores. Cumulative disease scores inversely mirrored the Kaplan-survival curve of the non-vaccinated or vaccinated mice and helped predict when mice would become morbid. Moribund mice in the NVC groups showed severe weight and temperature loss which paralleled the increase of the cumulative disease scores starting at day 5 post challenge (Supp. Fig.2, Fig. 2DE). Immunized mice had overall lower disease scores compared to NVC. Mice immunized with  $\beta$  RBD HBsAg+Al challenged with Alpha, or Beta showed elevated disease scores beginning at day 5 for Alpha challenged and day 6 for Beta challenged mice that mirrored survival data, whereas mice immunized with  $\beta$ /Wu RBD HBsAg+Al did not show disease progression and maintained weight and temperature through the course of the study (Fig.2DE, Supp. Fig.2). SWE adjuvanted  $\beta$  RBD HBsAg immunized mice challenged with Alpha, or Beta had little to no detectable signs of disease and sustained weight and temperature throughout the course of the study (Fig.2DE, Supp. Fig.2). However, without the HBsAg VLP, mice immunized with  $\beta$  RBD+SWE challenge with Alpha or Beta experienced a sharp increase of disease scores starting at days 5 and 6 post challenge, as well as dramatic weight and temperature loss (Fig.2DE, Supp. Fig.2). Pfizer mRNA immunized mice also did not

demonstrate disease onset during the study (Fig.2DE, Supp. Fig.2). Overall, survival and disease scores of the vaccinated K-18 hACE2 mice indicated that  $\beta$ /Wu RBD HBsAg+Al compared to  $\beta$  RBD HBsAg+Al and  $\beta$  RBD HBsAg+SWE compared to  $\beta$  RBD+SWE provided better protection encompassing survival and prevention of disease against Alpha or Beta challenge.

**Adjuvanted RBD VLP and mRNA vaccines significantly decreased viral RNA burden in the lung compared to no vaccine, VOC challenged animals.** To corroborate survival and disease data, viral RNA burden was measured in the lung and brain of VOC challenged animals. Both  $\beta$ /Wu RBD HBsAg+Al and  $\beta$  RBD HBsAg+Al immunized mice significantly decreased Alpha and Beta viral RNA burden in the lung compared to NVC (Fig.3A). However, in the brain,  $\beta$ /Wu RBD HBsAg+Al was capable of significantly lowering viral RNA burden against Alpha or Beta challenge but  $\beta$  RBD HBsAg+Al did not lower Alpha or Beta viral RNA burden (Fig.3B). The elevated levels of viral RNA in the brain in  $\beta$  RBD HBsAg+Al immunized mice suggested that dissemination into the brain increased mortality.  $\beta$  RBD HBsAg+SWE significantly lowered Alpha or Beta viral RNA burden to the limit of detection in both the lung and the brain compared to NVC and RBD+SWE (Fig. 3AB).  $\beta$  RBD+SWE failed to lower viral RNA burden compared to NVC Alpha or Beta in both the lung and brain suggesting that the Hepatitis B antigen VLP is necessary for a significant decrease of viral RNA burden (Fig.3AB). Lastly, Pfizer mRNA was also able to significantly reduce viral Alpha or Beta RNA in both the lung and brain (Fig.3AB). Altogether, this data suggested that both Beta and Wuhan RBDs are necessary in the Alum adjuvanted vaccine to prevent VOC dissemination into the brain. Furthermore,  $\beta$  RBD HBsAg+SWE similar to Pfizer mRNA can diminish viral replication and dissemination in the both the lung and brain.

**RBD HBsAg+SWE vaccination generated cross neutralizing antibodies against VOC.** Neutralizing antibodies of SARS-CoV-2 provide the first line of defense for COVID-19 vaccine protection (38,39). Since the antigens used in the  $\beta$  RBD HBsAg+Al and  $\beta$ /Wu RBD HBsAg+Al vaccine formulations in this study originated from Wuhan or Beta SARS-CoV-2 it is important to



determine vaccine generation of cross neutralizing antibodies against the various VOC. To evaluate antibody cross-neutralizing capacity of the RBD HBsAg VLP vaccines against Beta or Alpha VOC challenge, *in vitro* human ACE2 to RBD VOC binding were assessed using the MSD neutralization assay platform. In this study, the RBD of the five major Variants of Concern, Alpha, Beta, Gamma, Delta, and Omicron VOC were evaluated compared to the ancestral strain of SARS-CoV-2. Mice vaccinated with  $\beta$  RBD HBsAg+AI or  $\beta$ /Wu RBD HBsAg+AI had similar neutralization profiles across the RBD VOC; however, there was a reduction of neutralization against Omicron RBD in both challenge with Beta or Alpha VOC (Fig.4, Supp.Fig.3). However, mice vaccinated with  $\beta$  RBD HBsAg adjuvanted with SWE along with mice vaccinated with mRNA generated robust neutralizing antibodies across all RBD VOC (Fig.4).  $\beta$  RBD HBsAg adjuvanted with SWE provided a significant induction of cross neutralizing antibodies that could inhibit the binding of hACE2 to Wuhan, Alpha, Beta, Delta, and Omicron RBD compared to NVC (Fig.4, Supp. Fig 3). However, immunization with  $\beta$  RBD+SWE did not generate significant neutralizing titers against VOC RBD suggesting that HBsAg is needed to produce functional antibodies against SARS-CoV-2 (Fig. 4 and Supp. Fig. 3). Thus, the neutralizing antibody profiles demonstrate that RBD HBsAg VLP vaccines provided breath of neutralizing antibodies against all major VOC similar to Pfizer mRNA immunization compared to unconjugated RBD vaccines.

**$\beta$ /Wu RBD HBsAg+AI and Pfizer mRNA vaccinations lowered both acute and chronic inflammation in the lung during Alpha or Beta challenge.** COVID-19 can cause severe inflammation in the lungs (40). Therefore, histopathological analysis was performed on non-vaccinated or vaccinated mouse lungs at time of euthanasia due to morbidity or the end of the experiment at day 11 to investigate whether RBD HBsAg VLP vaccines in this study alleviated inflammation from Alpha or Beta challenge. Chronic and acute inflammation was assessed in the lung parenchyma, blood vessels, and airways (Supp. Fig.4AB). The presence of infiltrating lymphocytes and plasma cells characterized chronic inflammation and acute inflammation was

identified by recruitment of neutrophils and edema (Supp. Fig.4AB). Total inflammation scores were determined by the addition of both chronic and acute inflammation scores. Mice in the NVC group challenged with either Alpha or Beta exhibited mixed inflammation comprising of both chronic and acute inflammation present in the lung parenchyma and blood vessels showing large aggregates of inflammatory cells (Fig.5AB, Supp. Fig. 4CDEF). NVC groups challenged with Alpha, or Beta had average inflammation scores (average of total inflammation between chronic and acute scores) of 4.6 and 4.2 respectively (Fig.5DE). Mice immunized with  $\beta$  RBD+SWE and challenged with Alpha or Beta experienced higher chronic and acute inflammation scores than NVC groups with an average inflammation score of 7.2 and 5.2 respectively (Fig. 5DE, Supp Fig. 4CDEF).  $\beta$  RBD+SWE immunized mice challenged with Alpha also had significantly elevated chronic and acute inflammation scores and significantly increased acute inflammation scores in Beta challenged mice compared to NVNC (Fig. 5C, Supp. Fig. 4CDEF). Additionally, RBD+SWE vaccinated lungs also showed an infiltration of alveolar macrophages, neutrophils, presence of eosinophilic material, and exhibited vascular thrombosis which may indicate the poor disease prognosis of  $\beta$  RBD+SWE vaccinated mice (Supp. Fig.5). Interestingly,  $\beta$  RBD HBsAg+SWE vaccinated mice challenged with Alpha, or Beta also demonstrated relatively increased chronic and acute inflammation levels compared to other protective vaccines ( $\beta$ /Wu RBD HBsAg+Al and Pfizer mRNA) with average inflammation scores of 3.2 and 2.6 (Fig. 5DE). Alveolar macrophages and eosinophilic material in the alveoli were also found in  $\beta$  RBD HBsAg+SWE vaccinated in lungs primarily in the Alpha challenged group suggesting SWE adjuvant may be more inflammatory than Alum adjuvant (Fig. 5AB).  $\beta$ /Wu RBD HBsAg+Al and  $\beta$  RBD HBsAg+Al lungs had similar low chronic and acute inflammation scores against Beta challenge; however,  $\beta$ /Wu RBD HBsAg+Al immunization was able to significantly decrease total chronic inflammation scores against Alpha challenge compared to NVC (Fig. 5DE). Pfizer mRNA also demonstrated lowered chronic and acute inflammation compared to NVC (Fig. 5, Supp. Fig. 4CDEF). Overall, mice

immunized with SWE formulations had elevated inflammation in the lung compared to vaccines adjuvanted with Alum or Pfizer mRNA.

### **3.6 Discussion**

As the pandemic continues, global vaccine disparities remain a major problem. In lower income areas of the world, such as in Africa, 16% or less of the population have received a single dose of a COVID-19 vaccine. Organizations such as the WHO, Gavi, and CEPI have teamed together to provide global access to COVID-19 vaccines and treatments. However, due to many issues involving lack of funds, supply, and participation from upper income countries, these organizations have faced setbacks providing vaccines to lower-income countries. Despite these difficulties, at the end of 2021, these organizations delivered approximately 300 million doses to primarily 144 low- and middle-income countries (41). With 194 or more COVID-19 vaccine candidates in pre-clinical stages and greater than 120 vaccines in clinical trials, there is a possibility that the production of these vaccines can help alleviate the supply chain issues. The development of protein-based subunit COVID-19 vaccines can especially aid in relieving supply as well as delivery and storage issues to lower-income countries. Protein-based vaccines are distinguished by inexpensive manufacturing cost as well as stability at a wide range of temperatures for shipment and storage, all of which can benefit low-income countries (42,43).

Currently, the spike nanoparticle protein vaccine developed by Novavax is the only WHO approved protein subunit vaccine in distribution. Nevertheless, at this time, there are over 46 protein-based vaccines under clinical investigation (44). However, there are no approved COVID-19 VLP vaccines that are authorized for human use currently. Interestingly, three COVID-19 protein decorated VLP vaccines are in phase 1-3 clinical trials. CoVLP developed by Medicago is composed of a plant based VLP decorated with the ancestral spike protein and adjuvanted with Adjuvant System 03 (ASO3). In phase 3 clinical trials, the vaccine efficacy of CoVLP was 69.5% effective at preventing symptomatic infections and 78.8% against moderate-severe COVID-19 infections across multiple VOC (45,46). The second COVID-19 VLP vaccine in clinical trials is

VBI-2902a. VBI-2902a is developed by VBI Vaccines and formulated with Wuhan spike protein displayed on enveloped virus like particles derived from murine leukemia virus adjuvanted with Alum (47). In pre-clinical trials, VBI-2902a induced neutralizing antibodies against SARS-CoV-2 as well as decreased viral burden and lung inflammation in SARS-CoV-2 challenged hamsters (47). Furthermore, in phase 1 clinical trials, VBI-2902a was well tolerated amongst recipients and generated functional antibody titers (48). Lastly, SARS-CoV-2 VLP Vaccine, developed by The Scientific and Technological Research Council of Turkey is in phase 1 clinical trials. SARS-CoV-2 VLP Vaccine is composed of SARS-CoV-2 membrane, envelope, nucleocapsid and spike protein decorated on a VLP adjuvanted with alum and CPGoDN-K3 (49). Additionally, despite most protein vaccines utilizing the spike protein as the main vaccine antigen, there are multiple RBD based protein vaccines in clinical trials. For example, manufacturers such as Serum Institute of India, Biological E, and SK Bioscience have developed RBD based protein vaccines, as well as other institutes such as Finlay Vaccine Institute and The Center for Genetic Engineering and Biotechnology in Cuba, and Texas Children's Hospital and Baylor College of Medicine (27,50).

Altogether, the numerous protein COVID-19 vaccines that are under pre-clinical and clinical investigation can help alleviate the global shortage of COVID-19 vaccines.

Here, four experimental protein subunit COVID-19 vaccines utilizing a Hepatitis B surface antigen Virus-like particle decorated with RBD as the vaccine antigen, adjuvanted with either Alum or SWE, were evaluated in K18-hACE2 mice against Alpha or Beta challenge (51–53). All experimental RBD HBsAg VLP vaccines were compared to the standard 2 dose Pfizer mRNA vaccine. Our first goal was to assess the correlates of protection associated with utilizing both ancestral SARS-CoV-2 and Beta RBD VLP in a vaccine formulation compared to Beta RBD VLP. Interestingly, only RBD HBsAg from both Beta and Wuhan in one formulation adjuvanted with Alum was able to fully protect mice against Alpha or Beta challenge (100% survival) (Fig.2) and decreased viral RNA in the lung and brain. Whereas  $\beta$  RBD HBsAg+Al provided partial protection from Alpha (60% survival) or Beta (80% survival) challenge (Fig.2), and significantly lowered viral

burden in the lung against Alpha or Beta challenge (Fig. 3). However, both alum adjuvanted RBD HBsAg vaccines were able to generate functional antibodies against RBD (Fig.1, Fig. 2) and decrease inflammation in the lung (Fig.5). Next, our second goal was to evaluate whether HBsAg VLP was necessary for protection as well as assess the outcome of utilizing SWE instead of Alum adjuvant on vaccine efficacy and immunogenicity. Beta RBD HBsAg adjuvanted with SWE vaccinated K18-hACE2 mice were protected against both Alpha or Beta challenge, induced a robust systemic RBD IgG response (Fig. 1), generated broadly neutralizing antibodies against VOC RBDs (Fig. 4), and lowered viral RNA burden in the lung and brain (Fig. 3) similar to the outcome of Pfizer vaccinated mice. Without the HBsAg VLP, RBD alone adjuvanted with SWE was not able to protect mice from Alpha or Beta challenge (Fig.2) or induce an immune response (Fig. 1,4). We acknowledge our study contained limitations such as not measuring infectious particles through plaque forming units (PFUs) in the murine challenge studies. However, in this study we prioritized using survival as a measure of protection instead of determining infectious viral burden. Studies have shown that after day 2 of challenge, PFUs begin to decrease (54,55). In our vaccine and challenge studies, non-protected mice do not begin to become morbid until day 5 or 6, and protected mice do not develop disease throughout the 11- day study, limiting the possibility of obtaining infectious virus. For future murine vaccine and challenge studies with SARS-CoV-2, we plan on performing time points at day 2 post challenge to assess PFUs as well as day 11 post challenge to evaluate survival.

With the lack of vaccines being delivered to rural countries, it is pertinent that the COVID-19 vaccines that these countries are receiving can deliver strong, long lasting immune responses with limited dose series. Vaccine adjuvants can help increase immune responses (both cellular and humoral) to target antigens, as well promote long-term protection (56,57). In this study, we used both Aluminum hydroxide or SWE to enhance the response of the RBD HBsAg antigen. Alum has been safely used in many vaccine formulations to date and is known to elicit a strong antibody response. The squalene in water emulsion, SWE adjuvant was developed by the non-

profit organization, Vaccine Formulation Institute, and is made available to the entire vaccine community with the goal of accelerating the development of COVID-19 vaccines. Similar to its counterpart MF59, oil in water emulsions also generate robust antibody responses. In this study, Alum adjuvanted RBD HBsAg generated less breadth of cross reactive RBD IgG antibodies across 10 VOC (Fig.1) compared to the SWE adjuvanted VLP as well as did not significantly produce broadly neutralizing antibodies across 5 major SARS-CoV-2 VOC (Fig.4) Alternatively, RBD HBsAg adjuvanted with SWE was able to induce robust RBD IgG response similar to the Pfizer mRNA RBD IgG titers (Fig.1) as well as elicit a significant broadly neutralizing antibody response against 3 out of 5 RBD VOC (Fig.4). Both vaccines offered protection to mice after challenge with VOC; however only the SWE adjuvanted RBD HBsAg vaccine was able to induce cross neutralizing antibodies that recognized all 10 variants of SARS-CoV-2 suggesting that SWE elicited a stronger antibody response that was able to aid in protection. We hypothesize that since SWE significantly elevated the broadly neutralizing antibody response in vaccinated mice compared to Alum, that the SWE adjuvant would also increase longevity of vaccine efficacy. However, further studies are needed to evaluate long-term protection of SWE adjuvanted RBD-HBsAg vaccines. We also acknowledge in this study that three doses of the RBD HBsAg+SWE were used to immunize mice. However, due to the dose sparing nature of SWE, vaccine efficacy of one or two dose administration to mice of RBD HBsAg+SWE could have been further investigated and compared to receiving three doses of vaccine.

Neutralizing antibodies against SARS-CoV-2 are the first line of vaccine protection against COVID-19. Therefore, in this study, vaccine induced antibody responses against RBD on SARS-CoV-2 were characterized. Additionally, T-cell responses including CD4 and CD8 T-cells, also play a crucial role in controlling COVID-19 by decreasing viral replication (58–61). Evaluation of T-cell responses are essential to understand the full protection profile generated from both SWE or Alum adjuvanted RBD VLP vaccines. The robust RBD specific IgG antibody responses elicited

from RBD HBsAg + SWE suggests that antigen specific CD4+ T cells are playing a role in activating SARS-CoV-2 B-cell responses. In this study, Pfizer mRNA vaccinated mice also generated a strong antibody response and broadly neutralizing antibodies against multiple VOC similar to the RBD HBsAg+SWE. In humans, cellular responses remained detectable after 6 months after 2 doses of Pfizer mRNA with high detection of spike specific CD4+ T-cells (59). Thus, we hypothesized that SWE adjuvanted RBD-VLP vaccines will elicit antigen specific B and T cell responses compared to the Alum adjuvanted vaccines. Further investigation is needed to evaluate the T-cell populations generated after vaccination with RBD-HBsAg adjuvanted with SWE or Alum and how they play a role in protection during challenge with different VOC.

The target vaccine antigen utilized in this study was the receptor binding domain (RBD) of the SARS-CoV-2 spike protein. RBD is a relatively small protein with the molecular weight of 25kDA, whereas the full spike protein has a molecular weight of 78.3kDA. Currently, all the WHO approved vaccines utilize the spike protein as the primary vaccine antigen. Utilization of the full spike protein as a vaccine antigen offers numerous immunological benefits. The spike protein offers more immunodominant T-cell epitopes that can elicit CD4+, T follicular helper cell, and CD8 responses against SARS-CoV-2 compared to RBD alone (38,62–64). Despite numerous immunological advantages of using the spike protein compared to RBD alone, the spike protein is more difficult to manufacture compared to RBD that can be easily expressed and produced in large scale in microbial host such as yeast. Therefore, RBD-based vaccines may help facilitate COVID-19 vaccine production and distribution in lower-income countries (11,65–67).

Emergence of new SARS-CoV-2 VOC have dampened vaccine effectiveness causing vaccine breakthrough cases facilitating transmission of the virus. VOC also prompted vaccine manufacturers to begin designing variant specific vaccines to replace vaccines derived from the ancestral strain of SARS-CoV-2 (68). At the time of this study, outbreaks of the Beta variant had

started to occur in South Africa triggering concerns around the world (69,70). Therefore, to prevent further deleterious consequences from Beta, we decided to evaluate the RBD from the Beta variant in vaccine formulations in this study. Beta unlike its predecessor Alpha, contains 9 mutations located on the spike protein (18F, D80A, D215G, R246I, K417N, E484K, N501Y, D614G, and A701V) and from these, three mutations (K417N, E484K, N501Y) are on the RBD (2,71). Previous studies performed with human convalescent plasma obtained from a patient infected with the ancestral strain of SARS-CoV-2 demonstrated that convalescent plasma was not able to protect against Beta challenge in mice (26). Furthermore, these mutations on Beta were shown to decrease vaccine efficacy as well as reduce neutralization efficacy in monoclonal antibody and convalescent antibody treatments (72–74). However, the frequency of detection of Beta did not go above 13% and did not persist past July 2021 unlike Alpha or other variants (75,76). Even though the Beta variant did not persist, our studies demonstrated that RBD HBsAg vaccines formulated with Beta RBD HBsAg offered protection against Alpha VOC as well as generated a breadth of neutralizing antibodies against multiple SARS-CoV-2 VOC suggesting that these vaccines could be protective against other VOC.

In summary, RBD HBsAg is an immunogenic antigen but when adjuvanted with either Alum or SWE provided protection to mice challenged with Alpha or Beta variant. Protection profiles generated by RBD HBsAg vaccines were similar to those produced by mRNA Pfizer vaccination. Evaluation of RBD HBsAg adjuvanted with Alum or SWE in pre-clinical murine studies allowed for the advancement of these vaccines into phase 1/2 clinical trials in Australia. In the future, RBD-VLP vaccines as well as other protein subunit vaccines will help alleviate the vaccine disparity gap caused by COVID-19.

### **3.7 Acknowledgements**

We would like to thank Serum Institute of India for providing HBsAg VLP, SpyBiotech for providing their SpyTag and SpyCatcher technology, the Love Lab at MIT for providing the RBD antigens,



and SEPPIC and the Vaccine Formulation Institute for supplying SWE adjuvant. FHD and the VDC are supported by the Research Challenge Grant no. HEPC.dsr.18.6 from the Division of Science and Research, WV Higher Education Policy Commission. This project was supported by the Serum Institute of India. MSD QuickPlex SQ120 in the WVU Flow Cytometry & Single Cell Core Facility is supported by the Institutional Development Awards (IDeA) from the National Institute of General Medical Sciences of the National Institutes of Health under grant numbers P30GM121322 (TME CoBRE) and P20GM103434 751 (INBRE). We would also like to acknowledge Mary Tomago-Chesney at the WVU Pathology Department for sectioning and performing H&E staining on lung tissues, as well as Dr. Christopher Gibson (iHisto) for performing histopathologic scoring on the lungs.

**Author contributions.** Studies were designed by SII, FHD, and JRB. All authors contributed to the execution of these studies. SARA, NCD, RSJ, and JCL provided and produced RBD antigens for vaccine formulations. SII supplied HBsAg and provided vaccines for immunization. TYW, JK, and KSL vaccinated mice. MTW and IM prepared and provided viral stocks of Alpha and Beta variants for murine challenge. Animal daily disease assessment, necropsy and tissue processing were performed by FHD, MB, HAC, TYW, BPR, KSL and JRB. Serological analysis was conducted by SII. qPCR to determine viral RNA burden was performed by BPR and OAM. MSD neutralization was performed by MC. All authors contributed to the writing and revision of this manuscript. Data was analyzed by TYW and FHD.

### 3.8 Figures.

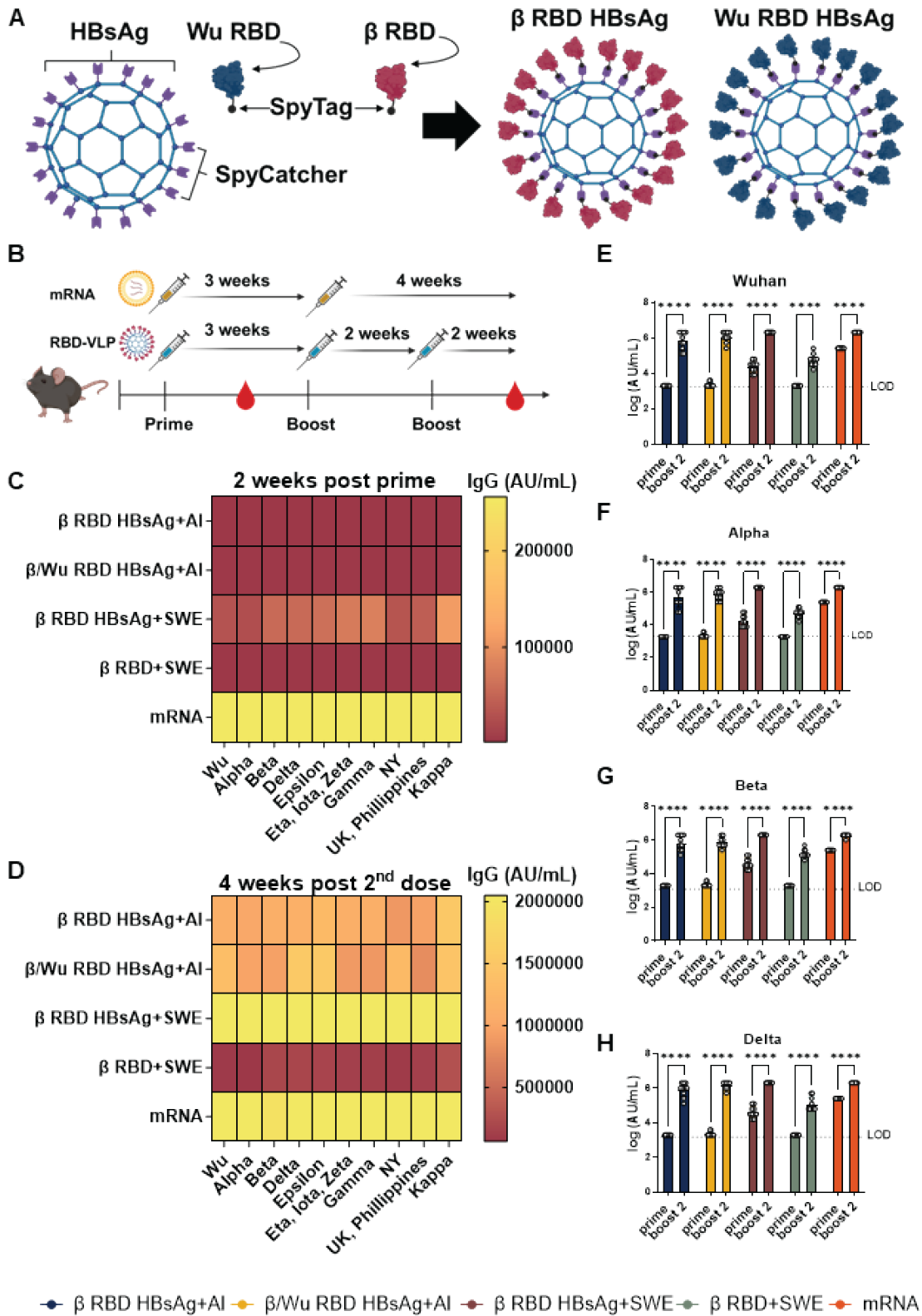


**Figure 1. Characterization of RBD IgG antibody responses against 10 SARS-CoV-2 VOC RBDs.** A) Depiction of assembly of  $\beta$  or Wuhan RBD on HBsAg using SpyTag and SpyCatcher technology. B) Schematic of K18 hACE2 mouse immunization and serological assessment schedule. C) MSD V-PLEX SARS-CoV-2 IgG Panel 11 was used to determine RBD IgG levels. Heat map depicts mean values of IgG (AU/mL) generated from each mouse RBD IgG titers were measured against 10 VOC RBDs at 2 weeks post prime. D) 4 weeks post 2<sup>nd</sup> dose RBD IgG titers against 10 VOC RBDs. E-H) RBD IgG titers from 2 weeks post prime and 4 weeks post 2<sup>nd</sup> dose against Wuhan, Alpha, Beta, and Delta RBD VOC respectively. IgG titers represented as log AU/mL. Two-Way ANOVA with Sidak's multiple comparisons test was performed for statistical analysis.  $P < 0.0001$  \*\*\*\*. Dotted line represents limit of detection for the specific RBD variant.

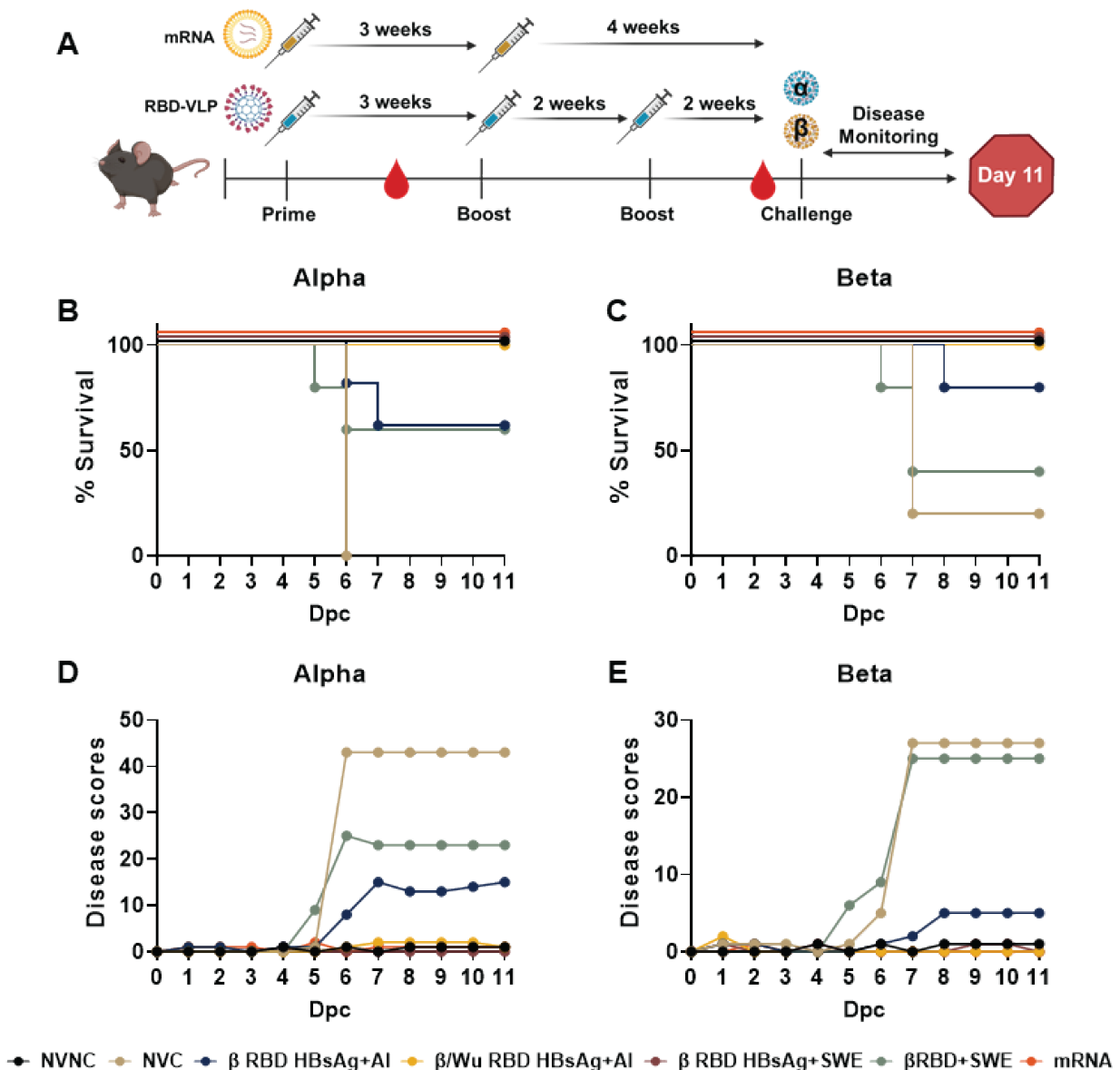


**Figure 2. Evaluation of RBD-VLP and mRNA vaccine protection against VOC challenge.** A) Vaccine and challenge experimental timeline in K18-hACE2 mice. Mice were intramuscularly administered three doses of either  $\beta$  RBD HBsAg+AI,  $\beta$ /Wu RBD HBsAg+AI,  $\beta$  RBD HBsAg + SWE, or  $\beta$  RBD+SWE. Pfizer mRNA vaccinated mice were administered 2 doses of vaccine. Vaccinated mice were bled every 2 weeks post vaccine dose. Mice were intranasally challenged with  $10^4$  PFU/dose of either Alpha or Beta variant and monitored for 11 days after challenge. B) Kaplan Meier survival curve shows percent survival of NVNC (n=5), NVC (n=5),  $\beta$  RBD HBsAg+AI

(n=5)  $P=0.0143^*$ ,  $\beta$ /Wu RBD HBsAg+AI (n=5)  $P=0.0027^{**}$ ,  $\beta$  RBD HBsAg + SWE (n=5)  $P=0.0027^{**}$ ,  $\beta$  RBD+SWE (n=5) or Pfizer mRNA (n=5)  $P=0.0027^{**}$  challenged with Alpha. C) Kaplan Meier survival curve of NVNC (n=5), NVC (n=5),  $\beta$  RBD HBsAg+AI (n=5)  $P=0.0411^*$ ,  $\beta$ /Wu RBD HBsAg+AI (n=4)  $P=0.0237^*$ ,  $\beta$  RBD HBsAg + SWE (n=5)  $P=0.0143^*$ ,  $\beta$  RBD+SWE (n=5) or Pfizer mRNA (n=5)  $P=0.0143^*$  challenged with Beta. Log-rank (Mantel-Cox) test determined statistical significance between NVC compared to respective vaccine groups. D-E) Daily disease scores of Alpha or Beta challenged mice respectively.

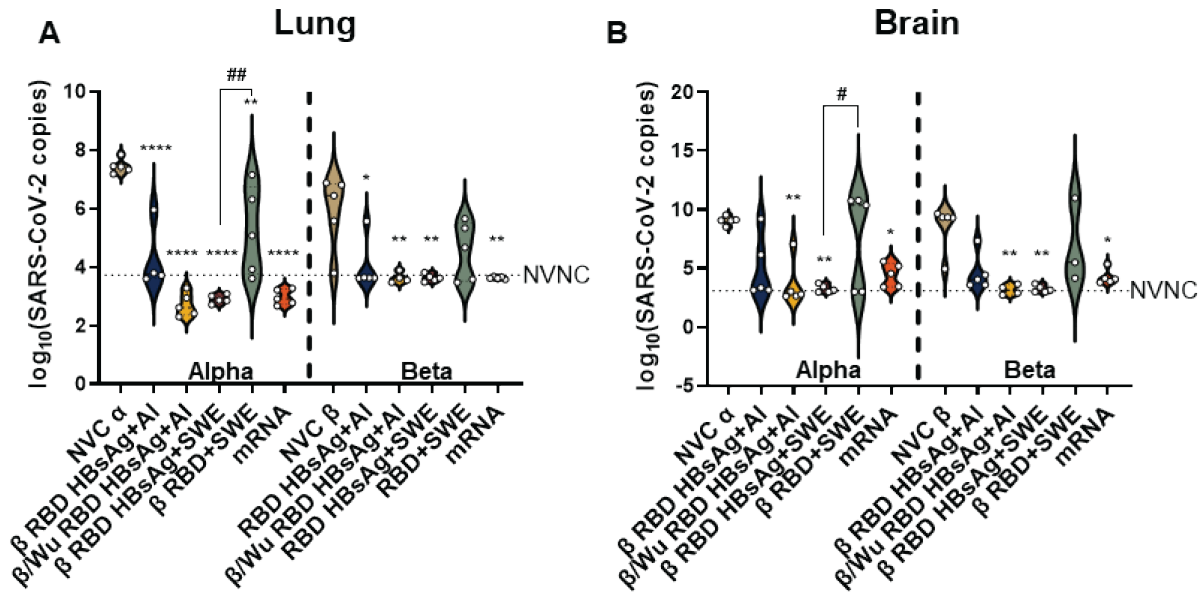


**Figure 3. Determination of viral RNA burden in VOC challenged mice.** 100ng of lung and brain were assessed for nucleocapsid RNA copies. Violin plots depict SARS-CoV-2 RNA copies in the A) right lobe of the lung and B) brain. Left side of the bold vertical dotted line represents mice challenge with Alpha and right side represents mice challenged with Beta. Horizontal dotted line represents the limit of detection calculated with the NVNC viral copy numbers. Ordinary one-way ANOVA with Tukey's multiple comparisons test was performed for statistical analysis amongst the Alpha or Beta challenged groups. Asterisks denote significant difference compared to NVC and # symbol indicates significant difference compared to RBD+SWE. For lung,  $P < 0.0001^{****}$ ,  $P = 0.0187^*$  (NVC $\beta$  vs  $\beta$  RBD HBsAg+AI),  $P = 0.0035^{**}$  (NVC $\alpha$  vs  $\beta$ /Wu RBD HBsAg+AI),  $P = 0.0014^{**}$  (NVC $\alpha$  vs  $\beta$  RBD HBsAg+SWE),  $P = 0.0089^{**}$  (NVC $\beta$  vs  $\beta$ /Wu RBD HBsAg+AI), and  $P = 0.0052^{**}$  (NVC $\beta$  vs  $\beta$  RBD HBsAg+SWE),  $P = 0.0014^{##}$  ( $\beta$  RBD HBsAg+SWE vs.  $\beta$  RBD+SWE). For brain,  $P = 0.0231^*$  (NVC $\alpha$  vs mRNA),  $0.0452^{\#}$  ( $\beta$  RBD HBsAg+SWE vs RBD+SWE),  $0.0495^*$  (NVC $\beta$  vs mRNA).  $P = 0.0035^{**}$  (NVC $\alpha$  vs  $\beta$ /Wu RBD HBsAg+AI),  $P = 0.0014^{**}$  (NVC $\alpha$  vs  $\beta$  RBD HBsAg+SWE),  $P = 0.0089^{**}$  (NVC $\beta$  vs  $\beta$ /Wu RBD HBsAg+AI), and  $P = 0.0052^{**}$  (NVC $\beta$  vs  $\beta$  RBD HBsAg+SWE).

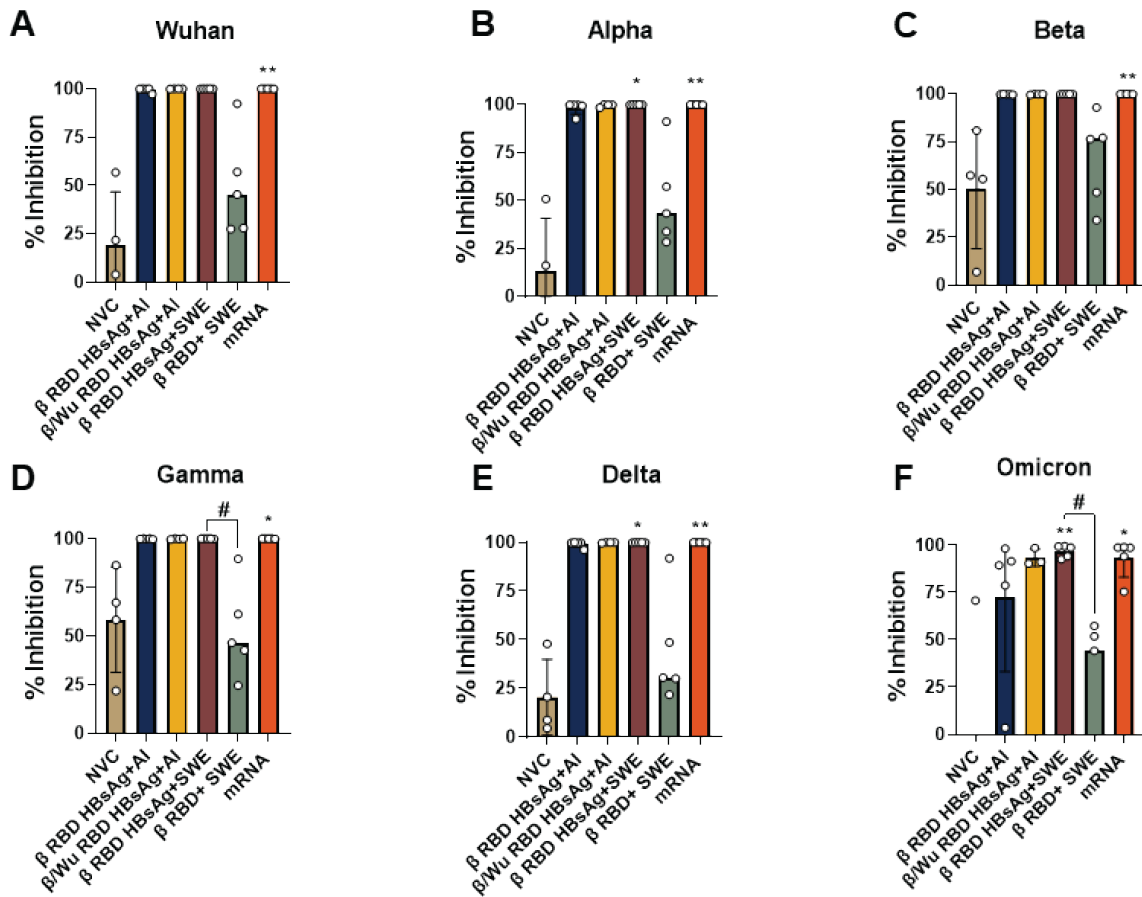


**Figure 4. RBD HBsAg+SWE induced broadly neutralizing antibodies against VOC RBD.**

MSD V-PLEX SARS-CoV-2 Panel 22 (ACE2) kit with 5 VOC and Wuhan RBD was used to measure serum antibody neutralization in Beta challenged mice in immunized and non-immunized mice. All values were depicted as % inhibition. Negative % inhibition values were not represented in the analysis. Percent inhibition of neutralizing antibodies measured against A) Wuhan, B) Alpha, C) Beta, D) Gamma, E) Delta, and F) Omicron respectively. Dotted line represents neutralizing antibody levels of NVNC. Results represented as mean  $\pm$  SD. Kruskal-Wallis test with Dunn's multiple comparisons test were conducted for statistical analysis. Asterisks denote significant difference compared to NVC and # symbol indicates significant difference compared to RBD+SWE. Wuhan.  $P=0.0063^*$ . Alpha.  $P=0.00319^*$  (NVC vs RBD HBsAg+SWE)

$P=0.0019^{**}$  (NVC vs mRNA) Beta.  $P=0.0081^*$  (NVC vs mRNA. Gamma.  $P=0.0151^*$  (NVC vs mRNA),  $P=0.0461\#$  (RBD HBsAg+SWE vs RBD+SWE). Delta.  $P=0.0319^*$  (NVC vs RBD HBsAg+SWE),  $P=0.0045^{**}$ (NVC vs mRNA). Omicron.  $P=0.0213^*$  (NVC vs mRNA),  $P=0.0029^{**}$  (NVC vs RBD HBsAg+SWE).



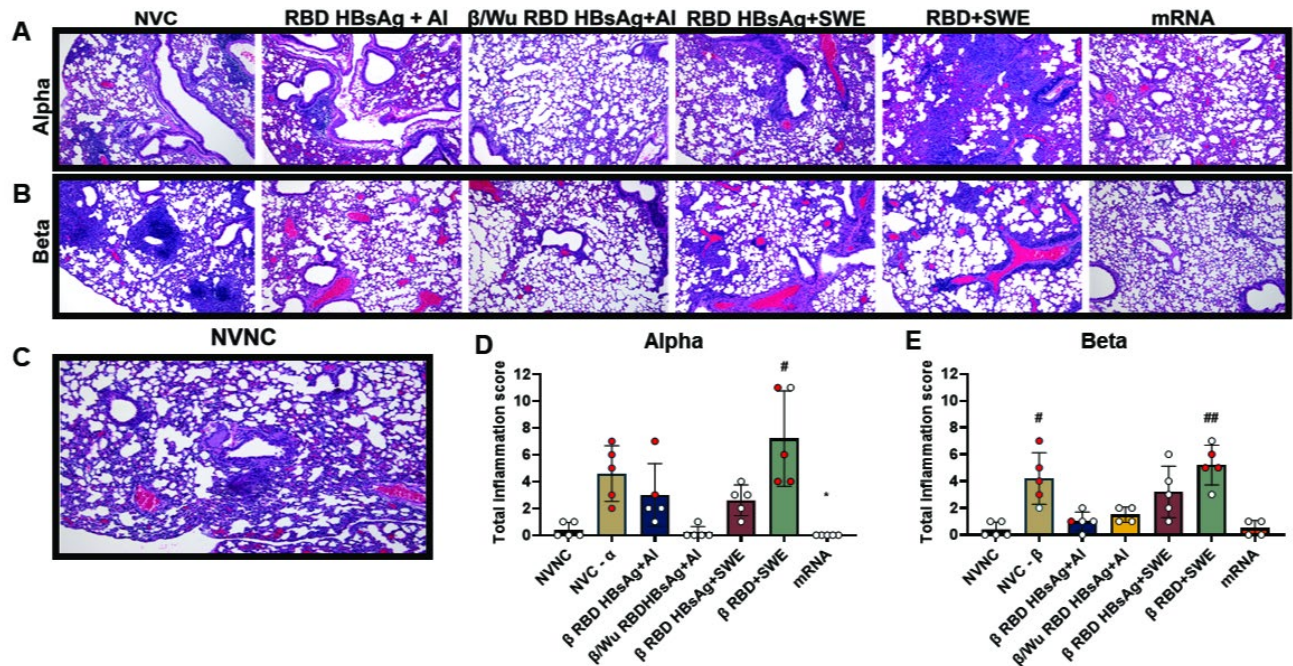


**Figure 5. Histopathological analysis of the lung in vaccinated mice challenged with VOC.**

A) H&E-stained lungs from vaccinated groups that were Alpha challenged. B) H&E-stained lungs from vaccinated groups that were Beta challenged. C) No vaccine no challenge (NVNC) H&E-stained lungs represented at 100X magnification. D) Alpha challenged total inflammation scores (chronic + acute inflammation scores).  $P=0.0213\#$  (NVNC vs.  $\beta$  RBD+SWE) and  $P=0.0251^*$  (NVC $\alpha$  vs mRNA). E) Beta challenged total inflammation scores.  $P=0.0341\#$  (NVNC vs. NVC- $\beta$ ), and  $P=0.0062\##$  (NVNC vs.  $\beta$  RBD+SWE). Red dots represent mice that were euthanized due to morbidity before the termination of the study at day 11. Results represented as mean  $\pm$  SD. Kruskal-Wallis with Dunn's multiple comparisons test was performed for statistical analysis. Asterisks denote significant difference compared to NVNC and # symbol indicates significant difference compared to NVNC.

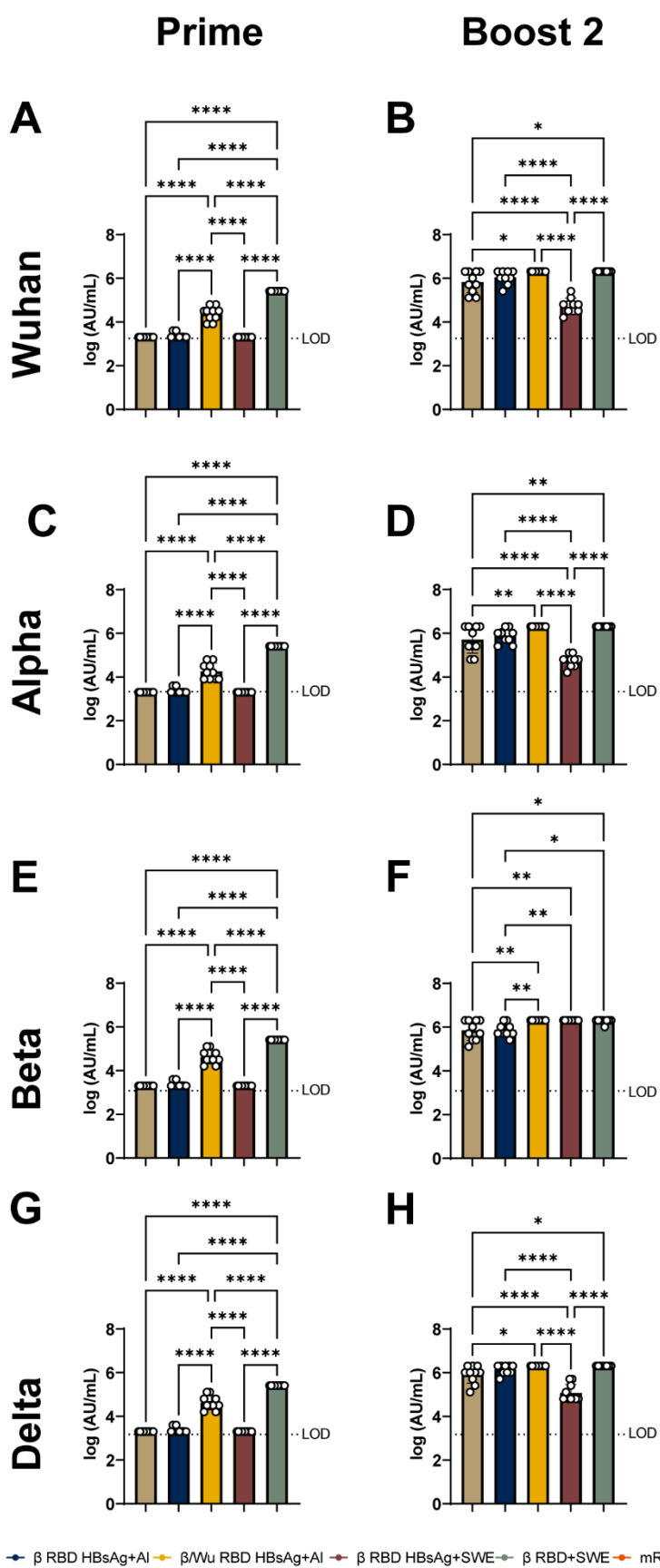
### 3.9 Supplemental Figures

<b>Vaccine</b>	<b>Composition</b>
<b>β RBD HBsAg+AI</b>	<b>10μg β RBD J HBsAg + 100μg AIOH</b>
<b>β/Wu RBD HBsAg+AI</b>	<b>5μg β RBD J HBsAg + 5μg Wu RBD HBsAg + 100μg AIOH</b>
<b>β RBD HBsAg + SWE</b>	<b>1.25μg β RBD J (N Tag) HBsAg + SWE</b>
<b>β RBD+SWE</b>	<b>2.5μg β RBD J (N Tag) + SWE</b>
<b>mRNA</b>	<b>3ug Pfizer mRNA</b>

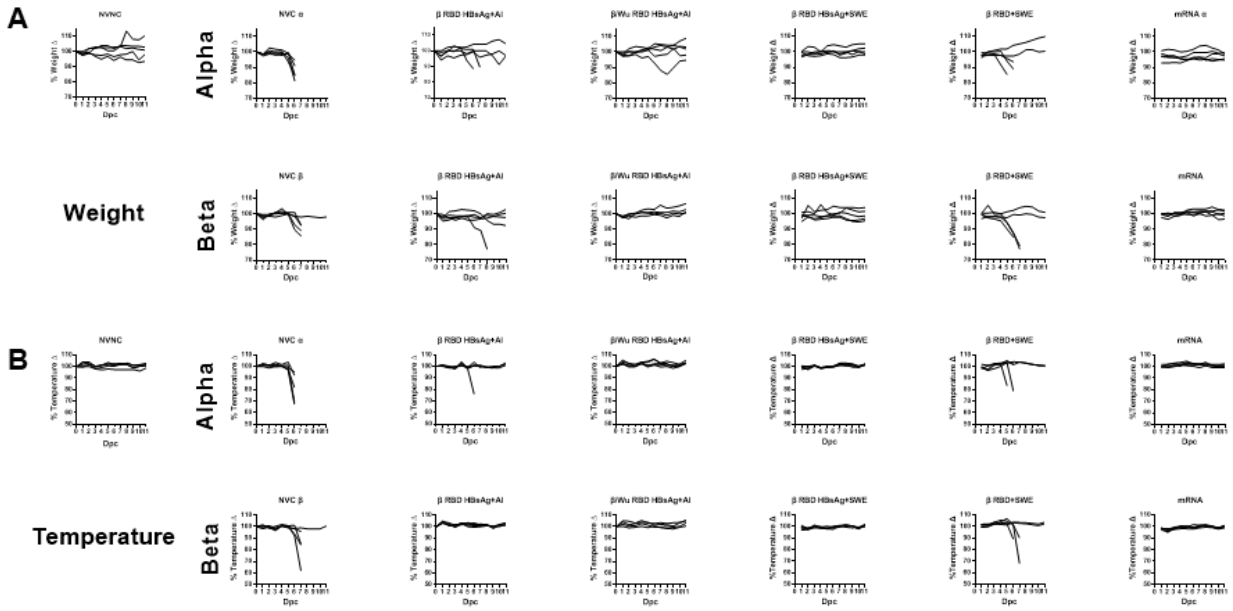
**Supplemental Table 1. COVID-19 vaccine formulations.** Composition of the five vaccines intramuscularly administered to K18-hACE2 mice.

Vaccine groups			
RBD strain	Prime	Summary	Adjusted P value
Wuhan	β RBD HBsAg+AI vs β RBD HBsAg+SWE	****	<0.0001
Wuhan	β RBD HBsAg+AI vs Pfizer mRNA	****	<0.0001
Wuhan	β/Wu RBD HBsAg+AI vs β RBD HBsAg+SWE	****	<0.0001
Wuhan	β/Wu RBD HBsAg+AI vs Pfizer mRNA	****	<0.0001
Wuhan	β RBD HBsAg+SWE vs β RBD+SWE	****	<0.0001
Wuhan	β RBD HBsAg+SWE vs Pfizer	****	<0.0001
Wuhan	β RBD+SWE vs Pfizer	****	<0.0001
Wuhan	<b>Boost 2</b>		
Wuhan	β RBD HBsAg+AI vs β RBD HBsAg+SWE	***	0.0003
Wuhan	β RBD HBsAg+AI vs β RBD+SWE	****	<0.0001
Wuhan	β RBD HBsAg+AI vs Pfizer mRNA	***	0.0007
Wuhan	β/Wu RBD HBsAg+AI vs β RBD+SWE	****	<0.0001
Wuhan	β RBD HBsAg+SWE vs β RBD+SWE	****	<0.0001
Wuhan	β RBD+SWE vs Pfizer	****	<0.0001
Wuhan			
RBD strain	Prime	Summary	Adjusted P value
Alpha	β RBD HBsAg+AI vs β RBD HBsAg+SWE	****	<0.0001
Alpha	β RBD HBsAg+AI vs Pfizer mRNA	****	<0.0001
Alpha	β/Wu RBD HBsAg+AI vs β RBD HBsAg+SWE	****	<0.0001
Alpha	β/Wu RBD HBsAg+AI vs Pfizer mRNA	****	<0.0001
Alpha	β RBD HBsAg+SWE vs β RBD+SWE	****	<0.0001
Alpha	β RBD HBsAg+SWE vs Pfizer	****	<0.0001
Alpha	β RBD+SWE vs Pfizer	****	<0.0001
Alpha	<b>Boost 2</b>		
Alpha	β RBD HBsAg+AI vs β RBD HBsAg+SWE	***	0.0003
Alpha	β RBD HBsAg+AI vs β RBD+SWE	****	<0.0001
Alpha	β RBD HBsAg+AI vs Pfizer mRNA	***	0.0001
Alpha	β/Wu RBD HBsAg+AI vs β RBD HBsAg+SWE	**	0.0069
Alpha	β/Wu RBD HBsAg+AI vs β RBD+SWE	****	<0.0001
Alpha	β/Wu RBD HBsAg+AI vs Pfizer mRNA	*	0.0123
Alpha	β RBD HBsAg+SWE vs β RBD+SWE	****	<0.0001
Alpha	β RBD+SWE vs Pfizer mRNA	****	<0.0001
Alpha			
RBD strain	Prime	Summary	Adjusted P value
Beta	β RBD HBsAg+AI vs β RBD HBsAg+SWE	****	<0.0001
Beta	β RBD HBsAg+AI vs Pfizer mRNA	****	<0.0001
Beta	β/Wu RBD HBsAg+AI vs β RBD HBsAg+SWE	****	<0.0001
Beta	β/Wu RBD HBsAg+AI vs Pfizer mRNA	****	<0.0001
Beta	β RBD HBsAg+SWE vs β RBD+SWE	****	<0.0001
Beta	β RBD HBsAg+SWE vs Pfizer	****	<0.0001
Beta	β RBD+SWE vs Pfizer	****	<0.0001
Beta	<b>Boost 2</b>		
Beta	β RBD HBsAg+AI vs β RBD HBsAg+SWE	***	0.0003
Beta	β RBD HBsAg+AI vs β RBD+SWE	****	<0.0001
Beta	β RBD HBsAg+AI vs Pfizer mRNA	**	0.0016
Beta	β/Wu RBD HBsAg+AI vs β RBD HBsAg+SWE	***	0.0005
Beta	β/Wu RBD HBsAg+AI vs β RBD+SWE	****	<0.0001
Beta	β/Wu RBD HBsAg+AI vs Pfizer mRNA	**	0.0038
Beta	β RBD HBsAg+SWE vs β RBD+SWE	****	<0.0001
Beta	β RBD+SWE vs Pfizer	****	<0.0001
Beta			
RBD strain	Prime	Summary	Adjusted P value
Delta	β RBD HBsAg+AI vs β RBD HBsAg+SWE	****	<0.0001
Delta	β RBD HBsAg+AI vs Pfizer mRNA	****	<0.0001
Delta	β/Wu RBD HBsAg+AI vs β RBD HBsAg+SWE	****	<0.0001
Delta	β/Wu RBD HBsAg+AI vs Pfizer mRNA	****	<0.0001
Delta	β RBD HBsAg+SWE vs β RBD+SWE	****	<0.0001
Delta	β RBD HBsAg+SWE vs Pfizer mRNA	****	<0.0001
Delta	β RBD+SWE vs Pfizer mRNA	****	<0.0001
Delta	<b>Boost 2</b>		
Delta	β RBD HBsAg+AI vs β RBD HBsAg+SWE	**	0.0015
Delta	β RBD HBsAg+AI vs β RBD+SWE	****	<0.0001
Delta	β RBD HBsAg+AI vs Pfizer mRNA	**	0.0032
Delta	β/Wu RBD HBsAg+AI vs β RBD+SWE	****	<0.0001
Delta	β RBD HBsAg+SWE vs β RBD+SWE	****	<0.0001
Delta	β RBD+SWE vs Pfizer mRNA	****	<0.0001
Delta			

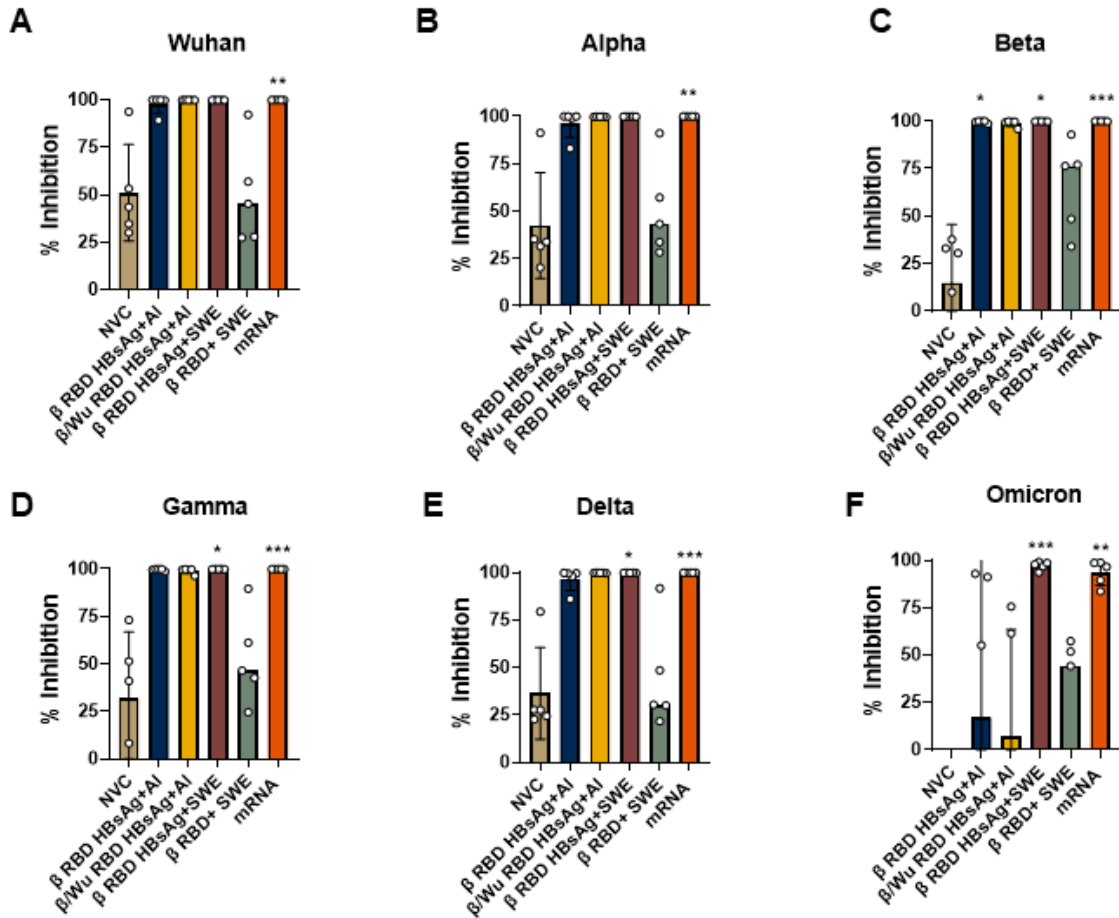
**Supplemental Table 2.** Statistical analysis of VOC RBD IgG levels at 2 weeks post prime and 4 weeks post second boost. Two-way ANOVA mixed-effects analysis was performed with Sidak's multiple comparisons test for statistical analysis.



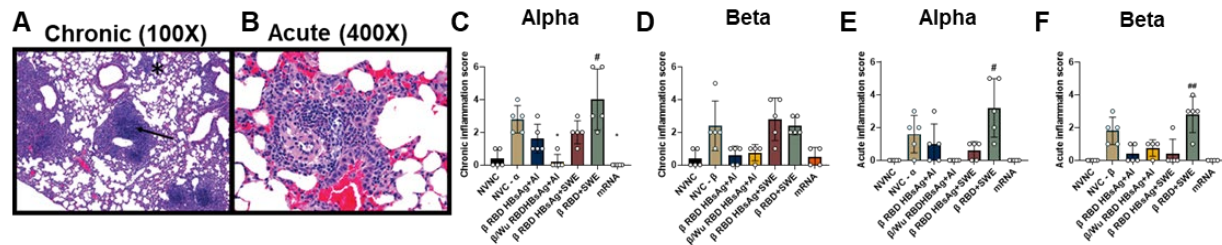
**Supplemental Figure 1.** RBD IgG titers from 2 weeks post prime (prime) and 4 weeks post 2<sup>nd</sup> dose (boost 2) against Wuhan, Alpha, Beta, and Delta RBD VOC respectively. Ordinary one-way ANOVA with Tukey's multiple comparisons test was performed for statistical analysis. Dotted line represents limit of detection for the specific RBD variant. IgG titers represented as log AU/mL. A) Wuhan RBD IgG titers from 2 weeks post prime.  $P < 0.0001$  \*\*\*\*. B) Wuhan RBD IgG from 4 weeks post 2<sup>nd</sup> dose.  $P < 0.0001$  \*\*\*\*,  $\beta$  RBD HBsAg+AI vs.  $\beta$  RBD HBsAg+SWE  $P < 0.0104^*$ , and  $\beta$  RBD HBsAg+AI vs. mRNA  $P < 0.0177^*$ . C) Alpha RBD IgG from 2 weeks post prime.  $P < 0.0001$  \*\*\*\*. D) Alpha from 4 weeks post 2<sup>nd</sup> dose.  $P < 0.0001$  \*\*\*\*,  $\beta$  RBD HBsAg+AI vs.  $\beta$  RBD HBsAg+SWE  $P < 0.0032^{**}$ , and  $\beta$  RBD HBsAg+AI vs. mRNA  $P < 0.0060^{**}$ . E) Beta RBD IgG from 2 weeks post prime.  $P < 0.0001$  \*\*\*\*. F) Beta from 4 weeks post 2<sup>nd</sup> dose.  $\beta$  RBD HBsAg+AI vs.  $\beta$  RBD HBsAg+SWE, and  $\beta$  RBD HBsAg+AI vs.  $\beta$  RBD+SWE  $P < 0.0023^{**}$ .  $\beta$ /Wu RBD HBsAg+AI vs.  $\beta$  RBD HBsAg+SWE, and  $\beta$ /Wu RBD HBsAg+AI vs.  $\beta$  RBD+SWE  $P < 0.0047^{**}$ .  $\beta$  RBD HBsAg+AI vs. mRNA  $P < 0.0106^*$ .  $\beta$ /Wu RBD HBsAg+AI vs. mRNA  $P < 0.0191^*$ . G) Delta RBD IgG titers from 2 weeks post prime.  $P < 0.0001$  \*\*\*\*. H) Delta from 4 weeks post 2<sup>nd</sup> dose.  $P < 0.0001$  \*\*\*\*.  $\beta$  RBD HBsAg+AI vs.  $\beta$  RBD HBsAg+SWE  $P < 0.0223^*$ , and  $\beta$  RBD HBsAg+AI vs. mRNA  $P < 0.0353^*$ .



**Supplemental Figure 2.** Evaluation of weight and temperature change from K18-hACE2 vaccinated mice against Alpha or Beta challenge. A) % weight change of NVNC and vaccinated mice challenged with Alpha or Beta. B) % temperature change of NVNC and vaccinated mice challenged with Alpha or Beta.

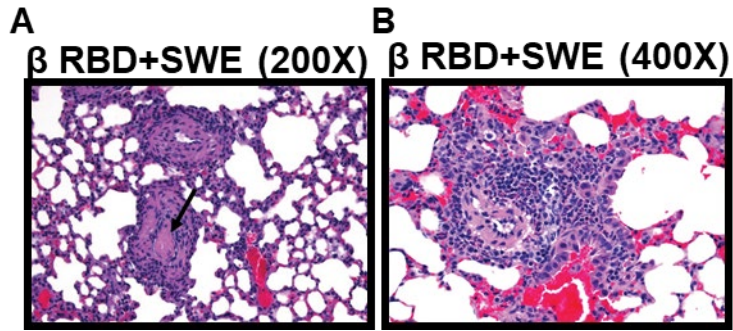


**Supplemental Figure 3.** Analysis of vaccine induced neutralizing antibodies against 5 major VOC during Alpha challenge. MSD V-PLEX SARS-CoV-2 Panel 22 (ACE2) kit with 5 VOC and Wuhan RBD was used to measure serum antibody neutralization in Alpha challenged mice in immunized and non-immunized mice. All values were depicted as % inhibition. Negative % inhibition values were not represented in the analysis. Percent inhibition of neutralizing antibodies measured against A) Wuhan, B) Alpha, C) Beta, D) Gamma, E) Delta, and F) Omicron respectively. Dotted line represents neutralizing antibody levels of NVNC. Results represented as mean  $\pm$  SD. Kruskal-Wallis test with Dunn's multiple comparisons test were conducted for statistical analysis. Wuhan.  $P=0.0024^{**}$ . Alpha.  $P=0.0012^{**}$ . Beta.  $P=0.0382^*$  (NVC vs. RBD HBsAg+AI),  $P=0.0208^*$  (NVC vs. RBD HBsAg + SWE),  $P=0.0005^{***}$  (NVC vs mRNA). Gamma.  $P=0.0484^*$ ,  $P=0.0007^{***}$ . Delta.  $P=0.0340^*$ ,  $P=0.0007^{***}$ . Omicron.  $P=0.0049^{**}$ ,  $P=0.0007^{***}$ .



**Supplemental Figure 4. Chronic and acute inflammation in non-vaccinated and vaccinated lungs.** A) Example of chronic inflammation denoted by infiltration of lymphocytes and plasma within the parenchyma shown by the asterisks, as well as surrounding blood vessels marked by the arrow. 100X magnification. B) Example of acute inflammation denoted by neutrophils surrounding blood vessels. 400X magnification. C) Alpha challenged chronic inflammation scores.  $P=0.0322^*$  (NVNC vs.  $\beta$  RBD+SWE),  $P=0.0470^*$  (NVC $\alpha$  vs  $\beta$ /Wu RBD HBsAg+AI)  $P=0.0164^*$  (NVC $\alpha$  vs mRNA)  $P=0.0109^*$  ( $\beta$ /Wu RBD HBsAg+AI vs  $\beta$  RBD+SWE) E) Beta challenged chronic inflammation scores. E) Alpha challenged total acute inflammation scores.  $P=0.0101$  (NVNC vs  $\beta$  RBD+SWE),  $P=0.0101^*$  ( $\beta$ /Wu RBD HBsAg+AI vs  $\beta$  RBD+SWE) ( $\beta$  RBD+SWE vs mRNA) (F) Beta challenged total acute inflammation scores.  $P=0.0150^*$ ,  $P=0.0070^{**}$ . Results represented as mean  $\pm$  SD. Kruskal-Wallis with Dunn's multiple comparisons test was performed for statistical analysis. Asterisks denote significant difference compared to NVC and # symbol indicates significant difference compared to NVNC.





**Supplemental Figure 5.**  $\beta$  RBD+SWE induced increased inflammation in the lung. A) Arrow denotes inflammation and thrombus in the blood vessel of the lung in  $\beta$  RBD+SWE immunized mouse (200X magnification). B) 400X magnification of the lung demonstrates neutrophil surrounding the blood vessel in  $\beta$  RBD+SWE immunized mouse.

### 3.9 References

1. Geers D, Shamier MC, Bogers S, den Hartog G, Gommers L, Nieuwkoop NN, et al. SARS-CoV-2 variants of concern partially escape humoral but not T-cell responses in COVID-19 convalescent donors and vaccinees. *Sci Immunol* [Internet]. 2021 May 1 [cited 2022 Mar 7];6(59):1750. Available from: <https://www.science.org/doi/abs/10.1126/sciimmunol.abj1750>
2. Aleem A, Samad Akbar Bari A, Slenker K A. Emerging Variants of SARS-CoV-2 And Novel Therapeutics Against Coronavirus (COVID-19) - PubMed [Internet]. StatPearls Publishing; 2022 [cited 2022 Feb 28]. Available from: <https://pubmed.ncbi.nlm.nih.gov/34033342/>
3. Planas D, Veyer D, Baidaliuk A, Staropoli I, Guivel-Benhassine F, Rajah MM, et al. Reduced sensitivity of SARS-CoV-2 variant Delta to antibody neutralization. *Nature* [Internet]. 2021 [cited 2022 Mar 7];596. Available from: <https://doi.org/10.1038/s41586-021-03777-9>
4. Mlcochova P, Kemp S, Dhar MS, Papa G, Meng B, Ferreira IATM, et al. SARS-CoV-2 B.1.617.2 Delta variant replication and immune evasion. *Nat* 2021 5997883 [Internet]. 2021 Sep 6 [cited 2021 Dec 16];599(7883):114–9. Available from: <https://www.nature.com/articles/s41586-021-03944-y>
5. Liu L, Iketani S, Guo Y, Chan JFW, Wang M, Liu L, et al. Striking antibody evasion manifested by the Omicron variant of SARS-CoV-2. *Nat* 2021 6027898 [Internet]. 2021 Dec 23 [cited 2022 Mar 7];602(7898):676–81. Available from: <https://www.nature.com/articles/s41586-021-04388-0>
6. WHO – COVID19 Vaccine Tracker [Internet]. [cited 2022 Feb 28]. Available from: <https://covid19.trackvaccines.org/agency/who/>
7. Tian JH, Patel N, Haupt R, Zhou H, Weston S, Hammond H, et al. SARS-CoV-2 spike glycoprotein vaccine candidate NVX-CoV2373 immunogenicity in baboons and protection in mice. *Nat Commun* 2021 121 [Internet]. 2021 Jan 14 [cited 2022 Feb 28];12(1):1–14.

Available from: <https://www.nature.com/articles/s41467-020-20653-8>

8. Heath PT, Galiza EP, Baxter DN, Boffito M, Browne D, Burns F, et al. Safety and Efficacy of NVX-CoV2373 Covid-19 Vaccine. <https://doi.org/10.1056/NEJMoa2107659> [Internet]. 2021 Jun 30 [cited 2021 Sep 14]; Available from: <https://www.nejm.org/doi/full/10.1056/NEJMoa2107659>
9. Dunkle LM, Kotloff KL, Gay CL, Áñez G, Adelglass JM, Barrat Hernández AQ, et al. Efficacy and Safety of NVX-CoV2373 in Adults in the United States and Mexico. *N Engl J Med* [Internet]. 2022 Feb 10 [cited 2022 Feb 18];386(6):531–43. Available from: <https://www.nejm.org/doi/full/10.1056/NEJMoa2116185>
10. Covid World Vaccination Tracker - The New York Times [Internet]. [cited 2022 Feb 25]. Available from: <https://www.nytimes.com/interactive/2021/world/covid-vaccinations-tracker.html>
11. Kleanthous H, Silverman JM, Makar KW, Yoon IK, Jackson N, Vaughn DW. Scientific rationale for developing potent RBD-based vaccines targeting COVID-19. *NPJ vaccines* [Internet]. 2021 Dec 1 [cited 2022 Feb 28];6(1). Available from: <https://pubmed.ncbi.nlm.nih.gov/34711846/>
12. Lee J, Liu Z, Chen WH, Wei J, Kundu R, Adhikari R, et al. Process development and scale-up optimization of the SARS-CoV-2 receptor binding domain–based vaccine candidate, RBD219-N1C1. *Appl Microbiol Biotechnol* [Internet]. 2021 May 1 [cited 2022 Mar 7];105(10):4153. Available from: [/pmc/articles/PMC8102132/](https://pubmed.ncbi.nlm.nih.gov/34711846/)
13. Dalvie NC, Rodriguez-Aponte SA, Hartwell BL, Tostanoski LH, Biedermann AM, Crowell LE, et al. Engineered SARS-CoV-2 receptor binding domain improves manufacturability in yeast and immunogenicity in mice. *Proc Natl Acad Sci U S A* [Internet]. 2021 Sep 21 [cited 2022 Feb 25];118(38). Available from: <https://www.pnas.org/content/118/38/e2106845118>
14. Vu MN, Kelly HG, Kent SJ, Wheatley AK. Current and future nanoparticle vaccines for COVID-19. *eBioMedicine* [Internet]. 2021 Dec 1 [cited 2022 Mar 7];74. Available from: <https://pubmed.ncbi.nlm.nih.gov/34711846/>

<http://www.thelancet.com/article/S235239642100493X/fulltext>

15. Wong TY, Lee KS, Russ BP, Horspool AM, Kang J, Winters MT, et al. Intranasal administration of BReC-CoV-2 COVID-19 vaccine protects K18-hACE2 mice against lethal SARS-CoV-2 challenge. *npj Vaccines* 2022 71 [Internet]. 2022 Mar 14 [cited 2022 Mar 21];7(1):1–15. Available from: <https://www.nature.com/articles/s41541-022-00451-7>
16. Ko EJ, Kang SM. Immunology and efficacy of MF59-adjuvanted vaccines. *Hum Vaccin Immunother* [Internet]. 2018 Dec 2 [cited 2022 Mar 7];14(12):3041. Available from: </pmc/articles/PMC6343625/>
17. Rivera-Hernandez T, Rhyme MS, Cork AJ, Jones S, Segui-Perez C, Brunner L, et al. Vaccine-Induced Th1-Type Response Protects against Invasive Group A Streptococcus Infection in the Absence of Opsonizing Antibodies. *MBio* [Internet]. 2020 Mar 1 [cited 2022 Feb 25];11(2). Available from: </pmc/articles/PMC7064752/>
18. de Jonge J, van Dijken H, de Heij F, Spijkers S, Mouthaan J, de Jong R, et al. H7N9 influenza split vaccine with SWE oil-in-water adjuvant greatly enhances cross-reactive humoral immunity and protection against severe pneumonia in ferrets. *NPJ Vaccines* [Internet]. 2020 Dec 1 [cited 2022 Feb 25];5(1). Available from: </pmc/articles/PMC7214439/>
19. Matthijs AMF, Auray G, Boyen F, Schoos A, Michiels A, García-Nicolás O, et al. Efficacy of three innovative bacterin vaccines against experimental infection with *Mycoplasma hyopneumoniae*. *Vet Res* [Internet]. 2019 Nov 8 [cited 2022 Feb 25];50(1). Available from: </pmc/articles/PMC6842239/>
20. Marcandalli J, Fiala B, Ols S, Perotti M, de van der Schueren W, Snijder J, et al. Induction of Potent Neutralizing Antibody Responses by a Designed Protein Nanoparticle Vaccine for Respiratory Syncytial Virus. *Cell* [Internet]. 2019 Mar 7 [cited 2022 Feb 25];176(6):1420. Available from: </pmc/articles/PMC6424820/>
21. Wang C, Dulal P, Zhou X, Xiang Z, Goharriz H, Banyard A, et al. A simian-adenovirus-vectored rabies vaccine suitable for thermostabilisation and clinical development for low-

- cost single-dose pre-exposure prophylaxis. *PLoS Negl Trop Dis* [Internet]. 2018 Oct 1 [cited 2022 Feb 25];12(10). Available from: [/pmc/articles/PMC6224154/](#)
22. Younis SY, Barnier-Quer C, Heuking S, Sommandas V, Brunner L, vd.Werff N, et al. Down selecting adjuvanted vaccine formulations: a comparative method for harmonized evaluation. *BMC Immunol* [Internet]. 2018 Jan 31 [cited 2022 Feb 25];19(1). Available from: [/pmc/articles/PMC5793412/](#)
  23. Deloizy C, Fossum E, Barnier-Quer C, Urien C, Chrun T, Duval A, et al. The anti-influenza M2e antibody response is promoted by XCR1 targeting in pig skin. *Sci Rep* [Internet]. 2017 Dec 1 [cited 2022 Feb 25];7(1). Available from: [/pmc/articles/PMC5550447/](#)
  24. Varypataki EM, Silva AL, Barnier-Quer C, Collin N, Ossendorp F, Jiskoot W. Synthetic long peptide-based vaccine formulations for induction of cell mediated immunity: A comparative study of cationic liposomes and PLGA nanoparticles. *J Control Release*. 2016 Mar 28;226:98–106.
  25. Westdijk J, Koedam P, Barro M, Steil BP, Collin N, Vedvick TS, et al. Antigen sparing with adjuvanted inactivated polio vaccine based on Sabin strains. *Vaccine* [Internet]. 2013 Feb 18 [cited 2022 Feb 25];31(9):1298. Available from: [/pmc/articles/PMC3570672/](#)
  26. Wong TY, Horspool AM, Russ BP, Ye C, Lee KS, Winters MT, et al. Evaluating antibody mediated protection against Alpha, Beta, and Delta SARS-CoV-2 variants of concern in K18-hACE2 transgenic mice. *J Virol* [Internet]. 2022 Jan 26 [cited 2022 Feb 25]; Available from: <https://pubmed.ncbi.nlm.nih.gov/35080423/>
  27. Hotez PJ, Bottazzi ME. Developing a low-cost and accessible COVID-19 vaccine for global health. *PLoS Negl Trop Dis* [Internet]. 2020 Jul 1 [cited 2022 Apr 5];14(7):e0008548. Available from: <https://journals.plos.org/plosntds/article?id=10.1371/journal.pntd.0008548>
  28. Love KR, Dalvie NC, Love JC. The yeast stands alone: the future of protein biologic production. *Curr Opin Biotechnol*. 2018 Oct 1;53:50–8.
  29. Dalvie NC, Biedermann AM, Rodriguez-Aponte SA, Naranjo CA, Rao HD, Rajurkar MP, et

- al. Scalable, methanol-free manufacturing of the SARS-CoV-2 receptor-binding domain in engineered *Komagataella phaffii*. *Biotechnol Bioeng* [Internet]. 2022 Feb 1 [cited 2022 Apr 5];119(2):657–62. Available from: [/pmc/articles/PMC8653030/](https://pubmed.ncbi.nlm.nih.gov/35303030/)
30. Dalvie NC, Tostanoski LH, Rodriguez-Aponte SA, Kaur K, Bajoria S, Kumru OS, et al. SARS-CoV-2 receptor binding domain displayed on HBsAg virus-like particles elicits protective immunity in macaques. *Sci Adv* [Internet]. 2022 Mar 18 [cited 2022 Apr 4];8(11):6015. Available from: <https://www.science.org/doi/full/10.1126/sciadv.abl6015>
31. Singh SK, Thrane S, Janitzek CM, Nielsen MA, Theander TG, Theisen M, et al. Improving the malaria transmission-blocking activity of a *Plasmodium falciparum* 48/45 based vaccine antigen by SpyTag/SpyCatcher mediated virus-like display. *Vaccine* [Internet]. 2017 Jun 27 [cited 2022 Apr 5];35(30):3726–32. Available from: <https://pubmed.ncbi.nlm.nih.gov/28578824/>
32. Tan TK, Rijal P, Rahikainen R, Keeble AH, Schimanski L, Hussain S, et al. A COVID-19 vaccine candidate using SpyCatcher multimerization of the SARS-CoV-2 spike protein receptor-binding domain induces potent neutralising antibody responses. *Nat Commun* 2021 121 [Internet]. 2021 Jan 22 [cited 2022 Feb 21];12(1):1–16. Available from: <https://www.nature.com/articles/s41467-020-20654-7>
33. Zhang W Bin, Sun F, Tirrell DA, Arnold FH. Controlling macromolecular topology with genetically encoded SpyTag-SpyCatcher chemistry. *J Am Chem Soc* [Internet]. 2013 Sep 18 [cited 2022 Feb 28];135(37):13988–97. Available from: <https://pubmed.ncbi.nlm.nih.gov/23964715/>
34. Brune KD, Leneghan DB, Brian IJ, Ishizuka AS, Bachmann MF, Draper SJ, et al. Plug-and-Display: decoration of Virus-Like Particles via isopeptide bonds for modular immunization. *Sci Reports* 2016 61 [Internet]. 2016 Jan 19 [cited 2022 Feb 21];6(1):1–13. Available from: <https://www.nature.com/articles/srep19234>
35. Cohen AA, Yang Z, Gnanapragasam PNP, Ou S, Dam KMA, Wang H, et al. Construction,

- characterization, and immunization of nanoparticles that display a diverse array of influenza HA trimers. *PLoS One* [Internet]. 2021 Mar 1 [cited 2022 Feb 21];16(3):e0247963. Available from: <https://journals.plos.org/plosone/article?id=10.1371/journal.pone.0247963>
36. Corrigan AR, Duan H, Cheng C, Gonelli CA, Ou L, Xu K, et al. Fusion peptide priming reduces immune responses to HIV-1 envelope trimer base. *Cell Rep*. 2021 Apr 6;35(1):108937.
  37. Perotti M, Perez L. Virus-Like Particles and Nanoparticles for Vaccine Development against HCMV. *Viruses* 2020, Vol 12, Page 35 [Internet]. 2019 Dec 28 [cited 2022 Feb 28];12(1):35. Available from: <https://www.mdpi.com/1999-4915/12/1/35/htm>
  38. Sette A, Crotty S. Adaptive immunity to SARS-CoV-2 and COVID-19. *Cell* [Internet]. 2021 Feb 18 [cited 2022 Feb 28];184(4):861–80. Available from: <https://pubmed.ncbi.nlm.nih.gov/33497610/>
  39. Dan JM, Mateus J, Kato Y, Hastie KM, Yu ED, Faliti CE, et al. Immunological memory to SARS-CoV-2 assessed for up to 8 months after infection. *Science* (80- ) [Internet]. 2021 Feb 5 [cited 2022 Feb 28];371(6529). Available from: <https://www.science.org/doi/abs/10.1126/science.abf4063>
  40. Bösmüller H, Matter M, Fend F, Tzankov A. The pulmonary pathology of COVID-19. *Virchows Arch* [Internet]. 2021 Jan 1 [cited 2022 Feb 28];478(1):137. Available from: </pmc/articles/PMC7892326/>
  41. Is Covax finally going to vaccinate the world? - Vox [Internet]. [cited 2022 Feb 28]. Available from: <https://www.vox.com/future-perfect/22872438/covax-omicron-covid-19-vaccine-global-inequity>
  42. Dolgin E. How protein-based COVID vaccines could change the pandemic. *Nature*. 2021 Nov 1;599(7885):359–60.
  43. Burgos RM, Badowski ME, Drwiega E, Ghassemi S, Griffith N, Herald F, et al. The race to a COVID-19 vaccine: opportunities and challenges in development and distribution. *Drugs*

- Context [Internet]. 2021 [cited 2022 Feb 28];10. Available from: <https://pubmed.ncbi.nlm.nih.gov/33643421/>
44. The COVID-19 vaccine race | Gavi, the Vaccine Alliance [Internet]. [cited 2022 May 3]. Available from: <https://www.gavi.org/vaccineswork/covid-19-vaccine-race>
  45. Hager KJ, Marc GP, Gobeil P, Diaz RS, Heizer G, Llapur C, et al. Efficacy and Safety of a Recombinant Plant-Based Adjuvanted Covid-19 Vaccine. <https://doi.org/10.1056/NEJMoa2201300> [Internet]. 2022 May 4 [cited 2022 May 10]; Available from: <https://www.nejm.org/doi/full/10.1056/NEJMoa2201300>
  46. Ward BJ, Gobeil P, Séguin A, Atkins J, Boulay I, Charbonneau PY, et al. Phase 1 randomized trial of a plant-derived virus-like particle vaccine for COVID-19. *Nat Med* 2021 276 [Internet]. 2021 May 18 [cited 2022 May 10];27(6):1071–8. Available from: <https://www.nature.com/articles/s41591-021-01370-1>
  47. Fluckiger AC, Ontsouka B, Bozic J, Diress A, Ahmed T, Berthoud T, et al. An enveloped virus-like particle vaccine expressing a stabilized prefusion form of the SARS-CoV-2 spike protein elicits highly potent immunity. *Vaccine*. 2021 Aug 16;39(35):4988–5001.
  48. VBI Vaccines Announces Initial Positive Phase 1 Data for its eVLP Vaccine Candidate Against COVID-19 - VBI Vaccines [Internet]. [cited 2022 May 10]. Available from: <https://www.vbivaccines.com/press-releases/covid-19-vaccine-phase-1-data/>
  49. Study of a Severe Acute Respiratory Syndrome CoV-2 (SARS-CoV-2) Virus-like Particle (VLP) Vaccine in Healthy Adults - Full Text View - ClinicalTrials.gov [Internet]. [cited 2022 May 10]. Available from: <https://clinicaltrials.gov/ct2/show/NCT04818281>
  50. Kleanthous H, Silverman JM, Makar KW, Yoon IK, Jackson N, Vaughn DW. Scientific rationale for developing potent RBD-based vaccines targeting COVID-19. *npj Vaccines* 2021 61 [Internet]. 2021 Oct 28 [cited 2022 Mar 7];6(1):1–10. Available from: <https://www.nature.com/articles/s41541-021-00393-6>
  51. Gan ES, Syenina A, Linster M, Ng B, Zhang SL, Watanabe S, et al. A mouse model of




- lethal respiratory dysfunction for SARS-CoV-2 infection. *Antiviral Res.* 2021 Sep 1;193:105138.
52. FS O, JG P, PA P, O G, A A, A A-G, et al. Lethality of SARS-CoV-2 infection in K18 human angiotensin-converting enzyme 2 transgenic mice. *Nat Commun* [Internet]. 2020 Dec 1 [cited 2021 Aug 8];11(1). Available from: <https://pubmed.ncbi.nlm.nih.gov/33257679/>
  53. PB M, L P, C W-L, M H, L M, L S, et al. Lethal infection of K18-hACE2 mice infected with severe acute respiratory syndrome coronavirus. *J Virol* [Internet]. 2007 Jan 15 [cited 2021 Aug 8];81(2):813–21. Available from: <https://pubmed.ncbi.nlm.nih.gov/17079315/>
  54. Yinda CK, Port JR, Bushmaker T, Owusu IO, Purushotham JN, Avanzato VA, et al. K18-hACE2 mice develop respiratory disease resembling severe COVID-19. *PLOS Pathog* [Internet]. 2021 Jan 19 [cited 2021 Aug 11];17(1):e1009195. Available from: <https://journals.plos.org/plospathogens/article?id=10.1371/journal.ppat.1009195>
  55. Winkler ES, Bailey AL, Kafai NM, Nair S, McCune BT, Yu J, et al. SARS-CoV-2 infection of human ACE2-transgenic mice causes severe lung inflammation and impaired function. *Nat Immunol* 2020 2111 [Internet]. 2020 Aug 24 [cited 2021 Aug 8];21(11):1327–35. Available from: <https://www.nature.com/articles/s41590-020-0778-2>
  56. De Gregorio E, Caproni E, Ulmer JB. Vaccine adjuvants: Mode of action. *Front Immunol.* 2013;4(JUL):214.
  57. O'Hagan DT, Lodaya RN, Lofano G. The continued advance of vaccine adjuvants – ‘we can work it out.’ *Semin Immunol.* 2020 Aug 1;50:101426.
  58. Grifoni A, Sidney J, Vita R, Peters B, Crotty S, Weiskopf D, et al. SARS-CoV-2 human T cell epitopes: Adaptive immune response against COVID-19. *Cell Host Microbe* [Internet]. 2021 Jul 14 [cited 2022 Feb 28];29(7):1076–92. Available from: <https://pubmed.ncbi.nlm.nih.gov/34237248/>
  59. GeurtsvanKessel CH, Geers D, Schmitz KS, Mykytyn AZ, Lamers MM, Bogers S, et al. Divergent SARS CoV-2 Omicron-reactive T- and B cell responses in COVID-19 vaccine

- recipients. *Sci Immunol* [Internet]. 2022 Feb 3 [cited 2022 Feb 28]; Available from: <https://www.science.org/doi/abs/10.1126/sciimmunol.abo2202>
60. Neidleman J, Luo X, George AF, McGregor M, Yang J, Yun C, et al. Distinctive features of SARS-CoV-2-specific T cells predict recovery from severe COVID-19. *Cell Rep* [Internet]. 2021 Jul 20 [cited 2022 Feb 28];36(3). Available from: <https://pubmed.ncbi.nlm.nih.gov/34260965/>
  61. Kundu R, Narean JS, Wang L, Fenn J, Pillay T, Fernandez ND, et al. Cross-reactive memory T cells associate with protection against SARS-CoV-2 infection in COVID-19 contacts. *Nat Commun* 2022 131 [Internet]. 2022 Jan 10 [cited 2022 Feb 28];13(1):1–8. Available from: <https://www.nature.com/articles/s41467-021-27674-x>
  62. Grifoni A, Weiskopf D, Ramirez SI, Mateus J, Dan JM, Moderbacher CR, et al. Targets of T Cell Responses to SARS-CoV-2 Coronavirus in Humans with COVID-19 Disease and Unexposed Individuals. *Cell* [Internet]. 2020 Jun 25 [cited 2022 Mar 1];181(7):1489. Available from: </pmc/articles/PMC7237901/>
  63. Tarke A, Coelho CH, Zhang Z, Dan JM, Yu ED, Methot N, et al. SARS-CoV-2 vaccination induces immunological T cell memory able to cross-recognize variants from Alpha to Omicron. *Cell* [Internet]. 2022 Jan [cited 2022 Feb 28];0(0). Available from: <http://www.cell.com/article/S0092867422000733/fulltext>
  64. Juno JA, Tan HX, Lee WS, Reynaldi A, Kelly HG, Wragg K, et al. Humoral and circulating follicular helper T cell responses in recovered patients with COVID-19. *Nat Med* [Internet]. 2020 Sep 1 [cited 2022 Mar 1];26(9):1428–34. Available from: <https://pubmed.ncbi.nlm.nih.gov/32661393/>
  65. Chen WH, Tao X, Agrawal AS, Algaissi A, Peng BH, Pollet J, et al. Yeast-expressed SARS-CoV recombinant receptor-binding domain (RBD219-N1) formulated with aluminum hydroxide induces protective immunity and reduces immune enhancement. *Vaccine*. 2020 Nov 3;38(47):7533–41.

66. Krammer F. SARS-CoV-2 vaccines in development. *Nat* 2020 5867830 [Internet]. 2020 Sep 23 [cited 2022 Mar 1];586(7830):516–27. Available from: <https://www.nature.com/articles/s41586-020-2798-3>
67. Dalvie NC, Biedermann AM, Rodriguez-Aponte SA, Naranjo CA, Rao HD, Rajurkar MP, et al. Scalable, methanol-free manufacturing of the SARS-CoV-2 receptor binding domain in engineered *Komagataella phaffii*. *bioRxiv* [Internet]. 2021 Apr 15 [cited 2022 Mar 1]; Available from: [/pmc/articles/PMC8057236/](https://pmc/articles/PMC8057236/)
68. Waltz E. COVID vaccine makers brace for a variant worse than Delta. *Nature*. 2021 Oct 1;598(7882):552–3.
69. Abu-Raddad LJ, Chemaitelly H, Ayoub HH, Yassine HM, Benslimane FM, Al Khatib HA, et al. Severity, Criticality, and Fatality of the Severe Acute Respiratory Syndrome Coronavirus 2 (SARS-CoV-2) Beta Variant. *Clin Infect Dis* [Internet]. 2021 Oct 17 [cited 2022 Mar 11]; Available from: <https://academic.oup.com/cid/advance-article/doi/10.1093/cid/ciab909/6398699>
70. Jassat W, Mudara C, Ozougwu L, Tempia S, Blumberg L, Davies MA, et al. Difference in mortality among individuals admitted to hospital with COVID-19 during the first and second waves in South Africa: a cohort study. *Lancet Glob Heal* [Internet]. 2021 Sep 1 [cited 2022 Mar 11];9(9):e1216–25. Available from: <https://pubmed.ncbi.nlm.nih.gov/34252381/>
71. Tragni V, Preziusi F, Laera L, Onofrio A, Mercurio I, Todisco S, et al. Modeling SARS-CoV-2 spike/ACE2 protein-protein interactions for predicting the binding affinity of new spike variants for ACE2, and novel ACE2 structurally related human protein targets, for COVID-19 handling in the 3PM context. *EPMA J* [Internet]. 2022 [cited 2022 Feb 28]; Available from: <https://pubmed.ncbi.nlm.nih.gov/35013687/>
72. Chen RE, Zhang X, Case JB, Winkler ES, Liu Y, VanBlargan LA, et al. Resistance of SARS-CoV-2 variants to neutralization by monoclonal and serum-derived polyclonal antibodies. *Nat Med* 2021 274 [Internet]. 2021 Mar 4 [cited 2022 Feb 28];27(4):717–26. Available from:

<https://www.nature.com/articles/s41591-021-01294-w>

73. Chen RE, Winkler ES, Case JB, Aziati ID, Bricker TL, Joshi A, et al. In vivo monoclonal antibody efficacy against SARS-CoV-2 variant strains. *Nat* 2021 5967870 [Internet]. 2021 Jun 21 [cited 2022 Feb 28];596(7870):103–8. Available from: <https://www.nature.com/articles/s41586-021-03720-y>
74. Madhi SA, Baillie V, Cutland CL, Voysey M, Koen AL, Fairlie L, et al. Efficacy of the ChAdOx1 nCoV-19 Covid-19 Vaccine against the B.1.351 Variant. *N Engl J Med* [Internet]. 2021 May 20 [cited 2022 Feb 28];384(20):1885–98. Available from: <https://www.nejm.org/doi/full/10.1056/nejmoa2102214>
75. Hadfield J, Megill C, Bell SM, Huddleston J, Potter B, Callender C, et al. NextStrain: Real-time tracking of pathogen evolution. *Bioinformatics*. 2018 Dec 1;34(23):4121–3.
76. Nextstrain / nCoV / gisaid / global [Internet]. [cited 2022 Mar 28]. Available from: <https://nextstrain.org/ncov/gisaid/global>



**Chapter 4: Intranasal administration  
of BReC-CoV-2 COVID-19 vaccine  
protects K18-hACE2 mice against  
lethal SARS-CoV-2 challenge**

## **Intranasal administration of BReC-CoV-2 COVID-19 vaccine protects K18-hACE2 mice against lethal SARS-CoV-2 challenge**

Ting Y. Wong<sup>1,2</sup>, Katherine S. Lee<sup>1,2</sup>, Brynna P. Russ<sup>1,2</sup>, Alexander M. Horspool<sup>1,2</sup>, Jason Kang<sup>1,2</sup>, Michael T. Winters<sup>1</sup>, M. Allison Wolf<sup>1,2</sup>, Nathaniel A. Rader<sup>1,2</sup>, Olivia A. Miller<sup>1,2</sup>, Morgane Shiflett<sup>6</sup>, Jerilyn Izac<sup>4</sup>, David Varisco<sup>4</sup>, Emel Sen-Kilic<sup>1,2</sup>, Casey Cunningham<sup>1,2</sup>, Melissa Cooper<sup>1,2</sup>, Holly A. Cyphert<sup>5</sup>, Mariette Barbier<sup>1,2</sup>, Ivan Martinez<sup>1,3</sup>, Justin R. Bevere<sup>1,2</sup>, Robert K. Ernst<sup>4</sup>, and F. Heath Damron<sup>1,2\*</sup>.

<sup>1</sup>Department of Microbiology, Immunology, and Cell Biology, West Virginia University, Morgantown, WV, USA

<sup>2</sup> Vaccine Development Center at West Virginia University Health Sciences Center, Morgantown, WV, USA

<sup>3</sup> West Virginia University Cancer Institute, Morgantown, WV, USA School of Medicine, Morgantown, WV, USA

<sup>4</sup> Department of Microbial Pathogenesis, University of Maryland School of Dentistry, Baltimore, Maryland, USA

<sup>5</sup> Department of Biological Sciences, Marshall University, Huntington, WV, USA

<sup>6</sup> Fina Biosolutions, LLC, Rockville, MD, USA

\* Corresponding author

Corresponding author email address: [fdamron@hsc.wvu.edu](mailto:fdamron@hsc.wvu.edu)

Lead contact email address: [fdamron@hsc.wvu.edu](mailto:fdamron@hsc.wvu.edu)

Keywords: SARS-CoV-2, COVID-19, K18-hACE2 transgenic mouse, vaccines, RBD, RBD-CRM, BECC, BECC470

DOI: <https://doi.org/10.1038/s41541-022-00451-7>

#### **4.1 Abstract**

SARS-CoV-2 is a viral respiratory pathogen responsible for the current global pandemic and the disease that causes COVID-19. All current WHO approved COVID-19 vaccines are administered through the muscular route. We have developed a prototype two-dose vaccine (BReC-CoV-2) by combining the Receptor Binding Domain (RBD) antigen, via conjugation to Diphtheria toxoid (EcoCRM®). The vaccine is adjuvanted with Bacterial Enzymatic Combinatorial Chemistry (BECC), BECC470. Intranasal (IN) administration of BreC-CoV-2 in K18-hACE2 mice induced a strong systemic and localized immune response in the respiratory tissues which provided protection against the Washington strain of SARS-CoV-2. Protection provided after IN administration of BReC-CoV-2 was associated with decreased viral RNA copies in the lung, robust RBD IgA titers in the lung and nasal wash, and induction of broadly neutralizing antibodies in the serum. We also observed that BReC-CoV-2 vaccination administered using an intramuscular (IM) prime and IN boost protected mice from a lethal challenge dose of the Delta variant of SARS-CoV-2. IN administration of BReC-CoV-2 provided better protection than IM only administration to mice against lethal challenge dose of SARS-CoV-2. These data suggest that the IN route of vaccination induces localized immune response that can better protect against SARS-CoV-2 than the IM route in the upper respiratory tract.

## 4.2 Introduction

As of January 2020, when the first SARS-CoV-2 genome was released, tremendous progress has been made in developing vaccines against COVID-19. To date, there are greater than 200 vaccines being developed worldwide to combat SARS-CoV-2, the causative agent of the COVID-19 pandemic (1). Currently, there are 8 vaccines that have been approved by WHO for administration that are being used around the world and more than 8 billion COVID-19 vaccines that have been given worldwide (2). Approved vaccinations for COVID-19 and most vaccines in development have been administered or designed to be given through the intramuscular route. Few COVID-19 vaccines under development are administered through the nasal route. Each route of vaccination provides a unique protection profile for respiratory viruses. Intramuscular vaccination produces a predominantly systemic immune response dominated mostly by serum IgG and, resulting in minimal to no detectable mucosal immune response at the site of infection (3,4). The vaccine response generated after intramuscular immunization can leave the upper respiratory tract vulnerable to viral replication and dissemination because it lacks the mucosal immune response generated by natural infection or intranasal vaccination (3). However, intranasal vaccination may provide both a systemic and a robust local IgA response, as what occurs during natural infection which may ultimately lead to total protection (3). In pre-clinical studies, non-human primates vaccinated intramuscularly with Pfizer-BioNTech (BNT162b2) intramuscularly and then challenged with SARS-CoV-2 had detectable SARS-CoV-2 RNA copies in the nasal and oropharyngeal swabs collected after challenge (5). We hypothesize that a vaccine must induce both mucosal and systemic immune responses to achieve sterilizing immunity against SARS-CoV-2.

Vaccine platforms that utilize nanoparticles, carrier proteins, and virus like particles (VLPs) can increase the immunogenicity of antigens increasing the size and quantity of the antigen presented to the immune system(6). Novavax utilizes recombinant nanoparticle technology to increase immunogenicity of the spike protein in their COVID-19 vaccine formulation(7). SpyBiotech and



Serum Institute of India have developed a recombinant protein vaccine utilizing Hepatitis B surface antigen VLP to display RBD in order to enhance immunogenicity by increasing the quantity of RBD presented to the immune system (8). In our studies, we have generated a recombinant COVID-19 vaccine containing the Receptor Binding Domain (RBD) of the SARS-CoV-2 spike antigen conjugated to EcoCRM<sup>®</sup> (an *E. coli* expressed CRM<sub>197</sub>) (9). CRM<sub>197</sub> has been used in licensed vaccines for *Streptococcus pneumoniae*, *Haemophilus influenzae b*, and *Neisseria meningitidis* to help increase the immunogenicity of polysaccharide antigens by promoting a T cell dependent response (10–13). CRM<sub>197</sub> has also been used to enhance the immunogenicity of weakly immunogenic proteins. EcoCRM<sup>®</sup> has been shown to be highly effective with poorly immunogenic malaria proteins (14) Crosslinking of CRM<sub>197</sub> and a candidate target antigen protein can create nanoparticle-like structures containing multiple copies of the target antigen. This approach has been successfully used to enhance the immunogenicity of malaria proteins (14,15).

Optimal COVID-19 vaccine immunity requires the activation of both cellular and humoral responses in regard to 1) activation of CD4 T cells to activate B-cell maturation to produce functional antibodies to neutralize SARS-COV-2 as well as B-memory responses and 2) stimulation of CD8 T cell production to eliminate virus infected cells and the activation of CD8 T memory cells (16). Bacterial Enzymatic Combinatorial Chemistry (BECC) is a novel adjuvant methodology developed to synthesize TLR4-agonists, lipid A mimetics. The BECC system uses lipid A biosynthetic and/or modification enzymes expressed in a bacterial background to rationally engineer lipid A structures with altered binding to the host TLR4 receptor and immunostimulatory properties (17). BECC adjuvants have been successfully used in both viral and bacterial pre-clinical vaccine formulations (18). Viral vaccine studies with Influenza virus H1N1 showed decreased viral titers and weight loss when influenza hemagglutinin antigen was adjuvanted with BECC470, as well as elicited a balanced Th1/Th2 immune response (19).

Overall, the aim in this study was to evaluate the efficacy of intramuscular and intranasal vaccination with BReC-CoV-2 against SARS-CoV-2 using the K18-ACE2 mouse challenge model (20–25). We hypothesized that intranasal immunization which induces a combination of both mucosal and systemic immune responses, would lead to better protection against SARS-CoV-2 than intramuscular vaccination with BReC-CoV-2. Here, we describe a series of murine immunogenicity and challenge studies that led us to a protective vaccine formulation and route of administration. Our findings demonstrate that unlike intramuscular administration, intranasal administration of BReC-CoV-2 provided protection against lethal doses of both the ancestral strain as well as Delta SARS-CoV-2.

### 4.3 Results

**Assessing different combinations of RBD-EcoCRM<sup>®</sup> and adjuvants in vaccine formulations against SARS-CoV-2.** It has been hypothesized that nasal vaccination offers a unique protection profile and advantages to muscular vaccination against SARS-CoV-2 (3). To test this hypothesis, we evaluated numerous antigens and adjuvants to identify a highly immunogenic vaccine formulation that would be subsequently evaluated in a K18-hACE2-transgenic mouse model. Since RBD has a small molecular weight, to improve responses to RBD, we conjugated RBD to EcoCRM<sup>®</sup>, a genetically detoxified diphtheria toxoid carrier protein (26). The conjugation of RBD to EcoCRM<sup>®</sup> yielded a product with approximately one EcoCRM<sup>®</sup> fused to 7-8 RBD molecules. The purpose behind the crosslinking of RBD with EcoCRM<sup>®</sup> was to enhance the immunogenicity and subsequent recognition of RBD by the immune system. Based on vaccine immunogenicity screens in CD1 mice (Figure 1), we hypothesized that a TLR4-agonist adjuvant would promote a robust antibody response. To test this hypothesis, we utilized Bacterial Enzymatic Combinatorial Chemistry (BECC). BECCs, are a TLR4-agonist that can help drive a balanced Th1/Th2 immune response that can help clear viral infections. We evaluated different adjuvants including: CpG (TLR9 agonist), IRI-1501 (Beta-glucan from yeast), BECC438 (biphosphorylated lipid A), and

BECC470 (monophosphorylated lipid A) (Supplementary table 1). In these studies, female CD1 outbred mice were immunized with the vaccine formulations indicated in Supplementary table 1, either through an intranasal or intramuscular route. Mice were boosted 3 weeks later with the same formulation through the same routes. Serological analysis was performed at 2 weeks post prime and 2 weeks post boost (Fig.1). Overall, mice demonstrated modest improvement in immunogenicity with RBD-EcoCRM<sup>®</sup> compared to RBD alone supplemented with different adjuvant combinations, both through the IM and IN routes. Intramuscular administration of RBD or RBD-EcoCRM<sup>®</sup> adjuvanted with BECC438 resulted in similar RBD IgG titers at 2 weeks post boost; however, when administered intranasally, RBD-EcoCRM<sup>®</sup> with BECC438 elicited greater RBD IgG titers compared to RBD (Fig1). Intranasally, BECC470 induced similar RBD-IgG responses formulated with RBD or RBD-EcoCRM (Fig 1A). Intramuscular vaccination with RBD-EcoCRM<sup>®</sup> adjuvanted with CpG generated increased RBD IgG titers compared to intranasal vaccination (Fig. 1AB). In humans, CpG is only administered IM and would not likely be an ideal candidate IN adjuvant. RBD-EcoCRM<sup>®</sup> adjuvanted with BECC470 generated a robust RBD-IgG response both intranasally and intramuscularly compared to other adjuvants tested (Fig.1).

### **RBD-EcoCRM<sup>®</sup> adjuvanted with BECC470 elicits robust antibody responses in CD1 mice.**

In this study, we focused on further investigating RBD-EcoCRM<sup>®</sup> and BECC470 (BReC-CoV-2). Initially, IM BReC-CoV-2 generated elevated production of RBD IgG titers after 1 week and 2 weeks post prime compared to the other vaccines (Fig.2A). We observed that IN and IM administration of BReC-CoV-2 produced robust RBD-IgG titers in the serum after boost (Fig.2A). The IN BReC-CoV-2 generated a 3-log increase of anti-RBD IgG 1-week post boost from 2 weeks post prime. Whereas the IM BReC-CoV-2 produced a 2-log increase of anti-RBD IgG from 2 weeks post prime to 1-week post boost (Fig. 2A). Overall, at 1 and 2 weeks post prime IM BReC-CoV-2 generated significant anti-RBD IgG titers compared to IN BreC-CoV-2 vaccination (Supplementary data 1). However, there were no statistical differences measured between RBD

alone and RBD-EcoCRM<sup>®</sup> with BECC470 (Supplementary data 1). An ideal COVID-19 vaccine would need to protect long-term; therefore, we measured RBD IgG titers at 22 weeks post boost were consistent with 2 weeks post boost in both IN and IM BReC-CoV-2 vaccinated groups (Fig.2A). In addition to serological analyses, we also confirmed antibodies generated were able to neutralize RBD binding to ACE2 *in vitro* at 2 weeks post boost (Fig. 2B). Overall, the collective data from the pilot immunogenicity study indicated that IM and IN BReC-CoV-2 vaccines produced long lasting strong anti-RBD IgG responses.

**Intranasal administration of BReC-CoV-2 protected mice from SARS-CoV2 challenge.** We next tested the protective capacity of IN and IM BReC-CoV-2 in a SARS-CoV-2 challenge model. K18-hACE2 mice were vaccinated with IN and IM formulations of BReC-CoV-2 (Fig. 3A). At 2 weeks post boost, IN (n=9), IM BReC-CoV-2 (n=10), and no vaccine challenged (NVC) (n=8) groups were challenged with a 10<sup>4</sup> PFU/dose of WA-1 variant of SARS-CoV-2 and monitored for disease outcomes for a 14-day period. We assessed disease manifestations such as weight loss, appearance, activity, eye closure, respiration, and hypothermia (Supplementary Figure 1). Mice were euthanized if they achieved a disease score 5 or greater, which determined that they were morbid. We calculated the cumulative disease score by adding the total scores of each mouse in one group. When animals become morbid and require euthanasia, we retained the animal's score in the sum of the remaining days of the experiment. This disease scoring system helps us predict when mice will become morbid and is inverse to the falling Kaplan Meier curve. Throughout this 14-day period, we observed that NVC and IM BReC-CoV-2 vaccinated mice began decreasing in weight at day 7 post challenge, whereas the IN BReC-CoV-2 vaccinated mice gradually gained weight (Fig.3D). IN vaccinated animals compared to NVC and IM maintained stable rectal temperatures throughout 2-week monitoring period which corroborated their disease scores (Fig. 3CE). However, NVC and IM vaccinated mice rectal temperature plummeted at days 7 and 8 post challenge (Fig.3E). Unlike the IM, NVC was not able to recover in temperature as IM vaccinated

mice. When evaluating the groups based on their disease scores, NVC began to increase in disease scores at day 7 and continually increased in disease scores until day 10 (Fig.3C). IM BReC-CoV-2 vaccinated mice peaked in disease scores at day 8, but then returned to normal health scores throughout the rest of the challenge trial (Fig.3C). IN BReC-CoV-2 vaccinated mice maintained low disease scores throughout the entirety of the 14-day monitoring period compared to both the NVC and IM vaccinated mice (Fig.3C). Weight and temperature loss along with disease scores correlated with poor survival outcome (25% survival) in NVC group (Fig. 3B). IM vaccinated mice portrayed a better disease outcome than NVC, with 60% survival (Fig.3B), and IN vaccinated mice experienced significant survival compared to NVC ( $P=0.0332$ ) with 89% survival (Fig.3B). Overall, the protection profile indicated that IN vaccination with BReC-CoV-2 compared to IM and NVC protected mice from SARS-CoV-2 challenge suggesting that the mucosal immune response may play a role in driving protection from SARS-CoV2.

**IN vaccination with BReC-CoV-2 decreases viral RNA burden in the lung and brain.** As the disease monitoring data suggested, IN vaccination with BReC-CoV-2 was superior in protection compared to IM mice. To corroborate the observed disease monitoring data, the viral RNA burden of the vaccinated mice compared to the NVC was determined. For this analysis, we measured RNA copies of nucleocapsid to SARS-CoV-2 in the lung (Fig.4A), brain (Fig.4B), and nasal wash (NW) for each animal (Fig.4C). In the lung, IN vaccination of BReC-CoV-2 significantly decreased viral RNA compared to NVC and IM vaccinated BReC-CoV-2 (Fig.4A) indicating that IN vaccination limits viral burden. Studies have shown that K18-ACE2 mice succumb to SARS-CoV-2 brain infection after challenge (22,27,28). IN vaccination with BreC-CoV-2 significantly decreased viral RNA in the brain compared to NVC suggesting that IN vaccination prevented the dissemination of virus into the brain (Fig.4B). IN vaccination also decreased viral copies in the NW compared to NVC and IM; however, these differences were not statistically significant (Fig. 4C). Overall, there was a significant reduction of viral RNA copies in the lung of IN vaccinated mice compared to IM and NVC, significant decrease of viral RNA in the brain compared to NVC

as well as fewer viral RNA copies in the NW. Decreased detection of viral RNA suggested that IN BReC-CoV-2 diminished viral replication at the site of infection aided in survival compared to IM BReC-CoV-2.

**Both IM and IN BReC-CoV-2 RBD antibody responses increase during SARS-CoV-2 challenge.** To investigate the antibody responses generated by BReC-CoV-2 vaccination, we first analyzed RBD specific IgG production systemically and then locally in the lung. Systemic RBD IgG was measured before challenge and after challenge with SARS-CoV-2. In order to measure serum RBD IgG before challenge, blood was collected at 2 weeks post prime and 2 weeks post boost (Fig.5A). At 2 weeks post prime, both IN and IM begin to generate detectable RBD IgG titers, with the IM generating higher RBD titers than both NVC and IN (Fig.5A). Both IN and IM BReC-CoV-2 vaccinated groups induced a robust response to boosting, but IM vaccination elicited increased RBD-IgG titers than IN and NVC (Fig.5A). Post challenge, serum RBD IgG was significantly elevated in both IN and IM vaccinated groups compared to NVC suggesting challenge may increase antibody production (Fig.5B). In the lung supernatant, similar to the serum, RBD IgG were significantly increased in both the IN and IM vaccinated mice compared to the NVC (Fig.5C) indicating no difference between the IN and IM RBD IgG titers in the lung.

**IN BReC-CoV-2 generated a robust localized IgA response compared to IM vaccination.**

To characterize the mucosal antibody response to BReC-CoV-2 vaccination, IgA titers were measured in the lung and nasal wash. In the lung supernatant, NVC and IM vaccinated mice did not generate RBD specific IgA compared to IN BReC-CoV-2 vaccination (Fig.5E). To further confirm the findings that the mucosal antibody response was contributing significantly to protection, anti-RBD IgA in the nasal wash was analyzed. Similar to the lung supernatant, IN vaccination significantly increased RBD-IgA compared to the undetectable IgA amounts in the NVC and IM vaccinated groups (Fig.5D). Serum RBD IgA titers were also examined. The results indicated that IgA was released systemically because pre-challenge IgA was slightly elevated in IN vaccinated mice but not in the NVC and IM groups. However, post challenge, there was no

change in the serum RBD IgA titers in any groups (Fig.5F). In summary, both IN and IM vaccination generated similar IgG responses in the lung and serum. However, IN vaccination induced a stronger IgA response in the lung and NW compared to IM, suggesting that the mucosal antibody response is potentially important in facilitating clearance of SARS-CoV-2 in the respiratory tract.

**BECC470 induces Th1/Th2 responses in both IN and IM BReC-CoV-2 vaccination.** Previous pre-clinical vaccine studies using BECC470 as an adjuvant have shown that BECC470 generated a balanced Th1/Th2 immune response(19). To investigate the Th1 and Th2 immune response elicited by IN and IM BReC-CoV-2 vaccination, IgG1 (Th2) and IgG2c (Th1) subtypes were analyzed in the serum. Both IN and IM BReC-CoV-2 vaccination induced significant RBD specific IgG2c and IgG1 responses compared to NVC (Supplementary Figure 2). IM BReC-CoV-2 vaccination also generated a significant increase in IgG1 compared to IN vaccination indicating a Th2 biased response with IM vaccination compared to IN (Supplementary Figure 2B). NVC mice had an expected increase in IgG2c compared to IgG1 indicating a Th1 response to viral infection (Supplementary Figure 2). IgG2/IgG1 ratios of less than one are considered Th1-biased whereas ratio of greater than one would indicate Th2 responses. Overall, IN and IM vaccination induced IgG1/IgG2c ratios of 0.8 and 1.1, respectively. Both vaccines induce Th2 responses, but IN immunization is driving slightly more Th1 antibody responses.

**Both IN and IM BReC-CoV-2 vaccination induced neutralizing antibodies.** Antibody analysis of IN and IM BReC-CoV-2 vaccination detected high levels of RBD specific IgG and IgA; therefore, we determined if these antibodies were functional in neutralizing RBD binding to ACE2. The MSD COVID-19 ACE2 neutralization multiplex assay was used to analyze neutralization of the RBD and spike protein of the variants of concern (VOC) (Alpha, Beta, and Gamma). Neutralization of RBD or Spike binding to ACE2 was measured through electrical chemiluminescent (ECL) signal intensity for NVC, IN, and IM vaccinated mice. The higher the signal the less neutralization and the less intense the signal the more neutralization capability. Both IN and IM vaccinated mice had

significant neutralizing antibody titers compared to NVC in the serum demonstrating that both IN and IM vaccination generated functional antibodies (Fig.6). NVC mice, as expected, had no neutralization against the VOCs (Fig.6). IN vaccinated mice had significantly higher neutralization capacity than NVC for Alpha, Beta, and Gamma (Fig.6A-B); whereas IM vaccinated mice had increased neutralization capacity compared to NVC against Beta (Fig.6C-D). For whole spike neutralization, IN vaccination generated significant neutralizing titers against the Wuhan strain of spike compared to IM vaccination (Fig.6A-B). Overall, IN vaccination with BReC-CoV-2 showed superior neutralization capacity over IM in the ability to neutralize multiple VOCs RBD from binding to ACE2.

**Increased levels of serum CXCL13 in NVC and IM BReC-CoV-2 vaccinated mice indicate poor disease prognosis.** CXCL13 is an important chemokine marker for germinal center activity, B-cell maturation, memory B-cell, and plasma cell formation. Conversely, in non-vaccinated COVID-19 patients, increased CXCL13 levels have been shown to be a marker of a poor clinical outcome compared to patients who survived COVID-19 (29,30). In the context of immunization (pre-challenge), CXCL13 was detectable in IN immunized mice, but higher in IM immunized mice, suggesting germinal centers were more active after IM immunization (Fig. 7A). After challenge, NVC mice had higher CXCL13 compared to naïve mice as would be expected (Fig.7B). IN immunized mice had the lowest CXCL13 levels. These data suggest that germinal centers were not activated due to the mucosal protection and levels of circulating systemic antibodies in the IN immunized mice.

**IN BReC-CoV-2 decreased IFN- $\gamma$  in the lung.** SARS-CoV-2 is known to cause inflammation in the lung and induce interferon responses (22,23,31). Therefore, we hypothesized that IN vaccination should help decrease inflammatory markers in the lung. To test this hypothesis, we measured inflammatory cytokines in the lung supernatant post SARS-CoV-2 challenge. Compared to the NVC and IM vaccination, IN vaccination significantly lowered IFN $\gamma$  in the lung supernatant (Supplementary Figure 3C), whereas other pro-inflammatory cytokines remained



similar between NVC, IN and IM (Supplementary Figure 3A-D). C reactive protein (CRP) was also measured as a marker to evaluate inflammation during SARS-CoV-2 challenge. CRP was significantly decreased in IN and IM vaccinated groups compared to NVC in the lung (Supplementary Figure 3D). Overall, vaccination decreased inflammation in the lung, with IN vaccination decreasing both IFN- $\gamma$  and CRP compared to NVC.

**IM vaccination decreases both chronic and acute inflammation in the lung whereas IN vaccination decreases acute inflammation only.** We next hypothesized that IN vaccination would reduce total inflammation due to decreasing inflammatory cytokines in the lung. The left lobe of the lung was subjected to H&E staining and evaluated for histopathological analysis for chronic and acute inflammation. Chronic inflammation was scored by the presence of recruited lymphocytes, plasma cells, and macrophages in the parenchyma and blood vessels. Acute inflammation was denoted by the infiltration of neutrophils and the presence of edema in the parenchyma, blood vessels, and airways. IN vaccinated mice had increased chronic inflammation scores (3.8) compared to NVNC (0.33), NVC (3.1), and IM (2.7) with the presence of plasma cells, lymphocytes, and macrophages localized around blood vessels (Fig. 8CDH). IN mice scored an average inflammation score of 4.1, lower than NVC (Fig. 8GH). Mice vaccinated IM with BReC-CoV-2 had the lowest chronic and acute inflammation scores compared to NVNC, NVC, and IN mice with an overall mean inflammation score of 2.8 (Fig. 8EFGH). IM mice had mostly chronic inflammation found in the parenchyma, blood vessels and bronchi (Fig. 8EFG). Overall, IM vaccinated mice had less acute and chronic inflammation than NVNC, NVC, and IN suggesting that IN vaccination mimicked natural infection by recruiting cells into the lung to fight viral infection.

**IN BReC-CoV-2 vaccination upregulates specific immune genes in response to SARS-CoV-2 challenge.** To capture the transcriptional profile of intranasal and intramuscular BReC-Cov-2 vaccination during SARS-CoV-2 challenge, the lung was analyzed using RNA sequencing. IN BReC-CoV-2 compared to NVC had 174 activated genes and 130 repressed genes whereas IM

BReC-CoV-2 compared to NVC had 82 activated genes with 167 repressed genes (Fig.9A, Supplementary data 2). Immunoglobulin genes involved in regulating the adaptive immune response were significantly upregulated in IN BReC-CoV-2 vaccination and challenge compared to NVC (Fig.9B-D). Genes responsible for general T-cell regulation and activation such as *Lat*, *Lef1*, *Mill1*, *Trat1*, *Tespa1*, *Themis*, *Tox*, *Tcf7*, *H2M2*, *Cd163l1*, *Cd226*, and *Cd4* hint at the presence of effector and resident T-cells in the lung (Fig.9D) However, IM vaccinated compared to NVC only had three immunoglobulin genes (*Igkv3-5*, *Ighv11-2*, and *Igkv14-126*) significantly upregulated, and no significant fold changes in the adaptive immune response gene set (Fig.9C-D). Over-Representation Analysis was used to enrich GO-terms of the biological processes in IN BReC-CoV-2 challenged mice compared to NVC. We observed gene set enrichment and significant upregulation in genes involved in a variety of important immune responses such as leukocyte activation, lymphocyte activation, leukocyte mediated immunity, somatic recombination, somatic diversification of immune receptors, and somatic diversification of T-cell receptor genes (Fig.9E). Conversely, there were increased repressed genes involved in cellular response to interleukin-1 suggesting that IN BReC-CoV-2 helped decrease inflammation in the lung (Fig.9E). Overall, the transcriptomic data generated from sequencing the lung from IN and IM BReC-CoV-2 vaccination during SARS-CoV-2 challenge mirrored the correlates of protection collected throughout this study.

**IM BReC-CoV-2 prime followed by IN boost afforded survival against SARS-CoV-2 Delta variant challenge.** SARS-CoV-2 Delta variant is the predominant circulating variant in the world as of December 2021(32–34). Therefore, we wanted to evaluate whether BReC-CoV-2 vaccination can protect against Delta challenge in mice. K18-hACE2 mice were vaccinated with 2 doses of BReC-CoV-2 through the IN route, IM route and lastly, primed through the IM route and boosted through the IN route (IM/IN). IN and IM BReC-CoV-2 vaccination generated similar RBD IgG titers as the previous vaccine and challenge study with WA-1 (Fig. 10A). IM/IN vaccination elicited similar RBD IgG titers as IM vaccination (Fig. 10A). NVC (n=5), IN (n=5), IM

(n=5), and IM/IN (n=3) were challenged with a lethal  $10^4$  PFU/dose of Delta variant and monitored similarly for disease manifestations as the previous challenge trial with WA-1 SARS-CoV-2. NVC mice began succumbing to disease at day 6, and by day 7 post challenge, remaining mice were morbid and were euthanized. Severity of disease caused by the Delta variant in the NVC group was reflected by the increase of the cumulative disease scores as well as in the sharp decrease in weight and temperature. (Fig. 10BCD). IN BReC-CoV-2 vaccinated mice had increased survival compared to NVC (60% survival); however, 2 mice succumbed to Delta at day 7 post challenge (Fig. 10B). Cumulative disease scores peaked at day 7 in the IN vaccinated group mirroring the moribund mice. The morbid mice in the IN vaccinated group had increased disease scores as well as decreased temperature and weight compared to the rest of the group. Mice administered BReC-CoV-2 through the IM route had increased mortality compared to IN with a 40% survival rate. Disease scores reflected the morbidity of the IM vaccinated mice; however, interestingly, IM mice that succumbed to disease had a sharp decrease in weight but maintained temperature unlike NVC and IN moribund mice (Fig. 10 CDE). Remarkably, all mice vaccinated with BReC-CoV-2 through IM prime and IN boost strategy survived a lethal challenge against the Delta variant (Fig. 10B). IM/IN group maintained stable weight and temperature throughout the course of challenge, as well as did not exhibit disease manifestations observed in NVC, IN and IM groups (Fig.10 CDE). Viral RNA burden in the brain (Fig. 10F), lung (Fig. 10G), and NW (Fig.10H) followed similar trends as the disease assessment and survival in IN, IM, and IM/IN BReC-CoV-2 immunized mice. Interestingly, despite IN BReC-CoV-2 having a better survival outcome than IM BReC-CoV-2 vaccinated mice, NVC, IN and IM groups had similar levels of viral RNA in the brain and lung (Fig. 10FG). However, IN BReC-CoV-2 vaccinated mice had decreased viral burden in the NW compared to NVC and IM BReC-CoV-2 (Fig. 10H). The heterologous prime (IM) and boost (IN) strategy provided significant decrease of viral RNA in the brain, lung and NW compared to NVC (Fig. 10FGH) suggesting that IM prime with BReC-CoV-2 followed by IN boost prevented viral dissemination. Overall,  $10^4$  PFU/dose of SARS-CoV-2 Delta variant was a lethal

dose in non-vaccinated mice. IM/IN BReC-CoV-2 vaccinated offered superior protection against lethal Delta challenge compared to NVC, IN, and IM vaccination. IN BReC-CoV-2 provided significant protection against Delta challenge compared to NVC; however, did not offer complete protection, and IM BReC-CoV-2 supplied limited protection against Delta.

#### **4.4 Discussion**

For protection against respiratory pathogens, nasal vaccines can offer both localized protection at the site of infection and activate systemic responses. Very few nasal vaccines have been approved for human use. To the best of our knowledge, only two examples are on the market: FluMist<sup>®</sup>, a live attenuated influenza FDA approved vaccine for seasonal flu and Nasovac<sup>®</sup>, an H1N1 pandemic flu vaccine (35). The chimpanzee adenovirus vectored vaccine encoding a pre-fusion stabilized spike (S) protein (ChAD-SARS-CoV-2-S) is an example of an adenovirus vectored COVID-19 vaccine that has been shown protective as a single dose nasal vaccination in non-human primates and other models as well (36,37). AdCovid<sup>™</sup> developed by Altimmune, is another adenovirus vectored (replication deficient adenovirus type 5) intranasal vaccine expressing RBD instead of the spike protein. In pre-clinical studies, a single dose of AdCovid<sup>™</sup> offered sterilizing immunity against SARS-CoV-2 challenge and induced a robust mucosal response in the respiratory tract in mice(38,39). However, AdCovid<sup>™</sup> demonstrated a lack of efficacy in phase 1 clinical trials and was discontinued. A few pre-clinical trials evaluating intranasal vaccines utilizing a recombinant spike protein with stimulator of interferon genes (STING) adjuvant showed robust systemic and localized immunogenicity. (40) And lastly, a live attenuated and vectored Newcastle Disease virus expressing spike protein demonstrated sterilizing immunity against SARS-CoV-2 when administered IN (41). Collectively, these studies hint that IN vaccines can protect against SARS-CoV-2.

In this study, our objective was to develop and evaluate a nasal vaccine against SARS-CoV-2 using RBD conjugated to EcoCRM<sup>®</sup> adjuvanted with BECC470 (BReC-CoV-2). Before we tested

BReC-CoV-2 in a SARS-CoV-2 challenge model, we performed an intensive immunogenicity screen for immunogenic vaccine antigen and adjuvant combinations in outbred mice (Fig.1). We screened 18 different vaccine combinations through both the intranasal and intramuscular route. Using the K18 hACE2 mouse model, we demonstrated that intranasal vaccination with BReC-CoV-2 offered protection against WA-1 SARS-CoV-2 compared to IM vaccination. We observed that IN vaccination with BReC-CoV-2 increased percent survival, decreased disease scores, and maintained weight and temperature in IN group throughout infection compared to IM and NVC (Fig.3). Intranasal vaccination was performed with 50 $\mu$ L of vaccine in order to deposit vaccine in both the upper respiratory tract and lungs. It is likely that this would cause both mucosal and systemic immune responses. Nasal vaccination decreased viral burden in the lung compared to IM and NVC (Fig.4), as well as increased RBD IgA titers in the lung and nasal wash compared to IM and NVC (Fig.5). Increased neutralizing antibodies against RBD of the variants of concern (Alpha, Beta, and Gamma) were found with IN compared to IM and NVC (Fig. 6). Intranasal vaccination with BReC-CoV-2 decreased IFN- $\gamma$  in the lung compared to IM and NVC (Supplementary Figure 3). However, histopathological analyses showed an increase of recruitment of lymphocytes, macrophages, and plasma cells to blood vessels in the lung compared to IM vaccination (Fig.8). RNAseq analysis performed on the lungs demonstrated that IN BReC-CoV-2 vaccination upregulated more genes involved in the adaptive immune response compared to NVC and IM groups (Fig. 9). Since the Delta variant of SARS-CoV-2 is the predominant strain in the world, a Delta challenge was performed in BReC-CoV-2 vaccinated mice. Compared to the WA-1 challenge, IN BReC-CoV-2 had significant survival compared to NVC and decreased disease scores. However, heterologous prime boost of BReC-CoV-2 offered 100% survival against Delta challenge (Fig. 10).

In our BReC-CoV-2 formulation we utilized a carrier protein and an adjuvant synthesized from bacterial components. Bacterial components can serve as potent adjuvants for either bacterial or viral vaccines. We used BECC470 as the candidate adjuvant to supplement RBD-EcoCRM.

Compared to GSK MPLA, they are both engineered forms of lipid A, TLR4-agonists, and drive a robust Th1 immune response, but there are significant differences in the way that they are synthesized. BECC was developed as an alternative route to produce lipid A mimetics. It uses novel methodology that generates products that are cost effective and easy to produce (17).. Carrier proteins are another important vaccine component for small molecular weight antigens such as RBD to increase antigen presentation thus immunogenicity. EcoCRM® the carrier protein of our immunogen is a genetically detoxified diphtheria toxin originally expressed in *Corynebacterium diphtheriae*(9). We used EcoCRM® which is CRM<sub>197</sub> expressed as a soluble, properly folded protein in the cytoplasm of an *E. coli* strain engineered to have an oxidative cytoplasm(26,42). Crosslinking of a carrier protein and RBD, forming a high MW nanoparticle like construct capable of presenting multiple molecules of RBD are likely critical for the enhanced response to the conjugate versus RBD alone.

In our studies, we acknowledge that the K18-hACE2 mouse model contains limitations such as increased sensitivity to SARS-CoV-2 challenge because of elevated expression of human ACE2 in the mouse compared to humans such as in the brain (25). The severity of this transgenic challenge model does likely have a caveat because brain SARS-CoV-2 infection is atypical of human infection (28,43). Future studies are needed to evaluate IN and IM administration of BReC-CoV-2 in other rodent models such as the Syrian hamster model. The hamster model results in pneumonia (44). Hamster ACE2 are similar to human ACE2 and disease phenotypes of SARS-CoV-2 infection recapitulate those of human pneumonia and inflammation in the hamster model (45). Unlike the K18-hACE2 mouse model, hamsters do not succumb to brain encephalitis, the majority of the virus remain in the lungs, and may spread to the GI tract (25).

Since the K18-hACE2 mouse model is sensitive to SARS-CoV-2, it was important to determine an appropriate lethal challenge dose to effectively evaluate vaccine protection. In previous studies, we evaluated  $10^4$  (n=12) and  $10^5$  (n=13) PFU/dose of SARS-CoV-2 WA-1 in K18-ACE2 mice (46). We observed that  $10^4$  and  $10^5$  PFU/dose resulted in 11% survival and 0% survival,

respectively. Our BReC-CoV-2 challenge study showed that  $10^4$  PFU/dose of WA-1 resulted in 25% survival in the non-vaccinated, challenged mice similar to the preliminary dose study. Other studies have shown that approximately  $10^4$  PFU/dose also show similar lethality in K18-hACE2 mice and  $10^5$  PFU/dose results in 100% lethality (22,23,28). Since the WA-1 viral stock that was used to challenge mice in this experiment was sequenced and contained no deletions in the furin cleavage site, discrepancies in mouse survival in the  $10^4$ -challenge dose could be due to deviations in delivery of the challenge dose per mouse. To further investigate the optimal dose for maximizing vaccine efficacy, more studies should be done characterizing the lethal and sublethal doses of SARS-CoV-2, especially in relation to VOC strains.

In our first protection study, we challenged mice with the ancestral SARS-CoV-2 WA-1; however, this clade of strain is currently virtually non-existent. Nevertheless, we evaluated the neutralizing capacity of sera of BReC-Cov-2 vaccinated mice to RBD and spike proteins from the VOCs (Fig. 6). Sera from mice IN immunized with BReC-CoV-2 vaccination were able to significantly inhibit hACE2 binding of the VOC RBDs. This suggests that IN administration of BReC-CoV-2 may be able to protect mice challenged with these VOCs. Since the Delta variant is currently the predominant global variant; we challenged BReC-CoV-2 vaccinated mice with Delta (Fig. 10). Even though, IN BReC-CoV-2 significantly improve survival compared to NVC, survival rate decreased from 89% with WA-1 challenge to 60% with Delta challenge, indicating a decrease in vaccine efficacy against the VOC. However, we demonstrated that mice immunized through the IM/IN vaccine strategy with BReC-CoV-2 had 100% survival against lethal Delta challenge suggesting that the IM/IN vaccine route is the optimal vaccine strategy with BReC-CoV-2 in this model. The RBD used in BReC-CoV-2 was generated from the WA-1 strain of SARS-CoV-2. Therefore, mutations in RBD will decrease antibody binding and virus neutralization which is likely causing decreased vaccine efficacy of IN and IM BReC-CoV-2. Our data suggest that administering a booster dose through the IN route after an IM prime might provide increased

protection against SARS-CoV-2. Further investigation is needed to evaluate the correlates of protection of BReC-CoV-2 IM/IN compared to IN or IM only routes with Delta challenge.

Neutralizing antibodies are important in diminishing the replication of SARS-CoV-2, whereas CD4<sup>+</sup> and CD8<sup>+</sup> T-cells play a large role in clearing and controlling SARS-CoV-2 infection (16,47,48). Studies have shown that in humans, resident T-cells in the lung instead of in circulation were linked with better disease prognosis and survival (49). We appreciate that in other intranasal vaccination studies for bacterial and viral pathogens that T resident memory cells are elevated in the lung and nasal associated lymphoid tissue (50). We hypothesize that since BECC470 is a driver of Th1 immune responses (Supplementary Figure 2A) that IN BReC-CoV-2 will also elicit robust T resident memory responses that will contribute to protection. However, further investigation is needed to study T resident memory cells in the lung as well as the nasal associated lymphoid tissue in the mouse.

Next generation sequencing is a powerful platform that can be used to profile vaccine responses. In this study we used bulk RNAseq to characterize the transcriptomic landscape of BReC-CoV-2 vaccinated lungs against WA-1 SARS-CoV-2 challenge (Fig.9). Interestingly, IN BReC-CoV-2 vaccinated and SARS-CoV-2 challenged lungs revealed activation of immunoglobulin genes compared to NVC suggesting the presence of antibody producing B cells in the lungs which could have contributed to protection of the IN BReC-CoV-2 mice. These data corroborate with serological analysis of IN BReC-CoV-2 lung, where we observed the increased induction of RBD IgG and IgA titers. Human COVID-19 studies observe the presence of memory B cells in the lung 6 months post infection which hint at the importance of memory B cells for protection against SARS-Co-2 infection(51). Additionally, IN BReC-CoV-2 lung showed transcriptional signatures of genes involved in T-cell signaling and differentiation, suggesting the presence of CD4<sup>+</sup> and CD8<sup>+</sup> T cells as well as T resident memory cells, which also has been shown in human COVID-19 cases (51). *Rag1* and *rag2* were significantly upregulated in IN BReC-CoV-2 vaccination suggesting that mature B and T cells were residing in the lung. Remarkably, we only observe differentiation in



the immune response genes in IN BReC-CoV-2 lungs and not in the IM BReC-CoV-2 lungs hinting that a localized immune response was occurring in the IN vaccinated. Overall, traditional RNAseq provides a snapshot of the immune response occurring during IN and IM BReC-CoV-2 vaccination; however, it does not detail antigen specificity of the immunoglobulin genes expressed (Fig. 9). Novel technology such as linking B cell receptor to antigen specificity through sequencing can aid in discovering antigen specific B and T cell receptors that are crucial to a protective vaccine response.

In summary, our study demonstrates that intranasal administration of BReC-CoV-2 confers protection against WA-1 SARS-CoV-2 challenge in hACE2 mice compared to intramuscular vaccination. IN administration with BReC-CoV-2 protected transgenic mice against challenge, but also reduced viral burden in the lung, inhibited hACE2 binding of VOC RBDs, and induced high titers of IgA in the lung and nasal wash. Importantly, we also demonstrated that BReC-CoV-2 administered via an IM prime and IN boost strategy protected transgenic mice from a lethal challenge of the Delta variant. In the future, our goal is to evaluate BReC-CoV-2 in the Syrian hamster model with emerging VOCs such as the Delta variant. We also want to further investigate the mucosal IgA response of nasal BReC-CoV-2 in the lungs and nasal tissue. In summary, intranasal vaccination with BReC-CoV-2 offered better protection at the site of infection than intramuscular vaccination, indicating that intranasal route of this vaccine candidate can be pursued in future studies.

## **4.5 Methods**

### **Animal welfare, Biosafety and Ethics statements.**

CD1 outbred mouse immunogenicity studies were performed under the approved West Virginia University IACUC protocol number 2004034204 whereas B6.Cg-Tg(K18-ACE2)2PrImn/J mouse vaccine and SARS-CoV-2 challenge studies were executed under IACUC protocol number 2009036460. All mice were humanely euthanized based on the disease scoring system, described below (Supplementary Figure 1), and no deaths occurred in the cage. All SARS-CoV-2 challenge studies were conducted in the West Virginia University Biosafety Laboratory Level 3 facility under the IBC protocol number 20-04-01. SARS-CoV-2 samples were inactivated with 1% Triton per volume before exiting high containment.

### **Mouse vaccination**

Female outbred CD1 mice were obtained from Charles River Laboratories (strain code: 022) at 4 weeks old and vaccinated at 8 weeks of age. Both male and female B6.Cg-Tg(K18-ACE2)2PrImn/J mice were purchased from Jackson Laboratory (stock no: 034860) at 8 weeks old and vaccinated at 10 weeks old for the WA-1 challenge study. Female B6.Cg-Tg(K18-ACE2)2PrImn/J mice were vaccinated at 13 weeks old and were used in the Delta (B.1.617.2) challenge study. Both CD1 and K18-hACE2 mice were administered 50 $\mu$ L immunizations through either the intramuscular route or intranasal route. For intranasal immunization, mice were anesthetized through intraperitoneal injection with ketamine/xylazine per approved protocols, then administered 25 $\mu$ L of vaccine into each nare.

### **Production of antigen**

Receptor binding domain (RBD) of the Wuhan original strain of SARS-CoV-2 was recombinantly produced by transient transfection in HEK293T cells using a pCAGGS expression vector with RBD construct with a C-terminal hexahistidine tag and codon optimized for mammalian expression (pCAGGS vector catalog #: NR-52309 BEI Resources) (9). RBD was then chemically conjugated to the carrier protein EcoCRM<sup>®</sup> by Fina Biosolutions LLC (Rockville,MD).

### **Determination of RBD-CRM ratio by mass spectrometry**

Proteins RBD, CRM, RBD-CRM (1 µg each) were electrophoresed in SDS-PAGE gel. The protein bands were excised and extracted protein was treated with trypsin. The resulting peptides were analyzed on a Q Exactive™ Plus Hybrid Quadrupole-Orbitrap™ Mass Spectrometer and peptide spectra matched (PSM) were aligned to RBD or CRM proteins. Unique peptides were determined and the RBD to CRM ratio was determined. CRM and RBD individual resulted in 150 PSM or 16.2 per pmol of protein, respectively. Conjugated RBD-CRM resulted in 112 PSM (0.74pmol) of CRM and 95 PSM (5.86 pmol) of RBD.  $5.86/0.74$  pmol results in a ratio of 7.92 RBD per CRM of conjugated antigen.

### **Vaccine composition**

20µg of RBD- EcoCRM® was used in the vaccine formulations. The adjuvants BECC 470 and BECC 438 were obtained from Dr. Robert Ernst at the University of Maryland(17). Briefly, 50µg BECC 470 or BECC 438 were sonicated in a water bath sonicator for 15 minutes prior mixing with RBD-EcoCRM® for 2 hours before vaccination. IRI-1501 beta glucan was provided by Immunoresearch. CpG adjuvant was acquired from Dynavax.

### **Luminex Magpix platform *in vitro* neutralization assay.**

Neutralization assay was developed using the Luminex Magpix platform(29). Briefly, 1:2 dilution of mouse serum was added to Greiner black non-binding 96 well plates. Serum was diluted 1:5 down the plate. Luminex Magpix® Microspheres (MC10012-YY) conjugated to RBD were added to the serum dilutions. After a 2-hour incubation period, plates were washed 2X with 1X PBS-TBN on a 96 well magnet, ACE2-biotin was added to the plates and incubated for 1 hour. Plates were washed again 2X on the magnet, and Streptavidin-phycoerythrin was added to the plates and incubated for 30 minutes at room temperature at 700rpm. After the Streptavidin-phycoerythrin

incubation, plates were washed again, and 100 $\mu$ L of 1XPBS-TBN was added to plates and analyzed on the Magpix to measure neutralizing ability of serum antibodies.

### **Serological analysis**

ELISAs were performed to assess the total IgG (Novus Biologicals NBP1-75130), and IgA (Novus Biologicals NB7504) in the serum, lung supernatant, and nasal wash (29,46). Total IgG titers were quantified in the serum. High binding plates (Pierce 15041) were coated overnight at 4°C with 2 $\mu$ g/mL of RBD in phosphate buffered saline. Plates were then blocked with 3% non-fat milk in PBS-0.1% Tween 20 overnight in the 4°C. After blocking, 1:20 dilution of serum from mice was added in the first row and diluted 1:2 down two plates (15 dilutions total) in 1% non-fat milk in PBS-0.1% Tween 20 leaving the last row on the last plate as a blank. Plates were incubated for 10 minutes at room temperature with shaking. Plates were then washed with PBS-0.1% Tween 20 4 times, then either goat-anti-mouse secondary IgG HRP (1:2000 dilution) was added to the plates and incubated as above (Novus Biosolutions). ELISAs were developed using TMB reagent (Biolegend 421101) (1:1 ratio) in the dark for 10 minutes, and the reaction was stopped using 25 $\mu$ L 2N sulfuric acid. ELISAs were read using the Synergy H1 plate reader at 450nm. Nasal wash, serum, and lung supernatant IgA titer quantification was performed using the same coating and blocking procedures as mentioned above. In separate ELISA assays, 100 $\mu$ L of nasal wash, 1:20 dilution of serum and 1:5 dilution of lung supernatant was added to the first rows of high binding plates and diluted down 2 plates at 1:2 dilution in 1% non-fat milk in PBS-0.1% Tween 20. Serum, nasal wash and lung supernatant samples were incubated for 2 hours at room temperature with shaking. Plates were washed according to the protocol mentioned above. Secondary goat-anti-mouse IgA HRP (1:10000) (Novus biologicals) was used in these assays and incubated for 1 hour at room temperature with shaking. IgA ELISAs were developed with TMB substrate (1:1) for 20 minutes in the dark before adding stopping solution and read on the Synergy H1 plate reader at 450nm. Serological data was also analyzed as antibody titer, IC50

and AUC. From our analysis, data followed nearly identical trends of titers per vaccine/control group as well as have the same statistical significance (one-way ANVOVA using Tukey's multiple comparisons test) between each method analyzed. Titers were represented as Area Under the Curve values calculated via GraphPad Prism v9.0.0.

### **SARS-CoV-2 propagation and mouse challenge.**

SARS-CoV-2 USA-WA-1/2020 (NR-52281) (GenBank accession number: MN985325) or SARS-CoV-2 Delta variant B.1.617.2 hCoV-19/USA/WV-WVU-WV118685/2021 (GISAID Accession ID: EPI\_ISL\_1742834) were the challenge strains used in K18-hACE2 vaccine studies. SARS-CoV-2 USA-WA-1/2020 (NR-52281) was obtained from BEI and hCoV-19/USA/WV-WVU-WV118685/2021 was obtained from a patient sample at WVU. Both strains were propagated in Vero E6 cells (ATCC-CRL-1586) and re-sequenced. K18-hACE2 mice were challenged with a  $10^4$  PFU/dose. Viral dose was prepared from the first passage of WA-1 at a concentration of  $3.7 \times 10^6$  PFU/mL diluted to a working concentration of  $10^6$  PFU/mL. B.1.617.2  $10^4$  PFU/dose was prepared from the first passage of a viral stock concentration of  $8.25 \times 10^5$  PFU/mL. Briefly, mice were anesthetized with IP injection of ketamine (Patterson Veterinary 07-803-6637) /xylazine (Patterson Veterinary 07-808-1947), and a total of 50 $\mu$ L of  $10^4$  PFU SARS-CoV-2 WA-1 or Delta was administered intranasally (25 $\mu$ L per nare).

### **Disease score of SARS-CoV-2 challenged mice**

Challenged K18-hACE2 mice were evaluated daily through both in-person health assessments in the BSL3 and SwifTAG Systems video monitoring for 12-14 days. Health assessments of the mice were scored based on five criteria: 1) weight loss (scale 0-5), 2) appearance (scale 0-2), 3) activity (scale 0-3), 4) eye closure (scale 0-2), and 5) respiration (scale 0-2) (Supplementary Figure 1). All five criteria were scored based off a scaling system where 0 represents no symptoms and the highest number on the scale denotes the most severe phenotype (52). Weight loss (0-5) was scored based off percent weight loss from original weight before challenge using the scale

0-5% (0), 5-10% (1), 10-15% (2) 15-20% (3), >20% (4-5). If mice reached 20% weight loss before the termination of the study, mice were humanely euthanized at that time point. Appearance (0-2) was scored by observation of piloerection of fur, score of (0) indicative of groomed, healthy fur whereas score of (2) represented ungroomed fur. Activity (0-3) was scored based off (0) normal activity for the time of day observed and (3) collapsed or immobile. Eye closure (0-2) was assigned (0) for mice with open eyes and (2) mice with eye discharge in both eyes in addition to eye closure. Lastly, respiration was scored visually (0) mice with 80-200 breaths per minute and (2) irregular breathing, or gasping marked by fewer than 80 or more rapid than 200 breaths per minute. Additive disease scores of the five criteria were assigned to each mouse after evaluation. Mice that scored an additive disease score of 5 or above among all 5 criteria, or weight loss of 20% or greater during the health assessment required immediate euthanasia. Cumulative disease scoring was calculated by adding the disease scores of each mouse from the group. Morbid mice that were euthanized during the study, before day 14, retained their disease score for the remainder of the experiment.

### **Euthanasia and tissue collection**

Challenged mice that were assigned a health score of 5 or above or reached the end of the experiment were euthanized with an IP injection of Euthasol (390mg/kg) (Pentobarbital) followed by secondary measure of euthanasia with cardiac puncture. Blood from cardiac puncture was collected in BD Microtainer gold serum separator tubes, centrifuged at 15,000 x *g* for 5 minutes and serum collected for downstream analysis. Nasal wash was acquired by pushing 1mL of PBS through the nasal pharynx. 500  $\mu$ L of nasal wash was added to 167  $\mu$ L of TRI reagent for RNA purification and the remainder of the nasal wash was frozen for serological analysis. Lungs were separated into right and left lobes. Right lobe of the lung was homogenized in 1mL of PBS in gentleMACS C tubes (order number: 130-096-334) using the m\_lung\_02 program on the gentleMACS Dissociator. 300 $\mu$ L of lung homogenate was added to 167 $\mu$ L of TRI Reagent (Zymo

research) for downstream RNA purification and 300  $\mu$ L of lung homogenate was centrifuged at 15,000  $\times g$  for 5 minutes and the lung supernatant was collected for downstream analyses. Brain was excised from the skull and separated into the right and left hemispheres. Right hemisphere was homogenized in 1mL PBS in gentleMACS C tubes using the same setting as lung on the gentleMACS Dissociator. 167 $\mu$ L of TRI Reagent was added to 500 $\mu$ L of brain homogenate for RNA purification.

### **qPCR SARS-CoV-2 viral copy number analysis of lung, brain and nasal wash**

RNA purification of the lung, brain and nasal wash was performed using the Direct-zol RNA miniprep kit (Zymo Research R2053) following the manufacturer protocol. SARS-CoV-2 copy numbers were assessed through qPCR using the Applied Biosystems TaqMan RNA to CT One Step Kit (Ref: 4392938). We utilized nucleocapsid primers (F: ATGCTGCAATCGTGCTACAA; R: GACTGCCGCCTCTGCTC); and TaqMan probe (IDT:/56-FAM/TCAAGGAAC/ZEN/AACATTGCCAA/3IABkFQ/) that were synthesized according to Winkler. *et al*, 2020 (23). The following final concentrations were used according to the Applied Biosystems TaqMan RNA to CT One Step Kit manufacturer protocol: TaqMan RT-PCR Mix 2X, Forward and reverse primers 900nM final, TaqMan probe 250nM final, TaqMan RT enzyme mix 40X and RNA template 100ng (with the exception of nasal wash). Nasal wash RNA concentrations were not quantifiable on the Qubit 3 fluorometer; therefore, we used 5.4  $\mu$ L of nasal wash RNA per reaction instead of 100ng. Triplicates were prepared for each sample, and samples were loaded into a MicroAmp Fast optical 96 well reaction plate (Applied Biosystems 4306737). Prepared reactions were run on the StepOnePlus Real-Time System machine using the parameters: Reverse transcription for 15 minutes at 48°C, activation of AmpliTaq Gold DNA polymerase for 10 minutes at 95°C, and 50 cycles of denaturing for 15 seconds at 95°C and annealing at 60°C for 1 minute.

### **Meso Scale Discovery COVID-19 ACE2 Neutralization assay**

SARS-CoV-2 challenged serum was analyzed using the SARS-CoV-2 Plate 7 Multi-Spot 96-well, 10 spot plate following the manufacturer protocol (catalog #: N05428A-1) on the MSD QuickPlex SQ120. The 10 spots contained: 1) CoV-2 Spike 2) RBD B.1.351 3) CoV-2 N 4) RBD P.1 5) BSA 6) RBD B.1.1.7 7) Spike P.1 8) Spike B.1.1.7 9) Spike B.1.351 and 10) CoV2 S1 RBD. Three dilutions of serum, 1:5, 1:50, and 1:500 was analyzed on the MSD neutralization assay for each mouse to perform Area Under the Curve analysis on the electrochemiluminescence using GraphPad Prism.

### **Cytokine analysis.**

R&D 5-plex mouse magnetic Luminex assay (Ref LXSAMSM) was used to quantify cytokines: CXCL13, TNF $\alpha$ , IL-6, IFN- $\gamma$ , and C reactive protein in the serum and lung supernatant. Manufacturer protocols were followed in preparing samples. 5 plex mouse cytokine plate was analyzed on the Luminex Magpix and pg/mL were calculated based off standard curves generated for each cytokine in the assay.

### **Histopathology**

Left lobes of lungs from each mouse in the NVC, IN and IM groups in the WA-1 challenge study were fixed in 10mL of 10% neutral buffered formalin. Fixed lungs were paraffin embedded into 5  $\mu$ m sections. Sections were stained with hematoxylin and eosin and sent to iHisto for pathological analysis. The pathologist was blinded to the experimental groups but was aware of groups that were challenged or not challenged with SARS-CoV-2. Lung samples were scored for chronic and acute inflammation in the lung parenchyma, blood vessels, and airways. Each mouse was scored individually using a standard qualitative toxicologic scoring criteria: 0-none; 1-minimal; 2-mild; 3-moderate; 4-marked; 5-severe. Chronic inflammation was denoted by presence of lymphocytes and plasma cells and acute inflammation was scored by the presence of neutrophils and edema.



### **Illumina library preparation, sequencing, and bioinformatic analysis**

RNA quantity was measured with Qubit 3.0 Fluorometer using the RNA high sensitivity (Life Technologies) and RNA integrity was assessed on an Agilent Bioanalyzer 2100 Eukaryote Total RNA Nano chip (Applied Biosystems). RNA was DNAased before library preparation. Illumina sequencing libraries were prepared with KAPA RNA HyperPrep Kit with RiboErase (Basel, Switzerland). Resulting libraries passed standard Illumina quality control PCR and were sequenced on an Illumina NovaSeq s4 4000 at Admera Health (South Plainfield, NJ). A total of 100 million 2 x 150 bp reads were acquired per sample. Sequencing data will be deposited to the Sequence Read Archive. The reads were trimmed for quality and mapped to the *Mus musculus* reference genome using CLC Genomics Version 21.0.5. An exported gene expression browser table is provided as supplemental materials Supplementary data 2. Statistical analysis was performed with the Differential Gene Expression tool and genes were annotated with the reference mouse gene ontology terms. Genes with an FDR p value of <0.05 were considered differentially regulated. Volcano plot was generated with statistically significant genes. Genes of interest were plotted in a heat map that was generated in GraphPad version 9.0. Genes that were differentially regulated were further analyzed via the online WEB-based GENE SeT AnaLysis Toolkit using over-representation analysis using the mouse enrichment category gene ontology and biological process. Heat maps were generated using Morpheus (53).

### **IgG1/IgG2c subtypes**

ELISAs were performed on the challenged serum to assay IgG1 (Novus Biologicals NB7511) and IgG2c (Novus Biologicals NBP2-68519) titers. ELISAs were coated with RBD following the same concentration and procedures mentioned above. Plates were blocked with 3% non-fat milk in PBS-0.1% Tween 20 for one hour at room temperature with shaking at 480rpm. Serum concentration (1:20) was used as above following a 10-minute incubation period. Secondary IgG1-HRP and IgG2c-HRP were used at a 1:10000 dilution in 1% non-fat milk in PBS-0.1% Tween

20 with a 10-minute incubation period. ELISAs were developed and stopped using the same protocol as above. Titers were represented as Area Under the Curve values.

### **Statistical analyses and data availability**

All statistical analyses were performed using GraphPad Prism version 9. Statistical analyses were performed with  $n \geq 8$  for K18-ACE2 mice studies challenged with WA-1,  $n \geq 3$  for K18-ACE2 mice studies challenged with Delta variant, and  $n \geq 3$  for the CD1 mice studies. Error bars represent standard deviation. Ordinary one-way ANOVA with Dunnett's multiple comparisons test or Two-Way ANOVA with Tukey's multiple comparisons test were used with single pooled variance for data sets following a normal distribution and Kruskal-Wallis with Dunn's multiple comparisons test for non-parametric distributed datasets. Kaplan-Meier survival curves were utilized, and Log-rank (Mantel-Cox) test were used to test significance of survival between sample groups. The datasets generated during and/or analyzed in this study are available from the corresponding author on reasonable request. Raw Illumina RNAseq reads were deposited on SRA at accession number PRJNA797362.

### **4.6 Acknowledgements**

This project was funded by the Vaccine Development Center at the West Virginia University Health Sciences Center. F.H.D. and the VDC are supported by the Research Challenge Grant no. HEPC.dsr.18.6 from the Division of Science and Research, WV Higher Education Policy Commission. MSD QuickPlex SQ120 in the WVU Flow Cytometry & Single Cell Core Facility is supported by the Institutional Development Awards (IDeA) from the National Institute of General Medical Sciences of the National Institutes of Health under grant numbers P30GM121322 (TME CoBRE) and P20GM103434 (INBRE). We would like to acknowledge Dr. James Denvir for sequencing the SARS-CoV-2-WA-1 strain and SARS-CoV-2 Delta variant that was used in the challenge studies. Thank you to Gaurav Deshmukh from MSD for helping design, run, and

analyze the MSD neutralization assays. We would like to acknowledge Mary Tomago-Chesney for sectioning and performing H&E staining on tissues. We would like to thank the pathologist, Dr. Christopher Gibson (iHisto) for scoring our lung H&E slides. Biorender figures throughout this manuscript was created with Biorender.com. Lastly, we thank Drs. Laura Gibson and Clay Marsh for supporting this COVID-19 vaccine research.

**Author contributions.** Studies were designed by FHD, JRB, and TYW. All authors contributed to the execution of the studies. MS prepared RBD EcoCRM<sup>®</sup> conjugation. JIG and DV facilitated in BECCs adjuvant preparation. TYW and JK vaccinated mice for both the immunogenicity studies, and the SARS-CoV-2 challenge studies. MTW and IM prepared and provided titered viral stocks of WA-1 and Delta SARS-CoV-2 for challenge. Animal health checks, necropsy, and tissue processing were performed by FHD, TYW, BRP, KSL, AMH, JRB, OAM, HAC, and MC. Viral RNA qPCR was performed by TYW, KSL, and CC. Serological analysis was executed by TYW, KSL, and NAR. MSD neutralization assays were performed by TYW and BPR. Luminex cytokine assays were completed by TYW and MAW. All authors contributed to the writing and revision of this manuscript. Data was analyzed by TYW and FHD.

**Conflicts of interest.** WVU Research Corporation has filed a patent application on nasal COVID-19 vaccines described in this study. Authors KSL, BPR, AMH, JK, MTW, MAW, NAR, OAM, MS, JI, DV, ESK, CC, MC, HAC, MB, IM and RKE declare no competing interests.

## 4.7 Figures

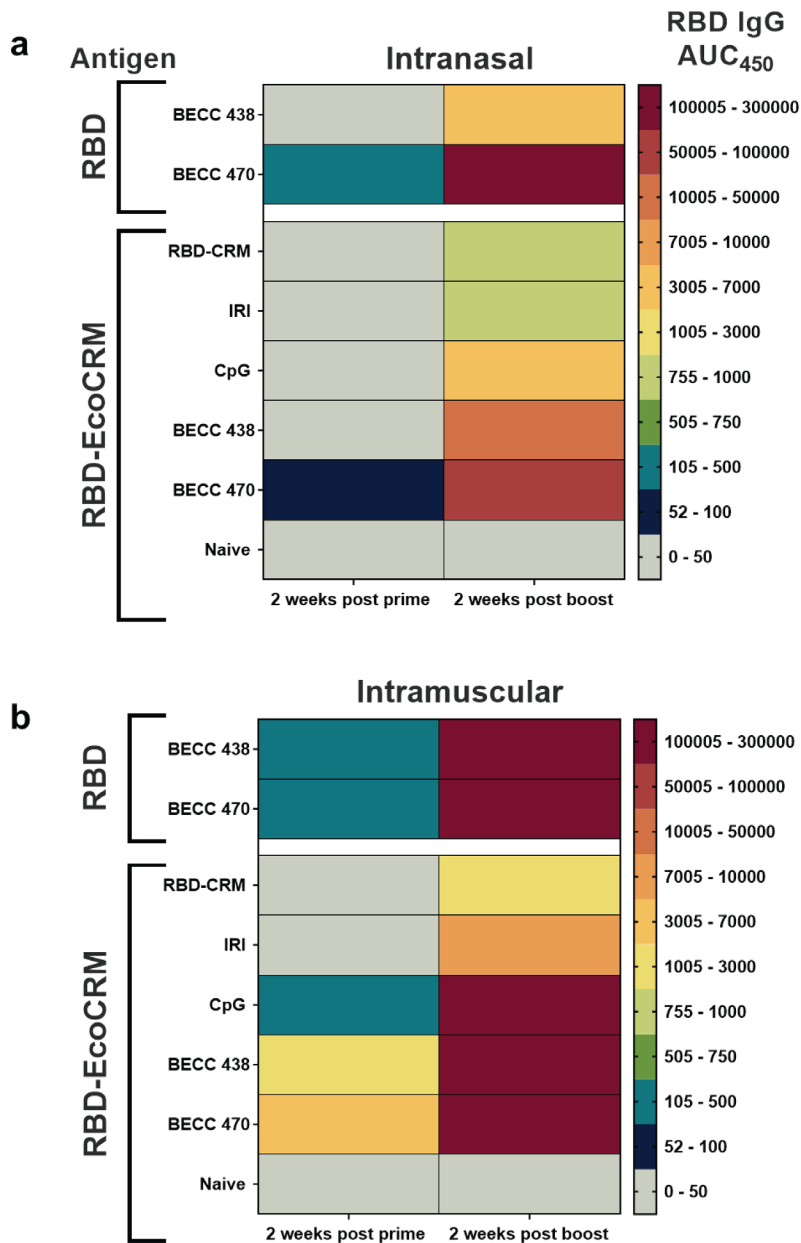


**Figure 1. Mouse immunogenicity studies to identify vaccine candidates.** 7 COVID-19 vaccine formulations were administered intranasally (A) or intramuscularly (B) in CD-1 mice in two doses. Heat map depicts the AUC<sub>450</sub> values from RBD-IgG titers at 2 weeks post prime (left) and 2 weeks post boost (right). The maximum AUC<sub>450</sub> value is set at 300,000, and the minimum is at 0.

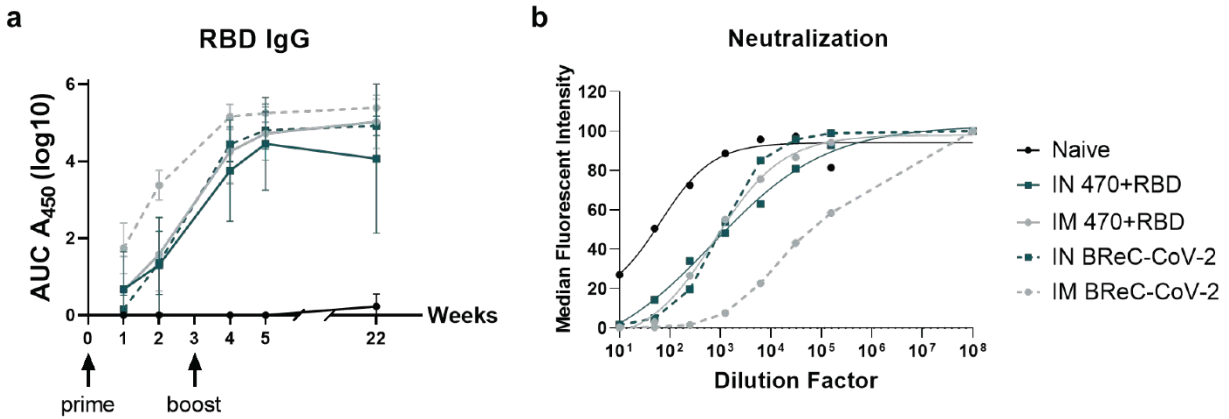


**Figure 2. Analysis of antibody responses and neutralization capacity of IN and IM BreC-CoV-2 vaccines.** CD-1 mice were IN or IM vaccinated with BECC470 with RBD or RBD-EcoCRM<sup>®</sup> in two doses. A) Serum was taken at 1 week and 2 weeks post prime, 1 week and 2 weeks post boost and 22 weeks post boost. Log<sub>10</sub> AUC<sub>450</sub> values from RBD-IgG titers are depicted for each vaccine. Results shown as mean ± SD. B) *In vitro* neutralization assay performed on the Luminex platform. Serum was obtained from 2 weeks post boost. Naïve represents the group that received no vaccine, BReC-CoV-2 denotes mice immunized with RBD-EcoCRM<sup>®</sup> adjuvanted with BECC 470, 470 represents BECC470 adjuvant, and receptor binding protein (RBD).

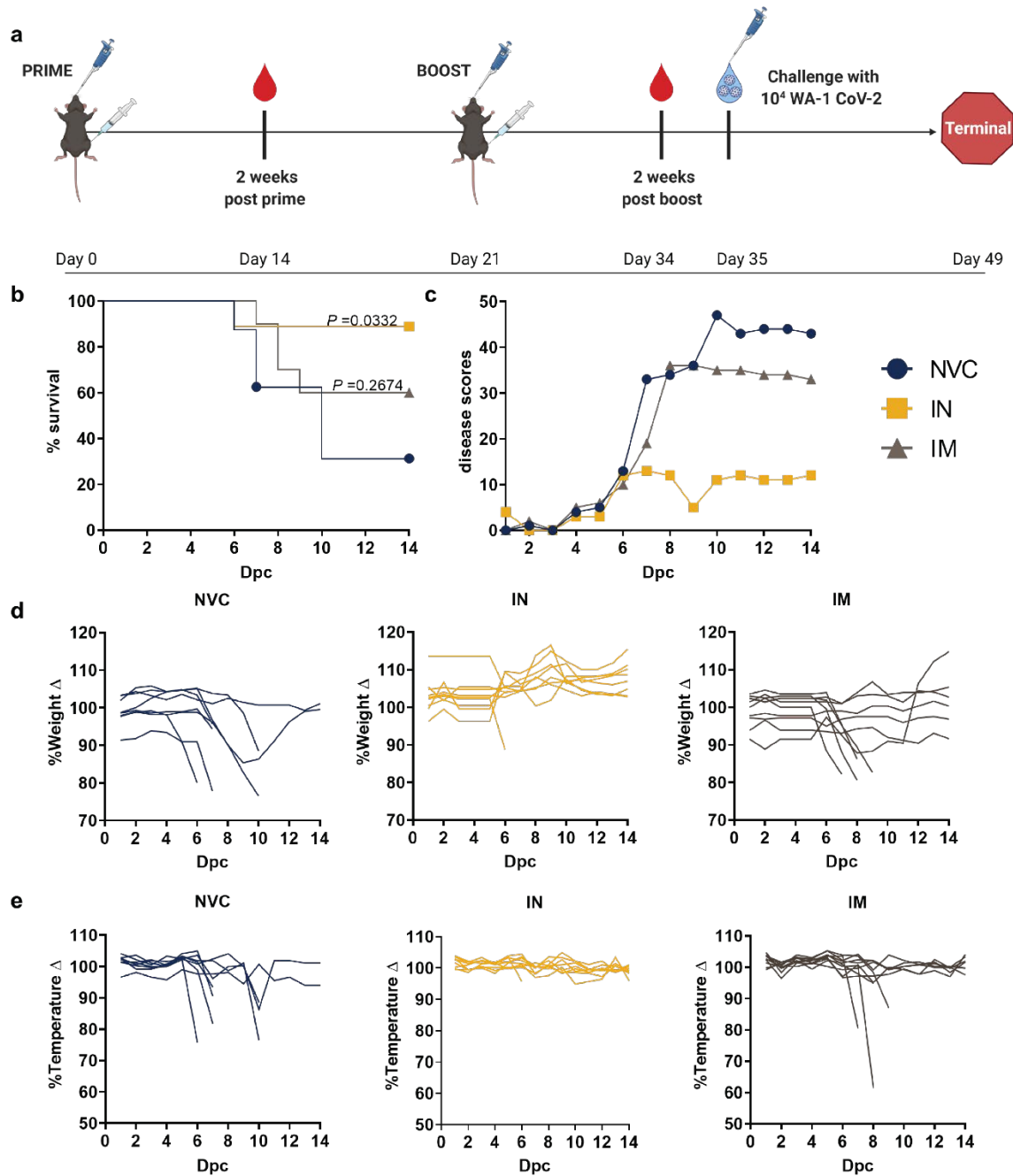


**Figure 3. Intranasal administration of BReC-CoV-2 protected mice from SARS-CoV2 challenge.** A) vaccine and challenge schematic in K18-ACE2 mice. Mice were primed and boosted with either IN or IM BReC-CoV-2, and blood for serological analysis was collected 2 weeks post prime and boost. Mice were challenged intranasally with  $10^4$  WA-1 SARS-CoV-2, and mice were monitored for 14 days post challenge. B) NVC (n=8), IN BreC-CoV-2 (n=9), and IM

BreC-CoV-2 (n=10) vaccinated animals Kaplan Meier survival curve. NVC had 31%, IN had 89%, and IM had 60% survival. Log-rank (Mantel-Cox) test were used to test significance of survival between sample groups. C) Disease scores were calculated each day for each mouse and added per group. If a mouse reached a disease score of 5 or above, the mouse was euthanized, but the score was retained downstream for disease score analysis. D) % weight change from 100% of the NVC, IN and IM groups. E) % temperature change from 100% of the NVC, IN and IM groups.

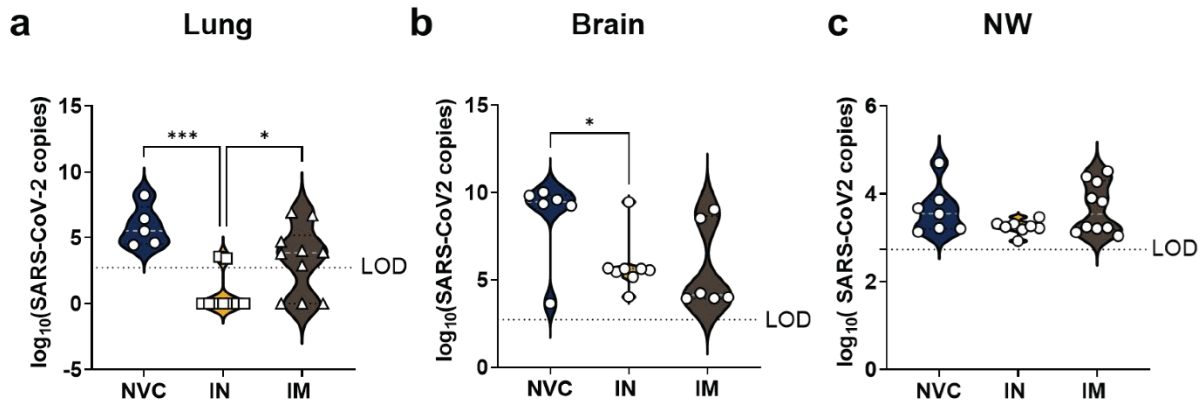


**Figure 4. Determination of viral RNA levels in challenged mice.** 100ng of lung and brain homogenate was used to perform qPCR analysis on the SARS-CoV-2 nucleocapsid RNA in the lung. A) Violin plots depicting the SARS-CoV-2 viral RNA copies in the right lobe of the lung, with white dotted line representing the median for each group plot. Ordinary one-way ANOVA with Sidak's multiple comparisons test was used to perform statistical analysis.  $P=0.0007^{***}$ , and  $P=0.0436^*$  B) Violin plots depicting the SARS-CoV-2 viral RNA copies in the left lobe of the brain, with white dotted line representing the median for each group plot. Unpaired T-test was performed for statistical analysis.  $P=0.0230^*$ . C) 500 $\mu$ L of nasal wash (NW) was assessed for qPCR quantification of viral nucleocapsid RNA. Violin plots representing the SARS-CoV-2 viral RNA copies.



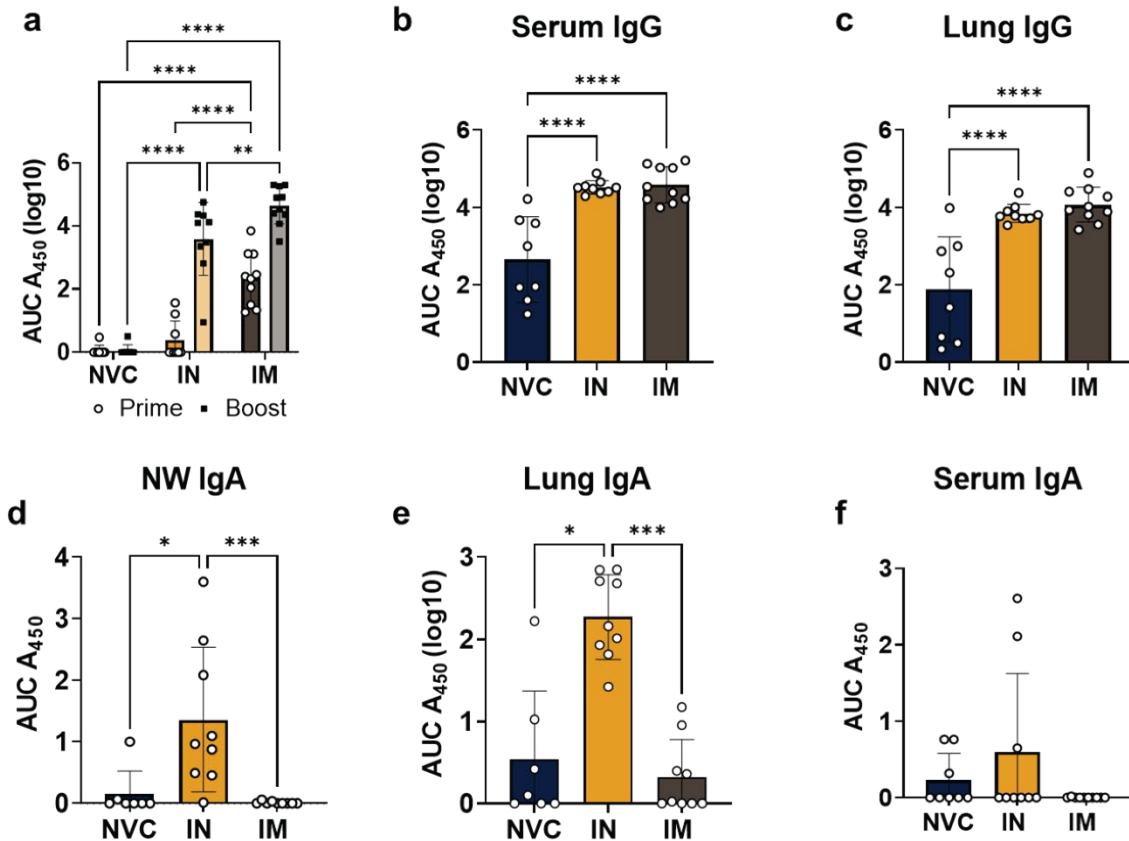


**Figure 5. Serological analysis of serum, lung, and nasal antibodies.** RBD IgG and IgA titers represented by log<sub>10</sub> AUC<sub>450</sub> values. Results represented as mean ± SD. A) Pre-challenged NVC, IN and IM RBD IgG titers at 2 weeks post prime (left column, circles) and 2 weeks post boost (right column, squares). Two-way ANOVA with Tukey's multiple comparisons test was used to determine *P* values.  $p < 0.0001$  \*\*\*\*,  $p = 0.0051$  \*\* B) Serum RBD-IgG titers post challenge. One way ANOVA performed for statistical analysis with Tukey's multiple comparisons test.  $p < 0.0001$  \*\*\*\* C) Lung supernatant RBD-IgG titers post challenge. One way ANOVA performed for statistical analysis with Tukey's multiple comparisons test.  $p < 0.0001$  \*\*\*\* D) NW RBD-IgA titers post challenge. Kruskal-Wallis test with Dunn's multiple comparisons test performed for statistical analysis.  $P = 0.0009$ \*\*\*,  $p < 0.0108$  \* E) Lung supernatant RBD-IgG titers post challenge. Kruskal-Wallis test with Dunn's multiple comparisons test performed for statistical analysis.  $P = 0.0009$ \*\*\*,  $P = 0.0129$ \* F) Serum RBD-IgA titers post challenge.

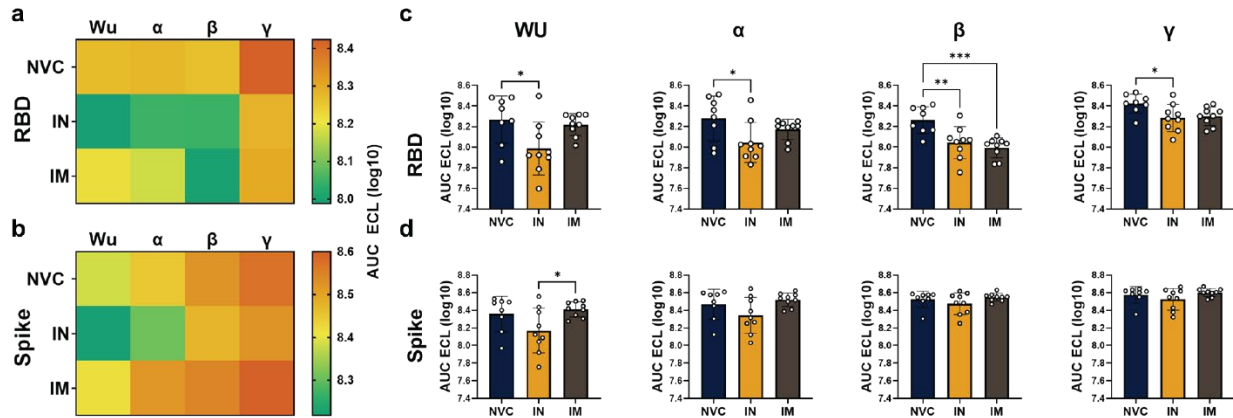


**Figure 6. Analysis of RBD-ACE2 neutralization capacity of serum.** MSD neutralization assay with RBD and Spike of the variants of concern with ACE2 was performed. All values are represented by the log10 AUC of the electrochemiluminescence emitted from the MSD plate reader. A) Heat map depicts the neutralization capacity of challenged serum of NVC, IN and IM groups against the RBD of different strains of SARS-CoV-2 (Wuhan, Alpha, Beta, and Gamma). B) Heat map depicts the neutralization capacity of challenged serum of NVC, IN and IM group against the Spike of different strains of SARS-CoV-2 (Wuhan, Alpha, Beta, and Gamma). C-D) Individual values of the neutralization capacity of RBD from the heat map of RBD and spike represented by the log10 AUC of ECL. Results represented as mean  $\pm$  SD. Two-way ANOVA with Tukey's multiple comparisons test performed for statistical analysis.  $P=0.0261^*$  (RBD-Wu),  $P=0.0322^*$  (RBD-Alpha),  $P=0.0062^{**}$ ,  $P=0.0009^{***}$ (RBD-Beta)  $P=0.0361^*$  (RBD-Gamma),  $P=0.0376^*$  (Spike-Wu).

**a Pre-challenge serum**   **b Challenged serum**

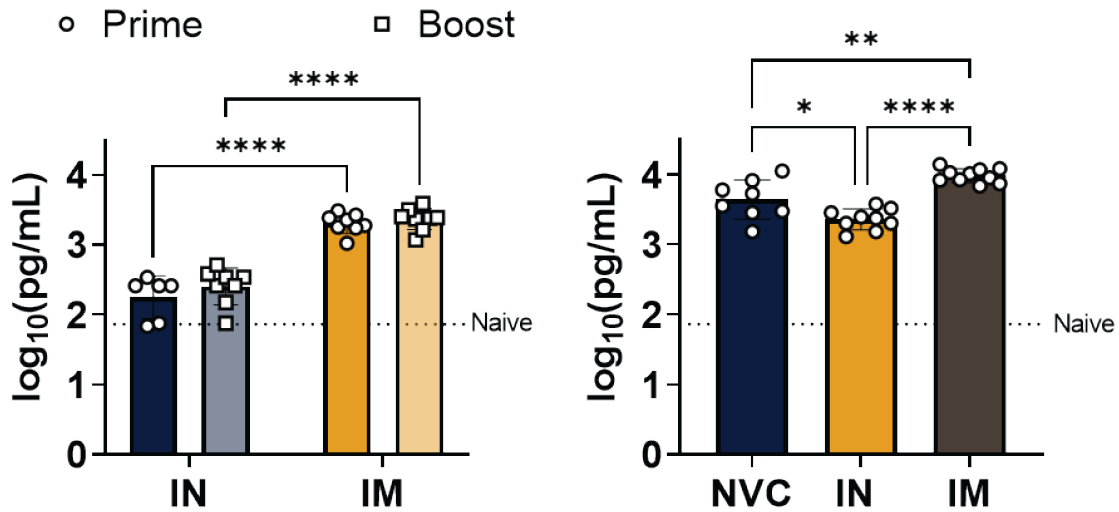


**Figure 7. Analysis of CXCL13 in serum or lungs in relation to immunization.** A) CXCL13 (log<sub>10</sub> pg/mL) in pre-challenged serum. Two-way ANOVA with Sidak's multiple comparisons test was performed for statistical analysis.  $P < 0.0001$  \*\*\*\*. Naïve baseline represented as dotted line at 1.861183. B) Post challenged CXCL13 levels in the serum. Ordinary one-way ANOVA with Tukey's multiple comparisons test was performed for statistical analysis.  $P = 0.0112^*$ ,  $P = 0.0018^{**}$ , and  $P < 0.0001^{****}$ . All results represented as mean  $\pm$  SD.

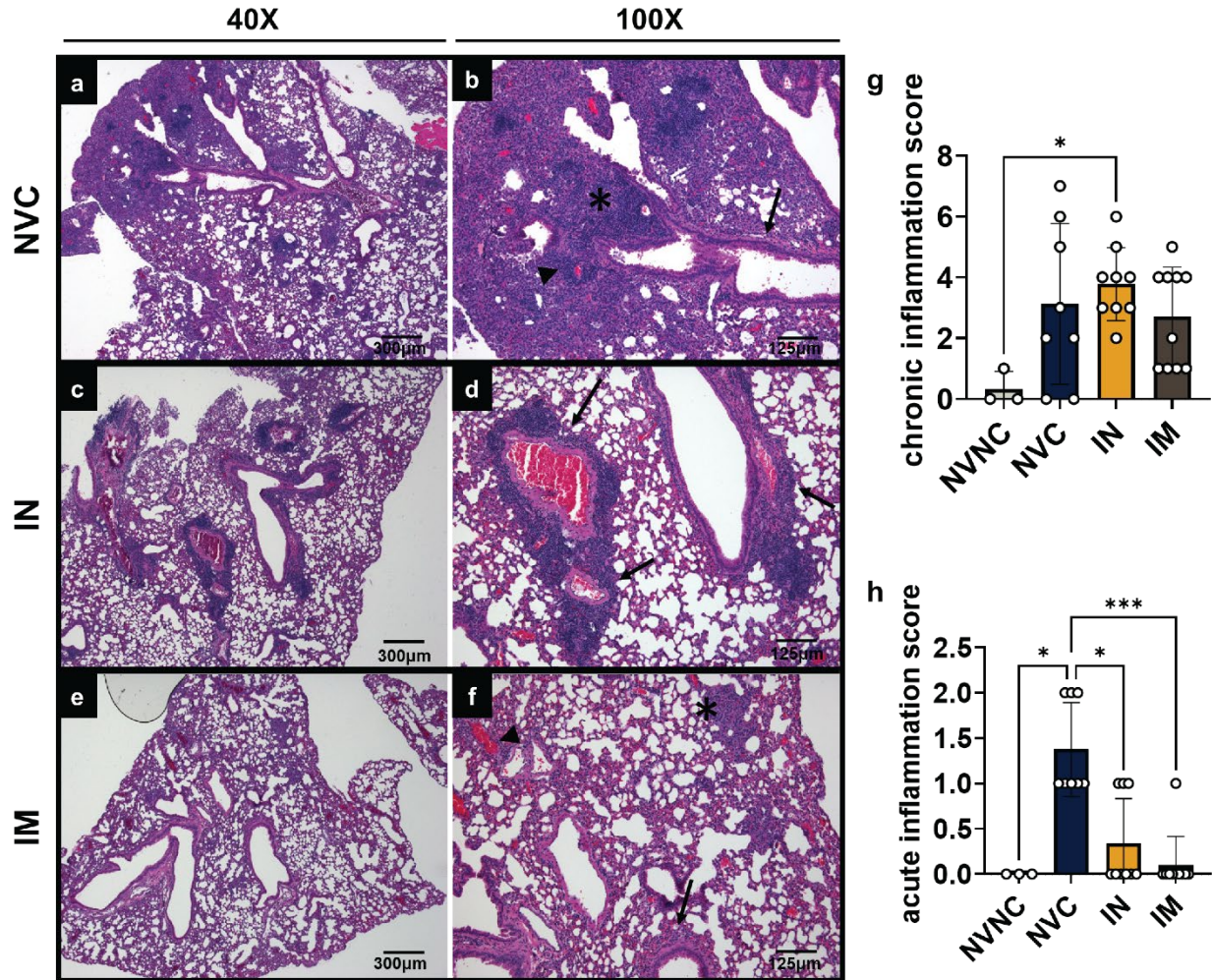


**Figure 8. Histopathological analysis of naïve or vaccinated mice challenged with SARS-CoV-2.** A) 40X magnification of the lung of NVC (scale bar = 300µm) B) 100X magnification of 8A. Inflammation in the parenchyma is denoted by the asterisk, inflammation surrounding the blood vessel is marked by an arrowhead, and inflammation in the airways are denoted by an arrow (scale bar = 125µm). C) 40X magnification of the lung of the IN BReC-CoV-2 vaccinated representative mouse (scale bar = 300µm). D) 100X magnification of 8C. Arrows show inflammation in the airways (scale bar = 125µm). E) 40X magnification of the lung of the IM BReC-CoV-2 vaccinated representative mouse (scale bar = 300µm). F) inflammation in the parenchyma is denoted by the asterisk, surrounding the blood vessels marked by an arrowhead and inflammation in the airways represented by arrows (scale bar = 125µm). G) Chronic inflammation

scores of each mouse. H) Acute inflammation score of each mouse. Results represented as mean  $\pm$  SD. All statistical analysis was performed using Kruskal-Wallis test with Dunn's multiple comparisons test.  $P=0.0449^*$  (chronic);  $P=0.0143$ ,  $0.150^*$ ,  $0.0004^{***}$  (acute).

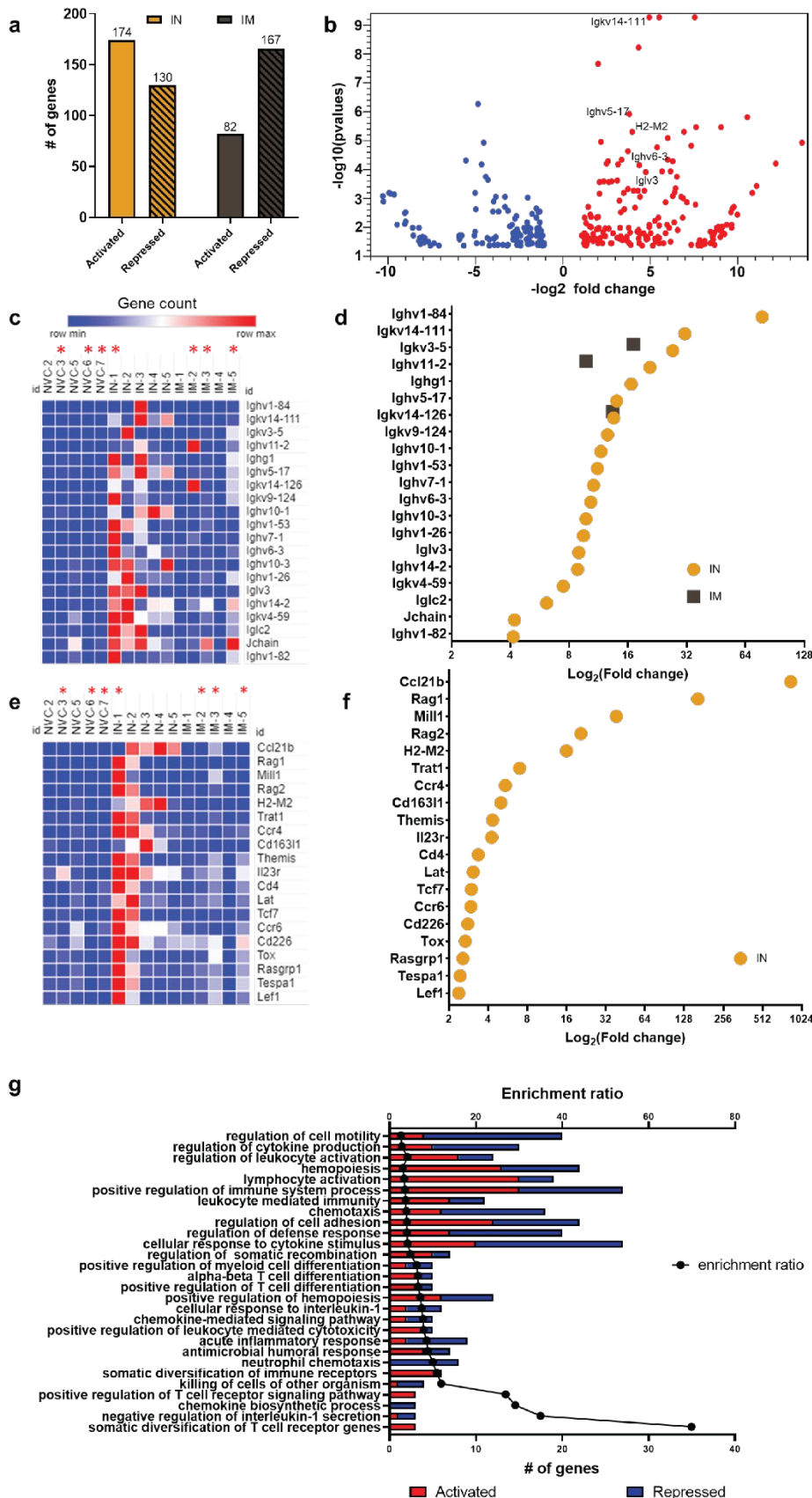


**Figure 9. RNAseq analysis reveals IN BReC-CoV-2 vaccination results in unique gene expression signatures enriched for T cell responses.** All analyses were performed on CLC genomics workbench 21. A) Number of significant (FDR  $p < 0.05$ ) activated and repressed genes in IN BReC-CoV-2 and IM BReC-CoV-2 groups. B) Volcano plot indicating significant gene expression profile of IN BReC-CoV-2 compared to NVC. Red circles denote upregulated genes and blue circles represent down regulated genes. C) Heat maps were generated by Morpheus. Heat map represents gene counts of immunoglobulin genes in each mouse lung. D) Significant fold changes of the immunoglobulin genes of interests in both IN and IM BReC-CoV-2 groups. E) Heat maps were generated by Morpheus. Heat map represents gene counts of adaptive immune response genes of interest in the mouse lung. F) Significant fold changes of adaptive immune response genes in both IN and IM groups. IM BReC-CoV-2 did not have significant fold changes. Red asterisks next to the sample ID indicate mouse morbidity before the termination of the study. NVC3 and N1 euthanized on day 6, IM5 euthanized on day 7, IM3 euthanized on day 8, IM2 euthanized on day 9, and NVC6 and 7 euthanized on day 10. G) Gene set enrichment analysis of IN BReC-CoV-2 compared to NVC was performed on WEB-based Gene SeT AnaLysis Toolkit. Enrichment ratio of significant GO-terms compared to the number of genes in each enriched gene set. Red represents activated genes and blue represents repressed genes.



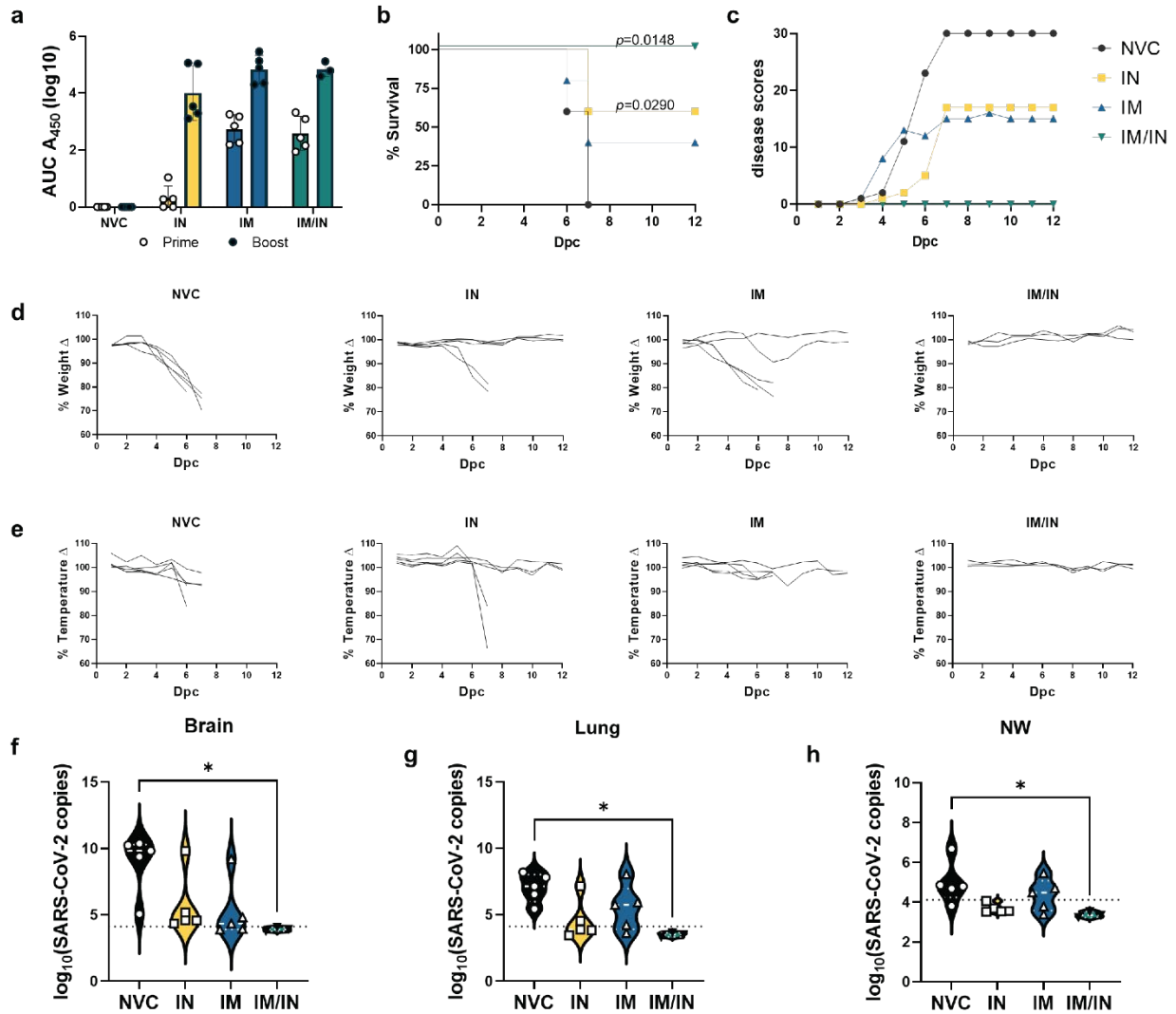


**Figure 10. IM BReC-CoV-2 prime followed by IN boost afforded protection against SARS-CoV-2 Delta variant challenge.** A) Serological analysis of 2 weeks post prime and boost of RBD IgG titers. Boost time points RB were significant compared to prime. RBD IgG titers represented by log<sub>10</sub> AUC<sub>450</sub> values. B) Kaplan Meier survival curve of BReC-CoV-2 vaccinated mice. Mantel-Cox test used to calculate significance between IN, IM and IM/IN BReC-CoV-2 compared to NVC. C) Cumulative disease scores of NVC, IN, IM, and IM/IN throughout 12-day course of study. D) % Weight change of NVC, IN, IM, and IM/IN BReC-CoV-2. E) % temperature change of NVC, IN, IM, and IM/IN BReC-CoV-2. F) Violin plots depicting the SARS-CoV-2 viral RNA copies in the brain, with white dotted line representing the median for each group plot. G) Violin plots



depicting the SARS-CoV-2 viral RNA copies in the right lobe of the lung, with white dotted line representing the median for each group plot. H) 500 $\mu$ L of nasal wash (NW) was assessed for qPCR quantification of viral nucleocapsid RNA. Violin plots representing the SARS-CoV-2 viral RNA copies. Ordinary One-way ANOVA with Tukey's multiple comparisons test was performed on the brain ( $P=0.0236$  \*), lung ( $P=0.0144$ \*) and NW ( $P=0.0391$ \*)).




















#### 4.7 Supplementary Figures

Vaccine route	SARS-CoV-2 antigen	Adjuvant
IN	RBD	BECC 438
IN	RBD	BECC 470
IN	RBD-EcoCRM	no adjuvant
IN	RBD-EcoCRM	IRI
IN	RBD-EcoCRM	CpG
IN	RBD-EcoCRM	BECC 438
IN	RBD-EcoCRM	BECC 470
IM	RBD	BECC 438
IM	RBD	BECC 470
IM	RBD-EcoCRM	no adjuvant
IM	RBD-EcoCRM	IRI
IM	RBD-EcoCRM	CpG
IM	RBD-EcoCRM	BECC 438
IM	RBD-EcoCRM	BECC 470

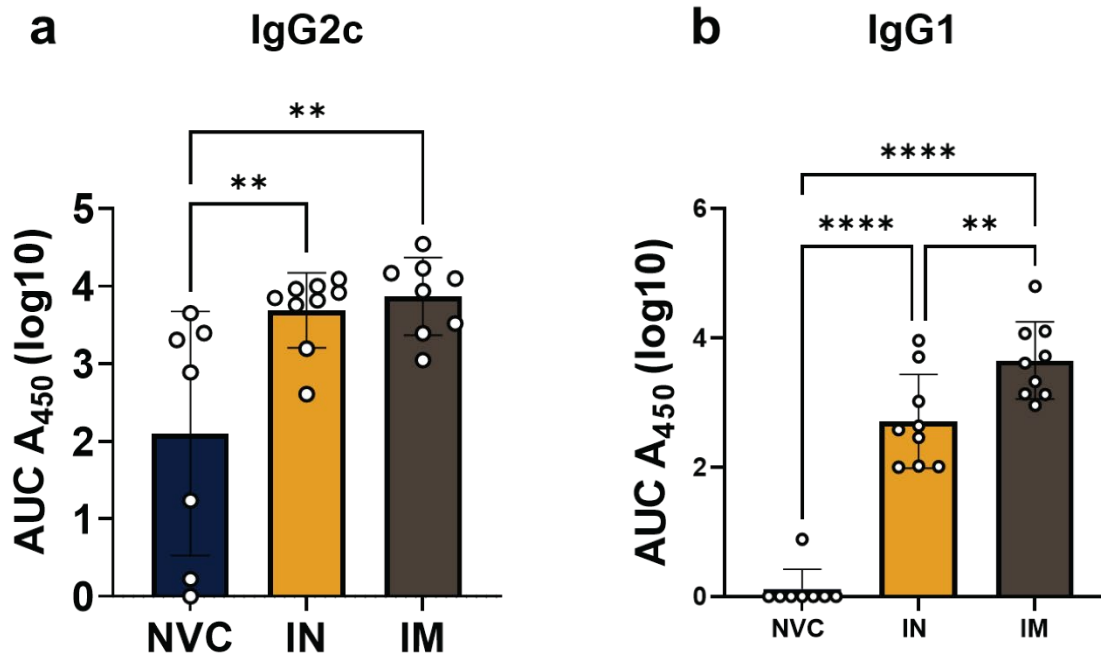
**Supplementary Table 1. COVID-19 vaccine formulations and routes for CD1 immunogenicity studies.** 7 different COVID-19 vaccine formulations and administered routes used in CD-1 mice immunogenicity studies.

Groups	Weeks	Summary	Adjusted P value
Naive vs. IM BReC-CoV-2	1	*	0.0186
IN 470+RBD-CRM vs. IM 470+RBD-CRM	1	*	0.0168
Naive vs. IM BReC-CoV-2	2	***	0.0002
IN BReC-CoV-2vs. IM BReC-CoV-2	2	*	0.016
Naive vs. IN 470+RBD	4	*	0.0142
Naive vs. IM 470+RBD	4	**	0.0016
Naive vs. IN BReC-CoV-2	4	***	0.0002
Naive vs. IM BReC-CoV-2	4	****	<0.0001
Naive vs. IN 470+RBD	5	**	0.0056
Naive vs. IM 470+RBD	5	***	0.0005
Naive vs. IN BReC-CoV-2	5	***	0.0001
Naive vs. IM BReC-CoV-2	5	****	<0.0001
Naive vs. IN 470+RBD	22	*	0.0485
Naive vs. IM 470+RBD	22	****	<0.0001
Naive vs. IN BReC-CoV-2	22	****	<0.0001
Naive vs. IM BReC-CoV-2	22	****	<0.0001

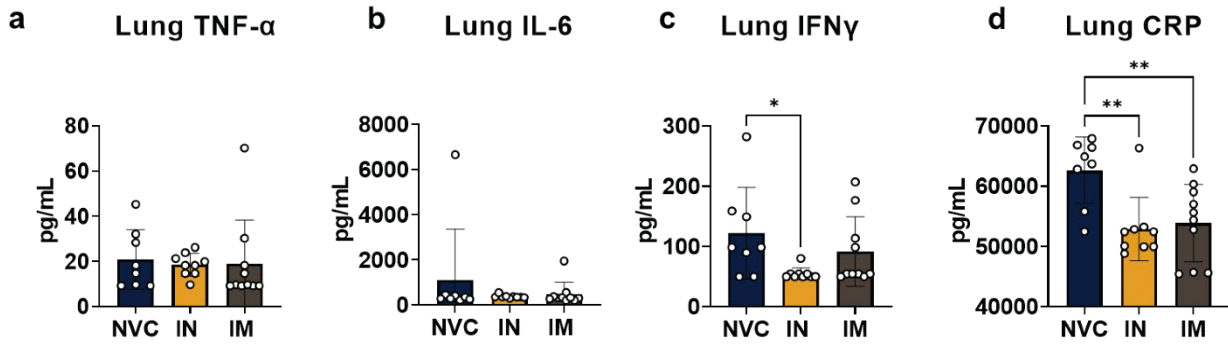
**Supplementary Table 2. Statistical analysis of RBD IgG titers in CD1 mice vaccinated with BREC-CoV-2 or RBD + BECC470 (figure 2).** Two-way ANOVA with Tukey's multiple comparisons test was performed on the RBD IgG titers represented in AUC values on week 1, 2, 4 5 and 22 weeks.

<b>Weight loss (0-5)</b> 	<div style="display: flex; justify-content: space-around; align-items: center;"> <div style="text-align: center;">0 </div> <div style="text-align: center;">1</div> <div style="text-align: center;">2</div> <div style="text-align: center;">3</div> <div style="text-align: center;">4</div> <div style="text-align: center;">5 </div> <div style="border: 1px solid black; padding: 5px; margin-left: 20px;">20% weight loss</div> </div>
<b>Appearance (0-2)</b> 	<div style="display: flex; justify-content: space-around; align-items: center;"> <div style="text-align: center;">0 </div> <div style="text-align: center;">1 </div> <div style="text-align: center;">2 </div> </div>
<b>Activity (0-3)</b> 	<div style="display: flex; justify-content: space-around; align-items: center;"> <div style="text-align: center;">0 </div> <div style="text-align: center;">1 </div> <div style="text-align: center;">2 </div> <div style="text-align: center;">3 </div> </div>
<b>Eye closure (0-2)</b>  	<div style="display: flex; justify-content: space-around; align-items: center;"> <div style="text-align: center;">0 </div> <div style="text-align: center;">1 </div> <div style="text-align: center;">2 </div> </div>
<b>Respiration (0-2)</b> 	<div style="display: flex; justify-content: space-around; align-items: center;"> <div style="text-align: center;">0 80-200 breaths per minute</div> <div style="text-align: center;">1</div> <div style="text-align: center;">2  fewer than 80 bpm/gasping</div> </div>

**Supplementary Figure 1.** Disease scoring schematic. 5 categories of disease manifestations that are observed daily. Symptoms in each category are scored from 0 being no symptoms to the highest number being the worst symptoms. All scores from each category are added up for each mouse, and if a mouse scores a 5 or above, the mouse will be humanely euthanized.



**Supplementary Figure 2.** BReC-CoV-2 vaccination demonstrated a balanced Th1/Th2 response. A) Serum IgG2c represented by log<sub>10</sub> AUC<sub>450</sub> in challenged mice. B) Serum IgG1 represented by log<sub>10</sub> AUC<sub>450</sub> in challenged mice. Results represented as mean ± SD. Ordinary one-way ANOVA with Tukey's multiple comparisons test was performed for statistical analyses.  $P=0.0047^{**}$  (IgG2c) and  $P<0.0001^{****}$  and  $P=0.0063^{**}$  (IgG1).



**Supplementary Figure 3. IN BReC-CoV-2 decreased IFN $\gamma$  in the lung.** A) TNF- $\alpha$  (pg/mL) in the lung supernatant. B) IL-6 measured in the lung supernatant. C) IFN $\gamma$  measured in the lung supernatant. Ordinary one-way ANOVA with Dunnett's multiple comparisons test was used for statistical analysis.  $P=0.0325^*$ . D) CRP measured in the lung supernatant. Results represented as mean  $\pm$  SD. Ordinary one-way ANOVA with Dunnett's multiple comparisons test was used for statistical analysis  $P=0.0041$  (NVC vs. IN) and  $P=0.0078$  (NVC vs. IM).

## 4.8 References

1. COVID-19 Vaccine and Therapeutic Drugs Tracker [Internet]. [cited 2021 Aug 8]. Available from: <https://biorender.com/covid-vaccine-tracker>
2. Ritchie H, Ortiz-Ospina E, Beltekian D, Mathieu E, Hasell J, Macdonald B, et al. Coronavirus Pandemic (COVID-19). Our World Data [Internet]. 2020 Mar 5 [cited 2021 Aug 8]; Available from: <https://ourworldindata.org/coronavirus>
3. Krammer F. SARS-CoV-2 vaccines in development. *Nat* 2020 5867830 [Internet]. 2020 Sep 23 [cited 2021 Jul 20];586(7830):516–27. Available from: <https://www.nature.com/articles/s41586-020-2798-3>
4. Chavda VP, Vora LK, Pandya AK, Patravale VB. Intranasal vaccines for SARS-CoV-2: From challenges to potential in COVID-19 management. *Drug Discov Today*. 2021 Nov 1;26(11):2619–36.
5. Vogel AB, Kanevsky I, Che Y, Swanson KA, Muik A, Vormehr M, et al. A prefusion SARS-CoV-2 spike RNA vaccine is highly immunogenic and prevents lung infection in non-human primates. *bioRxiv* [Internet]. 2020 Sep 8 [cited 2021 Sep 7];2020.09.08.280818. Available from: <https://www.biorxiv.org/content/10.1101/2020.09.08.280818v1>
6. Bachmann MF, Jennings GT. Vaccine delivery: a matter of size, geometry, kinetics and molecular patterns. *Nat Publ Gr* [Internet]. 2010 [cited 2021 Sep 10]; Available from: [www.nature.com/reviews/immunol](http://www.nature.com/reviews/immunol)
7. Heath PT, Galiza EP, Baxter DN, Boffito M, Browne D, Burns F, et al. Safety and Efficacy of NVX-CoV2373 Covid-19 Vaccine. <https://doi.org/10.1056/NEJMoa2107659> [Internet]. 2021 Jun 30 [cited 2021 Sep 14]; Available from: <https://www.nejm.org/doi/full/10.1056/NEJMoa2107659>
8. | Australian Clinical Trials [Internet]. [cited 2021 Sep 14]. Available from: <https://www.australianclinicaltrials.gov.au/anzctr/trial/ACTRN12620000817943>
9. Hickey JM, Toprani VM, Kaur K, Mishra RPN, Goel A, Oganesyanyan N, et al. Analytical

- Comparability Assessments of 5 Recombinant CRM197 Proteins From Different Manufacturers and Expression Systems. *J Pharm Sci*. 2018 Jul 1;107(7):1806–19.
10. MJ D, GL P. Pneumococcal conjugate vaccine (Pneumovax; PNCRM7): a review of its use in the prevention of *Streptococcus pneumoniae* infection. *Paediatr Drugs* [Internet]. 2002 [cited 2021 Aug 3];4(9):609–30. Available from: <https://pubmed.ncbi.nlm.nih.gov/12175274/>
  11. KK K, CL K, NS G, HL K, JR S. Immunization with Haemophilus influenzae type b-CRM(197) conjugate vaccine elicits a mixed Th1 and Th2 CD(4+) T cell cytokine response that correlates with the isotype of antipolysaccharide antibody. *J Infect Dis* [Internet]. 2001 [cited 2021 Aug 8];184(7):931–5. Available from: <https://pubmed.ncbi.nlm.nih.gov/11528593/>
  12. B C, L D, J S. Menveo®: a novel quadrivalent meningococcal CRM197 conjugate vaccine against serogroups A, C, W-135 and Y. *Expert Rev Vaccines* [Internet]. 2011 Jan [cited 2021 Aug 3];10(1):21–33. Available from: <https://pubmed.ncbi.nlm.nih.gov/21162617/>
  13. M B, P C, L D, ED M, R R. Biochemical and biological characteristics of cross-reacting material 197 CRM197, a non-toxic mutant of diphtheria toxin: use as a conjugation protein in vaccines and other potential clinical applications. *Biologicals* [Internet]. 2011 Jul [cited 2021 Aug 10];39(4):195–204. Available from: <https://pubmed.ncbi.nlm.nih.gov/21715186/>
  14. PV S, BB C, CG R, N A, OV M, EK B, et al. Comparison of carrier proteins to conjugate malaria transmission blocking vaccine antigens, Pfs25 and Pfs230. *Vaccine* [Internet]. 2020 Jul 22 [cited 2021 Aug 10];38(34):5480–9. Available from: <https://pubmed.ncbi.nlm.nih.gov/32600913/>
  15. Ou L, Kong W-P, Chuang G-Y, Ghosh M, Gulla K, O'Dell S, et al. Preclinical Development of a Fusion Peptide Conjugate as an HIV Vaccine Immunogen. *Sci Reports* 2020 101 [Internet]. 2020 Feb 20 [cited 2021 Aug 10];10(1):1–13. Available from: <https://www.nature.com/articles/s41598-020-59711-y>



16. Sette A, Crotty S. Adaptive immunity to SARS-CoV-2 and COVID-19. *Cell*. 2021 Feb 18;184(4):861–80.
17. Gregg KA, Harberts E, Gardner FM, Pelletier MR, Cayatte C, Yu L, et al. Rationally Designed TLR4 Ligands for Vaccine Adjuvant Discovery. *MBio* [Internet]. 2017 May 1 [cited 2021 Jul 20];8(3). Available from: [/pmc/articles/PMC5424205/](#)
18. Gregg KA, Harberts E, Gardner FM, Pelletier MR, Cayatte C, Yu L, et al. A lipid A-based TLR4 mimetic effectively adjuvants a *Yersinia pestis* rF-V1 subunit vaccine in a murine challenge model. *Vaccine* [Internet]. 2018 Jun 27 [cited 2021 Sep 14];36(28):4023. Available from: [/pmc/articles/PMC6057149/](#)
19. Robert E. Haupt, Erin M. Harberts, Robert J. Kitz, Shirin Strohmeier, Florian Krammer, Robert K. Ernst and MBF. Novel TLR4 Adjuvant Elicits Protection Against Homologous and Heterologous Influenza Infection. *Vaccine*. 2021;
20. McCray PB, Pewe L, Wohlford-Lenane C, Hickey M, Manzel L, Shi L, et al. Lethal Infection of K18-hACE2 Mice Infected with Severe Acute Respiratory Syndrome Coronavirus. *J Virol*. 2007 Jan 15;81(2):813–21.
21. JZ, LR W, K L, AK V, ME O, C W-L, et al. COVID-19 treatments and pathogenesis including anosmia in K18-hACE2 mice. *Nature* [Internet]. 2021 Jan 28 [cited 2021 Jul 20];589(7843):603–7. Available from: <https://pubmed.ncbi.nlm.nih.gov/33166988/>
22. FS O, JG P, PA P, O G, A A, A A-G, et al. Lethality of SARS-CoV-2 infection in K18 human angiotensin-converting enzyme 2 transgenic mice. *Nat Commun* [Internet]. 2020 Dec 1 [cited 2021 Aug 8];11(1). Available from: <https://pubmed.ncbi.nlm.nih.gov/33257679/>
23. Winkler ES, Bailey AL, Kafai NM, Nair S, McCune BT, Yu J, et al. SARS-CoV-2 infection of human ACE2-transgenic mice causes severe lung inflammation and impaired function. *Nat Immunol* 2020 2111 [Internet]. 2020 Aug 24 [cited 2021 Aug 8];21(11):1327–35. Available from: <https://www.nature.com/articles/s41590-020-0778-2>
24. R R, S S, F A, VL G, F K, A G-S, et al. Comparison of transgenic and adenovirus hACE2

- mouse models for SARS-CoV-2 infection. *Emerg Microbes Infect* [Internet]. 2020 [cited 2021 Aug 8];9(1):2433–45. Available from: <https://pubmed.ncbi.nlm.nih.gov/33073694/>
25. Muñoz-Fontela C, Dowling WE, Funnell SGP, Gsell P-S, Riveros-Balta AX, Albrecht RA, et al. Animal models for COVID-19. *Nat* 2020 5867830 [Internet]. 2020 Sep 23 [cited 2021 Jul 31];586(7830):509–15. Available from: <https://www.nature.com/articles/s41586-020-2787-6>
  26. Oganessian N, Lees A. *Expression and Purification of CRM197 and Related Proteins*. US; 10093704, 2018.
  27. Kumari P, Rothan HA, Natekar JP, Stone S, Pathak H, Strate PG, et al. Neuroinvasion and Encephalitis Following Intranasal Inoculation of SARS-CoV-2 in K18-hACE2 Mice. *Viruses* [Internet]. 2021 Jan 1 [cited 2021 Aug 11];13(1). Available from: </pmc/articles/PMC7832889/>
  28. Yinda CK, Port JR, Bushmaker T, Owusu IO, Purushotham JN, Avanzato VA, et al. K18-hACE2 mice develop respiratory disease resembling severe COVID-19. *PLOS Pathog* [Internet]. 2021 Jan 19 [cited 2021 Aug 11];17(1):e1009195. Available from: <https://journals.plos.org/plospathogens/article?id=10.1371/journal.ppat.1009195>
  29. AM H, T K, BP R, MA D, MA W, JM K, et al. Interplay of Antibody and Cytokine Production Reveals CXCL13 as a Potential Novel Biomarker of Lethal SARS-CoV-2 Infection. *mSphere* [Internet]. 2021 Feb 24 [cited 2021 Aug 8];6(1). Available from: <https://pubmed.ncbi.nlm.nih.gov/33472985/>
  30. Perreau M, Suffiotti M, Marques-Vidal P, Wiedemann A, Levy Y, Laouénan C, et al. The cytokines HGF and CXCL13 predict the severity and the mortality in COVID-19 patients. *Nat Commun* 2021 121 [Internet]. 2021 Aug 9 [cited 2021 Sep 9];12(1):1–10. Available from: <https://www.nature.com/articles/s41467-021-25191-5>
  31. Kim Y-M, Shin E-C. Type I and III interferon responses in SARS-CoV-2 infection. *Exp Mol Med* 2021 535 [Internet]. 2021 May 6 [cited 2021 Aug 8];53(5):750–60. Available from:

<https://www.nature.com/articles/s12276-021-00592-0>

32. McCallum M, Walls AC, Sprouse KR, Bowen JE, Rosen LE, Dang H V, et al. Molecular basis of immune evasion by the Delta and Kappa SARS-CoV-2 variants. *Science* [Internet]. 2021 Nov 9 [cited 2021 Dec 16];eabl8506. Available from: <http://www.ncbi.nlm.nih.gov/pubmed/34751595>
33. Saito A, Irie T, Suzuki R, Maemura T, Nasser H, Uriu K, et al. Enhanced fusogenicity and pathogenicity of SARS-CoV-2 Delta P681R mutation. *Nat* 2021 [Internet]. 2021 Nov 25 [cited 2021 Dec 16];1–10. Available from: <https://www.nature.com/articles/s41586-021-04266-9>
34. Mlcochova P, Kemp S, Dhar MS, Papa G, Meng B, Ferreira IATM, et al. SARS-CoV-2 B.1.617.2 Delta variant replication and immune evasion. *Nat* 2021 5997883 [Internet]. 2021 Sep 6 [cited 2021 Dec 16];599(7883):114–9. Available from: <https://www.nature.com/articles/s41586-021-03944-y>
35. Kulkarni PS, Raut SK, Dhere RM. A post-marketing surveillance study of a human live-virus pandemic influenza A (H1N1) vaccine (Nasovac®) in India. *Hum Vaccin Immunother* [Internet]. 2013 Jan [cited 2021 Jul 31];9(1):122. Available from: </pmc/articles/PMC3667925/>
36. Hassan AO, Kafai NM, Dmitriev IP, Fremont DH, Curiel DT, Diamond MS. A Single-Dose Intranasal ChAd Vaccine Protects Upper and Lower Respiratory Tracts against SARS-CoV-2. 2020 [cited 2021 Jul 31]; Available from: <https://doi.org/10.1016/j.cell.2020.08.026>
37. Hassan AO, Shrihari S, Gorman MJ, Ying B, Yaun D, Raju S, et al. An intranasal vaccine durably protects against SARS-CoV-2 variants in mice. *Cell Rep* [Internet]. 2021 Jul 27 [cited 2021 Jul 31];36(4):109452. Available from: <https://linkinghub.elsevier.com/retrieve/pii/S221112472100869X>
38. King RG, Silva-Sanchez A, Peel JN, Botta D, Dickson AM, Pinto AK, et al. Single-Dose Intranasal Administration of AdCOVID Elicits Systemic and Mucosal Immunity against

- SARS-CoV-2 and Fully Protects Mice from Lethal Challenge. *Vaccines* 2021, Vol 9, Page 881 [Internet]. 2021 Aug 9 [cited 2021 Aug 10];9(8):881. Available from: <https://www.mdpi.com/2076-393X/9/8/881/htm>
39. Tiboni M, Casettari L, Illum L. Nasal vaccination against SARS-CoV-2: Synergistic or alternative to intramuscular vaccines? *Int J Pharm* [Internet]. 2021 Jun 15 [cited 2021 Aug 10];603:120686. Available from: </pmc/articles/PMC8099545/>
  40. X A, M M-P, A R, M F, S S, S B, et al. Single-dose intranasal vaccination elicits systemic and mucosal immunity against SARS-CoV-2. *bioRxiv Prepr Serv Biol* [Internet]. 2020 [cited 2021 Aug 10]; Available from: <https://pubmed.ncbi.nlm.nih.gov/32743568/>
  41. Park J-G, Oladunni FS, Rohaim MA, Whittingham-Dowd J, Tollitt J, Hodges MDJ, et al. Immunogenicity and Protective Efficacy of an Intranasal Live-attenuated Vaccine Against SARS-CoV-2. *iScience* [Internet]. 2021 Aug 4 [cited 2021 Aug 11];102941. Available from: <https://linkinghub.elsevier.com/retrieve/pii/S2589004221009093>
  42. Oganessian N, Lees A. Expression and Purification of CRM197 and Related Proteins. USA; 10597664, 2020. p. 1–30.
  43. Song E, Zhang C, Israelow B, Lu-Culligan A, Prado AV, Skriabine S, et al. Neuroinvasion of SARS-CoV-2 in human and mouse brain. *J Exp Med* [Internet]. 2021 Mar 1 [cited 2021 Aug 12];218(3). Available from: <https://doi.org/10.1084/jem.20202135>
  44. Imai M, Iwatsuki-Horimoto K, Hatta M, Loeber S, Halfmann PJ, Nakajima N, et al. Syrian hamsters as a small animal model for SARS-CoV-2 infection and countermeasure development. *Proc Natl Acad Sci* [Internet]. 2020 Jul 14 [cited 2021 Aug 12];117(28):16587–95. Available from: <https://www.pnas.org/content/117/28/16587>
  45. Francis ME, Goncin U, Kroeker A, Swan C, Ralph R, Lu Y, et al. SARS-CoV-2 infection in the Syrian hamster model causes inflammation as well as type I interferon dysregulation in both respiratory and non-respiratory tissues including the heart and kidney. *PLOS Pathog* [Internet]. 2021 Jul 1 [cited 2021 Aug 12];17(7):e1009705. Available from:

<https://journals.plos.org/plospathogens/article?id=10.1371/journal.ppat.1009705>

46. Horspool AM, Ye C, Wong TY, Russ BP, Lee KS, Winters MT, et al. SARS-CoV-2 B.1.1.7 and B.1.351 variants of concern induce lethal disease in K18-hACE2 transgenic mice despite convalescent plasma therapy. *bioRxiv* [Internet]. 2021 Jan 1;2021.05.05.442784. Available from: <http://biorxiv.org/content/early/2021/05/05/2021.05.05.442784.abstract>
47. Grifoni A, Weiskopf D, Ramirez SI, Mateus J, Dan JM, Moderbacher CR, et al. Targets of T Cell Responses to SARS-CoV-2 Coronavirus in Humans with COVID-19 Disease and Unexposed Individuals. *Cell*. 2020 Jun 25;181(7):1489-1501.e15.
48. C RM, SI R, JM D, A G, KM H, D W, et al. Antigen-Specific Adaptive Immunity to SARS-CoV-2 in Acute COVID-19 and Associations with Age and Disease Severity. *Cell* [Internet]. 2020 Nov 12 [cited 2021 Jul 29];183(4):996-1012.e19. Available from: <https://pubmed.ncbi.nlm.nih.gov/33010815/>
49. Szabo PA, Dogra P, Gray JI, Wells SB, Connors TJ, Weisberg SP, et al. Longitudinal profiling of respiratory and systemic immune responses reveals myeloid cell-driven lung inflammation in severe COVID-19. *Immunity* [Internet]. 2021 Apr 13 [cited 2021 Jul 31];54(4):797-814.e6. Available from: <http://www.cell.com/article/S1074761321001175/fulltext>
50. AC A, MM W, A M, L B, D M, KHG M. Sustained protective immunity against *Bordetella pertussis* nasal colonization by intranasal immunization with a vaccine-adjuvant combination that induces IL-17-secreting T RM cells. *Mucosal Immunol* [Internet]. 2018 Nov 1 [cited 2021 Sep 8];11(6):1763–76. Available from: <https://pubmed.ncbi.nlm.nih.gov/30127384/>
51. Poon MML, Rybkina K, Kato Y, Kubota M, Matsumoto R, Bloom NI, et al. SARS-CoV-2 infection generates tissue-localized immunological memory in humans. *Sci Immunol* [Internet]. 2021 Oct 7 [cited 2021 Oct 21];eabl9105. Available from: <https://www.science.org/doi/abs/10.1126/sciimmunol.abl9105>

52. Moreau GB, Burgess SL, Sturek JM, Donlan AN, Petri WA, Mann BJ. Evaluation of K18-hACE2 Mice as a Model of SARS-CoV-2 Infection. *Am J Trop Med Hyg* [Internet]. 2020 Sep 1 [cited 2021 Dec 1];103(3):1215–9. Available from: <https://pubmed.ncbi.nlm.nih.gov/32723427/>
53. Morpheus [Internet]. [cited 2021 Oct 12]. Available from: <https://software.broadinstitute.org/morpheus/>

# Chapter 5: Discussion

## 5.1 Overview

Emerging SARS-CoV-2 variants of concern have added additional challenges to COVID-19 vaccine and therapeutic development as well as impacted the efficacy of currently available vaccines and therapeutics. Here, we utilized pre-clinical models to help understand the immune response against SARS-CoV-2 to improve upon COVID-19 vaccines. The culmination of this portfolio of work depicted in chapters 2-4 describes the utilization of the transgenic K18-hACE2 mouse model to establish a pipeline to: 1) study SARS-CoV-2 pathogenesis, 2) evaluate systemic and mucosal immune responses against SARS-CoV-2, and 3) develop vaccines and assess efficacy.

In chapter 2, we established a passive immunization model in K18-hACE2 mice to evaluate human convalescent plasma (HCP) obtained from a patient infected with the ancestral strain of SARS-CoV-2 against variants of concern, Alpha, Beta, and Delta. In this study, we evaluated survival, disease burden, viral RNA in the lung and brain, SARS-CoV-2 HCP antibody duration in systemic circulation, and histopathology in the lung post challenge. Passive immunization against VOC challenge demonstrated that ancestral strain polyclonal antibodies protected mice against ancestral SARS-CoV-2 (WA-1) (100% survival), and partially protected against Alpha (60% survival) which corresponded with decreased lung inflammation (Ch.2, Fig.5), disease (Ch.2, Fig. 2), and viral RNA burden (Ch.2, Fig. 3) compared to mice treated with healthy human sera and challenged with SARS-CoV-2. Mice treated with HCP and challenged with Beta resulted in high viral RNA burden in the lung and brain leading to 100% morbidity despite having similar RBD and nucleocapsid IgG titers in the serum and lung as the ancestral and Alpha challenged HCP treated mice (Ch.2, Fig. 2, 4). As an attempt to enhance protection against Delta challenge, we administered 6 consecutive doses of HCP to mice. Unfortunately, passively immunized mice did

not survive challenge with a lethal Delta dose, demonstrating severe disease outcomes and high viral RNA levels in the lung, brain, and nasal wash (Ch.2, Fig.6) Overall, the establishment of a passive immunization model allowed us to understand the antibody responses against different emerging VOC to better develop vaccines and therapeutics against COVID-19. Chapter 2 focused on understanding the antibody response against different VOC and provided a model to study emerging VOC *in vivo*.

In chapter 3, we utilized the VOC challenge model in K18-hACE2 mice from chapter 2 to evaluate vaccines against Alpha and Beta challenge. In this study, four RBD-VLP vaccines composed of RBD displayed on Hepatitis B surface antigen (HBsAg) adjuvanted with either Alum or SWE were evaluated and compared to the standard Pfizer-BioNTech mRNA vaccine. The experimental vaccines included: 1)  $\beta$  RBD HBsAg + Alum, 2)  $\beta$ /Wu RBD HBsAg +Alum, 3)  $\beta$  RBD HBsAg + SWE, and 4)  $\beta$  RBD +SWE (Ch.3, Table S1). Mice were administered 3 doses of the experimental vaccines or 2 doses of the mRNA vaccine intramuscularly and challenged with either Alpha or Beta VOC. Results demonstrated that mice immunized with RBD HBsAg experienced higher survival than mice immunized without the HBsAg; however, only mice immunized with  $\beta$ /Wu RBD HBsAg +Alum,  $\beta$  RBD HBsAg + SWE, and mRNA had 100% survival against both Alpha and Beta challenge (Ch. 3, Fig.2). Disease pathologies, viral RNA burden in the lung and brain, and lung inflammation were consistent with survival results (Ch.3, Fig. 2,3). Furthermore, the serological analysis revealed that  $\beta$  RBD HBsAg + SWE generated increased binding antibodies to multiple VOC RBD compared to Alum adjuvanted RBD-HBsAg vaccines (Ch.3, Fig.1). Also, all RBD-HBsAg vaccines elicited a broadly neutralizing antibody response against VOC RBD similar to Pfizer-BioNTech mRNA (Ch.3, Fig.4, S2).

In chapter 3, we focused on evaluating the efficacy of intramuscular COVID-19 vaccines in the K18-hACE model; however, in chapter 4, we shifted our emphasis to improving COVID-19 vaccines by developing an intranasal protein subunit vaccine. We developed a COVID-19 vaccine composed of RBD conjugated to a carrier protein EcoCRM adjuvanted with a lipid A mimetic,



BECC470 (BReC-CoV-2). Mice were primed and boosted with BReC-CoV-2 either through the intramuscular route or intranasal route and challenged with the ancestral strain of SARS-CoV-2. Results demonstrated that nasal administration of BReC-CoV-2 led to higher survival (89%) compared to intramuscular administration of BReC-CoV-2 (60%) (Ch.4, Fig.3). Mice vaccinated intranasally with BreC-CoV-2 also maintained weight and temperature throughout challenge and had lowered viral RNA burden in the lung, nasal wash, and brain. Additionally, intranasal vaccinated mice induced broadly neutralizing antibodies against VOC RBD, and elicited a robust RBD IgA response in the respiratory tract compared to intramuscular vaccination (Ch.4, Fig.3,4,5,6). Furthermore, bulk RNA sequencing revealed that intranasal administration of BreC-CoV-2 generated both B and T cell signatures in the lung during SARS-CoV-2 challenge (Ch.4, Fig. 9). In this study, we also evaluated a heterologous prime and boost vaccine approach with BReC-CoV-2. Here, mice were primed intramuscularly with BReC-CoV-2 followed by an intranasal boost with the same formulation and challenged with Delta VOC. Mice vaccinated via the heterologous prime and boost vaccine strategy with BReC-CoV-2 were protected against challenge, while homologous intranasal or intramuscular vaccination only resulted in partial protection (60% and 40% respectively). (Ch.4, Fig. 10). Overall, chapter 4 demonstrates that nasal vaccination can offer both localized and systemic protection against SARS-CoV-2 and a nasal booster following an intramuscular prime can help induce protection against VOC.

We acknowledge that studies performed in chapters 2-4 contain limitations. All *in vivo* studies in chapters 2-4 were performed in the K18-hACE2 mouse model. Despite the advantages of using the lethal mouse model to evaluate vaccine protection against SARS-CoV-2 challenge, the over expression of hACE2 in the brain leading to morbidity in the K18-hACE2 mouse is not reflective of human COVID-19 disease progression. Other model organisms such as hamsters, ferrets, and non-human primates have more similar COVID-19 symptoms and disease outcomes compared to the K18-hACE2 model. In order to evaluate vaccine effectiveness against pneumonia like symptoms caused by SARS-CoV-2 and transmission of the virus, future studies should utilize the

Syrian hamster model. Chapters 2-4 utilized qRT-PCR for viral RNA quantification in the lung, brain, and nasal wash. However, measuring total genomic viral RNA detected by qRT-PCR does not specify the presence of infectious virions. Therefore, future vaccine and challenge studies will focus on incorporating plaque forming unit (PFU) assays to the studies to measure infectious SARS-CoV-2 virions in the lung, brain and nasal wash along with viral RNA quantification. Additionally, all neutralization assays were performed using an *in vitro* RBD to hACE2 binding assay. Even though the *in vitro* neutralization assay provided crucial information on serum antibody neutralization across multiple RBDs from variants of concern, live virus neutralization should also be performed to further support *in vitro* neutralization assays. Furthermore, IM/IN studies performed with the BECC470 adjuvant in chapter 4 elicited highly immunogenic responses which could have contributed to toxicity in mice. Future vaccine studies utilizing BECC470 as an adjuvant should focus on titrating BECC470 to find the optimal immunogenic but safe dose.

Chapter 5 reflects on the current COVID-19 pandemic responses and discusses the repercussions caused by SARS-CoV-2. Overall, in this chapter, we apply the lessons learned from the pandemic to develop novel vaccine approaches to improve vaccine immunity against emerging SARS-CoV-2 VOC with the ultimate goal of preventing future outbreaks and pandemics caused by SARS-CoV-2.

## **5.2 Pandemic response**

Since the initial WHO declaration of the COVID-19 pandemic in March 2020, there has been over 535 million confirmed COVID-19 cases and over 6 million deaths worldwide (Our World in Data). The availability of COVID-19 vaccines and treatments have alleviated hospitalizations and deaths; but the pandemic is still ongoing. The COVID-19 pandemic united scientists worldwide to study SARS-CoV-2 in order to develop vaccines, therapeutics and treatments, but also learn from the challenges to improve upon future pandemic preparedness.

As soon as China released the genomic sequence of SARS-CoV-2 in January 2020, COVID-19 vaccine development was underway. Previous research performed on the endemic causing coronaviruses severe acute respiratory syndrome coronavirus (SARS-CoV) and Middle East respiratory syndrome coronavirus (MERS-CoV) aided in the swift development of current COVID-19 vaccines. Previous studies characterizing SARS-CoV and MERS-CoV as well as other coronaviruses showed the mechanism of infection through spike protein binding to ACE2 similar to SARS-CoV-2 infection (1). Therefore, characterizing the virology and pathogenesis of SARS-CoV and MERS-CoV helped in the selection of the spike protein as a candidate vaccine antigen for COVID-19 vaccine development. Furthermore, studies engineering the pre-fusion stabilization spike protein for SARS and MERS also contributed to the development of the current pre-fusion stabilized spike protein used in COVID-19 vaccines (2,3). COVID-19 mRNA vaccines were the first vaccines to obtain emergency use approval in the United States in December 2020 and were the first vaccines to gain FDA approval in the United States. The accelerated development of COVID-19 mRNA vaccines also comprised over 30 years of previous research involving the synthesis of mRNA, stabilization, and delivery of mRNA in lipid nanoparticles as therapeutics and vaccines (4). The culmination of mRNA research led to the first mRNA vaccines for rabies and influenza to enter clinical trials in 2013 and 2015 respectively before the utilization of mRNA technology for COVID-19 (4). Overall, with the previous research performed on coronaviruses and mRNA, companies and research institutes were able to quickly and safely develop potent vaccines that could decrease deaths and hospitalization due to COVID-19. However, gaps in the vaccine development response included limited research on the durability of the vaccine response at the time, unclear dosing schedules, and inclusion of only the ancestral strain of SARS-CoV-2 antigens in vaccine formulations.

### **5.2.1 Repurposing of animal models**

The global research effort to restrain COVID-19 also resulted in the repurposing of pre-clinical animal models such as the K18-hACE2 mouse, ferret, and the non-human primate models to

better understand pathogenesis, transmission, and immune responses against SARS-CoV-2 (5,6). Together, these pre-clinical models established platforms to evaluate vaccine and therapeutic efficacy as well as provided the avenue to improve current vaccines and therapeutics.

### **5.2.2 Implementation of antibody-based therapeutics and antivirals to treat COVID-19**

Along with vaccines, therapeutics and antivirals were also developed throughout the span of the pandemic to treat SARS-CoV-2 infection. In the beginning of the pandemic, human convalescent plasma from recovered SARS-CoV-2 patients was used as a treatment for severe COVID-19 cases. Currently, studies have demonstrated that convalescent plasma could improve severe cases of COVID-19 (7,8). In December 2021, WHO recommended against the use of convalescent plasma treatment for non-severe COVID-19 cases as studies have shown no benefit but proposed that convalescent plasma treatment for severe cases should be further investigated in clinical trials. The FDA also updated the guidelines on emergency use approval (EUA) on high titer convalescent plasma treatment to only be administered to immunocompromised patients or patients taking immunosuppressive drugs. Overall, the use of convalescent plasma for severe COVID-19 treatment still needs further evaluation in clinical trials but could be used as emergency first response treatments for future pandemics or outbreaks until vaccines or therapeutics are developed. EUA was granted to several monoclonal antibody therapies targeting the spike protein such as Sotrovimab, REGEN-COV (Casirivimab and Imdevimab), Bamlanivimab and Etesevimab, and Bebtelovimab in 2021 (CDC). In 2022, Omicron became the predominant VOC, with over 30 mutations accumulated on the spike protein. Therefore, because of the heavily mutated spike protein, monoclonal antibody therapies Sotrovimab, REGEN-COV (Casirivimab and Imdevimab), Bamlanivimab and Etesevimab were no longer efficacious against Omicron and EUA approval was revoked (FDA). However, the cocktail antibody therapy Bebtelovimab, maintained effectiveness against Omicron and subvariants and retained EUA approval. Lastly, the availability of antivirals also mitigated the severity of COVID-19 in most developed countries. In the US, the FDA has authorized 3 antivirals

to treat COVID-19: 1) Paxlovid, 2) Remdesivir, and 3) Molnupiravir (CDC). Paxlovid is a combination of both nirmatrelvir and ritonavir and is used to treat mild-moderate COVID-19 (9). Nirmatrelvir is a protease inhibitor that stops SARS-CoV-2 replication and ritonavir is a drug that prolongs the half-life of nirmatrelvir to better increase activity of nirmatrelvir (9). Paxlovid is prescribed orally and recommended to be taken within 5 days of symptom onset (9). Remdesivir stops viral replication by inhibition of viral RNA dependent RNA polymerase (10). Unlike Paxlovid, Remdesivir is reserved for high-risk patients with mild to moderate COVID-19 or hospitalized high-risk patients and is administered intravenously. Molnupiravir is a nucleoside analog antiviral drug that stops viral replication prematurely by integration into the viral RNA during synthesis (11). Additionally, Molnupiravir is recommended for high-risk patients with mild to moderate COVID-19 and is administered orally at least within 5 days of symptom onset.

### **5.2.3 Local community response to COVID-19**

The focus of the initial responses of the research community included helping their local community develop reagents and assays to detect SARS-CoV-2 in human samples. Here at West Virginia University, a COVID-19 task force comprised of biochemists, virologists, immunologists, and physicians were assembled by Drs. Laura Gibson and Clay Marsh and supported by the state of West Virginia. The objective of the COVID-19 task force was to provide West Virginia with the tools to mitigate the spread COVID-19. Reagents such as RBD and spike protein were produced in house, for antibody detection assays (12). Additionally, viral genomic sequencing was established for SARS-CoV-2 surveillance, and PCR assays were developed to detect nucleocapsid RNA. As a result, WVU established the in-house WVU Rapid Development Laboratory which provided the capability to test more residents of WV, provide better surveillance of circulating VOC in WV, and offer faster turnaround times for PCR results.

#### **5.2.4 Global response to vaccine inequity**

Lastly, the COVID-19 pandemic has intensified global health inequalities such as vaccine inequity. Currently, 11.99 billion COVID-19 vaccine doses have been administered with approximately 66% of the global population receiving at least one dose of a COVID-19 vaccine (Our World in Data). However, only 17.8% of the population in developing countries are vaccinated with at least one dose. For example, many countries in Africa have less than 10% of the population that has received at least one vaccine dose. The sparse vaccine distribution into developing countries not only is a large humanitarian crisis but scientists are worried that low vaccination and high transmission rates of SARS-CoV-2 could allow for the emergence of new variants of concern (13). To help achieve higher vaccination rates in developing countries, global organizations such as the Bill and Melinda Gates Foundation have donated over 2 billion dollars to aid in the global COVID-19 response (14). Funds from the Gates Foundation have been allocated to mitigate transmission in sub-Saharan Africa and South Asia by providing tests, treatments, and vaccines. Additionally, the Gates Foundation have funded grants to other programs for COVID-19 research, as well as invested in companies that can provide medical supplies for low- and middle-income countries (14). Furthermore, COVAX is one of the largest global collaboration programs with the goal of bringing vaccine equity around the world with the focus on accelerating the development of COVID-19 vaccines and through acquiring vaccines through large vaccine manufacturers to distribute to developing countries (15). COVAX is comprised of the Coalition for Epidemic Preparedness Innovations (CEPI), Gavi (Vaccine Alliance), the WHO, and UNICEF. The overall goal of COVAX was to distribute 2 billion vaccine doses by 2021. However, due to challenges such as vaccine hoarding by high-income countries, cold chain requirements, and supply chain issues, COVAX fell short of their goal, but still was able to distribute over 1 billion doses to 148 countries and territories (16). Overall, COVAX predicts that it will need an additional 350 million dollars to continue research and development on developing vaccines for emerging VOC, increase vaccine supply and to continue clinical trials for COVID-19 vaccines.

### **5.3 Manufacturability of COVID-19 vaccines for developing countries**

Chapters 3 and 4 investigate RBD-based vaccines that could benefit developing countries. In general, RBD serves as an optimal vaccine antigen choice that can be used to meet the vaccine demands in developing countries. Utilization of RBD instead of the spike protein in vaccine formulations can offer advantages such as cost efficiency, ease of production in large volumes, and temperature stability (17–20). Additionally, RBD similar to full-length spike protein is an immunogenic target which encompasses 90% of neutralizing antibody targets obtained from convalescent pools (21). Furthermore, vaccine components disclosed in chapter 3 such as RBD-HBsAg can be mass produced by the Serum Institute of India, and can be stored and transported at 4°C. In chapter 4, components of the BReC-CoV-2 can also be easily scaled up for production and require limited cold chain storage. In particular, BECC470 adjuvant can be lyophilized, avoiding cold-chain requirements. Future ideal vaccine preparations could yield both lyophilized vaccine antigen and adjuvant formulations to improve shelf life, and transportation and delivery of vaccines into developing countries (22).

### **5.4 The impact of SARS-CoV-2 zoonosis and recombination events**

Many infectious diseases throughout history originated from animal to human spillover events. Coronavirus outbreaks caused by SARS-CoV from 2002-2003 and MERS-CoV in 2012 were speculated to originate from bats and then moved into civics and dromedary camels as intermediate hosts to jump into the human population (23). Bats were also hypothesized to be the original reservoir to harbor SARS-CoV-2. Studies found that the coronavirus strain RaTG13 discovered in horseshoe bats had 96% genome similarity to SARS-CoV-2 (24). Intermediate hosts such as pangolins and minks have also been considered as reservoirs that aided in the SARS-CoV-2 spillover into humans (25) (Ch.5, Fig.1). The influenza pandemics were also caused by spillover events from avian and swine origins. There has been a total of four influenza pandemics that have occurred over the span of 100 years. The 1918 H1N1 pandemic was the first recorded influenza pandemic, followed by the H2N2 in 1957, H3N2 in 1968, and another

H1N1 pandemic in 2009 (26). Interestingly, the virus that caused the most recent H1N1 pandemic in 2009 was a result of antigenic shift caused by the reassortment of three previous influenza strains originating from birds, pigs and humans (27). Antigenic shift is defined as two or more flu strains that can exchange entire genetic segments via reassortment to generate a new flu variant with different antigen variations. Typically, humans have no pre-existing immunity to new flu variants resulting from antigenic shift which can thus lead to pandemics and outbreaks. Furthermore, reassortment events that happen during antigen shift can only happen in viruses that possess segmented genomes such as influenza; however, coronaviruses, do not have a segmented genome. Even though coronaviruses cannot undergo reassortment to generate new strains, coronaviruses can undergo recombination events similar to reassortment during antigenic shift. Studies showed that RaTG13, a betacoronavirus obtained from bat, possessed the highest genomic similarity to SARS-CoV-2; however, the receptor binding motif found on RaTG13 was genetically dissimilar. Nevertheless, coronaviruses found in pangolins were genetically divergent from SARS-CoV-2 but harbored a receptor binding motif that could bind to human ACE2. Therefore, data suggested that SARS-CoV-2 could have originated from the recombination of both bat and pangolin coronaviruses that ultimately spilled over into humans (25,28) (Ch.5, Fig.1).

#### **5.4.2 SARS-CoV-2 spillover and spillback events**

Furthermore, genomic surveillance of SARS-CoV-2 have detailed human to animal transmission in cats, dogs, lions, tigers (zoo setting), minks and white-tailed deer. From this spillover, animal to animal transmission also have occurred between minks and deer (Ch.5, Fig.1). The SARS-CoV-2 outbreak that occurred at the mink farm in Denmark in 2020 is an example of human to mink spillover and subsequently mink to human spillback. The variant of SARS-CoV-2 that was transmitted back from minks to humans contained a newly acquired Y453F mutation on the RDB that could enhance the binding of spike protein to human ACE2 (29,30). SARS-CoV-2 also has established a natural reservoir in the white-tailed deer population in North America with 30-40% seroprevalence (31,32) (Ch.5, Fig.1). However, studies have demonstrated that SARS-CoV-2 did



not acquire mutations that increased viral fitness in humans (31). Additionally, it is speculated that Omicron originated from mice and then jumped back into humans (Ch.5, Fig.1). Mutations accumulated following human to mouse transmission allowed for SARS-CoV-2 to acquire mutations in the spike protein to increase binding affinity to mouse ACE2 (33,34). Further evidence demonstrates that Omicron also accumulated mutations in the mouse that could cause further immune evasion in human hosts.

#### **5.4.3 Prediction on future emerging SARS-CoV-2 variants**

Altogether, even though SARS-CoV-2 mutation rate is slower than influenza viruses, the ability of SARS-CoV-2 to undergo recombination with other coronaviruses and establish reservoirs in mammalian host generates concern for the future of the COVID-19 pandemic. The ability of SARS-CoV-2 to establish animal reservoirs suggests that it will be difficult to fully eradicate SARS-CoV-2 from circulation. Additionally, animal hosts can also provide an opportunity for SARS-CoV-2 to undergo recombination with other variants to generate new strains of SARS-CoV-2. Despite limited evidence demonstrating that SARS-CoV-2 can accumulate mutations in animal reservoirs that could cause an increase of virulence and transmissibility in humans, potential spillback events from animals to humans could occur and lead to emergence of variants of high consequence. SARS-CoV-2 variant of high consequence are characterized as variants that can resist available therapeutics and treatments, increase hospitalizations, evade vaccine protection, and cannot be detected with available detection assays. To date, no variants of high consequence have been reported. Overall, to prevent future zoonotic spillover events, increased genomic surveillance of animals, waste water, and humans are necessary to detect newly emerging variants (25). Prompt responses to newly emerging variants could allow for more time to develop vaccines, therapeutics, and antivirals to curb future coronavirus outbreaks and pandemics.

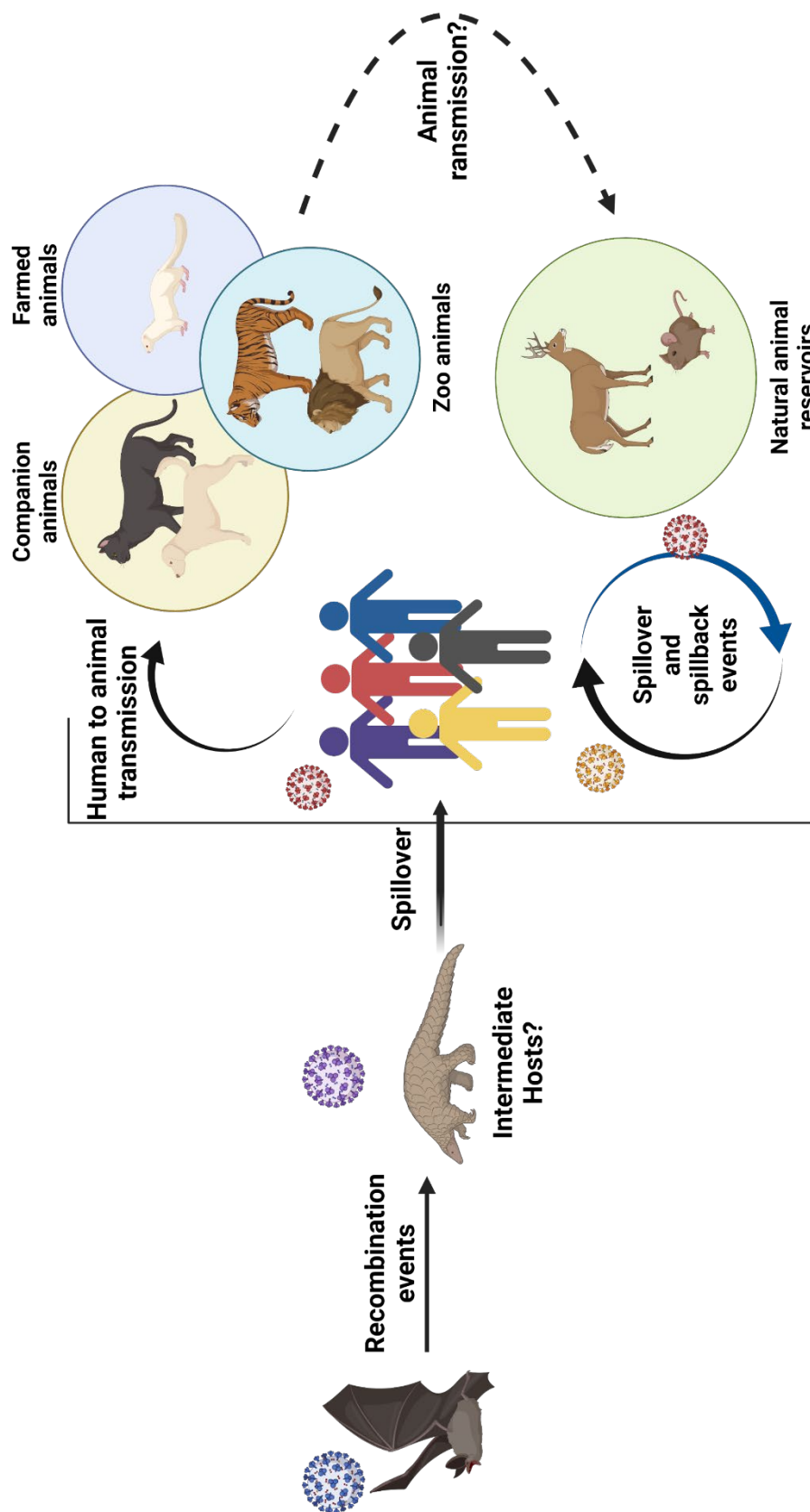


**Figure 1. SARS-CoV-2 zoonosis and VOC evolution.** SARS-CoV-2 is classified as a zoonotic disease. Spillover into humans is speculated to have originated in bats or through intermediate host such as the pangolin. SARS-CoV-2 transmission from humans to companion animals (dogs and cats), zoo animals (lions and tigers), and to farmed minks have been documented. Additionally, human transmission to animals in nature such as white-tailed deer and mice have also been documented. Spillover and spillback cases of transmission could potentially result in recombination of different variants of the virus leading to emerging variants of concern which could cause future SARS-CoV-2 outbreaks.

## **5.5 Improving COVID-19 vaccines**

Current available COVID-19 vaccines have mitigated the severity of COVID-19 by reducing hospitalizations and deaths. However, due to the accelerated development and production of approved COVID-19 vaccines, limited studies have been performed to assess the longevity of the vaccine response against SARS-CoV-2 as well as vaccine response against SARS-CoV-2 variants. COVID-19 vaccination and SARS-CoV-2 infection stimulate the optimal protection against SARS-CoV-2 compared to vaccine alone (Ch.5, Fig.2). Optimal protection included the production of broadly neutralizing antibodies against SARS-CoV-2, induction of mucosal IgA, stimulation of CD4 and CD8 cellular immune responses and lastly generation of memory B and T cells (35,36) (Ch.5, Fig.2). Therefore, in order to elicit long-term immunity and immunity against VOCs, vaccination strategies that mirror vaccination and infection immune responses could be investigated to increase protection against SARS-CoV-2.

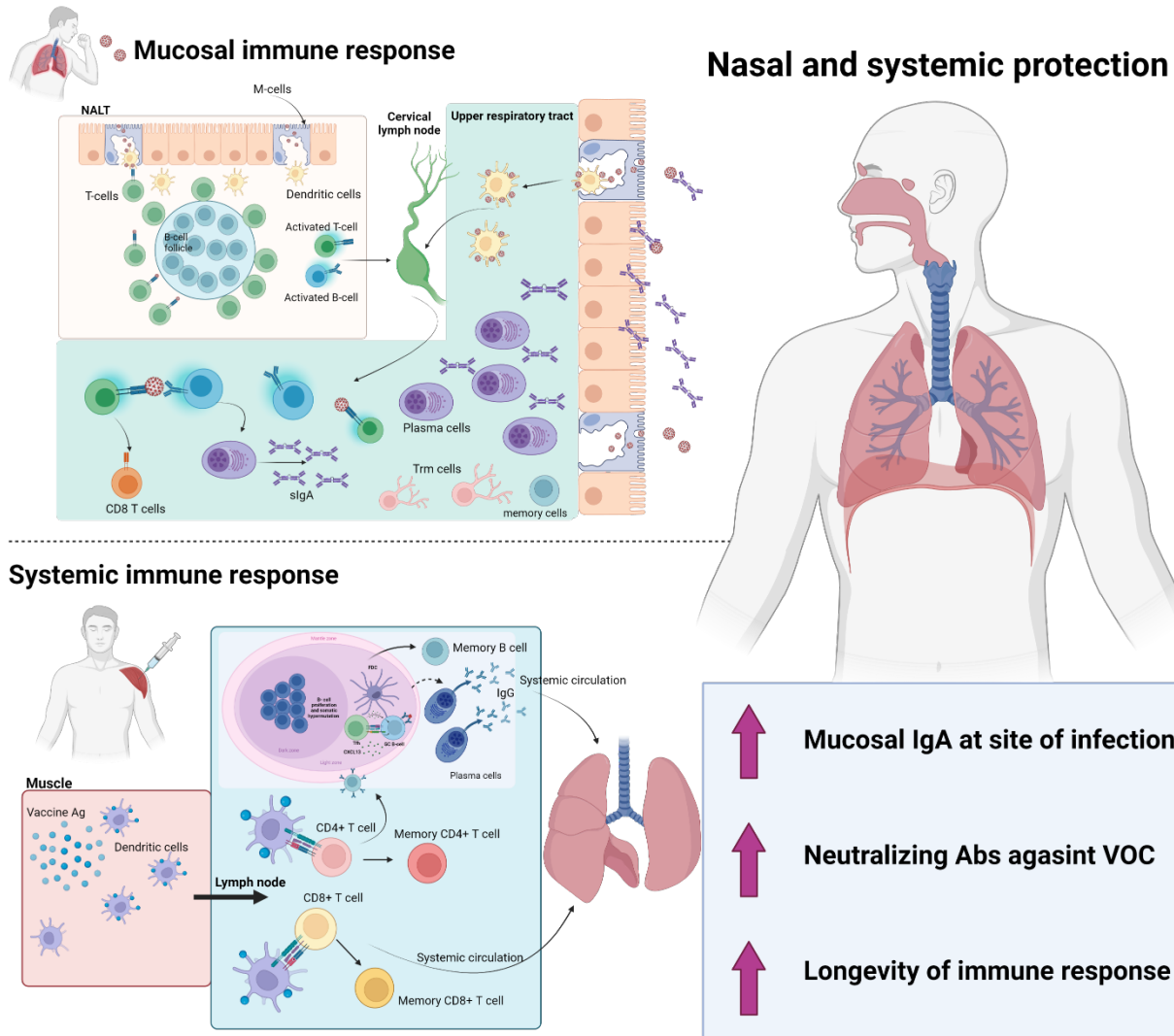


**Figure 2. Mucosal and systemic immunity against SARS-CoV-2.** The hybrid of both mucosal and systemic immunity are needed to provide optimal protection against SARS-CoV-2 infection. During infection or nasal vaccination, the mucosal immune response is initiated in the mucosal induction sites such as the NALT. The NALT is composed of M-cells, dendritic cells, B-cell dominated follicles and parafollicular zone surrounding the B-cell follicles largely inhabited by T-cells. Pathogen or vaccines are sampled by M-cells and distributed to dendritic cells for processing which are used to activate T-cells and B-cells. Activated T and B cells in the NALT then migrate through the cervical lymph node to effector sites, where T-cells help B-cells differentiate into IgA secreting B-cells. During intermuscular vaccination, antigen presenting cells process vaccine antigen and move into the draining lymph node to activate CD4 and CD8 T-cells. In the lymph node establishment of germinal centers by T-cell help allow for the maturation of B-cells into high affinity IgG secreting plasma cells. Activated cells can migrate to effector sites in the lung.

### 5.5.1 Improving longevity

Recent studies evaluating the mRNA COVID-19 vaccines (Comirnaty and Spikevax), adenovirus vectored vaccines (Ad26.COVS and Vaxzevria), and protein subunit vaccines (Nuvaxovid) have assessed vaccine mediated immune responses out to 6 months in fully vaccinated individuals. Studies overall demonstrated that after 6 months, vaccine immune responses begin to wane (37,38). Neutralizing antibody titers decreased in all vaccines evaluated after 6 months post vaccination, with the highest neutralizing titers belonging to individuals vaccinated with Spikevax, followed by Comirnaty and Nuvaxovid, and lastly trailed by Ad26.COVS vaccinated individuals with the lowest neutralizing titers (37). However, while neutralizing antibodies fell after 6 months, all vaccine platforms induced detectable spike specific CD4<sup>+</sup>, CD8<sup>+</sup> and B memory responses. (37). Overall, mRNA vaccines were more immunogenic than protein subunit and adenoviral vectored vaccinated individuals, stimulating either higher or similar memory responses compared to Nuvaxovid and Ad26.COVS (37).

Despite available COVID-19 vaccines retaining spike specific cellular and humoral memory responses against SARS-CoV-2, waning immunity remains an issue. Currently, the CDC recommends for adults to receive three doses of mRNA vaccine, and a 4<sup>th</sup> dose for people 50 or older. The vaccine schedule entails waiting 3-8 weeks after receiving the first dose of vaccine before obtaining the second dose, followed by at least a 5-month interval before acquiring the third dose. Constant boosting may elevate neutralizing titers and improve responses against emerging variants but is not a feasible plan of action for the future (39–41). To circumvent frequent dosing of COVID-19 vaccines, different approaches can be taken to improve longevity of COVID-19 vaccines. Heterologous prime and boost strategies with either different vaccine formulations or different routes of administration can be used to induce long-term immunity. In chapter 4, mice were primed intramuscularly with BReC-CoV-2 then boosted intranasally with the same formulation. The IM prime and IN boost strategy resulted in 100% survival from a lethal Delta challenge compared to 60% survival in homologous IN BReC-CoV-2 vaccination and 40%

survival in homologous IM BReC-CoV-2 vaccination (Ch.4, Fig.10). We hypothesized that the heterologous IM prime and IN boost strategy operated as a push-pull system to generate protection. IM vaccination pushed antibody magnitude and cellular responses and the IN boost not only induced an IgA response in the respiratory tract but also pulled circulating antibodies and effector cells generated from both IM and IN vaccination into the respiratory tract. Additionally, we hypothesize that the immunity generated after heterologous IM prime and IN boost mimics hybrid or vaccine breakthrough immunity. Studies demonstrated that the immunity generated from COVID-19 vaccination and SARS-CoV-2 infection could lead to long-term protection against re-infection for more than 1 year unlike COVID-19 vaccination only (42–44).

Furthermore, implementation of different vaccine boosters could also improve long-term immune responses. Heterologous prime and boost strategies have already been implemented into COVID-19 vaccination approaches for adenovirus vectored based vaccines. Clinical studies have shown that heterologous prime with ChAdOx1nCoV-19 and boost with mRNA generated enhanced broadly neutralizing antibodies against VOC, increased spike specific IgG and IgA responses, and elicited elevated levels of spike specific CD4 and CD8 T-cells compared to homologous administration of mRNA or ChAdOx1nCoV-19 (45–47). Therefore, the opportunity to stimulate both strong cellular responses from the adenovirus vaccine in combination with the robust humoral responses from the mRNA vaccine could overall potentially increase vaccine longevity. Overall, further studies need to be conducted in both the pre-clinical and clinical settings to evaluate COVID-19 vaccines long-term effectiveness. Additionally, COVID-19 vaccines in development currently should also focus on performing long-term studies in pre-clinical models to assess the durability of the immune response. More studies should also be performed assessing the effect of adjuvanted vaccines, administration strategies, timeline of dose administration, and/or delivery strategies to promote longer and stronger immune responses.

### **5.5.2 Improving vaccine responses against VOC**

All current approved COVID-19 vaccines utilize the spike protein of the ancestral strain of SARS-CoV-2. However, the ancestral strain that was circulating in 2019 and 2020 is essentially non-existent. Approved COVID-19 vaccines have suffered a decrease in vaccine efficacy against past and present VOC resulting in less protection against symptomatic disease (48,49). Fortunately, COVID-19 vaccines were still effective at preventing hospitalizations and death due to infection. With the emergence of new VOC, it is pertinent that COVID-19 vaccines provide broad protection amongst all variants of concern. The arrival of Omicron and its subvariants revealed the need for vaccine boosters to increase protection against infection. Two doses with mRNA or ChAdOx1nCoV-19 were not able to protect against symptomatic infection with Omicron; however a subsequent boost with either mRNA or ChAdOx1 provided an increase of vaccine efficacy against Omicron but only for a few months until responses began to wane (50,51). Currently both Pfizer and Moderna are developing Omicron specific mRNA vaccines to help increase vaccine efficacy against Omicron. Moderna has developed a bivalent Omicron booster candidate mRNA-1273.214 containing both the original Spikevax vaccine accompanied with candidate Omicron specific mRNA. In a press release, Moderna announced that administration of mRNA-1273.214 booster in people who have already received 2-3 doses of an approved COVID-19 vaccine resulted in an eight-fold increase of neutralizing antibody titers against Omicron above baseline (52,53). Similar to the Moderna bivalent COVID-19 vaccine, we have shown in chapter 3, that vaccination with both Beta RBD-HBsAg and Wuhan RBD-HBsAg adjuvanted with Alum in mice resulted in 100% protection against both Alpha or Beta challenge whereas Beta RBD-HBsAg + Alum alone resulted in 60% survival against Alpha challenge and 80% survival against Beta challenge (Ch.3, Fig. 2).

Furthermore, developing variant specific boosters may alleviate short-term problems that arise; however, do little to prevent future outbreaks or pandemics caused by coronaviruses that could spillover from animal reservoirs. Therefore, the development of pan-coronavirus vaccines could

help lessen the severity of future coronavirus outbreaks. Studies have demonstrated that humans first infected with SARS-CoV then vaccinated with Comirnaty generated pan-coronavirus neutralizing antibodies that could recognize SARS-CoV, SARS-CoV-2 Wuhan, Alpha, Beta, Delta and 10 other coronaviruses found in animals (54). Pre-clinical development of pan-coronavirus vaccines are underway. Currently, there are approximately four vaccines utilizing mosaic nanoparticles and VLPs to display different coronavirus spike and RBD proteins (55,56).

### **5.6 Developing protective nasal COVID-19 vaccines**

As mentioned in chapter 1, Flumist is the only approved intranasal vaccine. However, 12 nasal COVID-19 vaccines are in clinical trials and even more nasal vaccines are currently being evaluated in pre-clinical trials. Interestingly, the majority of COVID-19 vaccines in clinical trials are live viral vectored vaccines. No protein subunit vaccines are currently in clinical trials, and less than ten nasal vaccines in pre-clinical studies utilize the protein-based vaccine platform (57). We hypothesize that nasally administered viral vectored vaccines can lead to greater induction of mucosal immune responses since it shares similarity to a live infection. The mucosal tissue in general maintains a high tolerance or lack of responsiveness to foreign antigens. Therefore, to generate an immunogenic mucosal vaccine response, mucosal tolerance must be broken. T regulatory cells drive tolerogenic mucosal immune responses after mucosal antigen exposure by downregulating the activation of Th1 effector cells and decreasing the release of pro-inflammatory cytokines such as INF-gamma. Infections in the mucosa can break mucosal tolerance by releasing Pathogen Associated Molecular Patterns (PAMPs) that can trigger Toll-like Receptors to stimulate and activate the mucosal immune response (58). Therefore, we speculate that the mucosal immune response generated by viral vectored vaccines can be induced by intranasal administration of adjuvanted protein-based vaccines to the same or greater magnitude.

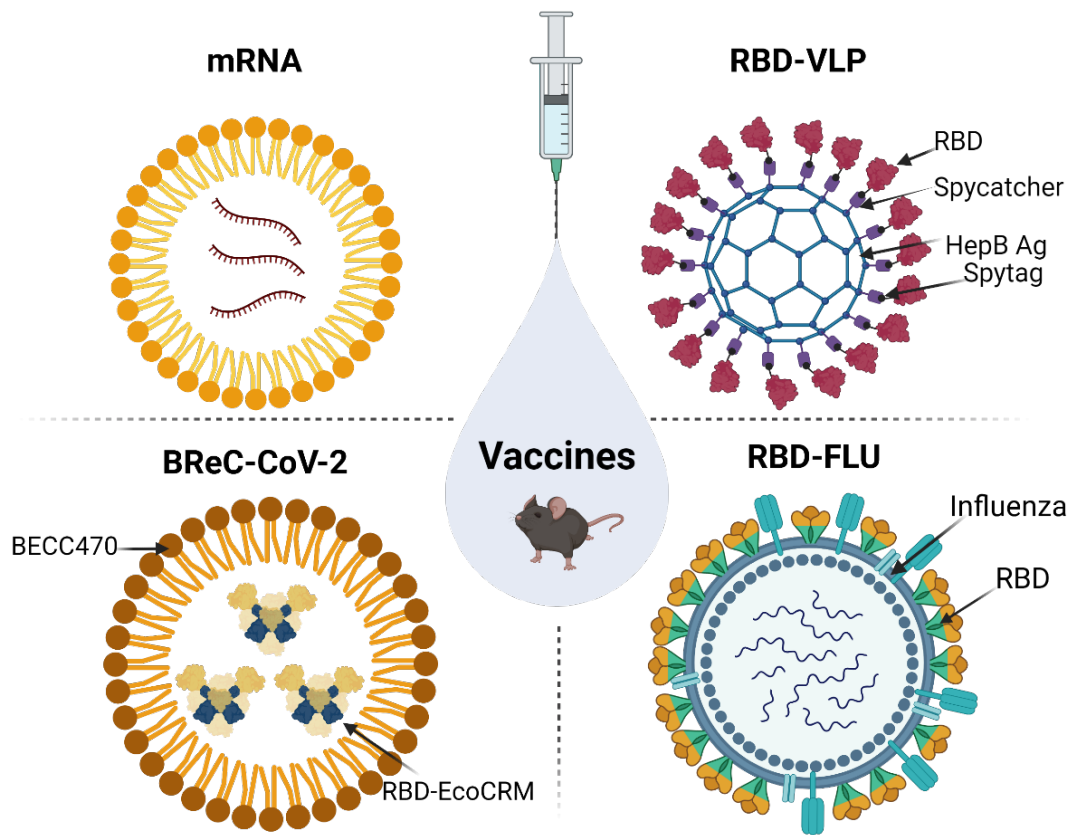
In chapter 3, we evaluated the vaccine efficacy of the VLP-based vaccine antigen RBD-HBsAg in mice. We showed that RBD-HBsAg VLP was needed to induce a protective immune response against Alpha or Beta challenge and elicit broadly neutralizing antibodies against VOC (Ch.3,



Fig.1,2,4). Additionally, in chapter 4, we evaluated intranasal administration of BreC-CoV-2, a bacterial carrier protein-based vaccine adjuvanted with a strong TLR4 agonist BECC470. In the same study, we showed that the RBD-CRM antigen was less immunogenic when administered intranasally alone, or adjuvanted with CpG or IRI (Beta-glucan adjuvant) (Ch.4, Fig.1). Therefore, in order to develop a more efficacious intranasal COVID-19 vaccine formulation we combined the immunogenic RBD-HBsAg vaccine antigen evaluated in chapter 3 with the immunostimulatory BECC470 adjuvant assessed in chapter 4. We assessed the vaccine efficacy of the new prototype vaccine RBD-HBsAg+BECC470 in the K18-hACE2 mouse challenge model and found that RBD-HBsAg+BECC470 protected mice (100% survival) against lethal Delta challenge as well as induced broadly neutralizing antibodies against VOC (data not shown). Future studies with RBD-HBsAg+BECC470 should focus on evaluating RBD-HBsAg+BECC470 as an intranasal booster to mRNA vaccinations to increase the longevity of immune responses. Similar studies assessing intranasal boost after mRNA prime has demonstrated stimulation of protective mucosal cellular and humoral responses (Ch.5, Fig.3) (59). Additionally, RBD-HBsAg+BECC470 should be studied in the context of transmission in either hamster or ferret models to evaluate the ability of RBD-HBsAg+BECC470 to inhibit transmission of SARS-CoV-2.

Moreover, we also evaluated attenuated viral vectored vaccines as nasal vaccine candidates. We collaborated with the Bloom lab at Fred Hutchinson Cancer Research Center to evaluate their attenuated influenza expressing SARS-CoV-2 RBD vaccine candidate (RBD-Flu) in the K18-hACE2 challenge model (Ch.5, Fig.3). The RBD-Flu vaccine antigen was generated by replacing neuraminidase on the surface of influenza virions with RBD (60). Mice vaccinated with 2 doses of RBD-Flu and challenged with Delta were partially protective against lethal Delta challenge (60% survival) (data not shown). Future studies with RBD-Flu could include evaluating the RBD-Flu and mRNA as a heterologous IN prime and IM boost strategy with the hypothesis that the live viral vectored vaccine will stimulate robust cellular mucosal response and the IM boost with mRNA will

boost neutralizing antibody responses against SARS-CoV-2 to generate improved immunity against SARS-CoV-2 infection.



**Figure 3. Experimental vaccine approaches to improve COVID-19 vaccine efficacy.** Prototype intranasal boosters after mRNA prime with RBD-VLP, RBD-Flu and BreC-CoV-2 to induce both mucosal and systemic immunity.

### 5.5.1 Potential nasal adjuvants

In chapter 4, we evaluated IRI (beta glucan), CpG, and two forms of BECC adjuvants as potential nasal vaccines (Ch.4, Fig.1). The BECC adjuvants were overall the most immunogenic adjuvants followed by CpG and then IRI. In order to develop a protective mucosal vaccine, an immunogenic vaccine formulation must be used to circumvent the quick mucosal clearance of antigen and maintain vaccine retention in the upper respiratory tract. Therefore, for protein-based vaccines, adjuvants are necessary to increase immunogenicity.

Even though the Beta glucan, IRI was not as immunogenic as BECCs, previous studies evaluating improving intranasal Pertussis vaccines demonstrated that Beta glucan adjuvants obtained from yeast could increase vaccine retention in the nasal cavity and induce long-lived antibody responses (61,62). Other intranasal Pertussis vaccine studies have demonstrated the use of c-di-GMP, an intracellular receptor stimulator of interferon genes (STING agonist), along with LP1569, a TLR2 agonist, as a combinatorial nasal adjuvant that can induce both Th1 and Th17 immune responses (63). Additional adjuvants that have shown immunogenic properties in nasal vaccine formulations include Alum and CpG. Intranasal administration of inactivated SARS-CoV-2 vaccine adjuvanted with Alum generated increased production of IgG and IgA in the mucosa compared to intramuscular administration of the same formulation (64). Lastly, lipid A mimetic adjuvants such as MPL and BECCs have been used in pre-clinical intranasal vaccine formulations. BECC adjuvants have shown immunostimulatory properties in nasal COVID-19 vaccines and in nasal Pertussis vaccine formulations. However, since BECCs are derived from Gram-negative bacteria, the toxicity of the Lipid A is a concern. Further toxicity and adjuvant dosing studies with BECC adjuvants need to be performed to ensure safety. Additionally, the generation of synthetic BECC molecules could also decrease the potential toxicity due to biologically derived endotoxin. Altogether, adjuvants in nasal vaccines serve as a tool to climb over the barriers of accelerated mucosal clearance as well as mucosal tolerance.

### **5.5.2 Other uses for nasal vaccination**

Conventional standards of administering antibody therapeutics in humans is through the intravenous route. Approved monoclonal antibody therapies for COVID-19 are administered as single IV dose, whereas convalescent plasma therapy is administered as an infusion. However, there are no approved intranasal antibody therapeutics. Pre-clinical passive immunization studies utilizing intranasal delivery of antibodies have demonstrated that IgM monoclonal antibody therapy targeting RBD maintained nasal cavity retention, neutralized SARS-CoV-2 VOC, protected mice against challenge, and was able to therapeutically treat mice with SARS-CoV-2 (65). RBD nanobody intranasal nebulization was also able to neutralize SARS-CoV-2 VOC *in vitro* and therapeutically decrease COVID-19 associated symptoms in Syrian hamsters (66). Influenza passive immunization studies also demonstrated that intranasal administration of Influenza specific IgA was able to protect against H1N1 challenge in a human challenge model (67).

Furthermore, antivirals could also be administered intranasally to diminish the transmission and spread of SARS-CoV-2 (68). We speculate that intranasal administration of antivirals, in theory, could alleviate systemic viral dissemination if administered early during the infection course, decrease transmission by eliminating viral replication at the site of infection and potentially help decrease or alleviate respiratory symptoms faster. Altogether, more studies need to be performed in order to evaluate the plausibility of intranasal antiviral delivery.

### **5.6 Concluding remarks**

The emergence of SARS-CoV-2 VOC has driven the continuation of the COVID-19 pandemic. Vaccines developed against the ancestral strain of SARS-CoV-2 towards the beginning of the pandemic have experienced a decrease in vaccine efficacy against newly emerging variants. Therefore, the development of improved COVID-19 vaccines and vaccine approaches are necessary to improve immunity against emerging VOC. We have utilized the K18-hACE2 mouse model to study the pathogenesis of VOC, characterize the antibody mediated responses against emerging VOC, as well as assessed different vaccine delivery systems and administration routes

to improve vaccine responses against VOC. Overall, we have demonstrated that the induction of both systemic and mucosal immunity results in the optimal protection against SARS-CoV-2.

## 5.7 References

1. Li Y Der, Chi WY, Su JH, Ferrall L, Hung CF, Wu TC. Coronavirus vaccine development: from SARS and MERS to COVID-19. *J Biomed Sci* 2020 271 [Internet]. 2020 Dec 20 [cited 2022 Jun 23];27(1):1–23. Available from: <https://jbiomedsci.biomedcentral.com/articles/10.1186/s12929-020-00695-2>
2. Hsieh CL, Goldsmith JA, Schaub JM, DiVenere AM, Kuo HC, Javanmardi K, et al. Structure-based design of prefusion-stabilized SARS-CoV-2 spikes. *Science* (80- ) [Internet]. 2020 Sep 1 [cited 2022 Jun 20];369(6509):1501–5. Available from: <https://www.science.org/doi/10.1126/science.abd0826>
3. Walls AC, Park YJ, Tortorici MA, Wall A, McGuire AT, Velesler D. Structure, Function, and Antigenicity of the SARS-CoV-2 Spike Glycoprotein. *Cell* [Internet]. 2020 Apr 16 [cited 2022 May 3];181(2):281-292.e6. Available from: <https://pubmed.ncbi.nlm.nih.gov/32155444/>
4. Dolgin E. The tangled history of mRNA vaccines. *Nature*. 2021 Sep 1;597(7876):318–24.
5. Muñoz-Fontela C, Dowling WE, Funnell SGP, Gsell P-S, Riveros-Balta AX, Albrecht RA, et al. Animal models for COVID-19. *Nat* 2020 5867830 [Internet]. 2020 Sep 23 [cited 2021 Jul 31];586(7830):509–15. Available from: <https://www.nature.com/articles/s41586-020-2787-6>
6. Muñoz-Fontela C, Widerspick L, Albrecht RA, Beer M, Carroll MW, de Wit E, et al. Advances and gaps in SARS-CoV-2 infection models. *PLOS Pathog* [Internet]. 2022 Jan 1 [cited 2022 Jun 23];18(1):e1010161. Available from: <https://journals.plos.org/plospathogens/article?id=10.1371/journal.ppat.1010161>
7. Cao H, Ming L, Chen L, Zhu X, Shi Y. The Effectiveness of Convalescent Plasma for the Treatment of Novel Corona Virus Disease 2019: A Systematic Review and Meta-Analysis. *Front Med*. 2021 Sep 27;8:1618.
8. Sullivan DJ, Gebo KA, Shoham S, Bloch EM, Lau B, Shenoy AG, et al. Early Outpatient Treatment for Covid-19 with Convalescent Plasma. *N Engl J Med* [Internet]. 2022 May 5

- [cited 2022 Jun 20];386(18):1700–11. Available from: <https://www.nejm.org/doi/full/10.1056/NEJMoa2119657>
9. Pfizer’s Novel COVID-19 Oral Antiviral Treatment Candidate Reduced Risk of Hospitalization or Death by 89% in Interim Analysis of Phase 2/3 EPIC-HR Study | Pfizer [Internet]. [cited 2022 Jun 23]. Available from: <https://www.pfizer.com/news/press-release/press-release-detail/pfizers-novel-covid-19-oral-antiviral-treatment-candidate>
  10. Beigel JH, Tomashek KM, Dodd LE, Mehta AK, Zingman BS, Kalil AC, et al. Remdesivir for the Treatment of Covid-19 — Final Report. *N Engl J Med* [Internet]. 2020 Nov 5 [cited 2022 Jun 20];383(19):1813–26. Available from: <https://www.nejm.org/doi/full/10.1056/nejmoa2007764>
  11. Fischer WA, Eron JJ, Holman W, Cohen MS, Fang L, Szewczyk LJ, et al. A phase 2a clinical trial of molnupiravir in patients with COVID-19 shows accelerated SARS-CoV-2 RNA clearance and elimination of infectious virus. *Sci Transl Med* [Internet]. 2022 Jan 19 [cited 2022 Jun 23];14(628):7430. Available from: <https://www.science.org/doi/10.1126/scitranslmed.abl7430>
  12. AM H, T K, BP R, MA D, MA W, JM K, et al. Interplay of Antibody and Cytokine Production Reveals CXCL13 as a Potential Novel Biomarker of Lethal SARS-CoV-2 Infection. *mSphere* [Internet]. 2021 Feb 24 [cited 2021 Aug 8];6(1). Available from: <https://pubmed.ncbi.nlm.nih.gov/33472985/>
  13. Mallapaty S. Researchers fear growing COVID vaccine hesitancy in developing nations. *Nature*. 2022 Jan 1;601(7892):174–5.
  14. COVID-19 | Bill & Melinda Gates Foundation [Internet]. [cited 2022 Jul 15]. Available from: <https://www.gatesfoundation.org/ideas/campaigns/covid-19>
  15. COVAX: CEPI’s response to COVID-19 – CEPI [Internet]. [cited 2022 Jul 15]. Available from: <https://cepi.net/covax/>
  16. Yoo KJ, Mehta A, Mak J, Bishai D, Chansa C, Patenaude B. COVAX and equitable access



- to COVID-19 vaccines. Bull World Health Organ [Internet]. 2022 May 5 [cited 2022 Jun 21];100(5):315. Available from: /pmc/articles/PMC9047429/
17. Kleanthous H, Silverman JM, Makar KW, Yoon IK, Jackson N, Vaughn DW. Scientific rationale for developing potent RBD-based vaccines targeting COVID-19. NPJ vaccines [Internet]. 2021 Dec 1 [cited 2022 Feb 28];6(1). Available from: <https://pubmed.ncbi.nlm.nih.gov/34711846/>
  18. Dalvie NC, Biedermann AM, Rodriguez-Aponte SA, Naranjo CA, Rao HD, Rajurkar MP, et al. Scalable, methanol-free manufacturing of the SARS-CoV-2 receptor-binding domain in engineered *Komagataella phaffii*. Biotechnol Bioeng [Internet]. 2022 Feb 1 [cited 2022 Apr 5];119(2):657–62. Available from: /pmc/articles/PMC8653030/
  19. Malladi SK, Singh R, Pandey S, Gayathri S, Kanjo K, Ahmed S, et al. Design of a highly thermotolerant, immunogenic SARS-CoV-2 spike fragment. J Biol Chem [Internet]. 2021 Jan 1 [cited 2022 Jun 22];296:100025. Available from: <http://www.jbc.org/article/S0021925820000113/fulltext>
  20. Hotez PJ, Bottazzi ME. Developing a low-cost and accessible COVID-19 vaccine for global health. PLoS Negl Trop Dis [Internet]. 2020 Jul 1 [cited 2022 May 11];14(7):e0008548. Available from: <https://journals.plos.org/plosntds/article?id=10.1371/journal.pntd.0008548>
  21. Piccoli L, Park YJ, Tortorici MA, Czudnochowski N, Walls AC, Beltramello M, et al. Mapping Neutralizing and Immunodominant Sites on the SARS-CoV-2 Spike Receptor-Binding Domain by Structure-Guided High-Resolution Serology. Cell [Internet]. 2020 Nov 12 [cited 2022 Mar 1];183(4):1024-1042.e21. Available from: <http://www.cell.com/article/S0092867420312344/fulltext>
  22. Preston KB, Randolph TW. Stability of lyophilized and spray dried vaccine formulations. Adv Drug Deliv Rev. 2021 Apr 1;171:50–61.
  23. Henrique Ellwanger J, Artur Bogo Chies J. Zoonotic spillover: Understanding basic aspects for better prevention. Genet Mol Biol [Internet]. 2021 [cited 2022 Jun 23];44(1):20200355.

Available from: <https://doi.org/10.1590/1678-4685-GMB-2020-0355>

24. Singh D, Yi S V. On the origin and evolution of SARS-CoV-2. *Exp Mol Med* 2021 534 [Internet]. 2021 Apr 16 [cited 2022 Jun 21];53(4):537–47. Available from: <https://www.nature.com/articles/s12276-021-00604-z>
25. Wang Q, Chen H, Shi Y, Hughes AC, Liu WJ, Jiang J, et al. Tracing the origins of SARS-CoV-2: lessons learned from the past. *Cell Res* 2021 3111 [Internet]. 2021 Sep 29 [cited 2022 Jun 21];31(11):1139–41. Available from: <https://www.nature.com/articles/s41422-021-00575-w>
26. Krammer F, Smith GJD, Fouchier RAM, Peiris M, Kedzierska K, Doherty PC, et al. Influenza. *Nat Rev Dis Prim* 2018 41 [Internet]. 2018 Jun 28 [cited 2022 Jun 21];4(1):1–21. Available from: <https://www.nature.com/articles/s41572-018-0002-y>
27. Zeng H, Pappas C, Katz JM, Tumpey TM. The 2009 Pandemic H1N1 and Triple-Reassortant Swine H1N1 Influenza Viruses Replicate Efficiently but Elicit an Attenuated Inflammatory Response in Polarized Human Bronchial Epithelial Cells. *J Virol* [Internet]. 2011 Jan 15 [cited 2022 Jun 21];85(2):686–96. Available from: <https://journals.asm.org/doi/full/10.1128/JVI.01568-10>
28. Li X, Giorg EE, Marichannegowda MH, Foley B, Xiao C, Kong XP, et al. Emergence of SARS-CoV-2 through recombination and strong purifying selection. *Sci Adv* [Internet]. 2020 Jul 1 [cited 2022 Jun 21];6(27). Available from: <https://www.science.org/doi/10.1126/sciadv.abb9153>
29. Munnink BBO, Sikkema RS, Nieuwenhuijse DF, Molenaar RJ, Munger E, Molenkamp R, et al. Transmission of SARS-CoV-2 on mink farms between humans and mink and back to humans. *Science* [Internet]. 2021 Jan 8 [cited 2022 Jun 21];371(6525):172–7. Available from: <https://pubmed.ncbi.nlm.nih.gov/33172935/>
30. Telenti A, Arvin A, Corey L, Corti D, Diamond MS, García-Sastre A, et al. After the pandemic: perspectives on the future trajectory of COVID-19. *Nat* 2021 5967873 [Internet].

- 2021 Jul 8 [cited 2022 Jun 21];596(7873):495–504. Available from: <https://www.nature.com/articles/s41586-021-03792-w>
31. Tan CCS, Lam SD, Richard D, Owen CJ, Berchtold D, Orengo C, et al. Transmission of SARS-CoV-2 from humans to animals and potential host adaptation. *Nat Commun* 2022 131 [Internet]. 2022 May 27 [cited 2022 Jun 21];13(1):1–13. Available from: <https://www.nature.com/articles/s41467-022-30698-6>
  32. Hale VL, Dennis PM, McBride DS, Nolting JM, Madden C, Huey D, et al. SARS-CoV-2 infection in free-ranging white-tailed deer. *Nat* 2022 6027897 [Internet]. 2021 Dec 23 [cited 2022 Jun 21];602(7897):481–6. Available from: <https://www.nature.com/articles/s41586-021-04353-x>
  33. Wei C, Shan KJ, Wang W, Zhang S, Huan Q, Qian W. Evidence for a mouse origin of the SARS-CoV-2 Omicron variant. *J Genet Genomics*. 2021 Dec 1;48(12):1111–21.
  34. Cameroni E, Bowen JE, Rosen LE, Saliba C, Zepeda SK, Culap K, et al. Broadly neutralizing antibodies overcome SARS-CoV-2 Omicron antigenic shift. *Nat* 2021 6027898 [Internet]. 2021 Dec 23 [cited 2022 Jun 21];602(7898):664–70. Available from: <https://www.nature.com/articles/s41586-021-04386-2>
  35. Crotty S. Hybrid immunity. *Science* (80- ) [Internet]. 2021 Jun 25 [cited 2022 Jun 22];372(6549):1392–3. Available from: <https://www.science.org/doi/10.1126/science.abj2258>
  36. Callaway E. Breakthrough COVID powers up immune response to variants — including Omicron. *Nature*. 2022 Feb 3;
  37. Zhang Z, Mateus J, Coelho CH, Dan JM, Moderbacher CR, Gálvez RI, et al. Humoral and cellular immune memory to four COVID-19 vaccines. *Cell* [Internet]. 2022 May 27 [cited 2022 Jun 21]; Available from: <https://linkinghub.elsevier.com/retrieve/pii/S0092867422006535>
  38. Feikin DR, Higdon MM, Abu-Raddad LJ, Andrews N, Araos R, Goldberg Y, et al. Duration

- of effectiveness of vaccines against SARS-CoV-2 infection and COVID-19 disease: results of a systematic review and meta-regression. *Lancet* [Internet]. 2022 Mar 5 [cited 2022 Jun 22];399(10328):924–44. Available from: <http://www.thelancet.com/article/S0140673622001520/fulltext>
39. Gruell H, Vanshylla K, Tober-Lau P, Hillus D, Schommers P, Lehmann C, et al. mRNA booster immunization elicits potent neutralizing serum activity against the SARS-CoV-2 Omicron variant. *Nat Med* 2022 283 [Internet]. 2022 Jan 19 [cited 2022 Jun 22];28(3):477–80. Available from: <https://www.nature.com/articles/s41591-021-01676-0>
  40. Shen X. Boosting immunity to Omicron. *Nat Med* 2022 283 [Internet]. 2022 Feb 24 [cited 2022 Jun 22];28(3):445–6. Available from: <https://www.nature.com/articles/s41591-022-01727-0>
  41. Cheng SMS, Mok CKP, Leung YWY, Ng SS, Chan KCK, Ko FW, et al. Neutralizing antibodies against the SARS-CoV-2 Omicron variant BA.1 following homologous and heterologous CoronaVac or BNT162b2 vaccination. *Nat Med* 2022 283 [Internet]. 2022 Jan 20 [cited 2022 Apr 27];28(3):486–9. Available from: <https://www.nature.com/articles/s41591-022-01704-7>
  42. Cerqueira-Silva T, Andrews JR, Boaventura VS, Ranzani OT, de Araújo Oliveira V, Paixão ES, et al. Effectiveness of CoronaVac, ChAdOx1 nCoV-19, BNT162b2, and Ad26.COVS.2.S among individuals with previous SARS-CoV-2 infection in Brazil: a test-negative, case-control study. *Lancet Infect Dis* [Internet]. 2022 Jun 1 [cited 2022 Jun 22];22(6):791–801. Available from: <http://www.thelancet.com/article/S1473309922001402/fulltext>
  43. Nordström P, Ballin M, Nordström A. Risk of SARS-CoV-2 reinfection and COVID-19 hospitalisation in individuals with natural and hybrid immunity: a retrospective, total population cohort study in Sweden. *Lancet Infect Dis* [Internet]. 2022 Jun 1 [cited 2022 Jun 22];22(6):781–90. Available from: <http://www.thelancet.com/article/S1473309922001438/fulltext>

44. Hall V, Foulkes S, Insalata F, Kirwan P, Saei A, Atti A, et al. Protection against SARS-CoV-2 after Covid-19 Vaccination and Previous Infection. *N Engl J Med* [Internet]. 2022 Mar 31 [cited 2022 Jun 22];386(13):1207–20. Available from: <https://www.nejm.org/doi/10.1056/NEJMoa2118691>
45. Schmidt T, Klemis V, Schub D, Mihm J, Hielscher F, Marx S, et al. Immunogenicity and reactogenicity of heterologous ChAdOx1 nCoV-19/mRNA vaccination. *Nat Med* 2021 279 [Internet]. 2021 Jul 26 [cited 2022 Jun 22];27(9):1530–5. Available from: <https://www.nature.com/articles/s41591-021-01464-w>
46. Barros-Martins J, Hammerschmidt SI, Cossmann A, Odak I, Stankov M V., Morillas Ramos G, et al. Immune responses against SARS-CoV-2 variants after heterologous and homologous ChAdOx1 nCoV-19/BNT162b2 vaccination. *Nat Med* 2021 279 [Internet]. 2021 Jul 14 [cited 2022 Jun 22];27(9):1525–9. Available from: <https://www.nature.com/articles/s41591-021-01449-9>
47. Deming ME, Lyke KE. A ‘mix and match’ approach to SARS-CoV-2 vaccination. *Nat Med* 2021 279 [Internet]. 2021 Jul 26 [cited 2022 Jun 22];27(9):1510–1. Available from: <https://www.nature.com/articles/s41591-021-01463-x>
48. Hayawi K, Shahriar S, Serhani MA, Alashwal H, Masud MM. Vaccine versus Variants (3Vs): Are the COVID-19 Vaccines Effective against the Variants? A Systematic Review. 2021 [cited 2022 Jun 22]; Available from: <https://doi.org/10.3390/vaccines>
49. Abu-Raddad LJ, Chemaitelly H, Ayoub HH, AIMukdad S, Yassine HM, Al-Khatib HA, et al. Effect of mRNA Vaccine Boosters against SARS-CoV-2 Omicron Infection in Qatar. *N Engl J Med* [Internet]. 2022 May 12 [cited 2022 Jun 22];386(19):1804–16. Available from: <https://www.nejm.org/doi/full/10.1056/NEJMoa2200797>
50. Andrews N, Stowe J, Kirsebom F, Toffa S, Rickeard T, Gallagher E, et al. Covid-19 Vaccine Effectiveness against the Omicron (B.1.1.529) Variant. *N Engl J Med* [Internet]. 2022 Apr 21 [cited 2022 Jun 22];386(16):1532–46. Available from:

<https://www.nejm.org/doi/full/10.1056/NEJMoa2119451>

51. Chemaitelly H, Ayoub HH, AlMukdad S, Coyle P, Tang P, Yassine HM, et al. Duration of mRNA vaccine protection against SARS-CoV-2 Omicron BA.1 and BA.2 subvariants in Qatar. medRxiv [Internet]. 2022 Mar 13 [cited 2022 Jun 22];2022.03.13.22272308. Available from: <https://www.medrxiv.org/content/10.1101/2022.03.13.22272308v1>
52. Moderna Announces Omicron-Containing Bivalent Booster Candidate mRNA-1273.214 Demonstrates Superior Antibody Response Against Omicron [Internet]. [cited 2022 Jun 22]. Available from: <https://investors.modernatx.com/news/news-details/2022/Moderna-Announces-Omicron-Containing-Bivalent-Booster-Candidate-mRNA-1273.214-Demonstrates-Superior-Antibody-Response-Against-Omicron/default.aspx>
53. A Study to Evaluate the Immunogenicity and Safety of Omicron Variant Vaccines in Comparison With mRNA-1273 Booster Vaccine for COVID-19 - Full Text View - ClinicalTrials.gov [Internet]. [cited 2022 Jun 22]. Available from: <https://clinicaltrials.gov/ct2/show/NCT05249829>
54. Tan C-W, Chia W-N, Young BE, Zhu F, Lim B-L, Sia W-R, et al. Pan-Sarbecovirus Neutralizing Antibodies in BNT162b2-Immunized SARS-CoV-1 Survivors. N Engl J Med [Internet]. 2021 Oct 7 [cited 2022 Jun 22];385(15):1401–6. Available from: <https://www.nejm.org/doi/10.1056/NEJMoa2108453>
55. Cohen AA, Gnanapragasam PNP, Lee YE, Hoffman PR, Ou S, Kakutani LM, et al. Mosaic nanoparticles elicit cross-reactive immune responses to zoonotic coronaviruses in mice. Science (80- ) [Internet]. 2021 Feb 12 [cited 2022 Jun 22];371(6530):735–41. Available from: <https://www.science.org/doi/10.1126/science.abf6840>
56. Dolgin E. Pan-coronavirus vaccine pipeline takes form. Nat Rev Drug Discov. 2022 May 1;21(5):324–6.
57. Alu A, Chen L, Lei H, Wei Y, Tian X, Wei X. Intranasal COVID-19 vaccines: From bench to bed. eBioMedicine [Internet]. 2022 Feb 1 [cited 2022 Jun 22];76:103841. Available from:

<http://www.thelancet.com/article/S2352396422000251/fulltext>

58. Phillip SD, Blumberg SR, Macdonald TT, editors. Principles of Mucosal Immunology. 2nd ed. CRC Press Taylor & Francis Group; 2020.
59. Mao T, Israelow B, Suberi A, Zhou L, Reschke M, Peña-Hernández MA, et al. Unadjuvanted intranasal spike vaccine booster elicits robust protective mucosal immunity against sarbecoviruses. [cited 2022 Jun 16]; Available from: <https://doi.org/10.1101/2022.01.24.477597>
60. Loes AN, Gentles LE, Greaney AJ, Crawford KHD, Bloom JD. Attenuated influenza virions expressing the SARS-CoV-2 receptor-binding domain induce neutralizing antibodies in mice. [cited 2022 Jun 22]; Available from: <https://doi.org/10.1101/2020.08.12.248823>
61. Wolf MA, Boehm DT, DeJong MA, Wong TY, Sen-Kilic E, Hall JM, et al. Intranasal immunization with acellular pertussis vaccines results in long-term immunity to *Bordetella pertussis* in mice. Infect Immun [Internet]. 2020 Dec 14;IAI.00607-20. Available from: <http://iai.asm.org/content/early/2020/12/10/IAI.00607-20.abstract>
62. Boehm DT, Wolf MA, Hall JM, Wong TY, Sen-Kilic E, Basinger HD, et al. Intranasal acellular pertussis vaccine provides mucosal immunity and protects mice from *Bordetella pertussis*. npj Vaccines. 2019 Dec 1;4(1):1–12.
63. AC A, MM W, A M, L B, D M, KHG M. Sustained protective immunity against *Bordetella pertussis* nasal colonization by intranasal immunization with a vaccine-adjuvant combination that induces IL-17-secreting T RM cells. Mucosal Immunol [Internet]. 2018 Nov 1 [cited 2021 Sep 8];11(6):1763–76. Available from: <https://pubmed.ncbi.nlm.nih.gov/30127384/>
64. Liang Z, Zhu H, Wang X, Jing B, Li Z, Xia X, et al. Adjuvants for Coronavirus Vaccines. Front Immunol. 2020 Nov 6;11:2896.
65. Ku Z, Xie X, Hinton PR, Liu X, Ye X, Muruato AE, et al. Nasal delivery of an IgM offers

- broad protection from SARS-CoV-2 variants. *Nat* 2021 5957869 [Internet]. 2021 Jun 3 [cited 2022 Jun 23];595(7869):718–23. Available from: <https://www.nature.com/articles/s41586-021-03673-2>
66. Esparza TJ, Chen Y, Martin NP, Bielefeldt-Ohmann H, Bowen RA, Tolbert WD, et al. Nebulized delivery of a broadly neutralizing SARS-CoV-2 RBD-specific nanobody prevents clinical, virological and pathological disease in a Syrian hamster model of COVID-19. *bioRxiv* [Internet]. 2021 Nov 12 [cited 2022 Jun 23]; Available from: </pmc/articles/PMC8597880/>
67. Gould VMW, Francis JN, Anderson KJ, Georges B, Cope A V., Tregoning JS. Nasal IgA provides protection against human influenza challenge in volunteers with low serum influenza antibody titre. *Front Microbiol*. 2017 May 17;8(MAY):900.
68. Higgins TS, Wu AW, Illing EA, Sokoloski KJ, Weaver BA, Anthony BP, et al. Intranasal Antiviral Drug Delivery and Coronavirus Disease 2019 (COVID-19): A State of the Art Review. *Otolaryngol - Head Neck Surg (United States)* [Internet]. 2020 Oct 1 [cited 2022 Jun 23];163(4):682–94. Available from: [https://journals.sagepub.com/doi/10.1177/0194599820933170?url\\_ver=Z39.88-2003&rfr\\_id=ori%3Arid%3Acrossref.org&rfr\\_dat=cr\\_pub++0pubmed](https://journals.sagepub.com/doi/10.1177/0194599820933170?url_ver=Z39.88-2003&rfr_id=ori%3Arid%3Acrossref.org&rfr_dat=cr_pub++0pubmed)